UiT The Arctic University of Norway

Faculty of Health Sciences

An investigation of BK Polyomavirus replication in tubular epithelial cells: new insights into kidney dissemination and neutralising antibodies

Elias Myrvoll Lorentzen

A dissertation for the degree of Philosophiae Doctor – March 2024

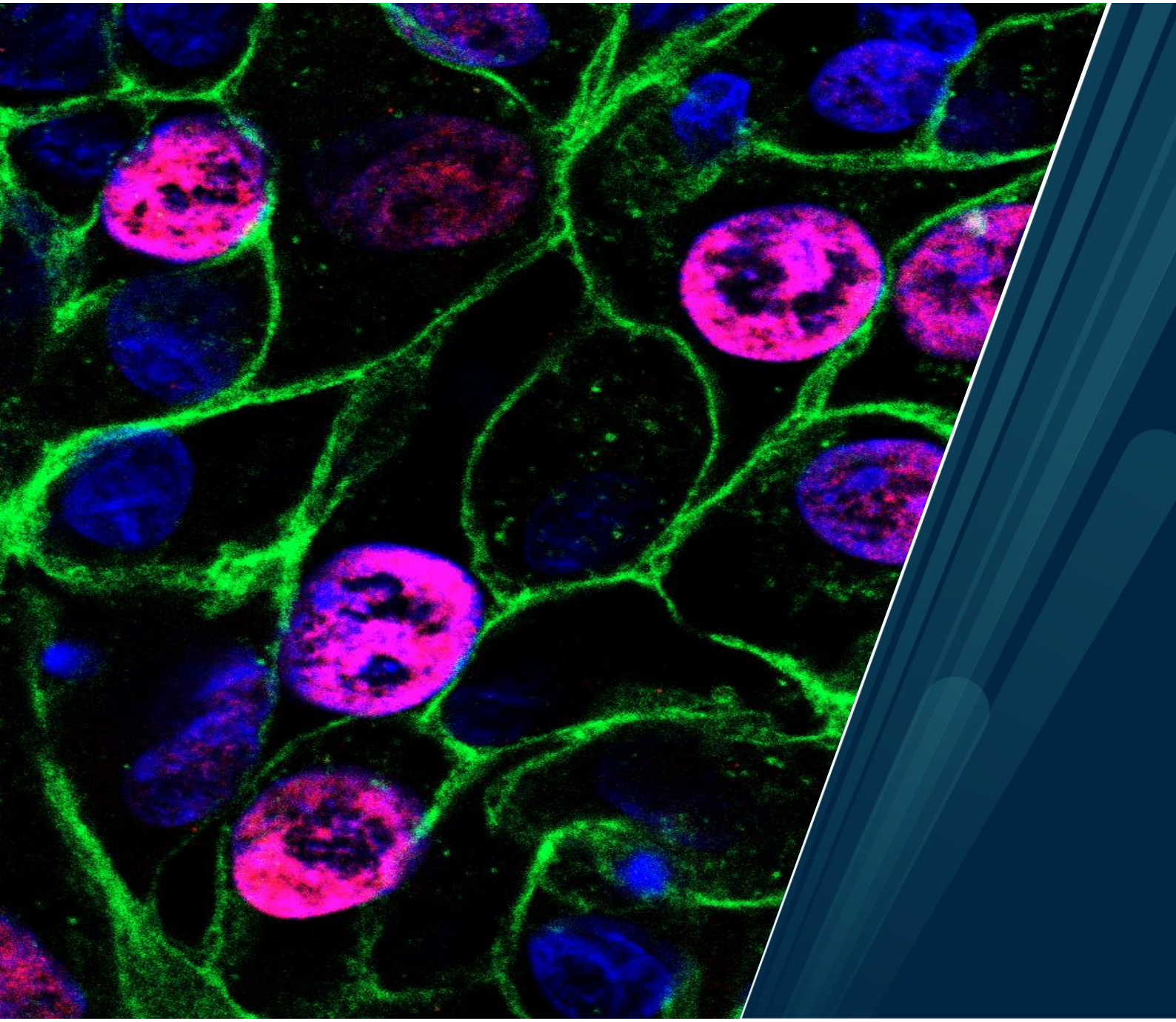

Front page image: Confocal image of BK Polyomavirus infected polarized renal proximal tubule epithelial cells at 3 days post-infection stained for sodium-potassium ATPase (green) and BKPyV large tumour antigen (red). Nuclei are shown in blue.

A dissertation for the degree of Philosophiae Doctor

An investigation of BK Polyomavirus replication in tubular epithelial cells: new insights into kidney dissemination and neutralising antibodies

Elias Myrvoll Lorentzen

Tromsø – March 2024

Department of Clinical Medicine

Faculty of Health Sciences

UiT The Arctic University of Norway

Acknowledgements

This work was carried out at the Department of Microbiology and Infection Control between 2017 to 2024. It was first initiated as a part of the medical student research program and later continued with a PhD-stipend from Helse Nord. I am grateful to Helse Nord and the medical student research program at the Faculty of Healthy Sciences, UiT – The Arctic University of Tromsø for funding. Thank you to the Department of Microbiology and Infection control for funding and for hosting me all these years.

First and foremost, I would like to thank my main supervisor Prof. Christine Hanssen Rinaldo for introducing me to virology and for your mentorship, positivity and support these past years. You have met all my questions, ideas and experiments (failed and successful) with guidance and encouragement. Your supervision and guidance have truly been essential for the completion of this thesis, and more importantly, for my development as a researcher.

I am grateful to Stian Henriksen for invaluable help in learning my way around lab. Thank you for patiently teaching me a multitude of lab skills, always answering all my questions, providing valuable feedback and for the collaboration these past years.

Thank you to my co-supervisors Dr. Garth D. Tylden and Prof. Kristian Prydz for assessing my work and providing valuable feedback. Thank you to all the co-authors that contributed to paper 1. I am grateful to Prof. Hans H. Hirsch and the Transplantation and Clinical Virology group at the University of Basel. The seminars in virology have expanded my interest and understanding of virology. Thank you to Randi Olsen and Kenneth Bowitz Larsen at the Advanced Microscopy Core Facility for processing of samples for electron microscopy and assistance with the microscopes. Kjersti, Linda and Merethe, thank you for good times in the office.

Throughout this PhD, I have had great support from friends and family. Thank you to Chris for office beers and last-minute assembly tips. I am grateful to PW for welcome distractions, good times and all our years of friendship. It means a lot. Thank you to my mom, dad and sister for all the encouragement, interest and support - you have been there the entire way. Thank you to my dear brother, Øyvind. In many ways it feels like we have gone through each other's PhD-journeys together. Thank you for all the breaks, discussions and time spent together.

Finally, elskede Isabell. Thank you for your love, patience and support. I am so grateful that I get to share life with you. I look forward to more time with you from now on.

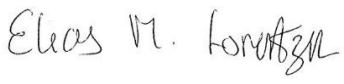

Tromsø, March 2024

Table of contents

Abbreviations

2D - Two-dimensional

2.5D - 2.5-dimensional

3D - Three-dimensional

ATM – Ataxia telangiectasia mutated

ATR – Ataxia telangiectasia and Rad3-related

APOBEC - Apolipoprotein B mRNA editing enzyme catalytic polypeptide-like

BKPyV – BK Polyomavirus

BKPyV-HC - BKPyV-associated haemorrhagic cystitis

BKPyV-UC - BK Polyomavirus-associated urothelial carcinoma

cGAS/STING - Cyclic GMP-AMP synthase/stimulator of interferon genes

CLIC/GEEC - clathrin-independent carrier/glycosylphosphatidylinositol-anchored protein enriched early endosomal compartment

ECM - Extracellular matrix

ELISA – Enzyme-linked immunosorbent assay

ERAD - ER-associated degradation

ER – Endoplasmic reticulum

EVs – Extracellular vesicles

HC – Haemorrhagic cystitis

HIA – Haemagglutination inhibition assay

hpi – Hours post-infection

HSCT - Haematopoietic stem cell transplantation

HSV-1 – Herpes Simplex virus 1

hTERT – Human telomerase reverse transcriptase

IVIGs - Intravenous immunoglobulins

JCPyV – JC Polyomavirus

LTag - Large Tumour antigen

MDCK - Madine-Darby canine kidney

miRNA – microRNA

MPyV - Murine polyomavirus

Na/K-ATPase - Sodium-potassium ATPase

NCCR – non-coding control region

NLS – Nuclear localisation signal

ORF – Open reading frame

Polymerase chain reaction – PCR

PP2A – Protein phosphatase 2A

pRB – Retinoblastoma protein

PyVAN – Polyomavirus-associated nephropathy

qPCR – Quantitative real-time PCR

RBCs – Red blood cells

RPTECs – Renal proximal tubule epithelial cells

sTag – Small tumour antigen

SV40 – Simian virus 40

T-antigen – Tumour antigen

TEM – Transmission electron microscopy

TruncTag – Truncated T-antigen

V-ATPase – Vacuolar H^+ ATPase

Vp1 – Viral protein 1

Vp2 – Viral protein 2

Vp3 – Viral protein 3

Vp4 – Viral protein 4

VLP – Virus-like-particle

ZO-1 –Zona occludens-1

List of papers

Paper 1: Early fulminant BK polyomavirus-associated nephropathy in two kidney transplant patients with low neutralising antibody titers receiving allografts from the same donor

Lorentzen E. M., Henriksen S., Kaur A., Kro G. B., Hammarström C., Hirsch H. H., Midtvedt K. and Rinaldo C. Virol J. 2020;17(5).

https://doi.org/10.1186/s12985-019-1275-9

Paper 2: Modelling BK Polyomavirus dissemination and cytopathology using polarised human renal tubule epithelial cells

Lorentzen E.M., Henriksen S. and Rinaldo C. H. PLOS Pathog. 2023;19(8): e1011622.

https://doi.org/10.1371/journal.ppat.1011622

Paper 3: Massive entry of BK Polyomavirus induces transient cytoplasmic vacuolisation of human renal proximal tubule epithelial cells

Lorentzen E. M., Henriksen S. and Rinaldo C. H. Manuscript.

Summary

BK Polyomavirus (BKPyV) is a DNA virus that infects the majority of the global population, causing a lifelong infection in epithelial cells of the reno-urinary tract. In healthy individuals, BKPyV does not cause disease but is intermittently shed in the urine. However, in immunosuppressed patients, especially kidney transplant recipients, BKPyV represents a major challenge. Up to 15% of kidney transplant recipients develop BKPyV nephropathy, a condition that reduces allograft function and ultimately may cause premature allograft loss. Despite years of study, there are still important knowledge gaps in our understanding of BKPyV biology. Unfortunately, no anti-viral therapies are available, and development of new therapies is hampered by incomplete knowledge of the viral replication cycle. This thesis examines several aspects of BKPyV biology a special focus on the viral replication cycle in polarised and non-polarised renal epithelial cells. to understand the spread of BKPyV but also the dynamic antibody response following BKPyV replication and BKPyV nephropathy and the effect of BKPyV-specific neutralizing antibodies *in vitro*.

In **paper 1**, we characterised the antibody response, quantitated plasma BKPyV DNA (BKPyV DNAemia) and characterised the BKPyV strains in two kidney transplant patients that both developed biopsy-proven BKPyV nephropathy early after transplantation of kidneys from the same deceased donor. Sequencing of BKPyV from plasma and urine revealed BKPyV of identical strain and genotype in the two recipients. Retrospective analysis of antibody titres with three different methods demonstrated that the recipients had low titres of BKPyV neutralising antibodies before transplantation, while the donor had a high titre that suggested recent BKPyV replication. After development of BKPyV DNAemia, both recipients developed high titres of BKPyV neutralising antibodies. Despite reduction of immunosuppression and a robust antibody response, only one of the recipients cleared the BKPyV DNAemia, indicating that high neutralising antibody titres alone is not sufficient for viral clearance. Our findings support that both recipients developed a donor-derived infection. Moreover, our findings of low antibody titres in the recipients and a high antibody titre in the donor support that this is an important risk factor for developing BKPyV nephropathy.

In **paper 2**, we developed a cell culture model of polarised renal proximal tubule epithelial cells (RPTECs) on permeable supports and used this more *in vivo*-like model to characterise major steps in the replication cycle of BKPyV. Viral entry is preferentially apical and BKPyV is mainly released into the apical compartment as cell-free virus and via extrusion of decoy-like

cells that harbour infectious virus. When BKPyV-specific neutralising antibodies are added to the basolateral compartment, they traverse the RPTEC-layer and partly inhibit new infections. Widespread lysis and disruption of the epithelial cell layer is necessary for leakage of BKPyV into the basolateral compartment. The work demonstrates how BKPyV in polarised RPTECs disseminate into the apical compartment. Based on this, we propose that BKPyV disseminate in the tubular fluid *in vivo*, partly inside decoy cells, and thereby may delay immune detection.

In **paper 3**, we determine that BKPyV induces cytoplasmic vacuolisation in RPTECs. This occurs in a fraction of RPTECs shortly after addition of a high infectious dose of BKPyV and after cell lysis. Vacuolisation is induced by a massive uptake of BKPyV into the endocytic pathway, leading to a transient accumulation of enlarged endo-/lysosomal vacuoles, possibly due to an overload of the endocytic pathway. Treatment with the V-ATPase inhibitor bafilomycin A or use of BKPyV-specific neutralising antibodies can block vacuolisation. In contrast to what has been reported for SV40, BKPyV-induced vacuolisation does not increase progeny release and cell death. That lytic progeny release causes focal vacuolisation, suggests cell-to-cell spread of BKPyV. The work demonstrates that cytoplasmic vacuolisation in RPTECs is an early event in the BKPyV replication cycle and contributes new insights to our understanding of BKPyV replication and dissemination.

1 Introduction

1.1 Polyomaviridae – history and main characteristics

Polyomaviridae is a family of viruses that infect a broad range of mammals and birds as well as some species of fish (1). The *Polyomaviridae* family consists of 6 genera: *Alphapolyomavirus*, *Betapolyomavirus*, *Deltapolyomavirus*, *Epsilonpolyomavirus* and *Zetapolyomavirus*, which is further divided into 117 species (1). Polyomaviruses are generally species-specific viruses with a narrow host range (1). Many polyomaviruses are ubiquitous as shown by a high prevalence in their hosts.

Polyomaviruses are small non-enveloped double-stranded DNA viruses with an icosahedral capsid (T = 7 icosahedral symmetry) of about 45 nm (1-3). The outer capsid consists of 72 pentamers of the major capsid protein Vp1 (4, 5). On the inside, the minor capsid proteins Vp2, and also Vp3 for some polyomaviruses, connect the genome to the outer capsid. Their genomes are small, consisting of only about 5 kilobases with a common genome architecture consisting of three regions - two transcriptional regions, the early and the late region, and a non-coding control region (NCCR) (1, 2). Typically, the genome encodes at least four viral proteins – two regulatory Tumour (T-) antigens, the large (LTag) and small T-antigen (sTag), and two capsid proteins. Some polyomaviruses also encode additional viral proteins such as the agnoprotein and express different T antigen variants due to alternative splicing (1).

In 1953, the first polyomavirus, murine polyomavirus (MPyV), was discovered. It was detected as a filterable infectious agent in extracts of mouse leukaemia and tumours that could induce several types of tumours in inoculated mice (6, 7). As MPyV could induce multiple types of tumours, it was named polyoma meaning multiple tumours in Greek (8). In 1960, Simian virus 40 (SV40), the first primate polyomavirus, was discovered as a contaminant in poliovirus vaccines that had been produced in simian cell cultures that harboured SV40 (9). MPyV and SV40 have since their discovery been extensively studied, especially the ability of the T-antigens to immortalise cells and induce cancer in a range of hosts. Furthermore, SV40 has been utilised as a model for eukaryotic DNA replication due to its double-stranded genome and use of the cellular DNA polymerase for genome replication (10). Lastly, SV40 and MPyV have also been used as model viruses in animal models to better understand diseases caused by human polyomaviruses, such as BKPyV nephropathy and progressive multifocal leukoencephalopathy (11-14). Due to the many shared features of the polyomaviruses, our

understanding of specific polyomaviruses is based on studies performed with the specific polyomavirus and extrapolated from similar studies on other polyomaviruses. For instance, the SV40 LTag has been viewed as a prototypic LTag and much of our understanding of LTag is based on the SV40 LTag (15).

To date, there are 12 confirmed human polyomaviruses. The two first human polyomavirus, BK Polyomavirus (BKPyV) and JC Polyomavirus (JCPyV) were discovered in 1971 in a kidney transplant recipient with ureteric stenosis and a patient with progressive multifocal leukoencephalopathy, respectively (16, 17). Since then, ten additional human polyomaviruses have been described, including Merkel Cell Polyomavirus which cause Merkel Cell Carcinoma (18). Despite their shared traits when it comes to the capsid and genome structure, human polyomaviruses exhibit significant sequence diversity. Moreover, they display distinct host cell tropism and are associated with different pathologies (3).

1.2 BK Polyomavirus (BKPyV)

1.2.1 Virion structure and viral genome

BKPyV belongs in the *Betapolyomavirus* genus. The capsid consists of Vp1, Vp2 and Vp3 (Figure 1A) (4, 19, 20). Beneath each pentamer, a single copy of the minor capsid proteins, Vp2 or Vp3, is bound to the inside of Vp1 pentamers and to the genome (Figure 1B). The viral genome is complexed on host histone proteins (H2A, H2B, H3, and H4) and condensed in approximately 20 nucleosomes (21, 22). Both the N-terminal arm of Vp1 and the minor capsid proteins are associated with the packaged viral genome (4).

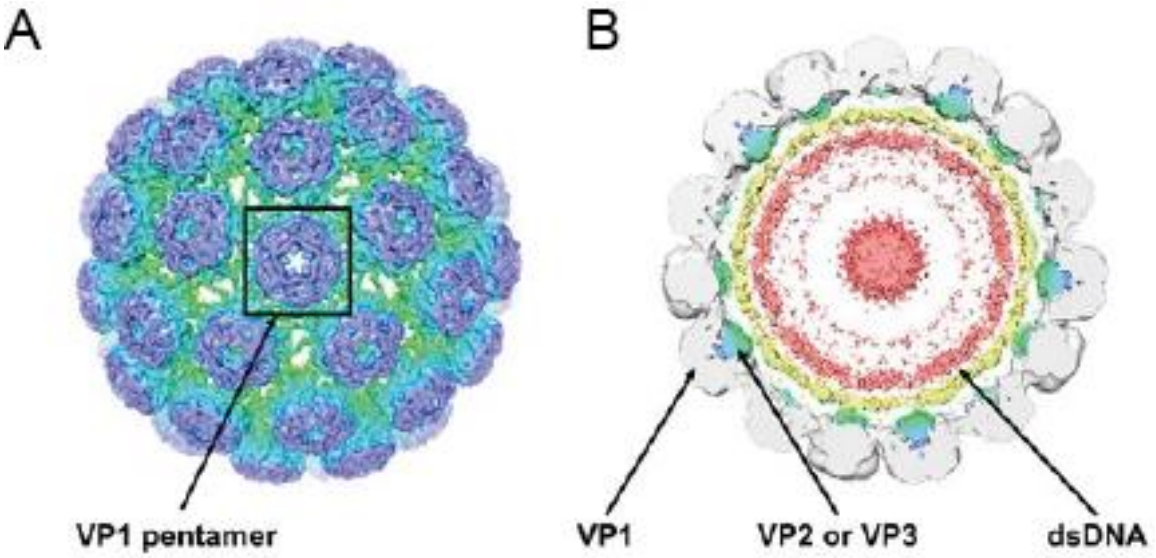

Figure 1: Structure of BKPyV capsid. A) External view of the BKPyV capsid which consists of 72 Vp1-pentamers with T = 7 icosahedral symmetry. The black box highlights a single Vp1-pentamer. B) 40-Å slab through the unmasked BKPyV capsid. Beneath the Vp1-pentamer, a blue/green pyramidal density representing Vp2/Vp3 is seen. The packaged double-stranded DNA is seen as two shells of electron densities adjacent to the inner capsid layer and is coloured yellow/pink. Reprinted from Helle et al. (23). The figure was originally adapted from Hurdiss et al. (4).

As previously mentioned, BKPyV has a double-stranded DNA genome of approximately 5000 bases (Figure 2A) (24). The early region of the BKPyV genome encodes the regulatory T-antigens - LTag, sTag (Figure 2A), truncated T-antigen (truncTag) and super T (25). Additionally, the early region encodes a pre-microRNA that is complimentary to the early viral mRNAs (26, 27). The late region encodes the capsid proteins, Vp1, Vp2 and Vp3, and the non-structural agnoprotein (2). A recent study analysing transcripts in BKPyV infected TERT-immortalised RPTECs with the use of short and long read RNA-sequencing technology, identified 21 to 23 transcripts of which only six were previously identified (25). Of note, both wraparound and non-wraparound transcripts were identified. The NCCR is a bidirectional regulatory region that separates the early and late region. It contains the origin of replication and the early and late promotors and enhancers. Transcription of the early and late region occur bidirectionally from the promotors and enhancers in the NCCR and uses the different DNA strands as template (2). Depending on its sequence, the NCCR is categorised as either an archetypal NCCR or a rearranged NCCR. The archetypal NCCR can be divided into five sequence blocks denoted the O-, P-, Q-, R and S-block, while rearranged-NCCRs have insertions, duplications and deletions in the sequence blocks (Figure 2B). The Dunlop variant

is an example of a rearranged variant that is widely used for *in vitro* experiments and has a NCCR where there are duplications of the P-box while the Q- and R-block is deleted (Figure 2B). As the NCCR regulate transcription of viral proteins and viral replication, rearrangements can affect the replication fitness of the virus. Archetypal strains are typically found in healthy individuals, while rearranged variants emerge in immunocompromised patients after extensive replication has occurred (2, 28-30).

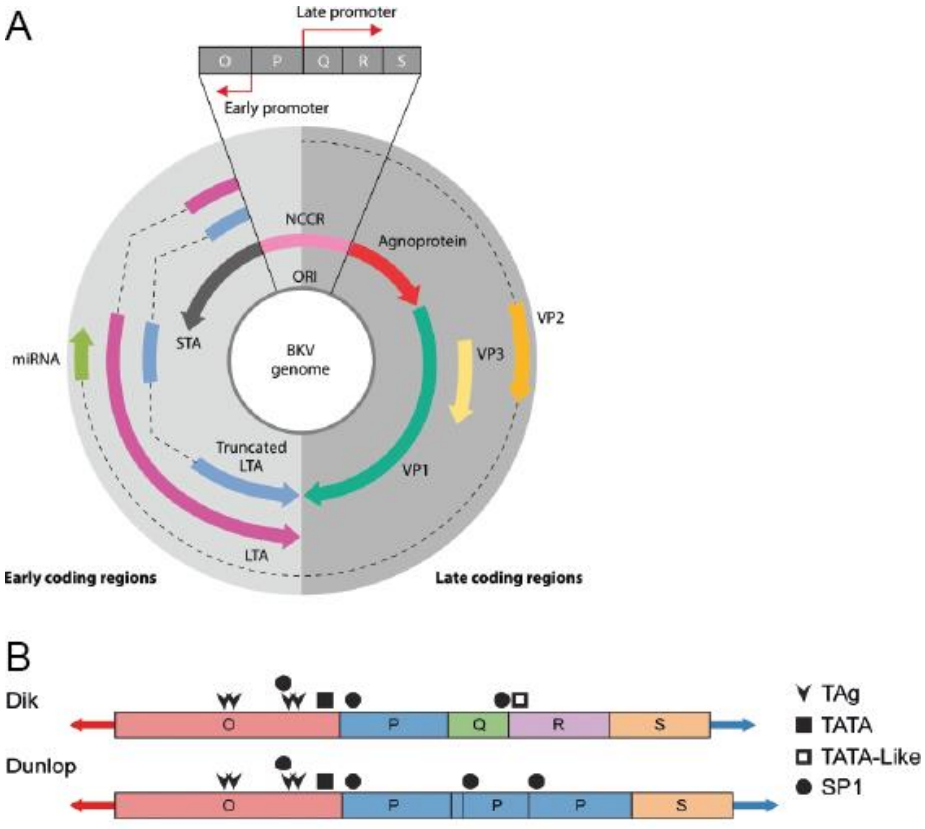

Figure 2: Genome of BKPyV. A) Diagram of the BKPyV genome. Reprinted from Ambalathingal et al. (31) with permission. Small T-antigen (STA), Large T-antigen (LTA), Truncated T-antigen (Truncated LTA). B) Diagram of archetype (Dik strain) and rearranged (Dunlop strain) NCCR. Reprinted from Zhao and Imperiale (28).

1.2.2 BKPyV proteins

The early T-antigens

The LTag of all polyomaviruses exhibit high sequence homology and contain conserved motifs and domains that are necessary for its functions (3, 15). The SV40 LTag is the prototypic LTag and much of our understanding of T antigens is derived from research on the SV40 LTag. The early regulatory T antigens are translated from individual mRNAs that are created by alternative splicing of the primary early mRNA transcript (15, 25). LTag is the major regulatory protein of all polyomaviruses, including BKPyV. It is a multifunctional protein that is essential for polyomavirus infection. In short, LTag both reprograms the host cell by forcing it into S-phase to promote viral DNA replication and it facilitates the replication of the viral DNA by binding to the viral origin of replication, unwinding the viral DNA and recruiting cellular proteins necessary for DNA replication, such as DNA polymerase α primase (3, 15). In addition, it prevents apoptosis.

The gene encoding BKPyV LTag consists of two exons separated by an intron and encodes an 80 kDa protein that consists of 695 amino acids (23). BKPyV LTag contains multiple conserved domains and motifs such as the J-domain, LXCXE-motif, nuclear localisation signal (NLS), origin-binding domain and the helicase domain (Figure 3) (3, 15). The J-domain is necessary for viral replication (3, 15, 32, 33). The LXCXE-motif allows LTag to bind the retinoblastoma-related tumour suppressor proteins, retinoblastoma protein (pRb), p130 and p107 (34, 35). Binding of LTag to retinoblastoma-related proteins break the interaction between these proteins and E2F transcription factors and drive unscheduled S-phase entry, increased cell proliferation and growth and may contribute to transformation (3, 15). Experimental studies have confirmed that the BKPyV LTag can bind and inactivate pRb-proteins to stimulate proliferation similar to SV40 LTag (36, 37). Additionally, the LXCXE-motif also participates in immune evasion by disrupting DNA sensing (38). Due to its NLS, LTag exhibit a nuclear location and it is in the nucleus where it executes most of its functions. The origin-binding domain is a DNA-binding domain that binds to the viral origin of replication by recognising and binding to the four GAGGC sequences that flanks the origin (15, 39). Via this interaction, LTag binds to the origin to initiate replication of the viral DNA. The helicase domain consists of a zinc-binding domain and an ATPase domain (15), where the zinc-binding domain contributes to the formation of the double LTag hexamer at the viral origin while the ATPase domain produces the energy that

drives helicase activity. In addition to its helicase function, the helicase domain can bind to and block the tumour suppressor p53 to hinder cell cycle arrest and apoptosis (15, 36).

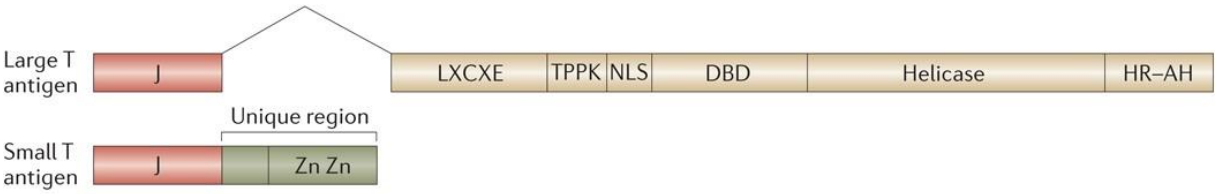

Figure 3 Diagram of the large T-antigen and small T-antigen. LTag contain a J-domain, LXCXE-motif, NLS, DNA-binding domain (DBD) also called origin-binding domain and aHelicase domain. sTag contains a J-domain and two zinc-fingers. Reprinted from DeCaprio and Garcea (3) with permission.

Due to alternative splicing of early mRNA, BKPyV express at least three other T-antigens – the sTag, truncTag and super T (2, 25, 40). The sTag is a 20 kDa protein that consists of an N-terminal J domain, that is shared with LTag, and a unique C-terminal region that resides in the intron of LTag (Figure 3)(3, 23). The C-terminal region contains two zinc fingers that are important to bind protein phosphatase 2A (PP2A) (3). The function of sTag is only partially understood. A recent report demonstrated that sTag negatively regulates virus replication (41) as removal of sTag lead to increased viral replication and gene expression. This regulation partially occurs via the interaction between sTag and PP2A. The authors also demonstrate that BKPyV sTag, unlike the sTag of Merkel cell polyomavirus and SV40 (42-44), is not important for transformation of cells (41).

TruncTag was first described in 2009 (40). It shares the first 133 amino acids with LTag, which contains the J domain, LXCXE-motif and NLS, except for the last valine residue of the NLS. Additionally, the TruncTag contains a second intron which causes a shift of translation into a different reading frame yielding a C-terminal with three unique amino acids. TruncTag is poorly characterised but it is located in the nucleus and has been proposed to deregulate cell growth and support transformation due to the J domain and LXCXE-motif (40). The previously mentioned transcriptomic study by Nomburg and colleagues (25) described additional polyomavirus early transcripts and ORFs. This includes the super T that contains two LXCXE-motifs. Although its function is unclear, it is expressed in BKPyV infected RPTEC-TERT cells and superT transcripts have been found in a BKPyV-associated urothelial carcinoma specimen (25).

The late capsid proteins

BKPyV encodes the three capsid proteins Vp1, Vp2 and Vp3. Vp1 is the major capsid protein and makes up the external capsid (23). Vp1 consists of 362 amino acids and has a size of approximately 42 kDa. Interaction with cellular receptors occurs via the receptor-binding groove that lies in the Vp1 pentamer (4, 45). Therefore, receptor usage and cell tropism of BKPyV is influenced by the Vp1 sequence (46-48). For instance, point mutations in the receptor binding site can switch BKPyV receptor specificity from B-series gangliosides to GM1 (48). The receptor-binding region of Vp1 also contains the epitopes that are responsible for antigenic determination and genotyping (49-51). There are four main genotypes of BKPyV, which each represent a serotype (47). Genotype I is the most abundant genotype (80%). Genotype IV is the second most prevalent (15%)(52), while genotypes II and III are rare. As genotype I and IV are geographically heterogenous, they have been further divided into subgroups. For genotype I there are the four subtypes (Ia, 1b-1, Ib-2 and Ic), while genotype IV is divided into six subtypes (Iva-1, Iva-2, Ivb-1, Ivb-2, Ivc-1 and Ivc-2) (51, 53). Subtype Ib-2 is the most common subtype in Europe (54, 55). The NLS of Vp1 leads to import of newly synthesised Vp1 into the nucleus, where viral assembly occurs.

Vp2 and Vp3 are the minor capsid proteins of BKPyV. They are internally located in the capsid, where one copy of Vp2 or Vp3 lies beneath each Vp1 pentamer (4). Vp2 consists of 351 amino acids and has a size of 38 kDa while Vp3 consists of 232 amino acids and has a size of 27 kDa. Vp2 and Vp3 are translated from the same transcript due to leaky ribosomal scanning and internal ribosomal entry sites upstream of Vp3, and therefore share a common C-terminus (56-58). The unique N-terminal of Vp2 contains an myristylation site that for MPyV was found to be necessary for correct viral entry (59). Furthermore, both Vp2 and Vp3 play a crucial role in correct viral entry and trafficking of BKPyV (56, 60) and other polyomaviruses, since removal of the minor capsid proteins perturb infectivity (61-66).

The late region contains additional open reading frames (ORFs) that potentially encodes the smaller proteins – Vp4, Vp5 and Vp6. Since the ORFs lie downstream and in frame of Vp2 and Vp3, the putative proteins are smaller proteins with a shared C-terminus with Vp2/Vp3 (56). The most studied of these is the putative protein Vp4. It has been proposed to be a viroporin as SV40 Vp4 supposedly could permeabilise membranes and was necessary for lytic release of SV40 (67-70). However, two other studies have demonstrated conflicting evidence. Henriksen et al. could not detect Vp4 in SV40 and BKPyV infected cells, and mutation of the Vp4 start

codon inhibited viral entry, not viral release (56). Similarly, Tange et al. (71) did not detect Vp4 and concluded that mutating the Vp4 ORF inhibited early steps in the replication cycle.

The late agnoprotein

Agnoprotein is expressed from an ORF in the late gene region region. Agnoprotein is a non-structural protein that consists of 66 amino acids with a size of 8 kDa (72). It is mainly detected in the cytoplasm of infected cells. Even though it only consists of 66 amino acids, the agnoprotein has several important functions. The N-terminal part of agnoprotein contains a mitochondrial targeting sequence while the middle region of the protein, amino acid 20-44, has the ability to form an amphipathic helix and interact with lipid droplets and intracellular membranes (73-75). The combination of the mitochondrial targeting domain of the N-terminal and the amphipathic helix allows agnoprotein to interact with and fragment the mitochondrial network to disrupt innate immune sensing (74).

In addition, agnoprotein have also been proposed to regulate the viral replication cycle and gene expression (29, 76), interact with cellular proteins (77, 78) and partake in virion assembly and egress (79-83).

1.2.3 BKPyV microRNAs

The BKPyV genome encodes a precursor microRNA (miRNA) in the early gene region on the DNA strand opposite of the LTag encoding DNA strand. The extended late transcripts produce precursor microRNAs that yields a 3p- and 5p-miRNAs that both are complementary to the LTag mRNA and cause reduced LTag expression (27, 84). These miRNAs are conserved and found in several other polyomaviruses, including SV40, JCPyV and Merkel Cell Polyomavirus (26, 27, 85). During infection with archetype BKPyV variants, microRNA expression leads to reduced viral replication and progeny production (84). In rearranged variants, where the early region is highly expressed, the amount of miRNA is insufficient to inhibit early gene expression and therefore has little effect on viral replication and progeny production (84).

Polyomavirus miRNA also protect infected cells from killing by cytotoxic T-cells and natural killer cells by downregulating T antigens and by reducing the expression of ULBP3, a ligand for the killer receptor NKG2D (26, 86).

1.2.4 Replication cycle

Attachment

The replication cycle of BKPyV (Figure 4) starts with attachment of the viral particle to the plasma membrane of a susceptible cell. Attachment occurs by binding of Vp1 to cellular receptors. As already mentioned, the entry tropism and receptor usage of BKPyV is determined by Vp1 and mutations in Vp1 can alter receptor usage (48, 87, 88). Sialylated gangliosides, specifically B-series gangliosides and α(2,3)-linked sialic acids were first identified as receptors for BKPyV, as BKPyV can bind to them and they are necessary for BKPyV entry (48, 87, 88). BKPyV binding to gangliosides is also necessary for BKPyV to haemagglutinate erythrocytes, a method used to quantitate viral particles (89). However, recent studies have demonstrated that BKPyV can use additional receptors for attachment, as ganglioside-deficient cells can be transduced with BKPyV. Moreover, the susceptibility of cells can vary between different BKPyV serotypes (47) and different BKPyV variants from kidney transplant patients show differential dependence on sialic acids, including sialic acid independent uptake (46).

Internalisation, intracellular transport and nuclear entry

Internalisation of BKPyV have been shown to occur via multiple endocytosis pathways. Initially, BKPyV was shown to enter simian Vero cells and human proximal tubular epithelial cells (RPTECs) by caveolae-mediated endocytosis (90, 91). However, a recent study reported that BKPyV can enter cells via a caveolin- and clathrin-independent entry mechanism (92). Similar results have also been demonstrated for SV40 (93-95).

After internalisation, the viral particle is transported to the endoplasmic reticulum (ER) (96-98). Early entry and trafficking steps depend on an intact microtubule network and correct acidification of organelles and endosomes (96, 97), while dynein and actin are not necessary (97, 99). Transport of the viral particle to the ER most likely occurs via the endocytic pathway as BKPyV has been shown to co-localise with Rab18 and BKPyV accumulates in late endosomes if ER-delivery is perturbed (98). Moreover, other polyomaviruses utilise endocytic pathways for ER-delivery. SV40 is transported to the ER via Rab5- and Rab7-positive endosomes while MPyV rely on Rab5, Rab7 and Rab11 for ER-delivery (100-103). BKPyV arrives in the ER at approximately 8 to 10 hours post-infection (97).

The role of the ER and subsequent nuclear entry of BKPyV is poorly characterized and our current understanding of this is mostly based on studies with SV40. First, ER-resident redox proteins such as protein disulfide isomerase, Erp57 and Erdj5, facilitate partial uncoating and disassembly of the SV40 viral particle by disrupting the disulfide bonds of the capsid (62, 66, 104-108). After partial uncoating, the SV40 viral particle inserts into the ER-membrane to form an ER-foci or exit site which the viral particle is ejected through to the cytosol. To facilitate formation of the exit site and insertion, SV40 hijacks a range of host proteins such as BiP, BAP31, DNAJ-proteins, Lunapark and Atlastin (61, 62, 66, 104, 106, 108-111). In the cytosol, the SV40 particle undergoes further disassembly to prepare the capsid for nuclear entry (112).

ER-processing and -exit of BKPyV is poorly understood, but parts of the process have been characterised in RPTECs infected with BKPyV. This has revealed that the BKPyV capsid also undergoes rearrangements and partial uncoating in the ER. The proteasome and the ER-associated degradation (ERAD) pathway may partake in this process (60, 96). After partial uncoating, the viral particle most likely translocates from the ER to the cytosol by interacting with the ERAD-protein Derlin-1 (60, 96). The shared features of SV40 and BKPyV and the similar experimental evidence of disassembly in the ER followed by translocation into the cytosol (60, 96), support that BKPyV undergoes a similar process in the ER as SV40.

As a DNA virus, BKPyV must deliver its viral genome into the nucleus of the host cell to replicate. Nuclear delivery of BKPyV is poorly characterised, but one study proposed that after translocation into the cytosol, BKPyV may enter the nucleus via an interaction between the NLS of the capsid proteins and importin β1 (113). This is further supported by studies on SV40, which have linked importins and the nuclear pore complex proteins to nuclear entry (114-116). Spriggs et al. recently proposed that SV40 first engage nesprin-2, which positions SV40 close to the nuclear pore complex, allowing it to bind SV40 and facilitate nuclear entry (114). Nuclear entry during nuclear envelope breakdown has been proposed as an alternative to import via the nuclear pore complex (117). For BKPyV, alternative nuclear entry pathways may exist as knockdown of importin β1 only partially inhibits BKPyV infection (113).

Gene expression and genome replication

Our understanding of BKPyV gene expression and genome replication is derived from studies on both BKPyV and SV40. Immediately after nuclear entry, gene expression is initiated by expression of the early viral genes. As mentioned, the early gene expression is driven by the

early promoter in the NCCR, leading to expression of a single primary early transcript which gives rise to the T-antigens (2, 23).

Genome replication is initiated directly after translation of the early regulatory T-antigens. LTag is essential for BKPyV genome replication. It both prepares the cell for viral DNA replication by causing early S-phase entry and it binds to the origin of replication in the NCCR. At the origin of replication, it unwinds the double-stranded viral DNA in both directions and recruits the cellular DNA polymerase complex required for replication. DNA synthesis occurs bidirectionally from the origin of replication (10, 118-121). Viral DNA replication leads to activation of the ataxia telangiectasia mutated (ATM)- and the ATM- and Rad3-related (ATR)-mediated DNA damage response (DDR) (122, 123). This response facilitates viral DNA replication as both knockdown of ATM/ATR and treatment with ATM- or ATR-inhibitors lead to reduced viral replication and reduced levels of progeny virus (122, 124). Activation of ATM and ATR facilitates viral replication by extending the S-phase, the cell cycle phase where viral replication occurs, and by inducing G2-arrest to prevent mitotic entry (122-125). Without this response, the cell enters premature mitosis causing reduced viral replication and severe chromosome damage (122-124).

After viral DNA replication is initiated, the late mRNAs are expressed and the structural capsid proteins and the non-structural agnoprotein are translated.

Assembly and virus release

The capsid proteins are imported into the nucleus via the NLS. In the nucleus, progeny viruses are formed by assembly of capsid proteins into capsids, each with a newly synthesised viral genome complexed with cellular histones (20, 21, 126). Progeny viruses accumulate in the nucleus, often arranged in a crystalline array pattern (127), leading to an enlarged nucleus with intranuclear inclusion bodies.

BKPyV host-cell release is poorly understood but the current dogma is that lytic release is the main mechanism. This is supported by studies on kidney biopsies from patients with BKPyV nephropathy, which have shown BKPyV infected cells with a necrotic morphology and extensive lysis (127, 128). Furthermore, BKPyV infection of both primary human renal epithelial cells and urothelial cells lead to loss of plasma membrane integrity and cell death with a necrotic morphology (129-132). The mechanism behind the lytic release of BKPyV is unknown. One suggestion is that the nuclear accumulation of progeny virus cause swelling of

the nucleus which leads to lysis of the nuclear envelope and the host cell (118). An alternative theory is that agnoprotein, in addition to disrupting immune sensing, acts as a viroporin and promotes lysis of the host cell. This is supported by studies on both BKPyV and JCPyV agnoprotein, which reported that agnoprotein have pore forming activity and that mutant viruses without agnoprotein have reduced progeny release (79, 81, 133, 134).

Non-lytic BKPyV release has been proposed as an alternative egress pathway for BKPyV. First, a study proposed that a small proportion of progeny BKPyV undergo non-lytic egress via endosomal/lysosomal compartments which can be inhibited by the chloride channel inhibitor 4,4′-diisothiocyano-2,2′-stilbenedisulfonic acid (DIDS) (135). Recently, non-lytic release of BKPyV via extracellular vesicles (EVs) was proposed as well (136). Non-lytic release has also been proposed for both SV40 and JCPyV. JCPyV seems to be released in EVs via secretory autophagy or exosome-related pathways, and this protects JCPyV from neutralising antibodies (137-139). Studies on SV40 in a polarised simian cell line, demonstrated directional virus release before cell lysis could be detected (140).

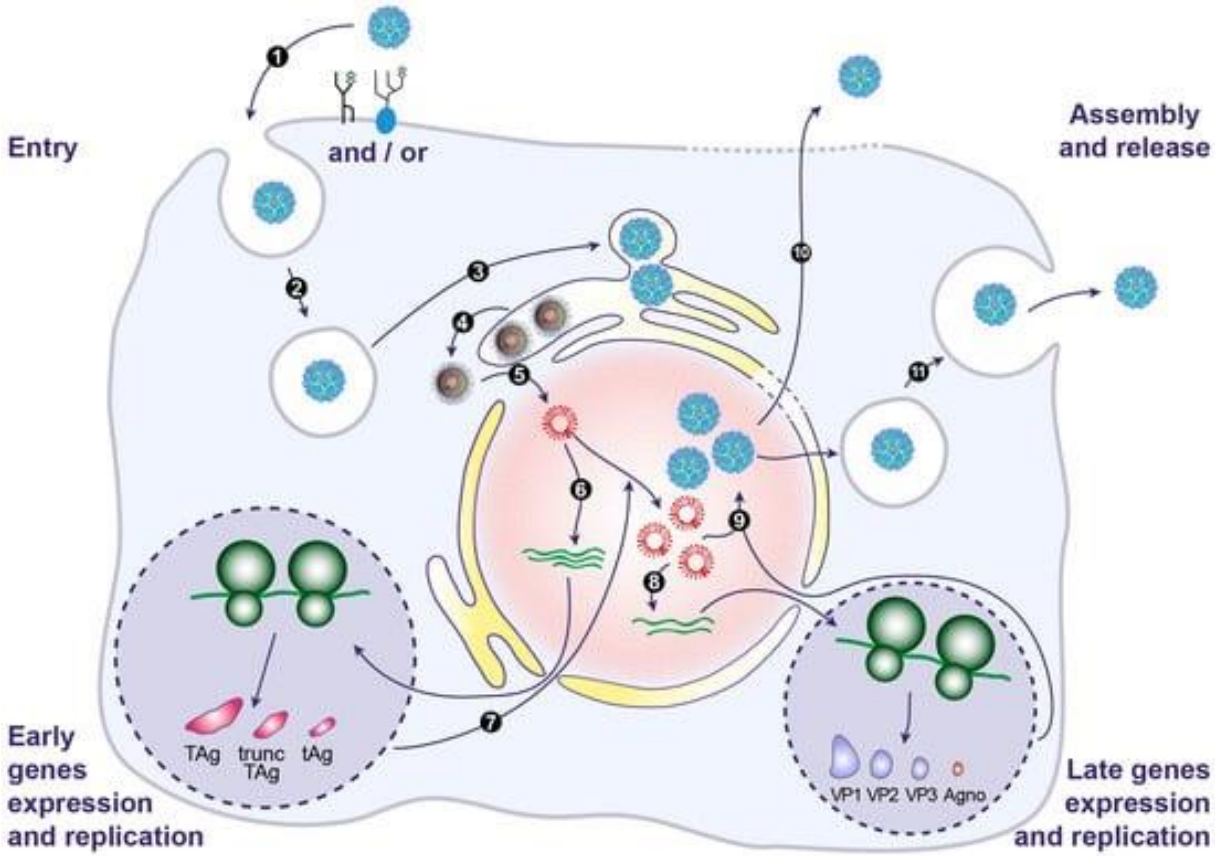

Figure 4: Schematic presentation of the replication cycle of BKPyV. 1) BKPyV binds to ganglioside receptors on the cell surface before it is internalised. 2) BKPyV enters endosomes. 3) Transport to the ER via endosomes. 4) Partial uncoating of the BKPyV capsid in the ER. 5) Nuclear entry. 6) After nuclear entry, the early genes are expressed. After translation, the early proteins are translocated into the nucleus where they initiate viral DNA replication. 8) The late gene region, encoding capsid proteins and agnoproteins, is immediately expressed after viral DNA replication is initiated. 9) After translation in the cytoplasm, the capsid proteins are imported into the nucleus where the viral DNA is packaged into self-assembling capsids. Progeny virus is released via host cell lysis (10) and possibly via a supplemental uncharacterised non-lytic egress pathway (11). Reprinted from Helle et al. (23).

Disruption of immune sensing

Human cells express pattern-recognition receptors, such as toll-like receptors, to sense viruses and initiate a protective response in the face of virus infection. The typical response after recognition of a viral structure, for instance viral DNA, RNA or proteins, is induction of an interferon- or anti-viral response (141, 142). To evade this response, viruses have developed mechanisms to either avoid sensing or disrupt the immune response. Proteomic and genomic studies on BKPyV infected RPTECs have detected little to no changes in expression of proteins and genes related to immunity and anti-viral responses (125, 132, 143-146), indicating that BKPyV avoid immune sensing.

Recent studies have identified multiple mechanisms BKPyV and other polyomaviruses utilise to evade immune detection. MPyV delay immune sensing by being transported to the nucleus in endosomes, as the interferon response is first induced after nuclear delivery and viral replication is initiated (147). Another related DNA tumour virus, human papillomavirus 16, evade immune sensing by the cyclic GMP-AMP synthase/stimulator of interferon genes (cGAS/STING) pathway by being transported to the nucleus via the Golgi hidden in vesicles (148). Since BKPyV is trafficked to the ER inside vesicles and endosomes, it is likely that BKPyV uses a similar strategy to avoid early immune sensing. SV40 LTag can inhibit immune sensing of SV40 DNA as the LXCXE motif antagonises the cGAS-STING-pathway (38). As BKPyV LTag contains an identical LXCXE motif, it is likely that it can also antagonise the cGAS-STING pathway. Work on JCPyV and BKPyV sTag have identified sTag as an interferon-antagonist that inhibit retinoic acid-inducible gene 1, an innate immunity RNA sensor (149). In addition, the late agnoprotein antagonises immune detection by disrupting the mitochondrial network leading to mitophagy and degradation of mitochondrial antiviral-signalling protein (74). This leads to an attenuated interferon-response and increased viral replication. Lastly, BKPyV encodes a miRNA that inhibits expression of ULBP3, a stress-induced ligand for natural killer cells, leading to reduced killing of infected cells *in vivo* (86). To summarise, BKPyV seemingly employs multiple mechanism to avoid immune sensing at different steps of the replication cycle.

1.2.5 BKPyV – persistent infection and disease

Definitions of BKPyV infection, replication and disease

BKPyV is ubiquitous and infects the majority of the global population as shown by a seroprevalence in adults ranging from 80 to over 90% (150-154). In humans, the virus appear in different states depending on individual factors (155). It is often in a latent or persistent state without active replication, for instance in an infected cell harbouring only the BKPyV genome. Alternatively, the virus can be replicating, defined as ongoing multiplication, with asymptomatic shedding in the urine. Lastly, in some immunocompromised patients lasting and high-level uncontrolled replication can cause disease. In a review, Hirsch and Steiger proposed the following definitions (155):

- BKPyV infection is defined as exposure to BKPyV. It can be shown by detection of the virus itself or viral DNA in urine or by evidence of previous exposure, for instance the presence of BKPyV-specific antibodies. This state does not differentiate between a latent non-replicating state and active replication, but rather states that an individual has been exposed to BKPyV.
- BKPyV replication is defined as ongoing multiplication of the virus. Examples of signs of viral multiplication include detection of infectious virus and increasing levels of BKPyV DNA or proteins.
- BKPyV disease is defined as organ damage secondary to BKPyV replication.

BKPyV in immunocompetent individuals

Primary infection is thought to occur during childhood as the seroprevalence of BKPyV increases markedly during the first years of life (156, 157). At the time of late childhood and adolescence the seroprevalence is around 80-90% (158, 159). The route of transmission for primary infection is unknown, but respiratory transmission has been proposed due to detection of BKPyV DNA and seroconversion in children with respiratory symptoms (160). Furthermore, salivary shedding of BKPyV has been described in healthy adults (161). Urinary shedding might be a source for oral transmission. During or after the primary infection, BKPyV somehow reaches the reno-urinary tract where it persists in epithelial cells (162-164). In healthy individuals, BKPyV will be intermittently shed in the urine but this does not cause any symptoms or disease (150, 165-167). In a cross-sectional study of 400 blood donors by Egli et al. (150), 7% of the participants excreted BKPyV in the urine. Similar results were found in

healthy adults in Tunisia where 6% had urinary shedding of BKPyV (168). Kling et al. (166), Polo et al. (165) and Urbano et al. (167) measured a higher BKPyV excretion prevalence in healthy adults of 12%, 15.7% and 22.5%, respectively. Furthermore, they noted a large day-to-day variability and occasional excretion was more common than continuous excretion. During pregnancy, urinary excretion of BKPyV is increased due to altered immune function (169). BKPyV DNAemia is seldom observed in healthy individuals. In Egli et al., none of the 28 blood donors with BKPyV DNA in urine had BKPyV DNA in plasma (150). Similar results were obtained in 1014 Dutch blood donors where only one participant had detectable BKPyV DNA in serum, showcasing how rare BKPyV DNAemia is in healthy individuals (170).

BKPyV nephropathy

Background, aetiology and pathogenesis

Solid organ transplant recipients, including kidney transplant recipients, must use immunosuppressive drugs to avoid immunological rejection of the allograft. A drawback of the immunosuppressive treatment is an increased risk of bacterial, fungal and viral infections, including BKPyV (171). BKPyV reactivation and replication is more common in kidney transplant recipients compared to healthy individuals (172). Replication of BKPyV in kidney transplant patients is a continuum and can have several outcomes, depending on the level of replication (172). Limited or low-level BKPyV replication only leads to low-level BKPyV viruria without or with low-level BKPyV DNAemia and does not affect allograft function. Summarised, 20 – 73% of kidney transplant recipients will develop BKPyV viruria or shed decoy cells while 8 – 62% will develop BKPyV DNAemia (31, 172). If BKPyV replication continues unchecked, patients can develop BKPyV disease, namely BKPyV nephropathy, previously called BK polyomavirus-associated nephropathy.

BKPyV nephropathy is a serious medical condition that reduce allograft function and can even cause premature allograft loss. BKPyV nephropathy emerged in the late 1990s after more potent immunosuppressive regimens with tacrolimus and mycophenolic acid were implemented for kidney transplant recipients (158, 173, 174). Today, 1 – 15% of kidney transplant recipients develop BKPyV nephropathy (172). BKPyV nephropathy commonly debuts the first year after transplantation (155), but up to a third of cases occur after the first year post-transplantation (175). The condition is characterised by uncontrolled BKPyV replication in the tubular epithelial cells of the allograft, leading to cytopathic loss of these cells. Histologically, infected renal tubular epithelial cells display cytopathic changes such as enlarged nuclei and intranuclear

inclusion bodies (127, 128, 176). Tubule cells with nuclear inclusions frequently display a necrotic morphology. Furthermore, infected renal tubule epithelial cells are frequently shed into the tubular lumen leading to tubular clogging and extensive urinary shedding of decoy cells (127, 128). Shedding and loss of tubule epithelial cells eventually causes denudation of the basement membrane and BKPyV DNAemia due to leakage of viral DNA into the plasma (128, 177). Allograft tubulointerstitial inflammation is another typical finding in biopsies from patients with BKPyV nephropathy (128, 176, 178). Intragraft inflammation has been linked with increased risk of reduced allograft function and ultimately loss, although the exact role of intragraft inflammation in BKPyV nephropathy is still unclear (179). Over time, uncontrolled BKPyV replication with accumulating tubule epithelial cell loss and inflammation eventually leads to tubular atrophy, interstitial fibrosis and reduced allograft function (128, 180, 181). Ultimately, the allograft can be lost and re-transplantation or return to dialysis will be necessary (172).

Immune response to BKPyV replication and nephropathy

Kidney transplant recipients with BKPyV replication typically show increased titres of BKPyV-specific antibodies. The antibody level correlates with BKPyV exposure and replication as patients with uncontrolled replication and high-level BKPyV DNAemia develop higher antibody titres than patients with limited replication (182-190). The role of BKPyV-specific neutralising antibodies in controlling active BKPyV replication and viral clearance is conflicting. Solis et al. (185) found that a weak neutralising antibody response were associated with increased risk of BKPyV DNAemia and nephropathy, while high titres were associated with viral clearance. Another study reported a similar finding where development of BKPyV-specific antibodies was linked to viral clearance (191). However, other studies have demonstrated that humoral immunity with BKPyV-specific antibodies offer incomplete protection against BKPyV and while BKPyV-specific antibodies may help contain BKPyV, it is not enough to clear the virus (182, 190, 192, 193).

Reduced BKPyV-specific cellular immunity, due to immunosuppressive drugs, is a prerequisite for loss of immune control of the virus, leading to uncontrolled replication and development of BKPyV disease (194). BKPyV-specific cellular immunity has therefore been extensively studied in an effort to better understand the interplay between cellular immunity and BKPyV, and why some patients fail to control replication. This has revealed that high levels of BKPyV-specific T-cells and a robust T-cell response are associated with viral clearance (190, 192, 193,

195-199). Cytotoxic CD8 T-cells are an important subset of T-cells that can kill infected cells and thus help clear infections. For BKPyV, increasing CD8 T-cell responses seem to be especially important for viral clearance (190, 198, 200, 201), while expression of exhaustion markers is associated with slower clearance and prolonged BKPyV DNAemia (202) and BKPyV nephropathy (201).

Risk factors

Risk factors for BKPyV DNAemia and nephropathy can be separated into donor factors, recipient factors and transplantation factors (155, 172). Recipient factors include male sex, old age, no prior exposure to BKPyV and protective HLA-classes, such as HLA-B7, while male donor is a donor risk factor. Transplantation factors linked to increased risk of BKPyV nephropathy include use of tacrolimus compared to cyclosporine, high dose corticosteroids, acute rejection, AB0-incompatiblity and ureteral stents.

Many important donor and recipient factors are related to the interplay between donor and recipient. BKPyV serostatus and levels of BKPyV-specific antibodies in donor and recipients have been identified as risk factors for developing BKPyV DNAemia and nephropathy (172, 194, 203). Specifically, transplantation of a renal allograft from a seropositive donor to a seronegative recipient is associated with increased risk of BKPyV DNAemia and nephropathy (187, 204-206). Moreover, there is limited cross-reactivity between different BKPyV serotypes and genotypes (47, 207). Therefore, serotype or genotype mismatch increase the recipient risk due to reduced titres or complete lack of neutralising antibodies against the BKPyV genotype in the allograft (185, 208). Increased risk for BKPyV replication has also been found in recipients with low titres of BKPyV-specific antibodies at the time of transplantation (182, 185, 187, 190, 209).

The donor's pre-transplant titre of BKPyV-specific antibodies alone is also of interest as a high titre in the donor is associated with increased risk of BKPyV replication and disease (182, 187, 210). A theory behind this is that the titre of BKPyV-specific antibodies is directly linked to ongoing replication or exposure to BKPyV. Consequently, the donor antibody titre represents the viral load in the transplanted allograft. A kidney from a donor with a high BKPyV-specific antibody titre potentially has a higher BKPyV load or even ongoing replication, leading to increased risk of BKPyV replication and disease. Similarly, active BKPyV replication in the donor is also a risk factor for BKPyV replication in the recipient (211-213). Antibody titres in the donor and recipients can be viewed together and the combination of a low titre in the

recipient and a high titre in the donor or seropositive donor and seronegative recipient is associated with increased risk of BKPyV DNAemia. Wunderink et al. found a 10-fold increase for BKPyV DNAemia in low titre recipients that received a kidney from a high titre donor (187).

Diagnostics

Quantitative nucleic acid testing

BKPyV replication and BKPyV nephropathy causes no symptoms until severe organ damage has occurred. International guidelines therefore recommend active screening of kidney transplant recipients for BKPyV replication (172). Quantitative detection of BKPyV DNA with quantitative real-time polymerase chain reaction (qPCR) is the preferred molecular diagnostic tool for this. Alternatively, BKPyV qPCR on urine can be performed if blood sampling is not possible. Urine cytology to screen for decoy cells is only recommended if BKPyV qPCR is not available. Screening should be performed monthly the first nine months after transplantation, followed by screening every three months until two years post-transplantation (172).

Immunological methods

Cellular immunity is typically measured directly in isolated peripheral blood mononuclear cells or after pre-stimulation with BKPyV peptides and short-term expansion (172). The read-out is typically based on presenting viral peptides to the cells and then measuring T-cell activation. A variety of read-outs can be used, such as interferon-gamma, tumour necrosis factor-alpha, interleukim-2 and proliferation markers.

BKPyV-specific antibodies can be measured with several different serological methods such as haemagglutination inhibition assay (HIA), neutralisation tests and enzyme-linked immunosorbent assay (ELISA) based on virus-like-particles or Vp1-fusion proteins (Figure 5) (194). For viruses that agglutinate red blood cells (RBCs), such as influenza virus and BKPyV, HIA can be utilised (214). When RBCs are incubated in a round-bottom plate, the RBCs will sediment in the bottom of the well leaving a characteristic red dot. The virus inhibits sedimentation by binding to sialic acid receptors on the surface of the RBC leading to a network of interconnected RBCs and virus that reduces sedimentation. Instead of a red dot, a foggy red cloud is seen in the well. In the HIA, the virus is preincubated with a dilution of an antibody or serum and if this serum contains antibodies that bind BKPyV, the network of RBCs and virus will not be made allowing RBCs to sediment. Pseudovirus, virus-like-particles (VLPs) and

infectious virus can all be utilised for HIA since the interaction with the RBCs is mediated by the outer virus capsid.

Indirect ELISA is the most common method to detect and measure antibodies against virus and other pathogens in serum. In short, microtiter plates are first coated with the antigen of choice. For polyomaviruses, Vp1 is the most used antigen (172) and it is typically used as a Vp1-fusion protein (208, 215) or a Vp1-derived VLP (154, 207). Next, a diluted serum sample is incubated in the wells, and this is followed by incubation with an enzyme-conjugated secondary antibody that is specific to the Fc fragment of the antibody one wants to detect. Lastly, a chromogenic substrate is added and if the secondary antibody is bound to the BKPyV-specific antibody, it will convert the substrate into a coloured product. The colour change can then be measured to quantify the antibody titre (214). Indirect ELISAs can also be bead-based where magnetic beads are coated with the antigen instead of microtiter plates.

Another way to measure the level of neutralising antibodies are neutralisation tests. In short, the virus or VLPs are preincubated with serial dilutions of serum or an antibody for a given time before infection of cells are performed. Successful infection or transduction is typically used as the assay output. This can either be done by using a packaged reporter gene, for instance GFP or luciferase (207, 216, 217), or by assessing virus replication by plaque formation or by detection of virus proteins with immunofluorescence staining (209, 218, 219). VLPs or pseudovirus are typically used if a packaged reporter gene is used for readout, while infectious virus is used if the output is viral replication. The neutralisation titre is defined as the highest dilution that inhibits the readout with 50% or 90%. Due to being more resource demanding than HIA and ELISA, neutralisation assays are less used.

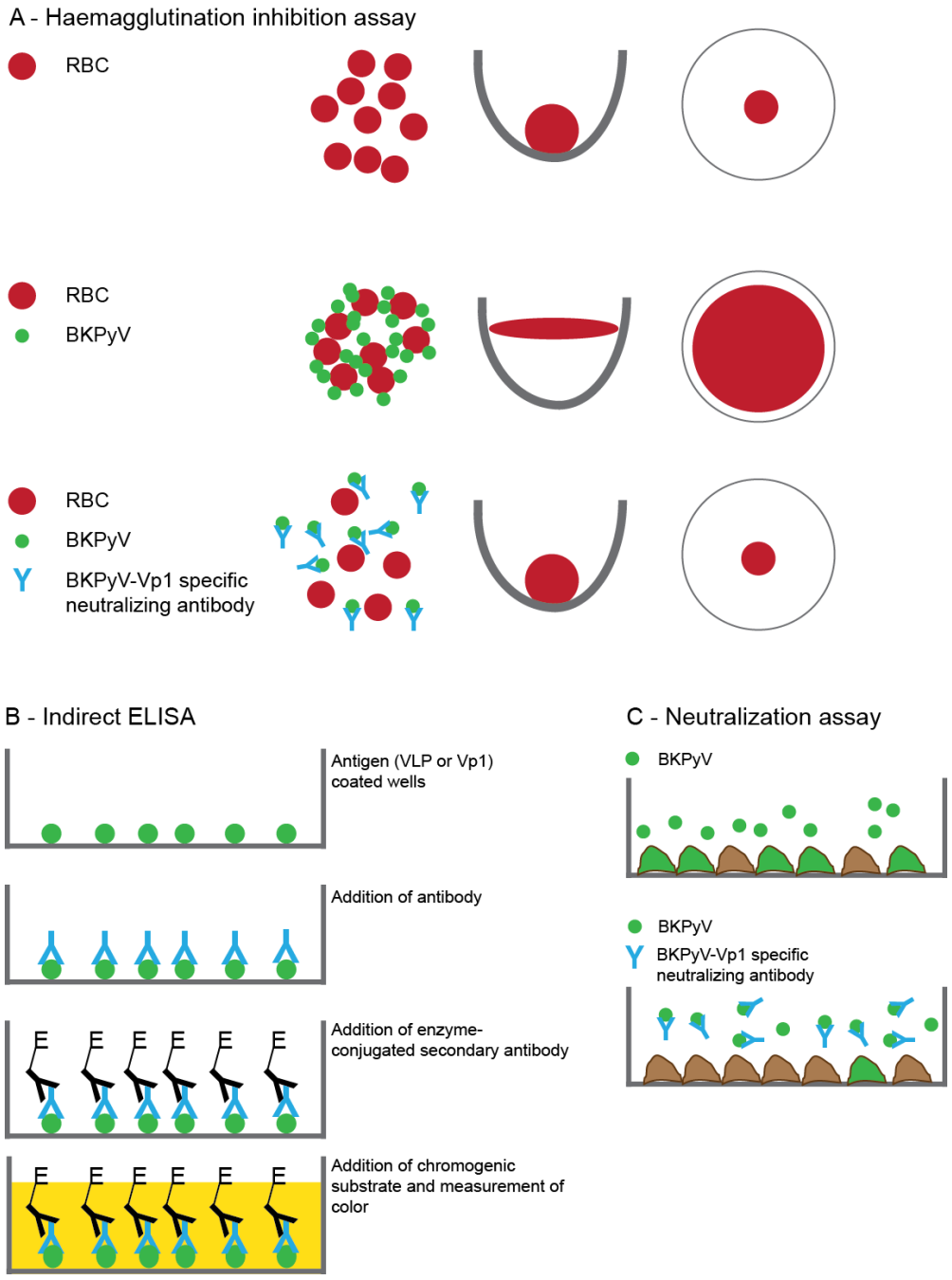

Figure 5: Haemagglutination inhibition assay, indirect ELISA and neutralisation assay. A) Haemagglutination inhibition assay. Top) RBCs incubated alone leads to sedimentation. Middle) RBCs and BKPyV leads to agglutination of RBCs. Bottom) Addition of neutralising antibodies inhibit BKPyV from agglutinating RBCs, causing sedimentation of RBCs. B) Microtiter plates are first coated with the antigen of choice – typically VLPs or Vp1 fusion-proteins. Next, serum is added. If BKPyV-specific antibodies are present, they will bind to the antigen. Next, an enzyme-conjugated secondary antibody that binds to the primary antibody is added. Lastly, the chromogenic substrate is added, and colour develops and can be measured. C) Diagram of a neutralisation assay with BKPyV-pseudovirus that carries an eGFP-plasmid. Top) Without antibodies present, the BKPyV-pseudovirus can infect the cells, leading to expression of eGFP. Bottom) Neutralising antibodies bind the BKPyV-pseudovirus and inhibit virus infection. Due to inhibition of infection, fewer green cells are detected.

Histology

Renal allograft biopsies are important for assessing allograft function and inform important treatment decisions in kidney transplant patients. Histological and immunohistochemical investigation of renal allograft biopsies were essential to identify BKPyV nephropathy as a new complication in kidney transplant recipients in the 1990s (173, 220). Due to this, diagnosis of BKPyV nephropathy was for several years dependent on detection of cytopathic effects and viral foci in renal allograft biopsies. However, renal allograft biopsies are no longer necessary as plasma BKPyV DNA can be used as a biological marker of BKPyV nephropathy (172, 221). BKPyV DNA in plasma is derived from active viral replication in the allograft as removal of the allograft leads to rapid reduction in plasma BKPyV DNA load (222, 223). Moreover, BKPyV nephropathy is a focal disease leading to discordant results in up to 30% of biopsies from patients with BKPyV DNAemia (179, 224). Limiting BKPyV nephropathy to biopsy-proven BKPyV nephropathy would both delay diagnosis and lead to false negatives, which again would delay treatment. BKPyV DNAemia is therefore not an indication for renal allograft biopsy alone and presumptive BKPyV nephropathy can be diagnosed without a renal allograft biopsy. However, renal allograft biopsies are still generally recommended in kidney transplant patients when clinically indicated or to investigate differential diagnoses (172).

Diagnostic criteria

Summarised, the diagnosis of BKPyV nephropathy is stratified into four different levels based on BKPyV DNA loads in plasma and urine, and biopsy results (172):

- Possible BKPyV nephropathy: high-level urine BKPyV loads defined as urinary BKPyV DNA load $>10^7$ copies/ml or decoy cells without detectable BKPyV DNAemia.
- Probable BKPyV nephropathy: sustained plasma BKPyV DNA load $>10^3$ copies/ml for over two weeks.
- Presumptive BKPyV nephropathy: plasma BKPyV DNA load $>10^4$ copies/ml.
- Biopsy-proven BKPyV nephropathy: biopsy with viral cytopathic effects as well as positive polyomavirus immunohistochemistry in combination with a specific test for BKPyV.

Treatment

Unfortunately, there is no efficient anti-viral therapy for BKPyV replication and nephropathy. The main treatment is reduction of the immunosuppressive drugs to promote viral clearance by

the immune system (172). Prompt reduction of immunosuppressive treatment is recommended in all patients with presumptive and biopsy-proven BKPyV nephropathy, while it can be considered for probable BKPyV nephropathy after thorough assessment.

Currently, multiple investigational therapies are being studied in clinical trials and laboratory experiments. This includes monoclonal antibodies against Vp1 and allogeneic virus-specific T-cells. In a phase 2 trial of kidney transplant recipients with high-level BKPyV DNAemia, treatment with a monoclonal Vp1-antibody was safe and was associated with a more rapid reduction in plasma BKPyV DNA load (225). Similarly, intravenous immunoglobulins (IVIGs), have been shown to neutralise and reduce spread of BKPyV *in vitro* (217, 226-228). Moreover, a recent meta-analysis concluded that reduction of immunosuppression in combination with intravenous immunoglobulins (IVIGs) offered additional benefit compared to reduced immunosuppression alone (229). However, the results must be carefully interpreted as the analysed IVIG studies were case series or retrospective studies. Since IVIGs are generally well tolerated and may have benefit, it can be considered for adjunctive treatment (172). Allogeneic virus-specific T-cells is a potential novel therapy against BKPyV replication. However, it has mostly been studied in the context of BKPyV-associated haemorrhagic cystitis (BKPyV-HC) in haematopoietic stem cell (HSCT) patients (230, 231). In a case report the BKPyV DNA load of a female kidney transplant recipient was reduced after T-cell adoptive immunotherapy (232). In another case series of two paediatric kidney transplant recipients, BKPyV DNAemia was reduced or cleared after virus-specific T-cell therapy. Lastly, a range of FDA-approved drugs, such as cidofovir, brincidofovir, leflunomide and levofloxacin, have been investigated in retrospective trials and clinical trials, but without convincing effect. Thus, they are not recommended for treatment of BKPyV replication or nephropathy (172, 229, 233).

BK Polyomavirus-associated haemorrhagic cystitis (BKPyV-HC)

Haemorrhagic cystitis (HC) is a serious complication of HSCT that is characterized by a painful and bleeding cystitis (234, 235). HC is split into two types – early and late onset HC. Early onset HC occurs due to toxic effects of the conditioning treatment on the bladder urothelium. It debuts within 1 week of HSCT and must occur during or shortly after (<48 hours) the conditioning treatment. Late onset haemorrhagic is a multi-factorial disease that is related to severe immune dysfunction due to HSCT, toxic damage to the urothelium and reactivation of BKPyV (234-237). Other viruses can also play a role in late onset HC, but BKPyV is the most common (236, 238, 239). Over 80% of HSCT patients develop high-level BKPyV viruria, while

7 to 54% develop BKPyV-HC. In paediatric HSCT patients, 8 to 25% develop BKPyV-HC (234).

BKPyV-HC typically occurs between two and eight weeks after transplantation, although cases has been described as late as six months after transplantation (234). Symptoms typically lasts two to four weeks but can in some cases last much longer (239). Patients presents with haematuria, urinary blood clots and symptoms of cystitis such as dysuria, increased urgency, pain in the lower abdomen or suprapubic region and urinary obstruction (239). The diagnosis is based on a diagnostic triad with symptoms of cystitis, haematuria (grade 2 or higher) and BKPyV viruria > 7 $\log^{10}$ copies/ml (234). The pathogenesis of BKPyV-HC is poorly understood but it is believed to be caused by a combination of BKPyV reactivation due to iatrogenic immune dysfunction and urothelial damage caused by the conditioning regimen (155, 234). Important risk factors includes high-level BKPyV viruria, allogeneic HSCT, haploidentical donor, graft-versus-host disease and cyclophosphamide treatment (234).

Like for BKPyV nephropathy, there is no effective anti-viral treatment for patients with BKPyV-HC either (234, 240). Intravenous cidofovir treatment has shown possible benefit in some retrospective and prospective trials but has not been investigated in a randomised clinical trial and use of it is therefore controversial. Due to lack of anti-viral therapies, supportive treatment such as pain treatment, bladder irrigation, hyperhydration, erythrocyte and platelet transfusions are used (234). Infusion of virus-specific T-cells have shown promise in HSCT-patients with BKPyV-HC and/or BKPyV DNAemia. A phase 2 trial by Tzannou et al. (231) reported that all 14 patients treated for BKPyV-HC achieved clinical benefit. In another phase 2 trial, Nelson et al. (230) reported an overall response rate of 86% in patients treated for BKPyV DNAemia and 100% in patients treated for BKPyV-HC.

BK Polyomavirus-associated urothelial carcinoma (BKPyV-UC)

Since their discovery, polyomaviruses and their potential role in oncogenesis and cancer in humans have been extensively studied. Although, BKPyV encodes T-antigens that can drive cellular transformation and even cause cancer in some animal models (241), its causal role in cancer has been controversial (242, 243). Early studies have examined a wide range of cancer specimens for the presence of BKPyV DNA and proteins, especially reno-urinary malignancies since BKPyV persists in the reno-urinary tract (244). However, the evidence is conflicting. Some studies have detected BKPyV oncogenes and proteins in human cancer specimens, while

others have not. False-positive PCRs and immunohistochemical examinations most likely contribute to the heterogeneity of the data, making it difficult to interpret (242, 244). Moreover, BKPyV is a ubiquitous and widespread virus, making interpretation of the early studies even more challenging. Based on this, the International Agency for Research on Cancer concluded in 2013 that BKPyV was possibly carcinogenic (243). Recent years, the interest in BKPyV and cancer has been renewed after several epidemiological studies demonstrated that kidney transplant patients with prolonged BKPyV replication or BKPyV nephropathy had greatly increased risk of developing urothelial carcinoma (245-248). Furthermore, BKPyV has also been associated with renal collecting duct carcinomas (249, 250).

Genomic accidents are thought to be the driving mechanism behind BK Polyomavirus-associated urothelial carcinoma (BKPyV-UC) (2, 242). Longer exposure time to BKPyV increases the risk of a genomic accident to occur. Kidney transplant patients that have been exposed to prolonged BKPyV replication therefore have increased risk for urothelial carcinoma. Although only partly understood, sequencing studies of urothelial carcinoma specimens and mechanistic studies in cell culture have highlighted two important mechanisms for BKPyV-UC – integration of the viral genome and induction of apolipoprotein B mRNA editing enzyme catalytic polypeptide-like (APOBEC) 3 (242, 249, 251).

Genome integration of BKPyV DNA can cause persistent expression of the early viral gene region and expression of T antigens can inactivate tumour suppressors and perturb cell cycle regulation, potentially leading to cancer. Of note, integration of BKPyV DNA and T-antigen expression has been detected in several cases of reno-urinary cancers (242, 249, 252, 253). APOBEC3 is a cytosine deaminase with important anti-viral functions that causes characteristic mutations of cytosine (C) to uracil (U) in single stranded DNA (254). Notably, APOBEC enzymes can also induce genome damage in the host and contribute to carcinogenesis (255). *In vitro*, BKPyV infection has been found to induce APOBEC-expression (256, 257) and APOBEC signature mutations have been found in BKPyV DNA from kidney transplant patients (258, 259). A recent *in vitro* study demonstrated how BKPyV-induced APOBEC3-mediated genomic damage in urothelium and that this could be a contributing factor to urothelial carcinoma (260). Deep sequencing of urothelial carcinoma specimens has revealed BKPyV DNA and expression of T-antigens in urothelial cancers as well as APOBEC3-signature mutations (253, 261). Summarised, it seems plausible that BKPyV can play a causal role in development of reno-urinary cancer, at least in organ transplant patients.

Diagnosis of BKPyV-UC is based on biopsy-taking with subsequent histological examination and radiological examinations. Immunohistochemical staining for LTag can be done but it does not necessarily influence treatment decisions. There are no specific guidelines for BKPyV-UC and treatment is similar to other urothelial carcinomas with surgical removal of the cancer and neo-adjuvant or adjuvant chemo- or immunotherapy depending on the histological and radiological staging, if there are metastases and if the patient still has a functioning allograft (262-264). The renal allograft is typically not affected of urothelial carcinoma, however, there are examples of allograft cancers (250, 265). In one of these cases, complete regression of a metastatic donor-derived allograft LTag-positive collecting duct carcinoma was achieved after allograft nephrectomy and withdrawal of immunosuppressive treatment (250).

Other manifestations of BKPyV

Although very rare, there are reports of BKPyV encephalopathy and pneumonia (266-271) as well as disseminated BKPyV disease in immunocompromised patients, typically HSCT and HIV/AIDS patients (155, 272). Similarly, systemic BKPyV disease affecting multiple organs have been reported in paediatric patients with severe immune deficiencies (269, 273).

1.3 Epithelial cells and tissues

Epithelial cells line most of the luminal surfaces in the body as well as the outside of the body (274). The lumen of the gastrointestinal tract, reno-urinary tract, hepatobiliary tract, airways and skin are examples of lumens and surfaces that are completely or partly lined with epithelial cells. Epithelial cells and tissues are essential as they form barriers between different bodily compartments and control the barrier function, uptake and secretion of molecules and regulate the flow of solutes and molecules across the barrier (274).

To fulfil their functions, prototypic epithelial cells have a distinct cell shape and apico-basal polarity (Figure 6). Apico-basal polarity yields two distinct membrane domains – an apical and a basolateral membrane. The two membrane domains differ and have a distinct composition of proteins, lipids and carbohydrates (274, 275). The apical membrane typically has microvilli to increase the surface of the membrane, a primary cilium and numerous transporter proteins that are necessary for secreting and absorbing molecules and solutes (275, 276). The basolateral membrane contains a range of transporter proteins that are necessary to create solute gradients between the lumen and the interstitial space and thus enable transport of solute and molecules across the epithelial cell. The lateral membrane contains the junctional complexes that form intercellular connections that separate the apical and the basolateral membrane. Lastly, the basal membrane is in contact with the basement membrane (274, 276). An important requirement for apico-basal polarity is differential intracellular sorting and trafficking of proteins, as this ensures that the apical and basolateral proteins are sorted to the correct membrane domain (277). Not only is intracellular protein sorting polarised, but release of extracellular vesicles has also been shown to be asymmetric as different types of extracellular vesicles are released from the apical and basolateral membrane via distinct mechanisms (278, 279).

Epithelial cells have several hallmark proteins and structures that are essential for their function (Figure 6) (276). Tight junctions are multiprotein junctional complexes localised on the border between the apical membrane and basolateral membrane. Here they form an intercellular barrier and connect the actin cytoskeleton of neighbouring cells together. Tight junctions determine the epithelial barrier function by both restricting the flow of water and solutes across the epithelium while simultaneously allowing selective transport of some molecules (280, 281). The leakiness of tight junctions is an important characteristic of the tight junctions that vary between different epithelial cells and depends on the composition and complexity of the tight junctions (280-282). Especially claudins and zona occludens-1 (ZO-1) have been shown to be

important determinants of tight junction permeability (245, 280, 282). Lastly, tight junctions are important for maintaining apico-basal polarity by inhibiting lateral diffusion of membrane proteins across tight junctions and thus restricting transmembrane proteins to their respective membrane domain (281, 283).

Adherens junctions are another type of cell-to-cell junctional complex that is located on the lateral membrane, beneath the tight junction complexes (275). These junctions make intercellular connections between the actin filaments of epithelial cells to mechanically link the cells together and give adherent strength to the epithelial cell layer.

On the basal membrane, extracellular matrix (ECM)-receptors, such as integrins and dystroglycans, interacts with matrix proteins to anchor the epithelial cell to the basement membrane (275, 284).

Polarised epithelial cells have numerous transmembrane transporter proteins. The transporter proteins are in one of the membrane domains or both depending on their function. An example of an essential transporter is the sodium-potassium ATPase (Na/K-ATPase) or Na-K pump (285-287). The Na/K-ATPase is located at the basolateral membrane of polarised epithelial cells where it exchanges sodium for potassium to regulate the intracellular concentration of sodium and potassium and uphold the sodium-ion gradient between the lumen and interstitial space (288). For one ATP-molecule the pump exports three sodium ions and imports two potassium ions against a concentration gradient. The lumen-to-interstitium sodium gradient is an essential gradient, as it drives sodium-dependent transport at the apical membrane via sodium/glucose and sodium/amino acid symporters and sodium/calcium and sodium/hydrogen exchangers.

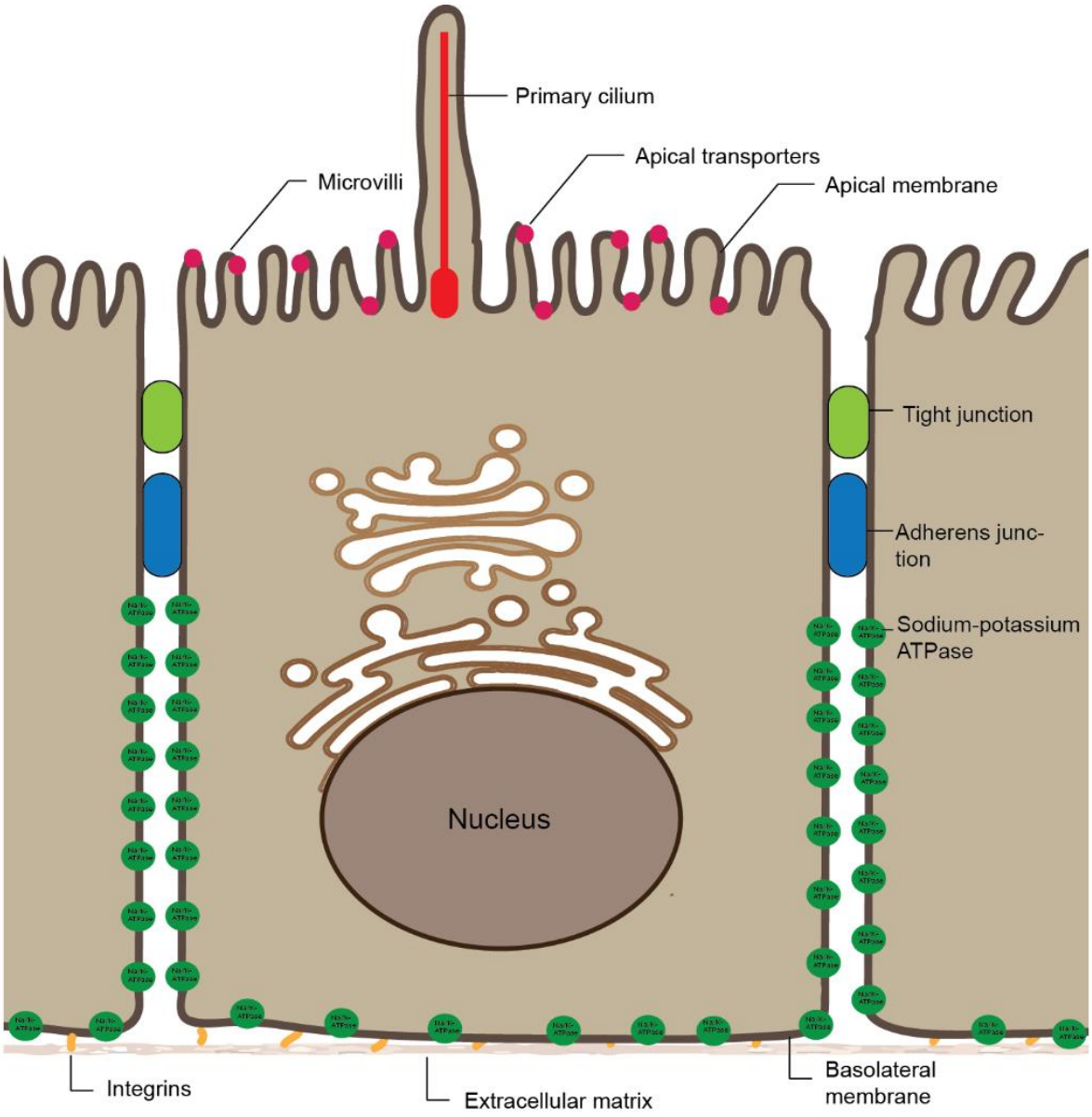

Figure 6: Prototypical epithelial cell with apico-basal polarity. Scheme of a polarised epithelial cell. Note the apical and basolateral membrane. The apical membrane has microvilli, apical transporters and a primary cilium, while the basolateral membrane has sodium-potassium ATPases (green circles) and integrins. Tight junctions and adherens junctions separate the two membrane domains. This scheme was created in Adobe Illustrator CS6.

As previously mentioned, epithelial cells share common features and functions across different tissues and organs. However, there are also significant variation between different epithelial cells based on the function of the tissue. In the gastrointestinal tract the intestinal epithelium is specialised to absorb nutrients from the intestinal lumen (289). The liver contains hepatocytes, a specialised epithelial cell with characteristic apico-basal polarity, that both absorb nutrients and molecules from the portal circulation and excrete bile into the bile ducts (290), and cholangiocytes that modify the composition of the bile and transport it to the duodenum (291). This is also the case for the nephron, the functional unit of the kidney, which contain several types of highly specialised epithelial cells with unique features and functions (285).

1.4 Endocytosis and the endocytic pathway

Endocytosis is a collective term of processes where cells internalise or absorb external materials and fluid. Endocytosis can occur via a range of different mechanisms (292), such as clathrin-mediated endocytosis, clathrin-independent carrier/glycosylphosphatidylinositol-anchored protein enriched early endocytic (CLIC/GEEC) endocytosis, macropinocytosis and caveolae-mediated endocytosis. In addition, there are numerous other endocytic mechanism that are characterised to a varying degree (292). Macropinocytosis is a constitutive large-scale process where membrane ruffles and cups engulf extracellular material and fluid (293). In contrast, endocytosis via other mechanisms such as caveolae-mediated endocytosis, clathrin-mediated endocytosis and CLIC/GEEC-endocytosis occur via inward budding pits (292).

In short, internalised cargo is typically delivered to the early endosome, also called sorting endosome (294, 295) (Figure 7). From the early endosome, the cargo can be recycled to the plasma membrane, or enter a degradative pathway where the early endosome will mature into a late endosome (294, 295). The late endosome will then fuse with a lysosome, a degradative organelle with acidic pH and lysosomal proteases, to form an endolysosome. This is a transient organelle with degradative capacity due to acidic pH and proteases, and after degradation is complete the endolysosome converts back to a lysosome.

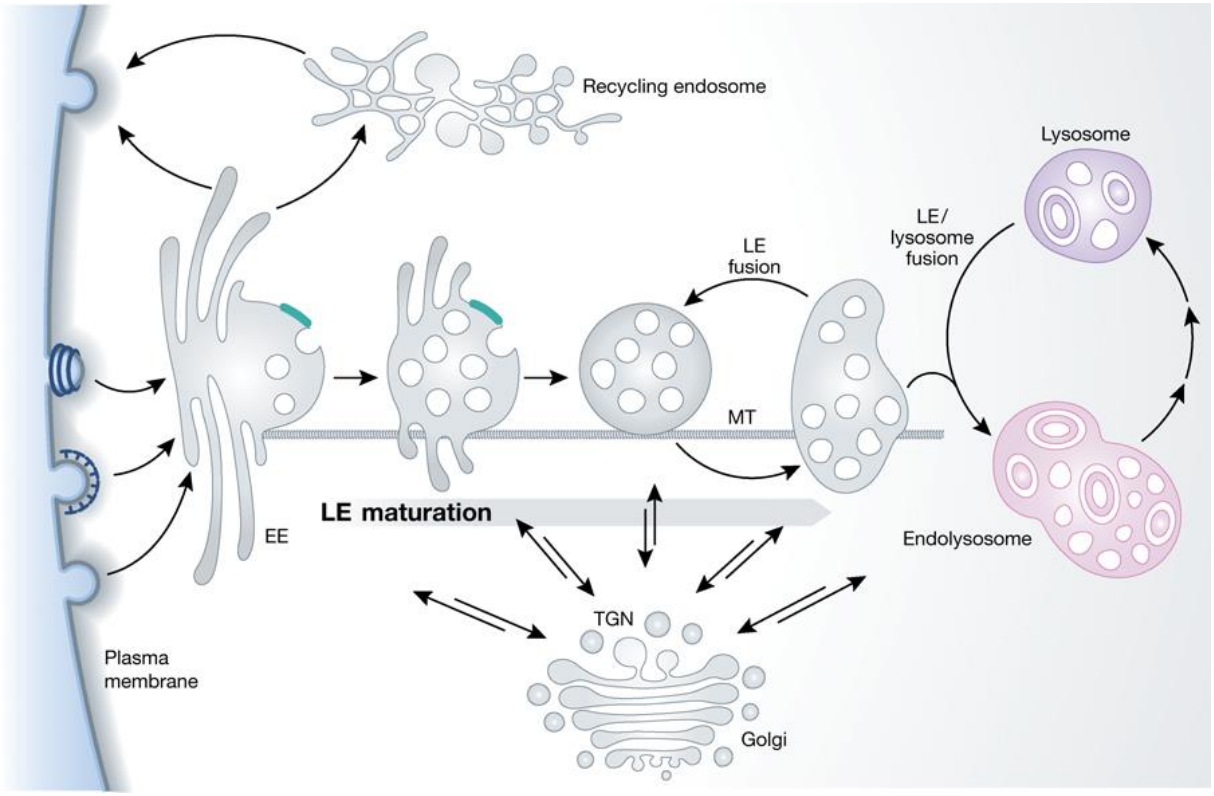

Figure 7: The endocytic pathway. Internalised cargo is routed to the early endosome (EE). From here, the cargo is either recycled to the plasma membrane via recycling endosomes or is destined for degradation. Early endosomes mature to late endosomes (LE). Late endosomes fuse with lysosomes to form endolysosomes, a transient degradative organelle with acidic pH and proteases. Reprinted from Huotari and Helenius (295) with permission.

1.5 The kidneys and urine production

BKPyV naturally persists in epithelial cells of the reno-urinary tract (162, 163). The kidneys and renal epithelial cells are therefore of special interest since this is where BKPyV both persists and reactivates to cause BKPyV nephropathy.

The kidneys are essential organs that remove waste products from the blood, regulate blood volume, acid-base balance and electrolyte concentrations and produce urine. Humans have two kidneys that are located on each side of the spine in the retroperitoneal space in the abdominal cavity. The kidneys receive blood from the renal arteries, while blood drains via the renal veins into the inferior vena cava. Urine from the kidneys and drains together into the renal pelvis via the calyces. From the renal pelvis, the urine drains via the ureters to the bladder, where urine is stored until urination occurs. The kidneys can be divided into two parts – the outer renal cortex and the inner renal medulla. Generally, the renal cortex contains the renal corpuscles as well as the proximal and distal tubules while the renal medulla contains loops of Henle and the collecting ducts (296).

The functional unit of the kidneys is the nephron and each kidney have over 1 000 000 nephrons. Each nephron is composed of a renal corpuscle and a tubular system (Figure 8A). The renal corpuscle filters the blood and consists of a capillary tuft called the glomerulus and its surrounding capsule called Bowman's capsule. The tubular system can be divided into the proximal convoluted tubule, the loop of Henle, the distal convoluted tubule and the collecting duct. Each of the tubular system's components perform specialised functions that are necessary to both produce and regulate the composition of the urine (296).

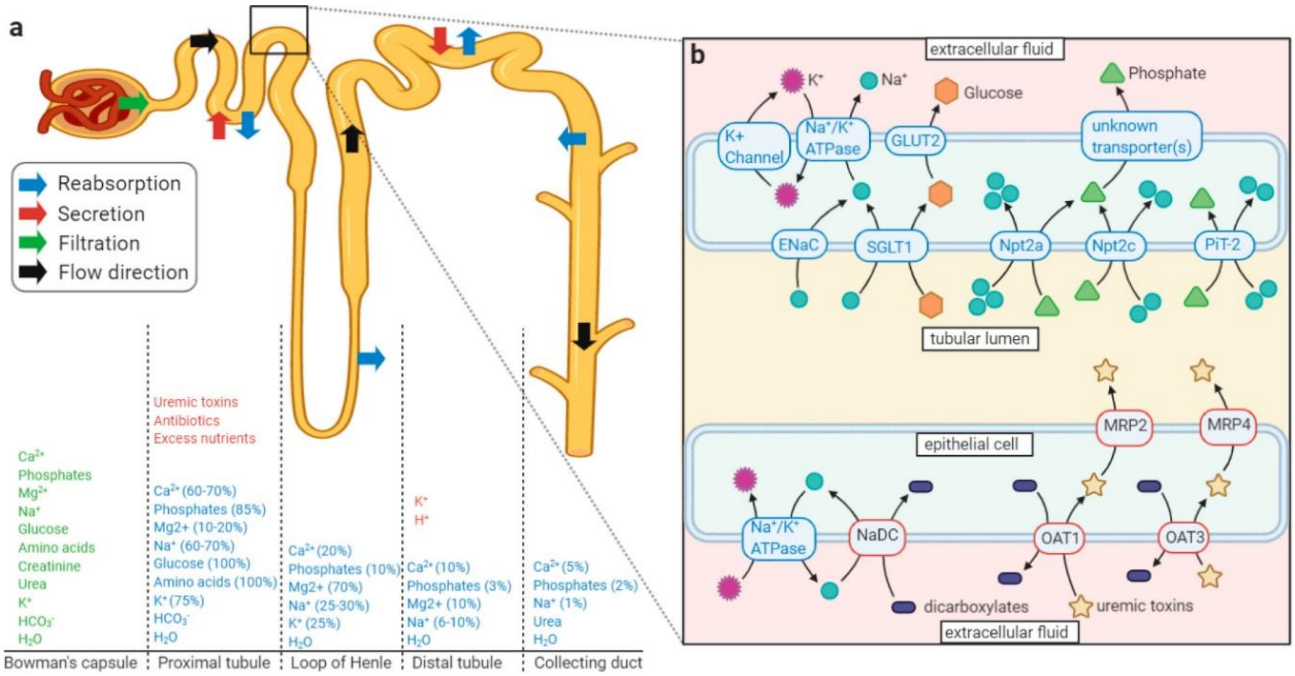

Figure 8 Schematic presentation of the nephron with special emphasis on the proximal tubule. A) The processes of the kidneys – filtration (green), reabsorption (blue) and secretion (red) and the examples of solutes and molecules is depicted with their respective colour. B) Examples of apical and basolateral membrane transporters in the proximal tubule epithelial cells: Na^+-glucose cotransporter (SGLT1), epithelial Na^+-channel (EnaC), facilitated glucose diffusion transporter (GLUT2), sodium-dependent phosphate transport proteins (Npt2a, Npt2c, PiT-2), divalent anion-sodium symporter (NaDC), organic anion transporter (OAT1, OAT3), multidrug resistance-associated protein 2 (MRP2, MRP4). Reprinted from Vermue et al. (297).

The first step of urine production occurs in the glomerulus, where the filtrate, also called pre-urine, is made by filtration of blood in the glomerulus. The filtration barrier of the glomerulus consists of the fenestrated endothelial cells in the glomerular capillaries, the basement membrane and specialised glomerular epithelial cells, podocytes, that together make up a permeable mesh that allows passage of fluid and small molecules from the blood into Bowman's space (298). Each day, the kidneys generate around 160-180 liters of filtrate (298, 299).

To avoid excessive loss of fluid, nutrients and solutes, the filtrate or pre-urine undergoes extensive modification via reabsorption of water, ions and solutes as well as directed secretion of ions and xenobiotics (285). From Bowman's space, the filtrate drains into the proximal tubule of the tubular system where the majority of the reabsorption occurs. The proximal tubule is lined with highly specialized epithelial cells that reabsorbs 60-70% of the filtered sodium and water. Furthermore, the kidneys filters up to 180 grams of glucose and 50 grams of amino acids daily and 99.8% of this is reabsorbed in the proximal tubule (299). Due to the importance of the proximal tubule and the massive reabsorption that occur there, the proximal tubule constitutes the majority of the kidney and 66% of all kidney cells are proximal tubule cells (285). Reabsorption of sodium, glucose and amino acids occurs via several apical transporter such as Na^+/H^+-exchangers and symporters that facilitate sodium-coupled uptake of glucose and amino acids. Water absorption occurs via osmotic gradient that the reabsorption of ions such as Na^+ create (Figure 8B) (285, 288, 299).

After the proximal tubule, the pre-urine drains through the loop of Henle where Na^+, K^+ and Cl^- are reabsorbed to establish the counter-current multiplication mechanism and the osmolality gradient along the collecting duct (300). The distal convoluted tubule is critical for homeostasis of sodium, potassium and cations. This regulation occurs in part via the responses of the epithelial cells of the distal convoluted tubule to hormones such as aldosterone and angiotensin II (301). In the collecting duct, the final regulation of the urine composition occurs. Here, the urine can be concentrated via absorption of water via antidiuretic hormone-sensitive aquaporins in principal cells, while the final excretion of sodium and potassium is regulated via the hormone-sensitive epithelial sodium channel and renal outer medullary K^+ channel (302). Lastly, the collecting duct intercalated cells are essential for acid-base homeostasis (303).

1.6 *In vitro* epithelial cell culture models

1.6.1 Two-dimensional cell cultures

The simplest and most widely used cell culture model of epithelial cells are two-dimensional (2D) cell cultures of non-polarised epithelial cells in plastic dishes or well plates. We used this model to cultivate RPTECs, Vero cells, CV-1 cells and Hela cells. In a 2D model, the cells are typically flat with few hallmarks of the cell's appearance *in vivo* such as an apico-basal polarity. A range of renal epithelial cell lines and primary renal epithelial cells from different species and organs have been cultured and characterised in such 2D cell cultures. Some renal epithelial cells and cell lines, such as Madine-Darby canine kidney (MDCK) cells and primary human renal tubule epithelial cells, develop some features of apico-basal polarity when grow to confluency in 2D cell cultures (304-307). A strength of 2D cell cultures is that they are cheap, require limited technical expertise and a wide range of cells can be cultured this way. However, cells cultured in 2D-models do not exhibit full apico-basal polarity and the physiology of the cells deviate from the physiology of the same cell type *in vivo* (308). Furthermore, 2D models are not suited to study transepithelial uptake, transport and secretion since there is only one compartment.

1.6.2 Cells cultured on cell culture inserts

Cell culture inserts, also called permeable supports, is a tool that allows development of more complex cell culture models by culturing cells on a permeable membrane. The inserts are placed in cell culture wells to yield a two-compartment model where the well constitutes the basal compartment while the inside of the insert is the apical compartment (Figure 9). Importantly, the pores of the permeable membrane allow flow of solutes, fluid and molecules between the two compartments. The cells of choice are cultured on the permeable membrane yielding a 2.5-dimensional (2.5D) cell culture model with a cell layer that separates the two compartments (309, 310). We used cell culture inserts to develop a 2.5D model of polarized RPTECs. Many types of epithelial cells, including both renal epithelial primary cells and cell lines, have been shown to develop apico-basal polarity when cultured on cell culture inserts (311-316). This has been utilised to examine issues such as transepithelial transport and epithelial barrier function (309, 310, 314, 317). A relevant example of this is the polarised cell culture model of MDCK cells, as this has been essential to characterise and understand the cell biology of apico-basal polarity (311, 318). Furthermore, polarised cell cultures on inserts have also been used to study host-pathogen interactions. For instance, it has been used to characterise how bacteria invade

polarised epithelial cell layers (319-321) and to examine if entry and release of viruses is polarised (140, 322-326).

1.6.3 Three-dimensional cell cultures

An important limitation of 2D and 2.5D cell culture models is the absence of biomechanical forces, and the lack of three-dimensional (3D) tissue architecture and microenvironment that is seen in tissues and organs *in vivo*. In an effort to close this gap and develop more *in vivo*-like cell models, 3D cell culture models and organoids have been extensively researched and utilised to model human development, physiology and disease (316, 327, 328). This has resulted in numerous systems and methods to develop 3D cell cultures.

Rotating wall vessel bioreactors can be used to generate polarised 3D cell cultures. It is a suspension-based system where cells are seeded on special beads or microcarriers coated in ECM (Figure 9). The cell-cell and cell-ECM as well as shear stress generated by the rotation stimulate the development of differentiated cells with *in vivo* features, including apico-basal polarity (328, 329). With this system, cell lines, primary cells and stem cells have been used to establish monotypic and co-culture 3D models of a wide range of tissues and organs. Moreover, the system has been used to study host-pathogen interactions (328, 330-334). Although this model can yield polarised cell layers, including epithelial and endothelial barriers, an important drawback is the lack of an accessible basal compartment since the cells are cultured on beads. This model is therefore not suited to examine issues where access to the basal compartment is necessary, such as invasion or release of pathogens via the basolateral membrane or polarised exocytosis.

Spheroids are self-assembled 3D cell cultures. They are often made by seeding cells in a low-adherence environment that allow aggregation of the cells and subsequent development of a spheroid (Figure 9). Many techniques have been developed for this, but three common techniques are low-adherence plates and microwells, the hanging drop method and rotating-wall vessel cultures (Figure 9) (335-338). LLC-PK1, MDCK II cells, mammary cell line EpH4, colon cancer cell line R2/7, primary retinal pigment epithelial cells and a human bronchial epithelial cell line are all examples of cell lines that develop into spheroids with stronger features of polarised epithelial cells (339-342). When cultured like this, a spheroid typically exhibit an apical-out morphology but does not have a lumen and therefore no accessible basal compartment (341).

An alternative to low-adherence techniques are ECM-embedded 3D cell cultures (316), where the cells are seeded in a matrix, for instance Matrigel or collagen, and allowed to differentiate (Figure 9). Epithelial cell lines, such as MDCK, LLC-PK1 and Caco cells, cultured in ECM can develop a cyst-like morphology with a circular polarised cell layer with a central lumen. Unlike spheroids, the ECM-cell contacts typically cause an apical-in morphology where the apical membrane faces in against the lumen of the cyst (341-343).

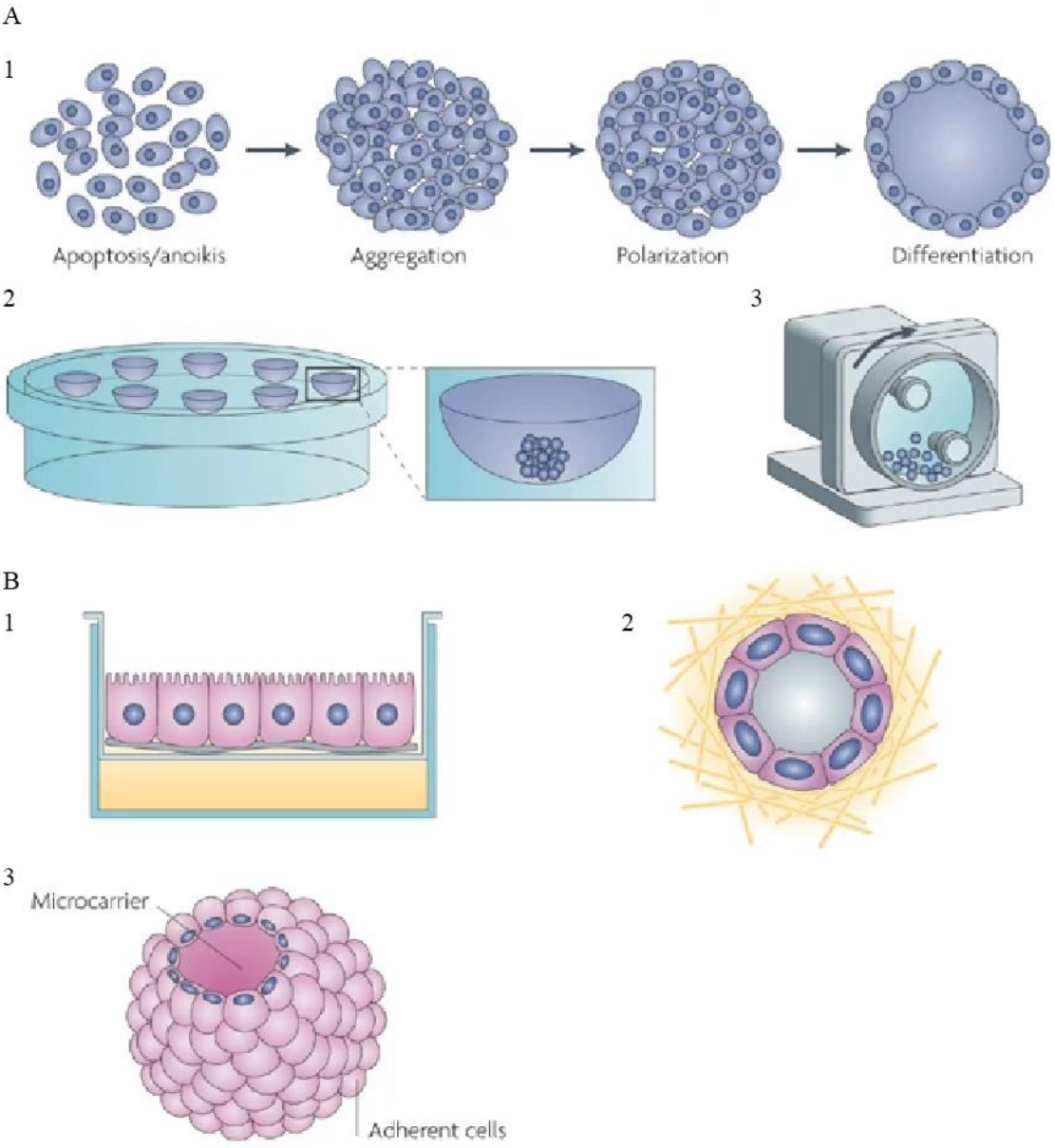

Figure 9: Examples of 2.5D and 3D cell culture models. A) Schematic examples of spheroid cell culture models that use aggregation techniques (1), such as hanging drop techniques (2) and rotating-wall vessel cultures (3). B) Example of cell culture techniques to develop polarised epithelial cells such as cell culture inserts (1), matrix-embedded culture (2) and microcarriers (3). Adapted from Pampaloni, Reynaud and Stelzer with permission (338).

Organoids are more complex 3D cell culture models compared to the previously discussed models and are a self-organised stem-cell derived 3D structures or tissues (344, 345). Stem cells used to generate organoids are typically either adult tissue derived stem cells or pluripotent stem cells, which can be further divided into embryonic stem cells or induced pluripotent stem cells. Pluripotent stem cell derived organoids can be generated by doing a stepwise differentiation of pluripotent stem cells ending in a fully differentiated organoid (Figure 10A). The differentiation process typically starts with germ layer specification followed by a guided differentiation using different growth factors and signalling inhibitors (346). For both stem cell types, different growth factors and inhibitors are used depending on which tissue one aims to develop (346). Adult stem cell derived organoids can be generated from a collected tissue sample (figure 10B). After collection, the sample is dissociated into a single cell suspension. The stem cells are then embedded in ECM and cultured in a medium with growth factors that mimic the *in vivo* stem cell niche, and after up to two weeks of culture, organoids have typically formed (344, 347). The organoids typically have a cystic apical-in morphology where the inside of the organoid represents the apical lumen.

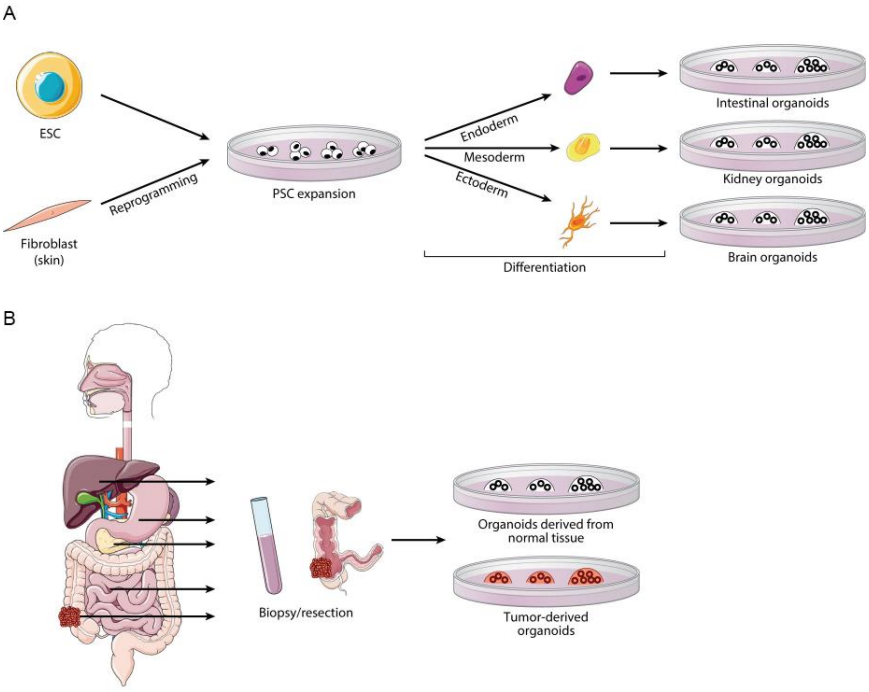

Figure 10: Schematic of how organoids are developed. A) Organoids generated from embryonic or induced pluripotent stem cells. Pluripotent stem cells are first differentiated toward one of the three germ layers, before a targeted differentiation is performed to generate the tissue of choice. B) Organoids generated from adult-derived stem cells. Adult-derived stem cells are first harvested before they are expanded and differentiated into an organoid of the same tissue that the cells were originally harvested from. Reprinted from Schutgens et al. (344) with permission.

The source of cells and methods used to generate organoid strongly influence its phenotype and complexity and an organoid model can range in complexity from a simple cystic organoid consisting of a single cell type (348, 349) to a complex mini-organ consisting of several cell types (345, 350, 351). Generally, pluripotent stem cells can give rise to all cell types while adult stem cells are limited to tissues that undergo regeneration such as epithelium. Therefore, organoids from pluripotent stem cells can typically yield more complex organoids with several different cell types while adult derived stem cells yield cystic organoids that mimic epithelial tissues (344). Using both methods, organoids have been developed from a wide range of organs (352) including but not limited to the lungs and airways (353, 354), the kidneys (349, 350), the brain (355) and the gastrointestinal tract (348, 356).

Although matrix-embedded 3D cultures can yield fully differentiated organoids with apico-basal polarity, there are also significant caveats with matrix-embedding. Organoids typically lack tissue interfaces and there is no shear stress such as flow of blood or tubular filtrate. Furthermore, organoids are not easily accessible due to being embedded in matrix, which makes sampling of supernatants and secreted products and examination of biological gradients difficult (357, 358). The apical-in morphology also complicates infections since the apical domain is not freely accessible. Apical infections must often by done with microinjection techniques. Furthermore, both basolateral infection is less controlled since the pathogen must diffuse through the matrix (359).

Flow systems such as organs-on-a-chip and other microfluidic systems try to answer some of these issues. In short, these systems allow seeding of cells in separate lumens or passages, thus enabling seeding of several cell types to create tissue interfaces. Furthermore, this also yields an apical compartment and basolateral compartment that can easily be sampled. Lastly, perfusion or induced shear stress in microfluidic systems contribute to a differentiated morphology and function of cells (357, 358, 360). Similar to organoids, organs-on-a-chip models have been generated for a wide range of organs (358). Polarised epithelial cell layers have been developed with cell lines (361), primary human cells (362) and cells from dissociated organoids (349). An example of this is kidney tubuloids that were dissociated and seeded in microfluidic cell culture plates denoted OrganoPlates in order to characterise the transport and barrier functions of the tubuloid cells (349).

2 Aims of the thesis

The overall aim of this thesis was to address important knowledge gaps in our understanding of BKPyV biology.

Paper 1:

The aim of the study was to characterise BKPyV replication and antibody response in two kidney transplant recipients that developed BKPyV nephropathy in parallel shortly after transplantation of allografts from the same donor, to better understand the role of antibodies in clearance of BKPyV nephropathy seen as resolving BKPyV DNAemia.

Paper 2:

The aim of the study was to increase our understanding of major aspects of the BKPyV replication cycle by employing an authentic polarised renal tubular epithelial cell culture model, with special focus on virus entry, virus release and dissemination of progeny virus.

Paper 3:

The aim of the study was to determine whether *in vitro* BKPyV infection of RPTECs induces cytoplasmic vacuolisation and to study the potential role of this in the BKPyV replication cycle.

3 Summary of papers

3.1 Paper 1

Early fulminant BK polyomavirus-associated nephropathy in two kidney transplant patients with low neutralising antibody titers receiving allografts from the same donor.

Lorentzen E. M., Henriksen S., Kaur A., Kro G. B., Hammarström C., Hirsch H. H., Midtvedt K. and Rinaldo C. H. Virol J. 2020;17(5).

In this study we retrospectively measured the plasma and urine BKPyV DNA load, analysed the BKPyV strain and subtype and characterised the humoral immune response in two older male kidney transplant recipients that both developed BKPyV nephropathy shortly after receiving a renal allograft from the same donor.

In recipient 1, BKPyV DNAemia of 8.58 x 10^4 copies/ml had been detected 5 weeks post transplantation, while in recipient 2 BKPyV DNAemia of 1.12 x 10^6 copies/ml had been detected 8 weeks post transplantation, giving both recipients the diagnosis of presumptive BKPyV nephropathy, previously called BK Polyomavirus-associated nephropathy. Recipient 2 had an increase in serum creatinine in week 8. Due to this, he underwent a renal allograft biopsy which was found to be negative for BKPyV LTag. Both patients were diagnosed with BKPyV nephropathy based on renal allograft biopsies at week 12 and immunosuppressive treatment was promptly reduced. One-year post-transplant, recipient 1 still exhibited high-level plasma BKPyV DNAemia, while recipient 2 had cleared the BKPyV DNAemia. Of note, we could retrospectively test five earlier plasma samples from recipient 2 and detected a BKPyV DNAemia of 2.59 x 10^3 already at 4 weeks post transplantation.

We characterised the BKPyV-specific antibody response in both recipients and the donor with ELISA, haemagglutination inhibition assay and neutralisation assay, the two latter methods analysing neutralising antibodies. The donor had a high titre of BKPyV-specific antibodies with all three methods, indicating recent exposure to BKPyV. As expected for an apparently immunocompetent individual, BKPyV DNA was not detectable in plasma. The recipients were seropositive but showed low levels of BKPyV-specific antibodies with all three methods prior to transplantation. Both recipient 1 and 2 developed a strong humoral response with a sharp increase in antibody titres at 10- and 8-weeks post-transplantation, respectively. At peak levels, both recipients demonstrated >6-fold increase in ELISA titre, >126-fold increase in HIA-titre

and >1000-fold increase in neutralisation titre. DNA sequencing demonstrated that the virus in early plasma and urine samples from both recipients were of the same strain and subtype.

Taken together, our results indicate a donor-derived infection and suggest that the combination of low titres of BKPyV-specific antibodies in the recipient and high titres of BKPyV-specific antibodies in the donor is a risk factor for BKPyV DNAemia and nephropathy. Lastly, this study show that a strong humoral response may not be enough for viral clearance.

3.2 Paper 2

Modelling BK Polyomavirus dissemination and cytopathology using polarised human renal tubule epithelial cells

Lorentzen E.M., Henriksen S. and Rinaldo C. H. PloS Pathog. 2023;19(8): e1011622.

In this study we established a polarised renal epithelial cell culture model by culturing RPTECs on cell culture inserts. After 8 eight days of culture, the RPTECs developed a polarised morphology and function.

We show that BKPyV entry is predominately apical, presumably due to asymmetric apical localisation of sialic acids. Progeny virus is mainly released into the apical compartment and leakage of BKPyV into the basolateral compartment first occurs when major cell lysis has started. In line with these results, the barrier function of the cell layer was maintained until 5 days post-infection. BKPyV infection of polarised RPTECs leads to apical extrusion of dead cells, that were similar to the decoy cells detected in urine of kidney transplant patients with BKPyV nephropathy. The decoy-like cells express BKPyV proteins and can transmit BKPyV to uninfected RPTECs. Neutralising antibodies added to the basolateral compartment can traverse the cell layer and inhibit spread of BKPyV infection.

Taken together, we demonstrate that BKPyV entry and dissemination occur in the apical compartment *in vitro*, suggesting that that BKPyV spread via the tubular lumen *in vivo*. Dissemination via the tubular fluid can help the virus delay immune detection. As the replication cycle progress, infected cells undergo lysis and progeny virus is released into the supernatant and inside extruded dead cells. Extrusion of dead infected cells is possibly protecting the barrier integrity of the renal epithelium during BKPyV infection and may protect the virus from neutralising antibodies.

3.3 Paper 3

Massive entry of BK Polyomavirus (BKPyV) induces transient cytoplasmic vacuolisation of human renal proximal tubule epithelial cells

Lorentzen E. M., Henriksen S. and Rinaldo C. H. 2023. Manuscript.

In this study we aimed to investigate whether *in vitro* BKPyV infection of RPTECs induces cytoplasmic vacuolisation and the potential role of this in the BKPyV replication cycle of RPTECs. We show that BKPyV induces massive cytoplasmic vacuolisation of RPTECs and that this occurs in two phases. Early vacuolization occurs only a few hours after infection with a high infectious dose and is reversed by 36 to 48 hours post-infection (hpi) while late vacuolization co-occurs with host cell lysis and progeny release.

Vacuolisation depends on BKPyV uptake as addition of a BKPyV-specific neutralising antibody inhibited vacuolisation. By using live-cell microscopy we demonstrate that both early and late vacuoles represent enlarged endo-/lysosomes. Moreover, using transmission electron microscopy the vacuoles were found to contain viral particles that lined the inside of the vacuole. Time-lapse microscopy and BKPyV qPCR reveal that cell death and progeny release precede late occurring vacuolisation. Intriguingly, late occurring vacuolisation is focal, mainly appearing in cells neighbouring lysed cells, suggesting that localised spread of BKPyV is favoured. By using chemical inhibitors, we show that BKPyV replication is sensitive to Rac1-inhibition but the inhibitor has little effect on early vacuolisation. Bafilomycin A treatment blocks vacuolisation, demonstrating that vacuolisation depends on a functioning V-ATPase and correct endosomal acidification and trafficking.

Taken together, massive entry of BKPyV induces transient vacuolisation of RPTECs. In contrast to what has been reported for the related polyomavirus SV40, vacuolisation does not increase cell death and progeny release, but is rather an early event in the BKPyV replication cycle that presumably is caused by a transient overload of the endocytic pathway. Focal vacuolisation suggests that BKPyV may undergo cell-to-cell spread.

4 Methodological considerations

4.1 Measuring BKPyV-specific antibodies

As previously mentioned, antibodies can be measured with different methods and commonly used methods include ELISA, HIA and neutralisation assays (Figure 5). Although the methods utilise different techniques and readouts, they should yield corresponding results, meaning that a high HIA titre should at least partially correlate with a high ELISA and neutralisation titre and vice versa. However, since the antigens used for the specific assays can vary, there are important nuances between the assays depending on the used antigen and assay readout.

A neutralising antibody is defined as an antibody that inhibit infection by binding to the viral particle, typically inhibiting virus binding and/or entry (363). Importantly, an antibody can be non-neutralising, meaning that it can bind the virus, but it does not inhibit infection. In a neutralisation assay, only antibodies that bind and neutralise the virus or pseudovirus and thus inhibit entry and successful infection of the host cell will affect the result of the assay. Neutralisation assays are therefore considered the gold standard to measure neutralising antibodies since it measures the actual reduction in virus infection or transduction (363). To inhibit haemagglutination in the HIA, the antibody must bind the antigen (infectious virus, pseudovirus or VLPs) in a way that hinders the capsid or viral particle from interacting with the viral receptor on RBCs. In contrast, a non-neutralising antibody will not disrupt receptor binding and therefore not inhibit haemagglutination. Therefore, the HIA titre correlates with the level of neutralising antibodies.

In an indirect ELISA, the used antigen, specifically if it is presented in a VLP or as a Vp1-fusion protein, can affect the assay and its interpretation (172). In VLPs, the external capsid surface of Vp1 is presented in its natural 3D conformation, similar to infectious virus. In contrast, with a Vp1-fusion protein the entire protein is available for binding, including the fusion protein, which may allow binding of lower affinity non-neutralising antibodies (172). This can potentially lead to a high ELISA titre, even when the patient has a low level of neutralising antibodies. In line with this, Bodaghi et al. (188), reported that an ELISA based on Vp1-derived VLPs was more sensitive than an ELISA with Vp1-fusion protein. The correlation to HIA titre was also stronger when VLPs were fused. Furthermore, Pastrana et al. (207) reported correlation between the VLP ELISA titre and the neutralisation titre, indicating that the VLP ELISA titre most likely reflects the level of neutralising antibodies.

In **paper 1** we measured BKPyV-specific antibody levels with both a VLP ELISA and HIA. By using both assays we could measure antibody levels with high sensitivity, as ELISA is more sensitive than HIA (188), and be certain that the antibodies had neutralising activity. We supplemented these assays by assessing the change in neutralisation titre between a pre-transplantation sample to a sample from week 20 post-transplantation. This confirmed that the patients developed high titres of neutralising antibodies. However, a drawback of our characterisation is that we only measured neutralising titre at pre-transplantation and at week 20. We can therefore not be completely certain when the level of neutralising antibodies first started to increase, although both HIA and VLP ELISA titre correlate with neutralising activity (188, 207).

4.2 Choice of cell type and cell culture model

Two important methodological aspects in **paper 2** and **3** were the choice of cell type and cell culture model. When examining virus-host interactions and pathogenesis *in vitro,* it is important to use a relevant cell type, which reflect the cells that the virus infects *in vivo*. Different cell types and cell lines exhibit different characteristics and functions. If using a less relevant cell type or cell line, the *in vitro* cell model may not produce representative results of how the virus interacts with the host cells *in vivo*. For instance, the two immortalised cell lines U2OS and HEK293T, lack STING, an important part of the innate immune system (142), and this can affect virus-host interactions (364-366). STING restricts several DNA viruses, including Herpes Simplex virus 1 (HSV-1) (142). In U2OS-cells, however, the growth-restricted HSV-1 mutant (ΔICP0) can replicate normally due to the absence of STING. Another issue with immortalised cell lines is that they typically express viral oncogenes such as human papillomavirus E6 and E7, polyomavirus LTag and adenovirus E1A, as this is a common method for immortalisation. As previously mentioned, all three oncogenes can inhibit the STING pathway via the LXCXE-motif (38). Immortalisation with persistent expression of these oncogenes can therefore potentially disrupt anti-viral signalling in immortalised cell lines. LTag can also have the opposite effect, as transfection of LTag into human fibroblasts lead to induction of interferon genes establishing an anti-viral state (367). Another relevant example is mouse embryo fibroblasts that only support myxoma virus infection after immortalisation due to a perturbed interferon-response (368).

Choice of cell type also influence BKPyV-host interactions. For BKPyV, its dependence on the ERAD machinery for ER-exit differ between primary human RPTECs and simian CV-1 cells

(60). Furthermore, a recent *in vitro* study demonstrated that some endothelial cells can restrict BKPyV replication via interferon signalling leading to a limited infection, while epithelial cells and fibroblasts are unable to restrict BKPyV replication resulting in a lytic infection with widespread cell death (132). These examples demonstrate how different cells can influence the interplay between virus and host and the importance of utilising relevant cells.

BKPyV infects renal tubular epithelial cells *in vivo* (127, 178, 369) and the ideal cell type for an *in vitro* cell culture model should therefore reflect a human renal tubule epithelial cell. Initially, different human and simian cells and cell lines, for instance Vero cells, were used to study the replication cycle of BKPyV (16, 36, 37, 72, 87, 90, 99, 370, 371). However, since *in vitro* BKPyV infection of human primary RPTECs was first described (129), they have been increasingly used to study BKPyV (73, 81, 91, 92, 96, 122, 125, 132, 372, 373). Previously, human RPTECs were mainly attained by isolating them from discarded renal tissue (129, 374, 375). However, from about 2006, RPTECs became commercially available from Lonza and later from other commercial sources such as ScienCell, American Type Culture Collection and PromoCell, making them an accessible cell type for researchers without access to renal tissue. Although primary RPTECs exhibit known features of the proximal tubule (371, 376-379), RPTECs have also been shown to express stress and injury markers that are usually detected in stressed and diseases kidneys. Since they are non-transformed cells, they have a limited passaging capacity before they enter senescence (380). An alternative source of renal epithelial cells are adult-derived stem cells, which can be differentiated into all the cell types of the nephron, including proximal tubule epithelial cells (349). Renal adult-stem cells can give rise to cell types of the nephron, develop a proximal tubule-like function and support BKPyV replication *in vitro* (344, 349). A drawback of adult-derived stem cells is that they are cultured in a matrix-embedded organoid. Moreover, they are typically less available as they are usually isolated from tissue, although renal tubuloids have also been generated from urinary cells (349).

For our cell culture model, we chose to use commercially sold primary human RPTECs since they are easily available and have been widely used to study BKPyV (60, 74, 81, 92, 96, 98, 113, 122, 125, 132, 135, 372, 373, 380-383). Importantly, RPTECs have previously been shown to develop a polarised morphology with a distinct apical and a basolateral membrane on cell culture inserts, in spheroids and in microfluidic devices (306, 384-389). Since we needed a polarised cell culture model of authentic cells for **paper 2**, this made RPTECs a suitable cell type.

In **paper 3**, the choice of cell type was especially important as the phenomenon we study, cytoplasmic vacuolisation, is known to be cell-type dependent. SV40 can induce cytoplasmic vacuolisation in 2D cultured CV-1 cells but fail to do the same in 2D cultured Vero cells due to lower levels of GM1 (376). The existing evidence on BKPyV and cytoplasmic vacuolisation is conflicting and have mainly been generated in less relevant cell types, such as simian cell lines and human cells that are not of renal origin (371, 376, 378, 379). BKPyV have been shown to induce cytoplasmic vacuolisation in human fibroblasts, foetal brain cells and Vero cells, but not in CV-1 cells. By using 2D cultured RPTECs, we could in **paper 3** determine that BKPyV induce cytoplasmic vacuolisation in a cell type that is relevant for BKPyV replication and disease *in vivo*. To minimise unwanted effects from extended passaging we only used RPTECs that had been passaged for a maximum of three passages.

The aim of **paper 2** was to characterise entry and release of BKPyV in polarised RPTECs to deepen our understanding of BKPyV dissemination *in vivo*. To do this, we needed a renal epithelial cell culture model with apico-basal polarity. As highlighted in the introduction, there are several cell culture models that can mimic polarised renal epithelium, including matrix-embedded spheroids and organoids that accurately mimic the 3D-organisation of epithelium (328, 344, 349). However, a big drawback of matrix-embedded spheroids and organoids is the lack access to the membrane domains. Apical or lumen infections can be performed, but this requires specialised techniques such as microinjection (359, 390). Moreover, organoids are typically developed with the use of stem cells which are more expensive and less available than commercially available primary cells (344).

Cell culture inserts are widely used to generate epithelial cell layers with apico-basal polarity. The inserts yield a two-compartment model where both the apical and basolateral membrane domain and compartment is accessible. Some drawbacks are that the cell culture inserts only yield a 2.5D cell culture model and do not accurately model the 3D organisation of the epithelial tissue *in vivo*. Moreover, cultures on inserts are static and without perfusion or shear stress. As previously mentioned, when RPTECs are cultured on cell culture inserts, they develop a more *in vivo*-like morphology and function compared to 2D cell cultures (306, 312, 374, 389, 391). Furthermore, cell culture inserts are widely used and are cheaper than organoids and microfluidic devices. We therefore chose to develop and utilise a polarised RPTEC model on cell culture inserts in **paper 2**. To do this, RPTECs are seeded on collagen-coated inserts and then cultured for seven to ten days, allowing the cells to differentiate and form a confluent polarised cell layer (Figure 11).

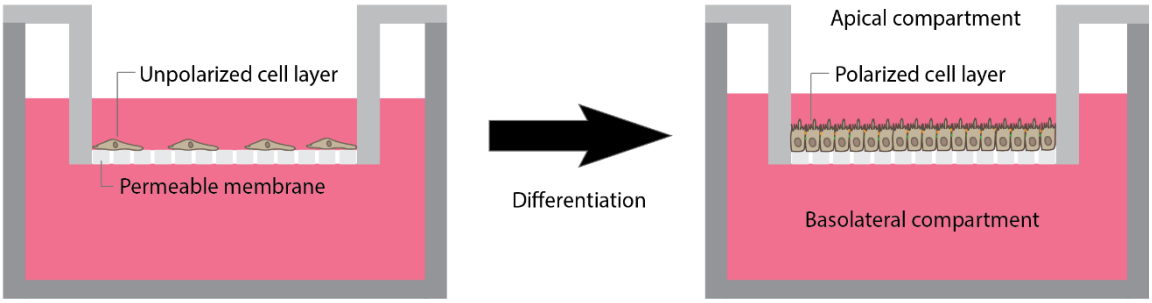

Figure 11: Scheme of establishment of polarised RPTECs on cell culture inserts. Reprinted from Lorentzen et al. (392).

4.3 Virus diffusion across cell culture inserts

An important aspect of using cell culture inserts is the diffusion of virus across the insert. When cells are infected from the basolateral side, the insert membrane acts as a mechanical hinder that the virus must traverse to access the basolateral membrane domain. When examining if virus entry is polarised, it is therefore essential to examine if the virus can diffuse across insert membrane and reach the basolateral membrane. Unless this is confirmed, a finding of preferential apical entry might be an artefact caused by limited virus diffusion across the insert membrane. Importantly, virus diffusion varies between different viruses. In the case of Epstein-Barr virus (enveloped virus, 80 – 100 nm (393)), only 20% of the purified applied virus traversed the membrane of Transwell filters with a pore size of 0.45 µm after 1 hour incubation (394). Furthermore, when using pelleted virus, only 10% traversed the membrane. Approximately 30% of Hantavirus (enveloped virus, 88-150 nm (395)) diffuse through 0.4 µm Transwell inserts (396), while only 0.1% of Rotavirus (non-enveloped virus, 60-100 nm in diameter (397)) diffused across 0.4 µm inserts (398). Importantly both pore size and insert-coating will affect virus diffusion rates. Larger pores typically lead to increased diffusion, while coating can reduce diffusion. Apical incubation with human cytomegalovirus (enveloped virus, 150 – 200 nm (399)) for 2 hours revealed that it could not traverse 0.45 µm pores, while there was relatively free diffusion across inserts with a pore size of 3.0 µm (400). Only 5-6% of applied Hepatitis A virus (non-enveloped virus, ~30 nm (401)) diffused across collagen-coated Transwell inserts with pore size 0.45 µm (402), while with a pore size of 3.0 µm virus diffusion was around 30% (403). Diffusion of HSV-1 (enveloped virus, 150 – 200 nm (404)) across Transwell inserts with 0.4 µm pore size is limited and was further reduced when the insert was coated (405). Similar results were shown for Mumps virus (enveloped virus, 300 – 600 nm

(406)), where around 10% of the inoculum diffused through inserts with pore size 0.4 µm, while around 30% diffused across 3.0 µm inserts (324).

Although cell culture inserts with a pore size of 3.0 µm allow greater virus diffusion, a critical caveat is that epithelial cells can migrate through 3.0 µm pores (407, 408). Thus, the cell culture model will no longer represent a polarised epithelial cell layer with an apical and basolateral compartment. Pore size must therefore be optimised to allow maximal virus diffusion without allowing epithelial cell migration across the insert. In **paper 2** we optimised this by first assessing diffusion rate of BKPyV for inserts with pore size 0.45, 1.0 and 3.0 µm. Since, RPTECs could migrate through pores of 3.0 µm, we chose pore size 1.0 µm since it allowed the greatest diffusion while still restricting the cells to the apical side of the insert.

4.4 The use of density gradient-purified virus

In **paper 3** we aimed to examine cytoplasmic vacuolisation, a cytopathic effect that BKPyV induces in some human cells. When studying viruses, viral infection can be initiated either by transfecting viral genomes into cells or by infection. Infections can be performed with purified virus or with infectious supernatants or lysates derived from infected cells. When studying cytopathic effects and cellular changes induced by a virus it is important to be aware that transfection and infection with supernatants or lysates can influence the host cells and induce cellular changes that can be misinterpreted as effects induced by the virus. For instance, supernatants and lysates can contain a range of molecules, including damage-associated and pathogen-associated molecular patterns that can influence a range of cellular processes and induce inflammation (409). Treatment of primary human RPTECs with supernatant from necrotic RPTECs induced pathogen-recognition receptors, MAP kinase signalling and stimulated inflammatory pathways (410). Transfection can have cytotoxic effects and induce interferon pathways and reduce cell viability (411). To avoid such artefacts, we used BKPyV purified by caesium-chloride density gradient ultracentrifugation. This separates the virus from the other proteins in the infectious supernatant or lysate by density, yielding a pure virus stock with few contaminants. Use of purified virus stocks allowed us to be sure that the induced changes were caused by the virus and not artefacts induced by transfection or by cellular factors in an infectious supernatant or lysate.

Use of density gradient-purified virus was also advantageous in **paper 2**, as purified virus has been shown to exhibit greater diffusion through cell culture inserts compared to more crude virus preparations such as pelleted virus (394).

4.5 Time-lapse microscopy to study BKPyV infected cells at the single-cell level

Studies of virus-induced effects have typically been conducted by studying cell populations in bulk. This has yielded immense knowledge and understanding of virus-host interactions. However, it can be challenging to detect rare or brief events in a bulk population, for instance the exact timepoint of progeny virus release or when the first cell undergoes cell death or vacuolisation. In an effort to answer this, we performed time-lapse microscopy to directly visualise these events at the single cell level.

In **paper 2** we investigated when progeny release and cell death occur in an effort to determine if progeny release is lytic or non-lytic. To do this, we measured progeny release by sampling the apical and basolateral supernatant at different timepoints and measuring BKPyV DNA load and infectious load (fluorescent focus units/ml). Cell death was measured by bulk techniques, measuring LDH release and CellTox-fluorescence, and at the single-cell level by time-lapse microscopy. For time-lapse microscopy we imaged cells with a 5x objective and 2x tube lens, which allowed us to directly visualise when cells became permeabilised. When we used bulk techniques, we could first detect an increase in cell death at 120 hpi. With time-lapse microscopy, we detected an increase in cell death already at 72 hpi. Furthermore, we observed new permeabilised cells before 48 hpi in some fields of view. This showcase the increased sensitivity single-cell methods can yield. One drawback of our approach is the limited resolution of live-cell imaging of cell culture inserts. This is caused by the distance between the insert and the objective, which surpasses the working distance of many objectives. We were therefore limited to a 5x objective with a 2x tube lens. This limited us to partially visualise single cells, but with little detail of their morphology. Despite this limitation, time-lapse microscopy allowed us to detect cell death earlier than the bulk methods used.

Another aspect of **paper 2** where time-lapse microscopy proved useful was examination of cell detachment. By first harvesting supernatants in bulk, we detected increased cell detachment from BKPyV infected inserts. Time-lapse microscopy then enabled us to visualise and describe how individual cells detached. Thus, revealing that a large fraction of cells underwent extrusion.

This highlights how time-lapse microscopy at the single-cell level can yield additional information compared to bulk analysis.

In **paper 3** we investigated a similar issue, namely if there is a link between BKPyV-induced vacuolisation, cell death and progeny release, as a recent study proposed that vacuolisation precedes cell death and progeny release during SV40 infection (412). In that study, cell cultures were investigated in bulk to assess vacuolisation, cell death and progeny release in parallel cell cultures at different timepoints throughout the replication cycle. When examining this question, the temporal resolution is especially important to keep in mind. Cytoplasmic vacuolisation occurs only a few hours after virus binding (376, 413). It is therefore necessary to have at least equally high temporal resolution to accurately determine what occurs first of cell death and vacuolisation. To investigate which of the two occurred first, we investigated single cells by time-lapse microscopy with a high temporal resolution of 15 to 30 minutes.

4.6 Imaging of vacuoles and endosomal compartments

In **paper 3** we utilised a combination of staining and imaging techniques to characterise BKPyV-induced vacuoles. Immunofluorescence staining is an essential method that is used to stain and visualise various molecules in a biological sample (414). Cells are first fixed and permeabilised before antibodies are used to label a specific target protein or molecule. For direct labelling the primary antibody must have a fluorochrome label, while for indirect labelling, which we used, an additional secondary fluorochrome-conjugated antibody is utilised. Fluorescence microscopy can then be used to visualise the distribution or location of the target molecule in the cell.

Endosomal compartments and vacuoles can be particularly challenging to image as fixation can alter their morphology and even disrupt them (102). To avoid fixation artefacts, live-cell imaging combined with transient expression of fluorescently tagged proteins or fluorescent dyes that mark specific subcellular compartments and organelles may be a good alternative (414). Transient expression of proteins has drawbacks as the protein is typically overexpressed, which can lead to unphysiological localisation and function of the protein compared to endogenously expressed protein (414, 415). Moreover, the fluorescent tag itself can affect protein localisation and function. Lastly, transfection and transient expression can cause cytotoxicity and induce inflammatory signalling such as interferon responses (411, 416). Alternatively, one can perform stable transfection to stably express a protein. This is done by

genomic integration of the gene or formation of an episomal plasmid with subsequent selection and expansion to establish stably transfected cells. However, primary cells are typically difficult to stably transfect (416) and stable transfection can induce a range of cellular changes, including altered proliferation, apoptosis and even cause mutations (417). Cytoplasmic vacuolisation has been shown to be cell-type dependent, it was therefore not an option to use stably transfected cell lines since stable transfection potentially could affect the cells' ability to undergo vacuolisation. Furthermore, a finding generated in relevant primary renal epithelial cells is possibly more transferable to *in vivo* BKPyV biology than if it is generated in a cell line.

We utilised several strategies to image vacuoles and vacuolisation. All phase-contrast and oblique contrast microscopy to visualise vacuolisation was performed on live-cells to avoid fixation artefacts. When visualising intracellular compartments, we performed both live-cell microscopy with fluorescent dyes and transient expression of fluorescently tagged proteins as well as immunofluorescence staining of endogenous proteins in fixed cells. For cells that transiently expressed proteins, we took care to image cells where the protein of interest was low to moderately expressed and avoided cells that strongly overexpressed the protein. Our use of both live-cell microscopy techniques and imaging of fixed and stained samples is a strength. This enables us to be more certain that our observations are accurate and not artefacts from overexpression or fixation.

To investigate if viral particles were associated with vacuoles, we used an antibody and an antiserum directed against BKPyV Vp1 in combination with an antibody directed against proteins in the vacuole membrane. We could then perform confocal microscopy to see whether Vp1 colocalised with the membrane protein and if there was Vp1-staining within the vacuole.

Lastly, we utilised transmission electron microscopy (TEM), an alternative imaging technique to light microscopy. With TEM, the sample is illuminated by an electron beam instead of light. This yields superior resolution compared to light microscopy since TEM is not limited by the diffraction limit (418-421). The sample preparation for TEM includes several steps including fixation, typically with aldehydes or high-pressure freezing, followed by resin-embedding, sectioning and staining with heavy metals. TEM is very useful to study viruses, as the high resolution allows direct visualisation of both cell-free and intracellular viral particles (418). Furthermore, TEM is useful to study vacuoles and endosomal structures as it enables examination of both the membrane and the contents of the structure (422, 423). We therefore utilised TEM to examine the ultrastructure of BKPyV-induced vacuoles and to see if they

contained viral particles. One drawback of TEM is a small field of view, which makes rare events challenging to detect (418). However, since vacuolisation is prevalent when a high infectious dose is used, vacuolised cells are reasonably easy to find. We could therefore perform conventional TEM and identify vacuolised cells. We used chemical fixation in our TEM preparation. Although widely used, chemical fixation can give fixation artefacts and endosomal structures look different after chemical fixation compared to cryofixation (422). Cryofixation is therefore viewed as better at preserving the intracellular ultrastructure and particularly membranes (422). For future studies of the ultrastructure of vacuoles, cryofixation would be preferred over chemical fixation.

5 Results and Discussion

5.1 BKPyV risk stratification and screening of kidney transplant recipients

BKPyV nephropathy is one of the most important infectious complications in kidney transplant patients. Up to 15% of all kidney transplant recipients develop BKPyV nephropathy. Importantly, BKPyV nephropathy is associated with reduced allograft function. Ultimately, the allograft can be lost, and the patient has to return to dialysis pending re-transplantation (172). Regrettably, there is no effective anti-viral treatment and reducing the immunosuppressive anti-rejection therapy is the only treatment option for BKPyV nephropathy.

Paper 1 is a case report on two kidney transplant recipients that developed BKPyV nephropathy in parallel shortly after transplantation of kidneys from the same deceased donor. The first plasma samples that were directly analysed for BKPyV DNA were taken from recipient 1 and 2 at 5- and 8-weeks post-transplantation, respectively. In both recipients this revealed a BKPyV DNAemia qualifying for the diagnosis of presumed BKPyV nephropathy. First at 12 weeks post-transplantation, when biopsy-proven BKPyV nephropathy was diagnosed in both recipients, was immunosuppression reduced. Retrospectively, we found that both recipients had low levels of BKPyV-specific neutralising antibodies prior to transplantation, while the donor exhibited high levels. After developing BKPyV DNAemia, a robust antibody response that included a large increase in BKPyV-specific neutralising antibodies was observed. Despite this, only one of the recipients had cleared the BKPyV DNAemia at one year post-transplantation.

The results in **paper 1** should be carefully interpreted since our study only includes two patients and one donor. However, it highlights some important aspects on management of BKPyV replication and disease in kidney transplant patients. The current guidelines recommend to screen kidney transplant patients monthly for BKPyV DNAemia during the first 9 months post transplantation (172). If patients have a BKPyV DNA load $>10^4$ copies/ml, the diagnosis of presumed BKPyV nephropathy can be set and immunosuppressive treatment should be promptly reduced. Our retrospect analysis revealed that both recipients had a BKPyV DNA load $>10^4$ copies/ml already at week 5. Despite this, reduction in immunosuppressive treatment was first performed 12 weeks post transplantation, when biopsy-proven BKPyV nephropathy was first diagnosed. Of note, in week 8, recipient 2 showed increasing serum creatinine and a BKPyV DNA load of 1.12×10^6 copies/ml and therefore underwent an allograft biopsy. Despite the high-level BKPyV DNAemia, the immunohistochemical staining for LTag was negative.

This illustrates why presumed BKPyV nephropathy should be diagnosed based on the plasma BKPyV DNA load and not depend on LTag staining in allograft biopsies. BKPyV replication can be focally distributed in the allograft, especially early in the disease. In a study by Drachenberg et al. up to 35% of examined allograft biopsies were negative despite active BKPyV replication (179). Importantly, an increase in serum creatinine suggests allograft damage and is therefore a slow marker of BKPyV nephropathy compared to BKPyV DNAemia which will increase prior to severe allograft damage (221). Delay in the diagnosis can have serious consequences as millions of renal tubule epithelial cells have been estimated to be lost per day when the plasma BKPyV DNA load is 5×10^4 copies/ml or more (424, 425), thereby reducing allograft function and survival (172, 426-428). Reduction of the immunosuppressive treatment is important since it contributes to resolution of BKPyV nephropathy and preserves allograft function (429-438). Although reduced immunosuppression can increase the risk of acute rejection and development of donor-specific antibodies (172). Summarised, whenever possible, an active screening for BKPyV DNAemia should be performed as a low adherence to the screening recommendations delay the diagnosis of BKPyV nephropathy.

As mentioned in the introduction, a low BKPyV-specific antibody titre in the recipient and/or high antibody titres in the donor have been associated with increased risk of BKPyV DNAemia and BKPyV nephropathy (52, 182, 187, 190, 209, 439). Serological assessment of donor and recipient has therefore been discussed as a potential risk stratification strategy (172). At the time of transplantation, both recipients were seropositive for BKPyV on ELISA and HIA but exhibited low levels of neutralising antibodies with a neutralisation titre of only 1:10. In contrast, the donor had very high levels of antibodies and neutralising antibodies measured with ELISA (normalised optical density of 2.329), HIA (titre of 320), and neutralisation assay (titre of >640 IC50), which suggested recent BKPyV replication. Although conclusions cannot be drawn from this limited study, our results agree with other studies that have investigated the association between BKPyV-specific antibody titres and risk of BKPyV replication and nephropathy. Solis and colleagues reported that the genotype-specific neutralising antibody titre pre-transplantation could predict development of BKPyV replication and nephropathy (185). Similar results have been reported by Dakroub et al., who found a protective effect of high BKPyV-specific antibody levels in recipients at the time of transplantation (439). Moreover, a seropositive donor is also associated with increased risk of BKPyV replication compared to a seronegative donor (187, 209, 439, 440). This can be further expanded to the antibody titre of the donor, as there is increasing risk for BKPyV replication and disease with increasing

antibody titre in the donor (187, 439). Importantly, Wunderink and colleagues found that recipients with low BKPyV-specific antibody titres that received an allograft from a highly seroreactive donor, just like we found in our donor and recipients, had a 10-fold increased risk of developing BKPyV DNAemia. Summarised, risk stratification based on donor/recipient serostatus and antibody titres is a promising strategy and our study is a contribution to the body of evidence that support this. One can imagine that this can be used to identify high-risk recipients in need of intensified screening or tapered immunosuppressive treatment. However, clinical studies are warranted to determine the clinical benefit of such strategies.

5.2 Host cell release of progeny virus

BKPyV is a non-enveloped virus and in general, the consensus has long been that non-enveloped viruses are mainly released via lysis of the host cell (441). This is supported by multiple *in vitro* studies demonstrating lytic release of non-enveloped viruses. Similar results have been shown for BKPyV and the related polyomaviruses SV40, which both cause extensive lysis in infected cell cultures (56, 129, 131, 132, 412). Moreover, infected lysed renal tubular epithelial cells can be seen in biopsies from patients with BKPyV nephropathy (127). Of note, non-lytic virus release via secretory autophagosome, exosomes, microvesicles and protrusion has been described for several non-enveloped enteric RNA viruses (442). Recently, Handala et al. (136) proposed non-lytic release of BKPyV via extracellular vesicles, while Evans et al. (135) reported that BKPyV can be released in a non-lytic manner that depend on anion homeostasis. Additionally, non-lytic release has been reported for the two related polyomaviruses SV40 (140) and JCPyV (137, 138).

In **paper 2** and **3** we investigated the relationship between lysis of BKPyV infected RPTECs and progeny release. We visualised lysis of BKPyV infected RPTECs, supporting the existing literature that BKPyV induces host cell lysis. Moreover, lysis co-occurred with progeny release in both non-polarised and polarised RPTECs, indicating that lytic release is the main release mechanism for BKPyV. It should be noted that we did not investigate potential non-lytic release mechanisms. Although the majority of progeny release from polarised RPTECs occurred concomitant with lysis, we did detect beginning progeny release before we could detect lysis. This could indicate a parallel non-lytic release mechanism that supplements lytic release. Alternatively, we missed some lysed cells due to the resolution of the time-lapse microscopy. In contrast, with non-polarised RPTECs, we could detect lysis prior to the first sampled timepoint for progeny release. Polarised RPTECs may be better equipped to perform non-lytic

release, perhaps due to apico-basal polarity or differences in the secretory systems. In support of this, in a 35 year old study, SV40 was reported to be released in a non-lytic manner from polarised simian epithelial cells (140). For future research, polarised RPTECs seem to be a more suitable model to investigate non-lytic release of BKPyV than non-polarised RPTECs.

5.3 Dissemination of BKPyV throughout the reno-urinary tract

In vivo studies have demonstrated that BKPyV is shed in the urine of both healthy and immunocompromised individuals, while BKPyV DNAemia is almost exclusively seen in immunocompromised patients with high-levels BKPyV replication (150, 170, 172). However, we know little of how the virus reaches these compartments. In **paper 2** we sought to answer this question by characterising viral entry and release in polarised RPTECs *in vitro*. Interestingly, entry of BKPyV mainly occurred via the apical membranes. As previously mentioned, virus release seemed to be mainly lytic, and progeny virus was first detected in the apical compartment. In our model the apical compartment represents the tubular filtrate or pre-urine. Our finding therefore indicates that *in vivo* BKPyV is spread downstream the tubular system in the tubular filtrate. Entry of BKPyV into the basolateral compartment occurred later in the infection, at a timepoint when widespread lysis was evident.

That BKPyV was mainly found in the apical compartment, despite lytic release, can be explained by a combination of factors. Firstly, as viral entry is apical, the released progeny virus will presumably bind to the apical membrane, thereby containing the virus in the apical compartment. Based on **paper 3**, we think that most virus will bind to the cells closest to the lysed cell. Furthermore, when we measured the transepithelial resistance, a measure for the tightness of the epithelium, the transepithelial resistance was largely unchanged indicating that the epithelium was intact at the time of the first progeny release. This will also contribute to restriction of the progeny virus in the apical compartment. Lastly, examination of the apical supernatants of BKPyV infected inserts revealed decoy-like cells. These cells were BKPyV infected and could transmit infection to uninfected RPTECs. We performed live-cell imaging of confluent RPTEC cell layers to examine the shedding process and observed extrusion of dead cells. Extrusion allows epithelial cell layers to remove or shed dead or infected cells without compromising the integrity of the epithelium (443) The process is often triggered by apoptosis, oncogenic transformation or overcrowding of cells. Infection is another inducer of extrusion. For instance, *Salmonella enterica* and Enterovirus A71 can induce extrusion of intestinal epithelial cells (444, 445). Respiratory syncytial virus and Measles virus have been reported to

induce cell shedding in airway epithelial cell cultures (326, 446). As far as we know, *in vitro* extrusion of infected RPTECs has not previously been reported. Thus, dead BKPyV infected cells are extruded into the apical compartment, leading to release of infectious virus and decoy-like cells into this compartment. Extrusion of dead BKPyV-infected cells possibly explains why the barrier integrity was maintained despite widespread lysis. Although, the mechanism behind the cell death was not investigated, the dead cells did not appear to undergo apoptosis and did not display features of extruded apoptotic cells (447, 448).

Importantly, our results of apical dissemination of cell-free virus and extrusion of infectious decoy-like cells agree with previous studies on kidney transplant recipients. Drachenberg et al. (127) observed that lysis of infected tubular cells leads to massive release of virus into the tubular lumen. The cell surface of nearby cells was covered with viral particles, showcasing how released progeny virus bind to cells after release. Cell-free viral particles did not cross the basement membrane and were restricted to tubules with infected cells. Detached tubular epithelial cells have been observed in the tubular lumen (128, 178, 449) and shedding of decoy cells is a hallmark of high-level BKPyV replication (178, 450, 451). An important caveat of our study is the lack of shear stress or flow since we used a static cell culture technique. We could therefore not assess if spread occurs locally or if released virus and detached cells can travel down an artificial tubular system to infect distant cells. However, since decoy cells is frequently seen in the urine of kidney transplant patients it seems plausible that at least decoy cells can spread BKPyV downstream in the tubular system and to the bladder. Interestingly, our findings of dissemination along the tubular system resonates with the model suggested by Funk et al. (424). They propose that BKPyV replication is initiated in allograft tubular epithelial cells before BKPyV is spread to the bladder, where viral amplification occurs followed by ureteric reflux back to the allograft for multi-site spread.

The importance of cell-to-cell spread of BKPyV is further highlighted in **paper 3**. Here, we studied cytoplasmic vacuolisation, a phenomenon that we propose is induced by uptake of massive amounts of BKPyV into RPTECs. Interestingly, when we did time-lapse microscopy of BKPyV infected RPTECs, we observed that cytoplasmic vacuolisation was concentrated around dead, infected cells. This supports the importance of dead infected cells for spread of BKPyV and indicates that cell-to-cell spread is important for BKPyV dissemination. We do not know how cell-to-cell spread of BKPyV occurs, but could be caused by locally increased concentration of BKPyV due to retention of BKPyV on the lysed cell and the closest neighbour

cells (452), as observed in BKPyV nephropathy biopsies (127). The latter study also noted that tubular epithelial cells seem to be infected via direct contact with dead infected cells.

Taken together, our results suggest that intra-renal BKPyV dissemination occurs via lytic release of cell-free virus and extrusion of infectious decoy-like cells into the tubular fluid. Moreover, *de novo* infection from progeny virus seems to occur via both cell-free virus and by cell-to-cell spread from dead infected cells.

5.4 Cytoplasmic vacuolisation is an early event in the BKPyV replication cycle

Cytoplasmic vacuolisation is a known cytopathic effect that can be caused by a range of causes including viral infection (376, 412, 413, 453), cell death (454, 455), chemical compounds (456, 457) and bacterial toxins (458, 459). Of particular interest to us, is the fact that SV40, a polyomavirus closely related to BKPyV, is known to cause cytoplasmic vacuolisation. SV40-induced cytoplasmic vacuolisation is reported to be triggered by SV40 binding to host cells (376, 413). Moreover, cytoplasmic vacuolisation has been reported to be related to SV40-induced cell death and progeny release (412). The evidence regarding BKPyV and cytoplasmic vacuolisation is conflicting as results differ between different cell types. Luo et al. (376) reported that BKPyV pseudovirus could not induce vacuolisation in CV-1 cells, but when the receptor-usage of the pseudovirus was changed to GM1, it was capable of inducing vacuolisation in CV-1 cells. In contrast, human foetal brain cells and human embryonic fibroblasts (371, 378) as well as simian Vero cells (377, 379) have been reported to develop vacuoles during BKPyV infection.

In **paper 3** we first determined that BKPyV infection of RPTECs induces cytoplasmic vacuolisation. Moreover, we show that this can occur at two timepoints. First, early vacuolization which occurs shortly after BKPyV addition to the cells, if a sufficiently high infectious dose is used. Second, a late round of vacuolisation follows and co-occurs with progeny release. Our results are in agreement with previous work on SV40 as both Luo et al. (376) and Miyamura and Kitahara (413) reported a similar pattern of vacuolisation. Using different staining and microscopy techniques we did a comprehensive characterisation of the origin of the vacuoles. The vacuoles were endo-/lysosomal structures as they were positive for several markers associated with the endocytic pathway, including Rab7 and Lamp1. TEM confirmed that the vacuoles looked like endosomes, lysosomes and endolysosomes and that they contained virus. The mentioned studies (376, 413), demonstrated that virus binding is a

requisite for vacuolisation as neutralising antibodies blocked vacuolisation. We observed the same in our study. Preincubating the virus with neutralising antibodies or treating cells with neutralising antibodies after infection, blocked early and late vacuolisation, respectively. Imaging of vacuolised cells that had been stained for Vp1 revealed that vacuolised RPTECs exhibited very strong Vp1-staining, indicating that vacuolisation is related to uptake of BKPyV. This was further strengthened by our time-lapse microscopy where we visualised that cell death preceded late vacuolisation and that late vacuolisation occurred in cells surrounding dead infected cells. Furthermore, disruption of vacuolization had little effect on progeny release and cell death. When we stained BKPyV infected RPTECs for LTag and Vp1, we observed that the majority of late vacuolised cells were negative for nuclear Vp1, while about 58% exhibited nuclear expression of LTag. Many vacuolised cells only exhibited strong cytoplasmic Vp1 staining, indicating that virus had recently been taken up and that cytoplasmic vacuolisation occurs in cells that have recently been infected with a high infectious load. Summarised, this thesis demonstrates that cytoplasmic vacuolisation is an early event in the replication cycle of BKPyV in RPTECs and that it is not related to BKPyV-induced cell death.

In **paper 2**, we observed late vacuolisation in BKPyV infected polarised RPTECs. In **paper 3**, this was further expanded upon as we observed early vacuolisation in polarised RPTECs after infection with a high infectious dose. Thus, demonstrating that cytoplasmic vacuolisation occurs in both non-polarised and polarised RPTECs.

5.5 Cytoplasmic vacuolization is caused by a massive uptake of BKPyV into the endocytic pathway

We sought to further characterise the role of vacuolisation in the replication cycle of BKPyV. As mentioned, vacuolisation relied on a high uptake of BKPyV into the endocytic pathway. Moreover, vacuoles were positive for Rab7 and Lamp1 and had an acidic pH and can therefore represent degradative endolysosomes (295, 460). Accumulation of degradative endolysosomes could be a potential host-defence strategy to degrade incoming virus. However, vacuolised cells became infected, thus vacuolisation did not protect the cells from BKPyV infection.

Anoth er possibility is that vacuolisation is related to trafficking of large amounts of incoming virus. BKPyV have previously been reported to exploit endosomes for ER-delivery (98, 100-103, 461). The vacuoles contained viral particles and were positive for markers of early (early endosome antigen 1) and late endosomes (Rab7) and can therefore potentially partake in

transport of BKPyV. Treatment with the vacuolar H^+-ATPase (V-ATPase) inhibitor bafilomycin A at 0 hpi blocked both vacuolisation and early transport steps of BKPyV. Treatment with bafilomycin A at 2 hpi blocked vacuolisation without affecting BKPyV replication, demonstrating that vacuolisation is related to BKPyV transport, but it is not obligate for BKPyV infection. Therefore, vacuolisation seems more likely to be caused by a transient overload of the endocytic pathway due to a massive uptake of BKPyV. After uptake, BKPyV is transported to early endosomes with subsequent maturation into late endosomes and endolysosomes, as shown by confocal microscopy and TEM. However, a caveat of **paper 3** is that we have not examined how BKPyV reaches the ER nor if vacuolisation is related to the amount of virus that successfully transport to the ER. We therefore do not know the full extent of similarities between the vacuoles and the transport pathway that BKPyV utilises. We believe that the vacuoles most likely end up as degradative endolysosomes. It therefore seems plausible that the successful viral particles that reach the ER must diverge from the vacuoles at some point or follow a parallel transport pathway to the ER.

5.6 The use of neutralising antibodies for treatment of BKPyV nephropathy

The benefit of BKPyV-specific neutralising antibodies in clearance of BKPyV nephropathy and the potential of utilizing commercial neutralising antibodies as a treatment of BKPyV nephropathy are currently unclear. Solis et al. reported that a robust humoral immune response with a neutralising titre of at least 10 000 was associated with viral clearance (185). However, other studies have failed to find similar associations between antibody titres and viral clearance (182, 193). Treatment of BKPyV DNAemia with IVIGs and a monoclonal antibody may also be beneficial, but randomised trials are lacking (225, 229).

In **paper 2** we utilised our polarised cell culture model to examine if a BKPyV Vp1-specific neutralising antibody could traverse the epithelial cell layer from the basolateral side to inhibit spread of BKPyV. We found that addition of neutralising antibodies led to a 35% decrease in infected cells. This suggests that the antibody can undergo transcytosis and neutralise progeny virus in the apical compartment. Similar *in vitro* results were recently reported by Sato et al., who reported that IVIGs could both block BKPyV infection and reduce spread (226). Although there are significant differences between the studies, both studies indicate that BKPyV-specific neutralising antibodies can reduce spread of BKPyV. An important aspect of neutralising antibodies for treatment of BKPyV nephropathy is renal penetration. Can the antibody access the tubular lumen to inhibit BKPyV infection? Our study suggests that antibodies that traverse

the epithelial cell layer inhibit BKPyV spread via the apical compartment. Of note, we have not determined how the antibodies enter the apical compartment, and it could occur via paracellular transport and not transcytosis. Our results support the potential utility of neutralising antibodies in treatment of BKPyV disease. However, there are still uncertainties. Our cell culture model only consists of a single cell layer on a permeable membrane but *in vivo*, the road from the blood to the renal tubular lumen has more obstacles. Antibodies must traverse the endothelium of the blood vessel, the renal interstitial space and basement membrane before they can undergo transcytosis into the renal tubular lumen. We can therefore not be certain that BKPyV-specific neutralising antibodies can reach the renal tubular lumen *in vivo*.

In **paper 1**, both recipients developed high levels of BKPyV-specific antibodies. Use of a neutralisation assay confirmed that the antibodies exhibited neutralising activity with a neutralisation titre >10 000. Despite high levels of neutralising antibodies, only one of the recipients cleared BKPyV DNAemia, showing that a robust neutralising antibody response is not enough to clear BKPyV replication. We did not examine the cell-mediated immunity of the patients but speculate that the BKPyV-specific cell-mediated immunity differed between the two recipients. In support of this, high levels of BKPyV-specific T-cells, especially $CD8^+$ cytotoxic T-cells, is associated with viral clearance (190, 192, 193, 197, 198).

In this thesis we also made some interesting observations that could be potential mechanisms for evasion from neutralising antibodies. In **paper 2** we demonstrated how BKPyV could be transmitted via extruded decoy-like cells. Extruded cells potentially act as vessels for distant spread of BKPyV while simultaneously protecting the virus from neutralising antibodies. Similar observations have been reported for Enterovirus A71, which induce extrusion of infected intestinal epithelial cells that can transmit enterovirus (444). In **paper 3**, we observed that BKPyV-induced late cytoplasmic vacuolisation was focal and concentrated around lysed cells. This indicates that dead infected cells can cause infection of the neighbouring cells via cell-to-cell spread. Another interesting observation in **paper 3** was that despite a strong inhibitory effect of neutralising antibodies on vacuolisation, we did observe some vacuolised cells with time-lapse microscopy. These cells were concentrated around lysed cells. Although vacuolisation was clearly inhibited it seems that some viral particles manage to enter surrounding cells in the presence of neutralising antibodies. We do not know the mechanism behind this, but it could be due to cell-to-cell spread that partially protects the virus from neutralisation (452). One possibility is that the retention of virus on dead cells increases the local concentration of virus to a level that exceed the amount of virus that the antibodies can

neutralise. Other potential escape mechanism include hiding within extracellular vesicles (136, 137) and neutralisation escape by accumulation capsid protein mutations (13, 46, 258, 462, 463). The latter did probably not apply to our study, as cells were only investigated until 5 days post-infection. Future *in vitro* studies should seek to elucidate if decoy cells and dead, infected cells can protect BKPyV from neutralisation.

Since BKPyV-specific anti-viral drugs are lacking, BKPyV-specific neutralising antibodies could be a promising therapy for BKPyV disease. Our *in vitro* studies demonstrate that BKPyV-specific neutralising antibodies can enter the tubular lumen, however we also observed potential mechanism for antibody evasion. Randomised clinical trials are urgently needed to determine if IVIGs and BKPyV-specific neutralising antibodies are efficient therapies for BKPyV nephropathy.

6 Conclusions

This thesis aimed to increase our understanding of important aspects of the BKPyV biology and how BKPyV interact with the human host.

In **paper 1** we characterised the antibody response and BKPyV strain in two kidney transplant recipients and their common donor after both recipients developed BKPyV nephropathy shortly after transplantation. Based on our results we conclude that the recipients had a donor-derived infection. Our study highlights the importance of screening for BKPyV DNAemia, as BKPyV DNAemia clearly preceded histology-proven BKPyV nephropathy. Moreover, our study demonstrates that a BKPyV negative kidney biopsy cannot rule out BKPyV nephropathy. We detected known risk factors for development of BKPyV DNAemia and nephropathy such as a very high BKPyV-specific antibody titre in the donor in combination with low BKPyV-specific antibody titres in the recipients at transplantation. Both recipients developed high titres of neutralising antibodies, but only one of them cleared the BKPyV DNAemia, showcasing that in some patients, high titres of neutralising antibodies are not enough to clear BKPyV.

In **paper 2**, we utilised a polarised cell culture model of RPTECs to demonstrate that entry and release of BKPyV mainly occur in the apical compartment, indicating that BKPyV spread in the kidney via the tubular fluid. BKPyV infection of polarised RPTECs ultimately ended in host cell lysis and release of progeny virus. Moreover, BKPyV infection caused apical extrusion of lysed infected cells into the apical compartment. These cells were similar to decoy-cells and could transmit infection. Furthermore, neutralising antibodies could traverse the renal epithelium to inhibit spread of BKPyV. Our results suggest that BKPyV *in vivo* can spread in the tubular fluid and potentially use decoy cells as a vessel to facilitate distant spread and avoid antibody neutralisation.

In **paper 3**, we determine that BKPyV induces cytoplasmic vacuolisation in RPTECs. Cytoplasmic vacuolisation was found to be an early event in the replication cycle and occur due to massive uptake of BKPyV that causes accumulation and enlargement of endo-/lysosomal structures. Blocking BKPyV uptake with neutralising antibodies inhibits vacuolisation, indicating that both binding and uptake of BKPyV is necessary for vacuolisation. TEM showed that vacuoles contained membrane bound BKPyV. We therefore speculate that vacuolisation is caused by a transient overload of the endocytic pathway. As late vacuolization occurred in cells

surrounding lysed infected cells, we suggest that BKPyV uses cell-to cell spread. Potentially this helps BKPyV to escape antibody neutralisation.

Collectively, this thesis deepens our understanding of how BKPyV interacts with the tubular epithelial cells and spread in the kidney. Our characterisation of two fulminant cases of BKPyV nephropathy complement the existing understanding of management of BKPyV nephropathy. Furthermore, the study demonstrates that in some patients, neutralising antibodies are not enough to clear BKPyV replication. We demonstrate how BKPyV disseminates via the apical compartment *in vitro* and propose that BKPyV disseminates via the tubular fluid *in vivo*. Lastly, this thesis unveils two new features of BKPyV replication, that decoy cells are released by extrusion and that BKPyV utilises cell-to-cell spread, indicating that BKPyV utilises several methods for successful spread.

7 Perspectives

This thesis lays the groundwork for future research on BK Polyomavirus. As mentioned, similar characteristics as those we found in the donor and recipients in **paper 1,** have already been described in larger retrospective and prospective studies on kidney transplant recipients. Risk stratification based on BKPyV serostatus and antibody levels is therefore a promising strategy for early detection or to start pre-emptive measures to prevent BKPyV nephropathy. However, before it can be implemented in the clinic, randomised interventional studies are needed to determine their clinical utility.

Paper 2 demonstrates the usefulness of a polarised cell culture model to study BKPyV-host interactions. This model can be used to address several knowledge gaps in BKPyV biology. BKPyV have been proposed to be spread via EVs (136). Our model can for instance be used to study if release of BKPyV-containing EVs is uni- or bidirectional. Moreover, **paper 2** demonstrates spread of BKPyV via extruded cells. We hypothesise that this can protect BKPyV from neutralising antibodies and support distant spread of BKPyV, but further studies are needed to fully understand the role of extrusion and if this occurs *in vivo*. Lastly, the model can be expanded to create a more complex model, for instance by incorporating shear stress or organoid technology. This can for instance be used to further examine how BKPyV disseminate through the tubular system.

In **paper 3**, we determine that BKPyV induces cytoplasmic vacuolisation and that this is an early event in the replication cycle. We speculate that vacuolisation is caused by a transient overload of the endocytic pathway. Our finding of viral particles in endosomes and endolysosomes indicate that this may be the regular transport pathway for BKPyV. However, we do not know for certain which transport pathway the successful viral particle that reaches the nucleus follows. More research is needed to fully map BKPyV trafficking to the ER and nucelus, and to understand the link between BKPyV-induced vacuolization and endocytic transport of BKPyV. Understanding how BKPyV transports to the ER and from there to the nucleus is necessary to fully understand BKPyV entry. Ultimately, this can aid in identifying targets for novel anti-viral drugs.

8 References

1. Moens U, Calvignac-Spencer S, Lauber C, Ramqvist T, Feltkamp MCW, Daugherty MD, et al. ICTV Virus Taxonomy Profile: Polyomaviridae. J Gen Virol. 2017;98(6):1159-60.
2. DeCaprio JA, Imperiale MJ, Hirsch HH. Polyomaviridae. In: Howley PM, Knipe DM, editors. Fields Virology: DNA Viruses. 7 ed: Lippincott Williams & Wilkins; 2021. p. 1-44.
3. DeCaprio JA, Garcea RL. A cornucopia of human polyomaviruses. Nat Rev Microbiol. 2013;11(4):264-76.
4. Hurdiss Daniel L, Morgan Ethan L, Thompson Rebecca F, Prescott Emma L, Panou Margarita M, Macdonald A, Ranson Neil A. New Structural Insights into the Genome and Minor Capsid Proteins of BK Polyomavirus using Cryo-Electron Microscopy. Structure. 2016;24(4):528-36.
5. Stehle T, Gamblin SJ, Yan Y, Harrison SC. The structure of simian virus 40 refined at 3.1 A resolution. Structure. 1996;4(2):165-82.
6. Gross L. A filterable agent, recovered from Ak leukemic extracts, causing salivary gland carcinomas in C3H mice. Proc Soc Exp Biol Med. 1953;83(2):414-21.
7. Stewart SE, Eddy BE, Gochenour AM, Borgese NG, Grubbs GE. The induction of neoplasms with a substance released from mouse tumors by tissue culture. Virology. 1957;3(2):380-400.
8. Buck CB, Van Doorslaer K, Peretti A, Geoghegan EM, Tisza MJ, An P, et al. The Ancient Evolutionary History of Polyomaviruses. PLOS Pathog. 2016;12(4):e1005574.
9. Sweet BH, Hilleman MR. The vacuolating virus, S.V. 40. Proc Soc Exp Biol Med. 1960;105:420-7.
10. Fanning E, Zhao K. SV40 DNA replication: From the A gene to a nanomachine. Virology. 2009;384(2):352-9.
11. Wilson JJ, Lin E, Pack CD, Frost EL, Hadley A, Swimm AI, et al. Gamma Interferon Controls Mouse Polyomavirus Infection In Vivo. J Virol. 2011;85(19):10126-34.
12. Han Lee ED, Kemball CC, Wang J, Dong Y, Stapler DC, Jr., Hamby KM, et al. A mouse model for polyomavirus-associated nephropathy of kidney transplants. Am J Transplant. 2006;6(5 Pt 1):913-22.
13. Lauver MD, Jin G, Ayers KN, Carey SN, Specht CS, Abendroth CS, Lukacher AE. T cell deficiency precipitates antibody evasion and emergence of neurovirulent polyomavirus. eLife. 2022;11:e83030.
14. Zaragoza C, Li R-m, Fahle Gary A, Fischer Steven H, Raffeld M, Lewis Andrew M, Kopp Jeffrey B. Squirrel Monkeys Support Replication of BK Virus More Efficiently than Simian Virus 40: an Animal Model for Human BK Virus Infection. J Virol. 2005;79(2):1320-6.
15. An P, Robles MTS, Pipas JM. Large T Antigens of Polyomaviruses: Amazing Molecular Machines. Annu Rev Microbiol. 2012;66(1):213-36.
16. Gardner SD, Field AM, Coleman DV, Hulme B. New human papovavirus (B.K.) isolated from urine after renal transplantation. Lancet. 1971;1(712):1253-7.
17. Padgett BL, Walker DL, ZuRhein GM, Eckroade RJ, Dessel BH. Cultivation of papova-like virus from human brain with progressive multifocal leucoencephalopathy. Lancet. 1971;1(7712):1257-60.
18. Feng H, Shuda M, Chang Y, Moore PS. Clonal integration of a polyomavirus in human Merkel cell carcinoma. Science. 2008;319(5866):1096-100.
19. Nilsson J, Miyazaki N, Xing L, Wu B, Hammar L, Li TC, et al. Structure and assembly of a T=1 virus-like particle in BK polyomavirus. J Virol. 2005;79(9):5337-45.

20. Li TC, Takeda N, Kato K, Nilsson J, Xing L, Haag L, et al. Characterization of self-assembled virus-like particles of human polyomavirus BK generated by recombinant baculoviruses. Virology. 2003;311(1):115-24.
21. Fang CY, Chen HY, Wang M, Chen PL, Chang CF, Chen LS, et al. Global analysis of modifications of the human BK virus structural proteins by LC-MS/MS. Virology. 2010;402(1):164-76.
22. Meneguzzi G, Pignatti PF, Barbanti Brodano G, Milanesi G. Minichromosome from BK virus as a template for transcription in vitro. Proc Natl Acad Sci U S A. 1978;75(3):1126-30.
23. Helle F, Brochot E, Handala L, Martin E, Castelain S, Francois C, Duverlie G. Biology of the BKPyV: An Update. Viruses. 2017;9(11):327.
24. Seif I, Khoury G, Dhar R. The genome of human papovavirus BKV. Cell. 1979;18(4):963-77.
25. Nomburg J, Zou W, Frost TC, Datta C, Vasudevan S, Starrett GJ, et al. Long-read sequencing reveals complex patterns of wraparound transcription in polyomaviruses. PLOS Pathog. 2022;18(4):e1010401.
26. Sullivan CS, Grundhoff AT, Tevethia S, Pipas JM, Ganem D. SV40-encoded microRNAs regulate viral gene expression and reduce susceptibility to cytotoxic T cells. Nature. 2005;435(7042):682-6.
27. Seo GJ, Fink LH, O'Hara B, Atwood WJ, Sullivan CS. Evolutionarily conserved function of a viral microRNA. J Virol. 2008;82(20):9823-8.
28. Zhao L, Imperiale MJ. A Cell Culture Model of BK Polyomavirus Persistence, Genome Recombination, and Reactivation. mBio. 2021;12(5):10.1128/mbio.02356-21.
29. Gosert R, Rinaldo CH, Funk GA, Egli A, Ramos E, Drachenberg CB, Hirsch HH. Polyomavirus BK with rearranged noncoding control region emerge in vivo in renal transplant patients and increase viral replication and cytopathology. J Exp Med. 2008;205(4):841-52.
30. Olsen GH, Andresen PA, Hilmarsen HT, Bjorang O, Scott H, Midtvedt K, Rinaldo CH. Genetic variability in BK Virus regulatory regions in urine and kidney biopsies from renal-transplant patients. J Med Virol. 2006;78(3):384-93.
31. Ambalathingal GR, Francis RS, Smyth MJ, Smith C, Khanna R. BK Polyomavirus: Clinical Aspects, Immune Regulation, and Emerging Therapies. Clin Microbiol Rev. 2017;30(2):503-28.
32. Kelley WL, Georgopoulos C. The T/t common exon of simian virus 40, JC, and BK polyomavirus T antigens can functionally replace the J-domain of the Escherichia coli DnaJ molecular chaperone. Proc Natl Acad Sci U S A. 1997;94(8):3679-84.
33. Peden KWC, Pipas JM. Simian virus 40 mutants with amino-acid substitutions near the amino terminus of large T antigen. Virus Genes. 1992;6(2):107-18.
34. Stubdal H, Zalvide J, Campbell KS, Schweitzer C, Roberts TM, DeCaprio JA. Inactivation of pRB-related proteins p130 and p107 mediated by the J domain of simian virus 40 large T antigen. Mol Cell Biol. 1997;17(9):4979-90.
35. DeCaprio JA, Ludlow JW, Figge J, Shew JY, Huang CM, Lee WH, et al. SV40 large tumor antigen forms a specific complex with the product of the retinoblastoma susceptibility gene. Cell. 1988;54(2):275-83.
36. Harris KF, Christensen JB, Imperiale MJ. BK virus large T antigen: interactions with the retinoblastoma family of tumor suppressor proteins and effects on cellular growth control. J Virol. 1996;70(4):2378-86.
37. Harris KF, Christensen JB, Radany EH, Imperiale MJ. Novel mechanisms of E2F induction by BK virus large-T antigen: requirement of both the pRb-binding and the J domains. Mol Cell Biol. 1998;18(3):1746-56.
38. Lau L, Gray EE, Brunette RL, Stetson DB. DNA tumor virus oncogenes antagonize the cGAS-STING DNA-sensing pathway. Science. 2015;350(6260):568-71.

39. Sowd GA, Fanning E. A Wolf in Sheep's Clothing: SV40 Co-opts Host Genome Maintenance Proteins to Replicate Viral DNA. PLOS Pathog. 2012;8(11):e1002994.
40. Abend JR, Joseph AE, Das D, Campbell-Cecen DB, Imperiale MJ. A truncated T antigen expressed from an alternatively spliced BK virus early mRNA. J Gen Virol. 2009;90(5):1238-45.
41. Zou W, Imperiale MJ. Regulation of Virus Replication by BK Polyomavirus Small T Antigen. J Virol. 2023;97(3):e0007723.
42. Shuda M, Kwun HJ, Feng H, Chang Y, Moore PS. Human Merkel cell polyomavirus small T antigen is an oncoprotein targeting the 4E-BP1 translation regulator. J Clin Invest. 2011;121(9):3623-34.
43. Verhaegen ME, Mangelberger D, Harms PW, Vozheiko TD, Weick JW, Wilbert DM, et al. Merkel cell polyomavirus small T antigen is oncogenic in transgenic mice. J Invest Dermatol. 2015;135(5):1415-24.
44. Hahn WC, Dessain SK, Brooks MW, King JE, Elenbaas B, Sabatini DM, et al. Enumeration of the Simian Virus 40 Early Region Elements Necessary for Human Cell Transformation. Mol Cell Biol. 2002;22(7):2111-23.
45. Hurdiss DL, Frank M, Snowden JS, Macdonald A, Ranson NA. The Structure of an Infectious Human Polyomavirus and Its Interactions with Cellular Receptors. Structure. 2018;26(6):839-47.e3.
46. Sorin MN, Di Maio A, Silva LM, Ebert D, Delannoy CP, Nguyen N-K, et al. Structural and functional analysis of natural capsid variants suggests sialic acid-independent entry of BK polyomavirus. Cell Rep. 2023;42(2):112114.
47. Pastrana DV, Ray U, Magaldi TG, Schowalter RM, Çuburu N, Buck CB. BK polyomavirus genotypes represent distinct serotypes with distinct entry tropism. J Virol. 2013;87(18):10105-13.
48. Neu U, Allen S-aA, Blaum BS, Liu Y, Frank M, Palma AS, et al. A structure-guided mutation in the major capsid protein retargets BK Polyomavirus. PLOS Pathog. 2013;9(10):e1003688.
49. Jin L, Gibson PE, Knowles WA, Clewley JP. BK virus antigenic variants: sequence analysis within the capsid VP1 epitope. J Med Virol. 1993;39(1):50-6.
50. Jin L, Gibson PE, Booth JC, Clewley JP. Genomic typing of BK virus in clinical specimens by direct sequencing of polymerase chain reaction products. J Med Virol. 1993;41(1):11-7.
51. Morel V, Martin E, François C, Helle F, Faucher J, Mourez T, et al. A Simple and Reliable Strategy for BK Virus Subtyping and Subgrouping. J Clin Microbiol. 2017;55(4):1177-85.
52. Wunderink HF, De Brouwer CS, Gard L, De Fijter JW, Kroes ACM, Rotmans JI, Feltkamp MCW. Source and Relevance of the BK Polyomavirus Genotype for Infection After Kidney Transplantation. Open Forum Infect Dis. 2019;6(3):ofz078.
53. Krumbholz A, Bininda-Emonds OR, Wutzler P, Zell R. Evolution of four BK virus subtypes. Infect Genet Evol. 2008;8(5):632-43.
54. Krumbholz A, Zell R, Egerer R, Sauerbrei A, Helming A, Gruhn B, Wutzler P. Prevalence of BK virus subtype I in Germany. J Med Virol. 2006;78(12):1588-98.
55. Ikegaya H, Saukko PJ, Tertti R, Metsarinne KP, Carr MJ, Crowley B, et al. Identification of a genomic subgroup of BK polyomavirus spread in European populations. J Gen Virol. 2006;87(Pt 11):3201-8.
56. Henriksen S, Hansen T, Bruun JA, Rinaldo CH. The presumed polyomavirus viroporin VP4 of simian virus 40 or human BK Polyomavirus is not required for viral progeny release. J Virol. 2016;90(22):10398-413.

57. Kozak M. Point mutations define a sequence flanking the AUG initiator codon that modulates translation by eukaryotic ribosomes. Cell. 1986;44(2):283-92.
58. Yu Y, Alwine JC. 19S late mRNAs of simian virus 40 have an internal ribosome entry site upstream of the virion structural protein 3 coding sequence. J Virol. 2006;80(13):6553-8.
59. Sahli R, Freund R, Dubensky T, Garcea R, Bronson R, Benjamin T. Defect in Entry and Altered Pathogenicity of a Polyoma Virus Mutant Blocked in VP2 Myristylation. Virology. 1993;192(1):142-53.
60. Bennett SM, Jiang M, Imperiale MJ. Role of Cell-Type-Specific Endoplasmic Reticulum-Associated Degradation in Polyomavirus Trafficking. J Virol. 2013;87(16):8843-52.
61. Goodwin Edward C, Lipovsky A, Inoue T, Magaldi Thomas G, Edwards Anne PB, Van Goor Kristin EY, et al. BiP and Multiple DNAJ Molecular Chaperones in the Endoplasmic Reticulum Are Required for Efficient Simian Virus 40 Infection. mBio. 2011;2(3):10.1128/mbio.00101-11.
62. Geiger R, Andritschke D, Friebe S, Herzog F, Luisoni S, Heger T, Helenius A. BAP31 and BiP are essential for dislocation of SV40 from the endoplasmic reticulum to the cytosol. Nat Cell Biol. 2011;13(11):1305-14.
63. Nakanishi A, Shum D, Morioka H, Otsuka E, Kasamatsu H. Interaction of the Vp3 nuclear localization signal with the importin α2/β heterodimer directs nuclear entry of infecting simian virus 40. J Virol. 2002;76(18):9368-77.
64. Gasparovic ML, Gee GV, Atwood WJ. JC virus minor capsid proteins Vp2 and Vp3 are essential for virus propagation. J Virol. 2006;80(21):10858-61.
65. Mannová P, Liebl D, Krauzewicz N, Fejtová A, Štokrová J, Palková Z, et al. Analysis of mouse polyomavirus mutants with lesions in the minor capsid proteins. J Gen Virol. 2002;83(Pt 9):2309-19.
66. Inoue T, Tsai B. A large and intact viral particle penetrates the endoplasmic reticulum membrane to reach the cytosol. PLOS Pathog. 2011;7(5):e1002037.
67. Daniels R, Sadowicz D, Hebert DN. A very late viral protein triggers the lytic release of SV40. PLOS Pathog. 2007;3(7):e98.
68. Giorda KM, Raghava S, Hebert DN. The Simian virus 40 late viral protein VP4 disrupts the nuclear envelope for viral release. J Virol. 2012;86(6):3180-92.
69. Raghava S, Giorda KM, Romano FB, Heuck AP, Hebert DN. SV40 late protein VP4 forms toroidal pores to disrupt membranes for viral release. Biochemistry. 2013;52(22):3939-48.
70. Raghava S, Giorda KM, Romano FB, Heuck AP, Hebert DN. The SV40 late protein VP4 is a viroporin that forms pores to disrupt membranes for viral release. PLOS Pathog. 2011;7(6):e1002116.
71. Tange S, Imai T, Nakanishi A. An SV40 mutant defective in VP4 expression exhibits a temperature-sensitive growth defect. Virus Res. 2011;157(1):116-20.
72. Rinaldo CH, Traavik T, Hey A. The agnogene of the human polyomavirus BK is expressed. J Virol. 1998;72(7):6233-6.
73. Unterstab G, Gosert R, Leuenberger D, Lorentz P, Rinaldo CH, Hirsch HH. The polyomavirus BK agnoprotein co-localizes with lipid droplets. Virology. 2010;399(2):322-31.
74. Manzetti J, Weissbach FH, Graf FE, Unterstab G, Wernli M, Hopfer H, et al. BK Polyomavirus Evades Innate Immune Sensing by Disrupting the Mitochondrial Network and Promotes Mitophagy. iScience. 2020;23(7):101257.
75. Unterstab G, Manzetti J, Hirsch HH. Corrigendum to “The polyomavirus BK agnoprotein co-localizes with lipid droplets” [Virology 399 (2) (2010) 322–331]. Virology. 2013;441(2):197-9.

76. Johannessen M, Myhre MR, Dragset M, Tummler C, Moens U. Phosphorylation of human polyomavirus BK agnoprotein at Ser-11 is mediated by PKC and has an important regulative function. Virology. 2008;379(1):97-109.
77. Gerits N, Johannessen M, Tümmler C, Walquist M, Kostenko S, Snapkov I, et al. Agnoprotein of polyomavirus BK interacts with proliferating cell nuclear antigen and inhibits DNA replication. Virol J. 2015;12:7.
78. Johannessen M, Walquist M, Gerits N, Dragset M, Spang A, Moens U. BKV agnoprotein interacts with alpha-soluble N-ethylmaleimide-sensitive fusion attachment protein, and negatively influences transport of VSVG-EGFP. PLOS One. 2011;6(9):e24489.
79. Swinscoe G, Prescott EL, Hurdiss DL, Morgan EL, Dobson SJ, Edwards T, et al. The virus-encoded ion channel "viroporin" activity of the agnoprotein is required for BK Polyomavirus release from infected kidney cells. bioRxiv. 2023:2023.01.30.526200.
80. Okada Y, Suzuki T, Sunden Y, Orba Y, Kose S, Imamoto N, et al. Dissociation of heterochromatin protein 1 from lamin B receptor induced by human polyomavirus agnoprotein: role in nuclear egress of viral particles. Embo Rep. 2005;6(5):452-7.
81. Panou MM, Prescott EL, Hurdiss DL, Swinscoe G, Hollinshead M, Caller LG, et al. Agnoprotein Is an Essential Egress Factor during BK Polyomavirus Infection. Int J Mol Sci. 2018;19(3).
82. Resnick J, Shenk T. Simian virus 40 agnoprotein facilitates normal nuclear location of the major capsid polypeptide and cell-to-cell spread of virus. J Virol. 1986;60(3):1098-106.
83. Sariyer IK, Saribas AS, White MK, Safak M. Infection by agnoprotein-negative mutants of polyomavirus JC and SV40 results in the release of virions that are mostly deficient in DNA content. Virol J. 2011;8:255.
84. Broekema NM, Imperiale MJ. miRNA regulation of BK polyomavirus replication during early infection. Proc Natl Acad Sci U S A. 2013;110(20):8200-5.
85. Seo GJ, Chen CJ, Sullivan CS. Merkel cell polyomavirus encodes a microRNA with the ability to autoregulate viral gene expression. Virology. 2008.
86. Bauman Y, Nachmani D, Vitenshtein A, Tsukerman P, Drayman N, Stern-Ginossar N, et al. An identical miRNA of the human JC and BK polyoma viruses targets the stress-induced ligand ULBP3 to escape immune elimination. Cell Host Microbe. 2011;9(2):93-102.
87. Dugan AS, Eash S, Atwood WJ. An N-linked glycoprotein with alpha(2,3)-linked sialic acid is a receptor for BK virus. J Virol. 2005;79(22):14442-5.
88. Low JA, Magnuson B, Tsai B, Imperiale MJ. Identification of gangliosides GD1b and GT1b as receptors for BK virus. J Virol. 2006;80(3):1361-6.
89. Sinibaldi L, Viti D, Goldoni P, Cavallo G, Caroni C, Orsi N. Inhibition of BK virus haemagglutination by gangliosides. J Gen Virol. 1987;68(Pt 3):879-83.
90. Eash S, Querbes W, Atwood WJ. Infection of vero cells by BK virus is dependent on caveolae. J Virol. 2004;78(21):11583-90.
91. Moriyama T, Marquez JP, Wakatsuki T, Sorokin A. Caveolar endocytosis is critical for BK virus infection of human renal proximal tubular epithelial cells. J Virol. 2007;81(16):8552-62.
92. Zhao L, Marciano AT, Rivet CR, Imperiale MJ. Caveolin- and clathrin-independent entry of BKPyV into primary human proximal tubule epithelial cells. Virology. 2016;492:66-72.
93. Damm EM, Pelkmans L, Kartenbeck J, Mezzacasa A, Kurzchalia T, Helenius A. Clathrin- and caveolin-1-independent endocytosis: entry of simian virus 40 into cells devoid of caveolae. J Cell Biol. 2005;168(3):477-88.
94. Anderson HA, Chen Y, Norkin LC. Bound simian virus 40 translocates to caveolin-enriched membrane domains, and its entry is inhibited by drugs that selectively disrupt caveolae. Mol Biol Cell. 1996;7(11):1825-34.

95. Pelkmans L, Kartenbeck J, Helenius A. Caveolar endocytosis of simian virus 40 reveals a new two-step vesicular-transport pathway to the ER. Nat Cell Biol. 2001;3(5):473-83.
96. Jiang M, Abend JR, Tsai B, Imperiale MJ. Early events during BK virus entry and disassembly. J Virol. 2009;83(3):1350-8.
97. Moriyama T, Sorokin A. Intracellular trafficking pathway of BK Virus in human renal proximal tubular epithelial cells. Virology. 2008;371(2):336-49.
98. Zhao L, Imperiale MJ. Identification of Rab18 as an Essential Host Factor for BK Polyomavirus Infection Using a Whole-Genome RNA Interference Screen. mSphere. 2017;2(4).
99. Eash S, Atwood WJ. Involvement of cytoskeletal components in BK virus infectious entry. J Virol. 2005;79(18):11734-41.
100. Liebl D, Difato F, Horníková L, Mannová P, Stokrová J, Forstová J. Mouse polyomavirus enters early endosomes, requires their acidic pH for productive infection, and meets transferrin cargo in Rab11-positive endosomes. J Virol. 2006;80(9):4610-22.
101. Mannová P, Forstová J. Mouse polyomavirus utilizes recycling endosomes for a traffic pathway independent of COPI vesicle transport. J Virol. 2003;77(3):1672-81.
102. Engel S, Heger T, Mancini R, Herzog F, Kartenbeck J, Hayer A, Helenius A. Role of endosomes in simian virus 40 entry and infection. J Virol. 2011;85(9):4198-211.
103. Qian M, Cai D, Verhey KJ, Tsai B. A Lipid Receptor Sorts Polyomavirus from the Endolysosome to the Endoplasmic Reticulum to Cause Infection. PLOS Pathog. 2009;5(6):e1000465.
104. Woo T-T, Williams JM, Tsai B. How host ER membrane chaperones and morphogenic proteins support virus infection. J Cell Sci. 2023;136(13):jcs261121.
105. Walczak Christopher P, Tsai B. A PDI Family Network Acts Distinctly and Coordinately with ERp29 To Facilitate Polyomavirus Infection. J Virol. 2011;85(5):2386-96.
106. Inoue T, Dosey A, Herbstman Jeffrey F, Ravindran Madhu S, Skiniotis G, Tsai B. ERdj5 Reductase Cooperates with Protein Disulfide Isomerase To Promote Simian Virus 40 Endoplasmic Reticulum Membrane Translocation. J Virol. 2015;89(17):8897-908.
107. Schelhaas M, Malmstrom J, Pelkmans L, Haugstetter J, Ellgaard L, Grunewald K, Helenius A. Simian Virus 40 depends on ER protein folding and quality control factors for entry into host cells. Cell. 2007;131(3):516-29.
108. Chen Y-J, Liu X, Tsai B. SV40 Hijacks Cellular Transport, Membrane Penetration, and Disassembly Machineries to Promote Infection. Viruses. 2019;11(10).
109. Ravindran MS, Engelke MF, Verhey KJ, Tsai B. Exploiting the kinesin-1 molecular motor to generate a virus membrane penetration site. Nat Commun. 2017;8(1):15496.
110. Bagchi P, Liu X, Cho WJ, Tsai B. Lunapark-dependent formation of a virus-induced ER exit site contains multi-tubular ER junctions that promote viral ER-to-cytosol escape. Cell Rep. 2021;37(10).
111. Pletan M, Liu X, Cha G, Chen Y-J, Knupp J, Tsai B. The atlastin ER morphogenic proteins promote formation of a membrane penetration site during non-enveloped virus entry. J Virol. 2023;97(8):e00756-23.
112. Ravindran M, Sudhan, Spriggs C, C., Verhey K, J., Tsai B. Dynein Engages and Disassembles Cytosol-Localized Simian Virus 40 To Promote Infection. J Virol. 2018;92(12):10.1128/jvi.00353-18.
113. Bennett SM, Zhao L, Bosard C, Imperiale MJ. Role of a nuclear localization signal on the minor capsid Proteins VP2 and VP3 in BKPyV nuclear entry. Virology. 2015;474:110-6.
114. Spriggs CC, Cha G, Li J, Tsai B. Components of the LINC and NPC complexes coordinately target and translocate a virus into the nucleus to promote infection. PLOS Pathog. 2022;18(9):e1010824.

115. Nakanishi A, Li PP, Qu Q, Jafri QH, Kasamatsu H. Molecular dissection of nuclear entry-competent SV40 during infection. Virus Res. 2007;124(1-2):226-30.
116. Nakanishi A, Itoh N, Li PP, Handa H, Liddington RC, Kasamatsu H. Minor capsid proteins of simian virus 40 are dispensable for nucleocapsid assembly and cell entry but are required for nuclear entry of the viral genome. J Virol. 2007;81(8):3778-85.
117. Butin-Israeli V, Ben-nun-Shaul O, Kopatz I, Adam SA, Shimi T, Goldman RD, Oppenheim A. Simian virus 40 induces lamin A/C fluctuations and nuclear envelope deformation during cell entry. Nucleus (Calcutta). 2011;2(4):320-30.
118. Bennett SM, Broekema NM, Imperiale MJ. BK polyomavirus: emerging pathogen. Microbes and infection / Institut Pasteur. 2012;14(9):672-83.
119. Danna KJ, Nathans D. Bidirectional replication of Simian Virus 40 DNA. Proc Natl Acad Sci U S A. 1972;69(11):3097-100.
120. Dodson M, Dean FB, Bullock P, Echols H, Hurwitz J. Unwinding of Duplex DNA from the SV40 Origin of Replication by T Antigen. Science. 1987;238(4829):964-7.
121. Mastrangelo IA, Hough PV, Wall JS, Dodson M, Dean FB, Hurwitz J. ATP-dependent assembly of double hexamers of SV40 T antigen at the viral origin of DNA replication. Nature. 1989;338(6217):658-62.
122. Jiang M, Zhao L, Gamez M, Imperiale MJ. Roles of ATM and ATR-mediated DNA damage responses during lytic BK polyomavirus infection. PLOS Pathog. 2012;8(8):e1002898.
123. Verhalen B, Justice JL, Imperiale MJ, Jiang M. Viral DNA replication-dependent DNA damage response activation during BK polyomavirus infection. J Virol. 2015;89(9):5032-9.
124. Justice JL, Needham JM, Thompson SR. BK Polyomavirus Activates the DNA Damage Response To Prolong S Phase. J Virol. 2019;93(14):10.1128/jvi.00130-19.
125. Caller LG, Davies CTR, Antrobus R, Lehner PJ, Weekes MP, Crump CM. Temporal Proteomic Analysis of BK Polyomavirus Infection Reveals Virus-Induced G(2) Arrest and Highly Effective Evasion of Innate Immune Sensing. J Virol. 2019;93(16).
126. Erickson KD, Bouchet-Marquis C, Heiser K, Szomolanyi-Tsuda E, Mishra R, Lamothe B, et al. Virion assembly factories in the nucleus of polyomavirus-infected cells. PLOS Pathog. 2012;8(4):e1002630.
127. Drachenberg CB, Papadimitriou JC, Wali R, Cubitt CL, Ramos E. BK polyoma virus allograft nephropathy: ultrastructural features from viral cell entry to lysis. Am J Transplant. 2003;3(11):1383-92.
128. Nickeleit V, Hirsch HH, Binet IF, Gudat F, Prince O, Dalquen P, et al. Polyomavirus infection of renal allograft recipients: from latent infection to manifest disease. J Am Soc Nephrol. 1999;10(5):1080-9.
129. Low J, Humes HD, Szczypka M, Imperiale M. BKV and SV40 infection of human kidney tubular epithelial cells in vitro. Virology. 2004;323(2):182-8.
130. Tylden GD, Hirsch HH, Rinaldo CH. Brincidofovir (CMX001) Inhibits BK Polyomavirus Replication in Primary Human Urothelial Cells. Antimicrob Agents Chemother. 2015.
131. Li R, Sharma BN, Linder S, Gutteberg TJ, Hirsch HH, Rinaldo CH. Characteristics of polyomavirus BK (BKPyV) infection in primary human urothelial cells. Virology. 2013;440(1):41-50.
132. An P, Sáenz Robles MT, Duray AM, Cantalupo PG, Pipas JM. Human polyomavirus BKV infection of endothelial cells results in interferon pathway induction and persistence. PLOS Pathog. 2019;15(1):e1007505.
133. Suzuki T, Orba Y, Okada Y, Sunden Y, Kimura T, Tanaka S, et al. The human polyoma JC virus agnoprotein acts as a viroporin. PLOS Pathog. 2010;6(3):e1000801.

134. Myhre MR, Olsen GH, Gosert R, Hirsch HH, Rinaldo CH. Clinical polyomavirus BK variants with agnogene deletion are non-functional but rescued by trans-complementation. Virology. 2010.
135. Evans GL, Caller LG, Foster V, Crump CM. Anion homeostasis is important for non-lytic release of BK polyomavirus from infected cells. Open Biology. 2015;5(8):150041.
136. Handala L, Blanchard E, Raynal P-I, Roingeard P, Morel V, Descamps V, et al. BK Polyomavirus Hijacks Extracellular Vesicles for En Bloc Transmission. J Virol. 2020;94(6):e01834-19.
137. Morris-Love J, Gee GV, O'Hara BA, Assetta B, Atkinson AL, Dugan AS, et al. JC Polyomavirus Uses Extracellular Vesicles To Infect Target Cells. mBio. 2019;10(2):e00379-19.
138. O'Hara BA, Morris-Love J, Gee GV, Haley SA, Atwood WJ. JC Virus infected choroid plexus epithelial cells produce extracellular vesicles that infect glial cells independently of the virus attachment receptor. PLOS Pathog. 2020;16(3):e1008371-e.
139. Morris-Love J, O'Hara BA, Gee GV, Dugan AS, O'Rourke RS, Armstead BE, et al. Biogenesis of JC polyomavirus associated extracellular vesicles. Journal of Extracellular Biology. 2022;1(5).
140. Clayson ET, Brando LV, Compans RW. Release of simian virus 40 virions from epithelial cells is polarized and occurs without cell lysis. J Virol. 1989;63(5):2278-88.
141. Bowie AG, Unterholzner L. Viral evasion and subversion of pattern-recognition receptor signalling. Nat Rev Immunol. 2008;8(12):911-22.
142. Sharma S, Fitzgerald KA. Innate Immune Sensing of DNA. PLOS Pathog. 2011;7(4):e1001310.
143. An P, Cantalupo PG, Zheng W, Sáenz-Robles MT, Duray AM, Weitz D, Pipas JM. Single-Cell Transcriptomics Reveals a Heterogeneous Cellular Response to BK Virus Infection. J Virol. 2021;95(6).
144. Abend JR, Low JA, Imperiale MJ. Global effects of BKV infection on gene expression in human primary kidney epithelial cells. Virology. 2010;397(1):73-9.
145. Justice JL, Verhalen B, Kumar R, Lefkowitz EJ, Imperiale MJ, Jiang M. Quantitative Proteomic Analysis of Enriched Nuclear Fractions from BK Polyomavirus-Infected Primary Renal Proximal Tubule Epithelial Cells. J Proteome Res. 2015;14(10):4413-24.
146. de Kort H, Heutinck KM, Ruben JM, Ede VSA, Wolthers KC, Hamann J, Ten Berge IJM. Primary Human Renal-Derived Tubular Epithelial Cells Fail to Recognize and Suppress BK Virus Infection. Transplantation. 2017;101(8):1820-9.
147. Ryabchenko B, Soldatova I, Šroller V, Forstová J, Huérfano S. Immune sensing of mouse polyomavirus DNA by p204 and cGAS DNA sensors. FEBS J. 2021;288(20):5964-85.
148. Uhlorn BL, Jackson R, Li S, Bratton SM, Van Doorslaer K, Campos SK. Vesicular trafficking permits evasion of cGAS/STING surveillance during initial human papillomavirus infection. PLOS Pathog. 2020;16(11):e1009028.
149. Chiang C, Dvorkin S, Chiang Jessica J, Potter Rachel B, Gack Michaela U. The Small t Antigen of JC Virus Antagonizes RIG-I-Mediated Innate Immunity by Inhibiting TRIM25's RNA Binding Ability. mBio. 2021;12(2):10.1128/mbio.00620-21.
150. Egli A, Infanti L, Dumoulin A, Buser A, Samaridis J, Stebler C, et al. Prevalence of Polyomavirus BK and JC infection and replication in 400 healthy blood donors. J Infect Dis. 2009;199(6):837-46.
151. Kamminga S, van der Meijden E, Feltkamp MCW, Zaaijer HL. Seroprevalence of fourteen human polyomaviruses determined in blood donors. PLOS One. 2018;13(10):e0206273.
152. Kean JM, Rao S, Wang M, Garcea RL. Seroepidemiology of human polyomaviruses. PLOS Pathog. 2009;5(3):e1000363.

153. Lim ES, Meinerz NM, Primi B, Wang D, Garcea RL. Common Exposure to STL Polyomavirus During Childhood. Emerg Infect Dis. 2014;20(9):1559-61.
154. Kardas P, Leboeuf C, Hirsch HH. Optimizing JC and BK polyomavirus IgG testing for seroepidemiology and patient counseling. J Clin Virol. 2015;71:28-33.
155. Hirsch HH, Steiger J. Polyomavirus BK. Lancet Infect Dis. 2003;3(10):611-23.
156. Laine HK, Waterboer T, Syrjänen K, Grenman S, Louvanto K, Syrjänen S. IgG Seroreactivites to Viral Capsid Protein VP1 of JC and BK Polyomaviruses in Children at Early Ages with Special Reference to Parental Cofactors. Children. 2023;10(10):1645.
157. Karachaliou M, Waterboer T, Casabonne D, Chalkiadaki G, Roumeliotaki T, Michel A, et al. The Natural History of Human Polyomaviruses and Herpesviruses in Early Life—The Rhea Birth Cohort in Greece. Am J Epidemiol. 2016;183(7):671-9.
158. Knowles WA, Pipkin P, Andrews N, Vyse A, Minor P, Brown DW, Miller E. Population-based study of antibody to the human polyomaviruses BKV and JCV and the simian polyomavirus SV40. J Med Virol. 2003;71(1):115-23.
159. Knowles WA. Discovery and epidemiology of the human polyomaviruses BK virus (BKV) and JC virus (JCV). Adv Exp Med Biol. 2006;577:19-45.
160. Goudsmit J, Dillen PW-v, van Strien A, van der Noordaa J. The role of BK virus in acute respiratory tract disease and the presence of BKV DNA in tonsils. J Med Virol. 1982;10(2):91-9.
161. Pena GPA, Mendes GS, Dias HG, Gavazzoni LS, Amorim AR, Santos N. Human polyomavirus KI, WU, BK, and JC in healthy volunteers. Eur J Clin Microbiol Infect Dis. 2019;38(1):135-9.
162. Chesters PM, Heritage J, McCance DJ. Persistence of DNA sequences of BK virus and JC virus in normal human tissues and in diseased tissues. J Infect Dis. 1983;147(4):676-84.
163. Heritage J, Chesters PM, McCance DJ. The persistence of papovavirus BK DNA sequences in normal human renal tissue. J Med Virol. 1981;8(2):143-50.
164. Randhawa P, Shapiro R, Vats A. Quantitation of DNA of polyomaviruses BK and JC in human kidneys. J Infect Dis. 2005;192(3):504-9.
165. Polo C, Perez JL, Mielnichuck A, Fedele CG, Niubo J, Tenorio A. Prevalence and patterns of polyomavirus urinary excretion in immunocompetent adults and children. Clin Microbiol Infect. 2004;10(7):640-4.
166. Kling CL, Wright AT, Katz SE, McClure GB, Gardner JS, Williams JT, et al. Dynamics of urinary polyomavirus shedding in healthy adult women. J Med Virol. 2012;84(9):1459-63.
167. Urbano PR, Oliveira RR, Romano CM, Pannuti CS, Fink MC. Occurrence, genotypic characterization, and patterns of shedding of human polyomavirus JCPyV and BKPyV in urine samples of healthy individuals in São Paulo, Brazil. J Med Virol. 2016;88(1):153-8.
168. Boukoum H, Nahdi I, Sahtout W, Skiri H, Segondy M, Aouni M. BK and JC virus infections in healthy patients compared to kidney transplant recipients in Tunisia. Microb Pathog. 2016;97:204-8.
169. McClure GB, Gardner JS, Williams JT, Copeland CM, Sylvester SK, Garcea RL, et al. Dynamics of pregnancy-associated polyomavirus urinary excretion: A prospective longitudinal study. J Med Virol. 2012;84(8):1312-22.
170. Kamminga S, van der Meijden E, de Brouwer C, Feltkamp M, Zaaijer H. Prevalence of DNA of fourteen human polyomaviruses determined in blood donors. Transfusion. 2019;59(12):3689-97.
171. van Delden C, Stampf S, Hirsch HH, Manuel O, Meylan P, Cusini A, et al. Burden and Timeline of Infectious Diseases in the First Year After Solid Organ Transplantation in the Swiss Transplant Cohort Study. Clin Infect Dis. 2020;71(7):e159-e69.

172. Kotton CN, Kamar N, Wojciechowski D, Eder M, Hopfer H, Randhawa P, et al. The Second International Consensus Guidelines on the Management of BK Polyomavirus in Kidney Transplantation. Transplantation, in press. 2024.
173. Binet I, Nickeleit V, Hirsch HH, Prince O, Dalquen P, Gudat F, et al. Polyomavirus disease under new immunosuppressive drugs: a cause of renal graft dysfunction and graft loss. Transplantation. 1999;67(6):918-22.
174. Purighalla R, Shapiro R, McCauley J, Randhawa P. BK virus infection in a kidney allograft diagnosed by needle biopsy. Am J Kidney Dis. 1995;26(4):671-3.
175. Imlay H, Whitaker K, Fisher CE, Limaye AP. Clinical characteristics and outcomes of late-onset BK virus nephropathy in kidney and kidney-pancreas transplant recipients. Transpl Infect Dis. 2018;20(4):e12928.
176. Randhawa PS, Finkelstein S, Scantlebury V, Shapiro R, Vivas C, Jordan M, et al. Human polyoma virus-associated interstitial nephritis in the allograft kidney. Transplantation. 1999;67(1):103-9.
177. Leuzinger K, Naegele K, Schaub S, Hirsch HH. Quantification of plasma BK polyomavirus loads is affected by sequence variability, amplicon length, and non-encapsidated viral DNA genome fragments. J Clin Virol. 2019;121:104210.
178. Drachenberg CB, Beskow CO, Cangro CB, Bourquin PM, Simsir A, Fink J, et al. Human polyoma virus in renal allograft biopsies: morphological findings and correlation with urine cytology. Hum Pathol. 1999;30(8):970-7.
179. Drachenberg CB, Papadimitriou JC, Hirsch HH, Wali R, Crowder C, Nogueira J, et al. Histological patterns of polyomavirus nephropathy: correlation with graft outcome and viral load. Am J Transplant. 2004;4(12):2082-92.
180. Menter T, Mayr M, Schaub S, Mihatsch MJ, Hirsch HH, Hopfer H. Pathology of Resolving Polyomavirus-Associated Nephropathy. Am J Transplant. 2013.
181. Drachenberg CB, Papadimitriou JC, Chaudhry MR, Ugarte R, Mavanur M, Thomas B, et al. Histological Evolution of BK Virus-Associated Nephropathy: Importance of Integrating Clinical and Pathological Findings. Am J Transplant. 2017;17(8):2078-91.
182. Bohl DL, Brennan DC, Ryschkewitsch C, Gaudreault-Keener M, Major EO, Storch GA. BK virus antibody titers and intensity of infections after renal transplantation. J Clin Virol. 2008;43(2):184-9.
183. Randhawa PS, Gupta G, Vats A, Shapiro R, Viscidi RP. Immunoglobulin G, A, and M responses to BK virus in renal transplantation. Clin Vaccine Immunol. 2006;13(9):1057-63.
184. Randhawa P, Bohl D, Brennan D, Ruppert K, Ramaswami B, Storch G, et al. Longitudinal analysis of levels of immunoglobulins against BK virus capsid proteins in kidney transplant recipients. Clin Vaccine Immunol. 2008;15(10):1564-71.
185. Solis M, Velay A, Porcher R, Domingo-Calap P, Soulier E, Joly M, et al. Neutralizing Antibody-Mediated Response and Risk of BK Virus-Associated Nephropathy. J Am Soc Nephrol. 2018;29(1):326-34.
186. Gras J, Nere ML, Peraldi MN, Bonnet-Madin L, Salmona M, Taupin JL, et al. BK virus genotypes and humoral response in kidney transplant recipients with BKV associated nephropathy. Transpl Infect Dis. 2023;25(2):e14012.
187. Wunderink HF, van der Meijden E, van der Blij-de Brouwer CS, Mallat MJK, Haasnoot GW, van Zwet EW, et al. Pretransplantation Donor-Recipient Pair Seroreactivity Against BK Polyomavirus Predicts Viremia and Nephropathy After Kidney Transplantation. Am J Transplant. 2017;17(1):161-72.
188. Bodaghi S, Comoli P, Bosch R, Azzi A, Gosert R, Leuenberger D, et al. Antibody responses to recombinant polyomavirus BK large T and VP1 proteins in young kidney transplant patients. J Clin Microbiol. 2009;47(8):2577-85.

189. DeWolfe D, Gandhi J, Mackenzie MR, Broge TA, Jr., Bord E, Babwah A, et al. Pre-transplant immune factors may be associated with BK polyomavirus reactivation in kidney transplant recipients. PLOS One. 2017;12(5):e0177339.
190. Leboeuf C, Wilk S, Achermann R, Binet I, Golshayan D, Hadaya K, et al. BK Polyomavirus-Specific 9mer CD8 T Cell Responses Correlate With Clearance of BK Viremia in Kidney Transplant Recipients: First Report From the Swiss Transplant Cohort Study. Am J Transplant. 2017;17(10):2591-600.
191. Hariharan S, Cohen EP, Vasudev B, Orentas R, Viscidi RP, Kakela J, DuChateau B. BK virus-specific antibodies and BKV DNA in renal transplant recipients with BKV nephritis. Am J Transplant. 2005;5(11):2719-24.
192. Blazquez-Navarro A, Schachtner T, Stervbo U, Sefrin A, Stein M, Westhoff TH, et al. Differential T cell response against BK virus regulatory and structural antigens: A viral dynamics modelling approach. PLoS Comput Biol. 2018;14(5):e1005998.
193. Schachtner T, Muller K, Stein M, Diezemann C, Sefrin A, Babel N, Reinke P. BK virus-specific immunity kinetics: a predictor of recovery from polyomavirus BK-associated nephropathy. Am J Transplant. 2011;11(11):2443-52.
194. Kaur A, Wilhelm M, Wilk S, Hirsch HH. BK polyomavirus-specific antibody and T-cell responses in kidney transplantation: update. Curr Opin Infect Dis. 2019;32(6):575-83.
195. Binggeli S, Egli A, Dickenmann M, Binet I, Steiger J, Hirsch HH. BKV Replication and Cellular Immune Responses in Renal Transplant Recipients. Am J Transplant. 2006;6(9):2218-9.
196. Binggeli S, Egli A, Schaub S, Binet I, Mayr M, Steiger J, Hirsch HH. Polyomavirus BK-specific cellular immune response to VP1 and large T-antigen in kidney transplant recipients. Am J Transplant. 2007;7(5):1131-9.
197. Schachtner T, Stein M, Babel N, Reinke P. The Loss of BKV-specific Immunity From Pretransplantation to Posttransplantation Identifies Kidney Transplant Recipients at Increased Risk of BKV Replication. Am J Transplant. 2015;15(8):2159-69.
198. Schaenman JM, Korin Y, Sidwell T, Kandarian F, Harre N, Gjertson D, et al. Increased Frequency of BK Virus-Specific Polyfunctional CD8+ T Cells Predict Successful Control of BK Viremia After Kidney Transplantation. Transplantation. 2017;101(6):1479-87.
199. Bae H, Jung S, Chung BH, Yang CW, Oh EJ. Pretransplant BKV-IgG serostatus and BKV-specific ELISPOT assays to predict BKV infection after kidney transplantation. Front Immunol. 2023;14:1243912.
200. van Aalderen MC, Remmerswaal EB, Heutinck KM, Ten Brinke A, Feltkamp MC, van der Weerd NC, et al. Clinically Relevant Reactivation of Polyomavirus BK (BKPyV) in HLA-A02-Positive Renal Transplant Recipients Is Associated with Impaired Effector-Memory Differentiation of BKPyV-Specific CD8+ T Cells. PLOS Pathog. 2016;12(10):e1005903.
201. Dekeyser M, de Goër de Herve MG, Hendel-Chavez H, Boutin E, Herr F, Lhotte R, et al. Heterospecific Immunity Help to Sustain an Effective BK-virus Immune Response and Prevent BK-virus-associated Nephropathy Research Square [Preprint]2022 [[05.02.2024]].
202. Stervbo U, Nienen M, Weist BJD, Kuchenbecker L, Hecht J, Wehler P, et al. BKV Clearance Time Correlates With Exhaustion State and T-Cell Receptor Repertoire Shape of BKV-Specific T-Cells in Renal Transplant Patients. Front Immunol. 2019;10:767.
203. Dakroub F, Touzé A, Akl H, Brochot E. Pre-Transplantation Assessment of BK Virus Serostatus: Significance, Current Methods, and Obstacles. Viruses. 2019;11(10).
204. Sood P, Senanayake S, Sujeet K, Medipalli R, Van-Why SK, Cronin DC, et al. Donor and Recipient BKV-Specific IgG Antibody and Posttransplantation BKV Infection: A Prospective Single-Center Study. Transplantation. 2013;95(6):896-902.

205. Andrews CA, Shah KV, Daniel RW, Hirsch MS, Rubin RH. A serological investigation of BK virus and JC virus infections in recipients of renal allografts. J Infect Dis. 1988;158(1):176-81.
206. Hisadome Y, Noguchi H, Nakafusa Y, Sakihama K, Mei T, Kaku K, et al. Association of Pretransplant BK Polyomavirus Antibody Status with BK Polyomavirus Infection After Kidney Transplantation: A Prospective Cohort Pilot Study of 47 Transplant Recipients. Transplant Proc. 2020;52(6):1762-8.
207. Pastrana DV, Brennan DC, Cuburu N, Storch GA, Viscidi RP, Randhawa PS, Buck CB. Neutralization serotyping of BK polyomavirus infection in kidney transplant recipients. PLOS Pathog. 2012;8(4):e1002650.
208. Wunderink HF, de Brouwer CS, van der Meijden E, Pastrana DV, Kroes ACM, Buck CB, Feltkamp MCW. Development and evaluation of a BK polyomavirus serotyping assay using Luminex technology. J Clin Virol. 2019;110:22-8.
209. Abend JR, Changala M, Sathe A, Casey F, Kistler A, Chandran S, et al. Correlation of BK virus neutralizing serostatus with the incidence of BK viremia in kidney transplant recipients. Transplantation. 2017;101(6):1495-505.
210. Bohl DL, Storch GA, Ryschkewitsch C, Gaudreault-Keener M, Schnitzler MA, Major EO, Brennan DC. Donor origin of BK virus in renal transplantation and role of HLA C7 in susceptibility to sustained BK viremia. Am J Transplant. 2005;5(9):2213-21.
211. Grellier J, Hirsch HH, Mengelle C, Esposito L, Hebral AL, Belliere J, et al. Impact of donor BK polyomavirus replication on recipient infections in living donor transplantation. Transpl Infect Dis. 2018;20(4):e12917.
212. Verghese PS, Schmeling DO, Knight JA, Matas AJ, Balfour HH, Jr. The impact of donor viral replication at transplant on recipient infections posttransplant: a prospective study. Transplantation. 2015;99(3):602-8.
213. Tan SK, Huang C, Sahoo MK, Weber J, Kurzer J, Stedman MR, et al. Impact of Pretransplant Donor BK Viruria in Kidney Transplant Recipients. J Infect Dis. 2019;220(3):370-6.
214. Ryu W-S. Chapter 4 - Diagnosis and Methods. In: Ryu W-S, editor. Molecular Virology of Human Pathogenic Viruses. Boston: Academic Press; 2017. p. 47-62.
215. Kamminga S, van der Meijden E, Wunderink HF, Touzé A, Zaaijer HL, Feltkamp MCW. Development and Evaluation of a Broad Bead-Based Multiplex Immunoassay To Measure IgG Seroreactivity against Human Polyomaviruses. J Clin Microbiol. 2018;56(4).
216. Buck CB, Pastrana DV, Lowy DR, Schiller JT. Generation of HPV pseudovirions using transfection and their use in neutralization assays. Methods Mol Med. 2005;119:445-62.
217. Randhawa P, Pastrana D, Zeng G, Huang Y, Shapiro R, Sood P, et al. Commercially available immunoglobulins contain virus neutralizing antibodies against all major genotypes of polyomavirus BK. Am J Transplant. 2015;15(4):1014-20.
218. Lau EHY, Tsang OTY, Hui DSC, Kwan MYW, Chan W-h, Chiu SS, et al. Neutralizing antibody titres in SARS-CoV-2 infections. Nat Commun. 2021;12(1):63.
219. Jelcic I, Combaluzier B, Jelcic I, Faigle W, Senn L, Reinhart BJ, et al. Broadly neutralizing human monoclonal JC polyomavirus VP1-specific antibodies as candidate therapeutics for progressive multifocal leukoencephalopathy. Sci Transl Med. 2015;7(306):306ra150.
220. Pappo O, Demetris AJ, Raikow RB, Randhawa PS. Human polyoma virus infection of renal allografts: histopathologic diagnosis, clinical significance, and literature review. Mod Pathol. 1996;9(2):105-9.
221. Hirsch HH, Mengel M, Kamar N. BK Polyomavirus Consensus. Clin Infect Dis. 2022;75(11):2046-7.

222. Funk GA, Steiger J, Hirsch HH. Rapid dynamics of polyomavirus type BK in renal transplant recipients. J Infect Dis. 2006;193(1):80-7.
223. Funk GA, Gosert R, Hirsch HH. Viral dynamics in transplant patients: implications for disease. Lancet Infect Dis. 2007;7(7):460-72.
224. Drachenberg CB, Papadimitriou JC, Ramos E. Histologic versus molecular diagnosis of BK polyomavirus-associated nephropathy: a shifting paradigm? Clin J Am Soc Nephrol. 2006;1(3):374-9.
225. Jordan S, Brennan D, Patick A, Gasink L, Lin C, Limaye A. A Randomized Phase 2 Study of Mau868 vs Placebo for Bk Viremia in Kidney Transplant Recipients: BK Viral Kinetics and Outcomes in Two Dosing Cohorts. Am J Transplant. 2023;23(6):S339-S613.
226. Sato N, Shiraki A, Mori KP, Sakai K, Takemura Y, Yanagita M, et al. Preemptive Intravenous Human Immunoglobulin G Suppresses BK Polyomavirus Replication and Spread of Infection In Vitro. Am J Transplant. 2023.
227. Randhawa PS, Schonder K, Shapiro R, Farasati N, Huang Y. Polyomavirus BK neutralizing activity in human immunoglobulin preparations. Transplantation. 2010;89(12):1462-5.
228. Urayama T, Takahashi K, Ideno S, Yunoki M, Saito M, Numakura K, et al. BK polyomavirus-neutralizing activity of intravenous immunoglobulin products derived from donated blood in Japan. Vox Sang. 2016;11(3):146-52.
229. Zhong C, Chen J, Yan Z, Xia R, Zeng W, Deng W, et al. Therapeutic strategies against BK polyomavirus infection in kidney transplant recipients: Systematic review and meta-analysis. Transpl Immunol. 2023;81:101953.
230. Nelson AS, Heyenbruch D, Rubinstein JD, Sabulski A, Jodele S, Thomas S, et al. Virus-specific T-cell therapy to treat BK polyomavirus infection in bone marrow and solid organ transplant recipients. Blood Adv. 2020;4(22):5745-54.
231. Tzannou I, Papadopoulou A, Naik S, Leung K, Martinez CA, Ramos CA, et al. Off-the-Shelf Virus-Specific T Cells to Treat BK Virus, Human Herpesvirus 6, Cytomegalovirus, Epstein-Barr Virus, and Adenovirus Infections After Allogeneic Hematopoietic Stem-Cell Transplantation. J Clin Oncol. 2017;35(31):3547-57.
232. Jahan S, Scuderi C, Francis L, Neller MA, Rehan S, Crooks P, et al. T-cell adoptive immunotherapy for BK nephropathy in renal transplantation. Transpl Infect Dis. 2020;22(6):e13399.
233. Wu Z, Graf FE, Hirsch HH. Antivirals against human polyomaviruses: Leaving no stone unturned. Rev Med Virol. 2021;31(6):e2220.
234. Cesaro S, Dalianis T, Rinaldo CH, Koskenvuo M, Pegoraro A, Einsele H, et al. ECIL guidelines for the prevention, diagnosis and treatment of BK polyomavirus-associated haemorrhagic cystitis in haematopoietic stem cell transplant recipients. J Antimicrob Chemother. 2017;73(1):12-21.
235. Azzi A, Cesaro S, Laszlo D, Zakrzewska K, Ciappi S, de Santis R, et al. Human polyomavirus BK (BKV) load and haemorrhagic cystitis in bone marrow transplantation patients. J Clin Virol. 1999;14(2):79-86.
236. Arthur RR, Shah KV, Baust SJ, Santos GW, Saral R. Association of BK viruria with hemorrhagic cystitis in recipients of bone marrow transplants. N Engl J Med. 1986;315(4):230-4.
237. Cesaro S, Facchin C, Tridello G, Messina C, Calore E, Biasolo MA, et al. A prospective study of BK-virus-associated haemorrhagic cystitis in paediatric patients undergoing allogeneic haematopoietic stem cell transplantation. Bone Marrow Transplant. 2008;41(4):363-70.
238. Dosin G, Aoun F, El Rassy E, Assi T, Lewalle P, Blanc J, et al. Viral-induced Hemorrhagic Cystitis After Allogeneic Hematopoietic Stem Cell Transplant. Clin Lymphoma Myeloma Leuk. 2017;17(7):438-42.

239. Imlay H, Xie H, Leisenring WM, Duke ER, Kimball LE, Huang ML, et al. Presentation of BK polyomavirus-associated hemorrhagic cystitis after allogeneic hematopoietic cell transplantation. Blood Adv. 2020;4(4):617-28.
240. Aldiwani M, Tharakan T, Al-Hassani A, Gibbons N, Pavlu J, Hrouda D. BK Virus Associated Haemorrhagic Cystitis. A systematic review of current prevention and treatment strategies. Int J Surg. 2019;63:34-42.
241. Noss G, Stauch G, Mehraein P, Georgii A. Oncogenic activity of the BK type of human papova virus in newborn Wistar rats. Arch Virol. 1981;69(3-4):239-51.
242. Starrett GJ, Buck CB. The case for BK polyomavirus as a cause of bladder cancer. Curr Opin Virol. 2019;39:8-15.
243. IARC. Malaria and some polyomaviruses (SV40, BK, JC, and Markel cell viruses). IARC Monogr Eval Carcinog Risks Hum. 2013;104:9-350.
244. Abend JR, Jiang M, Imperiale MJ. BK virus and human cancer: innocent until proven guilty. Semin Cancer Biol. 2009;19(4):252-60.
245. Kim S, Kim G-H. Roles of claudin-2, ZO-1 and occludin in leaky HK-2 cells. PLOS One. 2017;12(12):e0189221.
246. Gupta G, Kuppachi S, Kalil RS, Buck CB, Lynch CF, Engels EA. Treatment for presumed BK polyomavirus nephropathy and risk of urinary tract cancers among kidney transplant recipients in the United States. Am J Transplant. 2018;18(1):245-52.
247. Rogers R, Gohh R, Noska A. Urothelial cell carcinoma after BK polyomavirus infection in kidney transplant recipients: A cohort study of veterans. Transpl Infect Dis. 2017;19(5):e12752.
248. Li YJ, Wu HH, Chen CH, Wang HH, Chiang YJ, Hsu HH, et al. High Incidence and Early Onset of Urinary Tract Cancers in Patients with BK Polyomavirus Associated Nephropathy. Viruses. 2021;13(3).
249. Papadimitriou JC, Randhawa P, Rinaldo CH, Drachenberg CB, Alexiev B, Hirsch HH. BK Polyomavirus infection and renourinary tumorigenesis. Am J Transplant. 2016;16(2):398-406.
250. Meier RPH, Muller YD, Dietrich P-Y, Tille J-C, Nikolaev S, Sartori A, et al. Immunologic Clearance of a BK Virus-associated Metastatic Renal Allograft Carcinoma. Transplantation. 2021;105(2).
251. Kenan DJ, Mieczkowski PA, Burger-Calderon R, Singh HK, Nickeleit V. The oncogenic potential of BK-polyomavirus is linked to viral integration into the human genome. J Pathol. 2015;237(3):379-89.
252. Kenan DJ, Mieczkowski PA, Latulippe E, Côté I, Singh HK, Nickeleit V. BK Polyomavirus Genomic Integration and Large T Antigen Expression: Evolving Paradigms in Human Oncogenesis. Am J Transplant. 2017;17(6):1674-80.
253. Starrett GJ, Yu K, Golubeva Y, Lenz P, Piaskowski ML, Petersen D, et al. Evidence for virus-mediated oncogenesis in bladder cancers arising in solid organ transplant recipients. eLife. 2023;12:e82690.
254. Harris RS, Dudley JP. APOBECs and virus restriction. Virology. 2015;479-480:131-45.
255. Mertz TM, Collins CD, Dennis M, Coxon M, Roberts SA. APOBEC-Induced Mutagenesis in Cancer. Annu Rev Genet. 2022;56(1):229-52.
256. Starrett GJ, Serebrenik AA, Roelofs PA, McCann JL, Verhalen B, Jarvis MC, et al. Polyomavirus T Antigen Induces APOBEC3B Expression Using an LXCXE-Dependent and TP53-Independent Mechanism. mBio. 2019;10(1):10.1128/mbio.02690-18.
257. Verhalen B, Starrett GJ, Harris RS, Jiang M. Functional Upregulation of the DNA Cytosine Deaminase APOBEC3B by Polyomaviruses. J Virol. 2016;90(14):6379-86.

258. Peretti A, Geoghegan EM, Pastrana DV, Smola S, Feld P, Sauter M, et al. Characterization of BK Polyomaviruses from Kidney Transplant Recipients Suggests a Role for APOBEC3 in Driving In-Host Virus Evolution. Cell Host Microbe. 2018;23(5):628-35.e7.
259. McIlroy D, Peltier C, Nguyen ML, Manceau L, Mobuchon L, Le Baut N, et al. Quantification of APOBEC3 Mutation Rates Affecting the VP1 Gene of BK Polyomavirus In Vivo. Viruses. 2022;14(9).
260. Baker SC, Mason AS, Slip RG, Skinner KT, Macdonald A, Masood O, et al. Induction of APOBEC3-mediated genomic damage in urothelium implicates BK polyomavirus (BKPyV) as a hit-and-run driver for bladder cancer. Oncogene. 2022;41(15):2139-51.
261. Rao N, Starrett GJ, Piaskowski ML, Butler KE, Golubeva Y, Yan W, et al. Analysis of Several Common APOBEC-type Mutations in Bladder Tumors Suggests Links to Viral Infection. Cancer Prev Res. 2023;16(10):561-70.
262. Babjuk M, Burger M, Capoun O, Cohen D, Compérat EM, Dominguez Escrig JL, et al. European Association of Urology Guidelines on Non-muscle-invasive Bladder Cancer (Ta, T1, and Carcinoma in Situ). Eur Urol. 2022;81(1):75-94.
263. Cathomas R, Lorch A, Bruins HM, Compérat EM, Cowan NC, Efstathiou JA, et al. The 2021 Updated European Association of Urology Guidelines on Metastatic Urothelial Carcinoma. Eur Urol. 2022;81(1):95-103.
264. Hickman LA, Sawinski D, Guzzo T, Locke JE. Urologic malignancies in kidney transplantation. Am J Transplant. 2018;18(1):13-22.
265. Müller DC, Rämö M, Naegele K, Ribi S, Wetterauer C, Perrina V, et al. Donor-derived, metastatic urothelial cancer after kidney transplantation associated with a potentially oncogenic BK polyomavirus. J Pathol. 2018;244(3):265-70.
266. Darbinyan A, Major EO, Morgello S, Holland S, Ryschkewitsch C, Monaco MC, et al. BK virus encephalopathy and sclerosing vasculopathy in a patient with hypohidrotic ectodermal dysplasia and immunodeficiency. Acta Neuropathol Commun. 2016;4(1):73.
267. Antoniolli L, Borges R, Goldani LZ. BK Virus Encephalitis in HIV-Infected Patients: Case Report and Review. Case Report Med. 2017;2017:4307468.
268. Akazawa Y, Terada Y, Yamane T, Tanaka S, Aimoto M, Koh H, et al. Fatal BK virus pneumonia following stem cell transplantation. Transpl Infect Dis. 2012;14(6):E142-6.
269. Wang Y, Fang Y, Yan Z, Xia R, Zeng W, Deng W, et al. Fatal BK polyomavirus-associated pneumonia: report of two cases with literature review. BMC Infect Dis. 2023;23(1):592.
270. O'Kelly B, Keane A, Devitt E, Lockhart A, O'Rourke D, Lyons F. BK polyomavirus associated progressive multifocal leukoencephalopathy in a person living with HIV. Brain Behav Immun Health. 2021;15:100263.
271. Behzad-Behbahani A, Klapper PE, Vallely PJ, Cleator GM, Bonington A. BKV-DNA and JCV-DNA in CSF of patients with suspected meningitis or encephalitis. Infection. 2003;31(6):374-8.
272. Roy S, Mieczkowski PA, Weida C, Huo J, Roehrs P, Singh HK, Nickeleit V. BK polyomavirus nephropathy with systemic viral spread: Whole genome sequencing data from a fatal case of BKPyV infection. Transpl Infect Dis. 2020;22(2):e13269.
273. Espinosa-González R, E Aguilar León D, Rodríguez-Jurado R, Uribe-Uribe NO. Systemic BK Virus Infection in a Pediatric Patient With Severe Combined Immunodeficiency. Pediatr Dev Pathol. 2020;23(4):317-21.
274. St Johnston D, Ahringer J. Cell Polarity in Eggs and Epithelia: Parallels and Diversity. Cell. 2010;141(5):757-74.
275. Giepmans BNG, van Ijzendoorn SCD. Epithelial cell–cell junctions and plasma membrane domains. Biochim Biophys Acta - Biomembr. 2009;1788(4):820-31.

276. Buckley CE, St Johnston D. Apical–basal polarity and the control of epithelial form and function. Nat Rev Mol Cell Biol. 2022;23(8):559-77.
277. Stoops EH, Caplan MJ. Trafficking to the apical and basolateral membranes in polarized epithelial cells. J Am Soc Nephrol. 2014;25(7):1375-86.
278. Colombo F, Casella G, Podini P, Finardi A, Racchetti G, Norton EG, et al. Polarized cells display asymmetric release of extracellular vesicles. Traffic. 2021;22(4):98-110.
279. Matsui T, Osaki F, Hiragi S, Sakamaki Y, Fukuda M. ALIX and ceramide differentially control polarized small extracellular vesicle release from epithelial cells. Embo Rep. 2021;22(5):e51475.
280. Shen L, Weber CR, Raleigh DR, Yu D, Turner JR. Tight Junction Pore and Leak Pathways: A Dynamic Duo. Annu Rev Physiol. 2011;73(1):283-309.
281. Zihni C, Mills C, Matter K, Balda MS. Tight junctions: from simple barriers to multifunctional molecular gates. Nat Rev Mol Cell Biol. 2016;17(9):564-80.
282. Balkovetz DF. Claudins at the gate: determinants of renal epithelial tight junction paracellular permeability. Am J Physiol Renal Physiol. 2006;290(3):F572-F9.
283. Otani T, Furuse M. Tight Junction Structure and Function Revisited. Trends Cell Biol. 2020;30(10):805-17.
284. Johnston O, Jaswal D, Gill JS, Doucette S, Fergusson DA, Knoll GA. Treatment of polyomavirus infection in kidney transplant recipients: a systematic review. Transplantation. 2010;89(9):1057-70.
285. Balzer MS, Rohacs T, Susztak K. How Many Cell Types Are in the Kidney and What Do They Do? Annu Rev Physiol. 2022;84(1):507-31.
286. Aperia A. 2011 Homer Smith Award: To Serve and Protect: Classic and Novel Roles for Na: +: ,K: +: -Adenosine Triphosphatase. J Am Soc Nephrol. 2012;23(8):1283-90.
287. Dunbar LA, Caplan MJ. Ion Pumps in Polarized Cells: Sorting and Regulation of the Na^+,K^+- and H^+,K^+-ATPases. J Biol Chem. 2001;276(32):29617-20.
288. Lote CJ. The Proximal Tubule. Principles of Renal Physiology. New York, NY: Springer New York; 2012. p. 51-66.
289. Klunder LJ, Faber KN, Dijkstra G, van IJzendoorn SC. Mechanisms of cell polarity–controlled epithelial homeostasis and immunity in the intestine. Cold Spring Harb Perspect Biol. 2017;9(7):a027888.
290. Schulze RJ, Schott MB, Casey CA, Tuma PL, McNiven MA. The cell biology of the hepatocyte: A membrane trafficking machine. J Cell Biol. 2019;218(7):2096-112.
291. Maroni L, Haibo B, Ray D, Zhou T, Wan Y, Meng F, et al. Functional and structural features of cholangiocytes in health and disease. Cell Mol Gastroenterol Hepatol. 2015;1(4):368-80.
292. Doherty GJ, McMahon HT. Mechanisms of Endocytosis. Annu Rev Biochem. 2009;78(1):857-902.
293. Kay RR. Macropinocytosis: Biology and mechanisms. Cells Dev. 2021;168:203713.
294. Mayor S, Parton RG, Donaldson JG. Clathrin-independent pathways of endocytosis. Cold Spring Harb Perspect Biol. 2014;6(6).
295. Huotari J, Helenius A. Endosome maturation. EMBO J. 2011;30(17):3481-500-500.
296. Lote CJ. Essential Anatomy of the Kidney. Principles of Renal Physiology. New York, NY: Springer New York; 2012. p. 21-32.
297. Vermue IM, Begum R, Castilho M, Rookmaaker MB, Masereeuw R, Bouten CVC, et al. Renal Biology Driven Macro- and Microscale Design Strategies for Creating an Artificial Proximal Tubule Using Fiber-Based Technologies. ACS Biomater Sci Eng. 2021;7(10):4679-93.
298. Lote CJ. Glomerular Filtration. Principles of Renal Physiology. New York, NY: Springer New York; 2012. p. 33-44.

299. Curthoys NP, Moe OW. Proximal tubule function and response to acidosis. Clin J Am Soc Nephrol. 2014;9(9):1627-38.
300. Mount DB. Thick Ascending Limb of the Loop of Henle. Clin J Am Soc Nephrol. 2014;9(11):1974-86.
301. Subramanya AR, Ellison DH. Distal Convoluted Tubule. Clin J Am Soc Nephrol. 2014;9(12):2147-63.
302. Pearce D, Soundararajan R, Trimpert C, Kashlan OB, Deen PMT, Kohan DE. Collecting Duct Principal Cell Transport Processes and Their Regulation. Clin J Am Soc Nephrol. 2015;10(1):135-46.
303. Roy A, Al-bataineh MM, Pastor-Soler NM. Collecting Duct Intercalated Cell Function and Regulation. Clin J Am Soc Nephrol. 2015;10(2):305-24.
304. Rindler MJ, Chuman LM, Shaffer L, Saier MH. Retention of differentiated properties in an established dog kidney epithelial cell line (MDCK). J Cell Biol. 1979;81(3):635-48.
305. Elliget KA, Trump BF. Primary cultures of normal rat kidney proximal tubule epithelial cells for studies of renal cell injury. In Vitro Cell Dev Biol Anim. 1991;27(9):739-48.
306. Ronco P, Antoine M, Baudouin B, Geniteau-legendre M, Lelongt B, Chatelet F, et al. Polarized membrane expression of brush-border hydrolases in primary cultures of kidney proximal tubular cells depends on cell differentiation and is induced by dexamethasone. J Cell Physiol. 1990;145(2):222-37.
307. Wilmer MJ, Saleem MA, Masereeuw R, Ni L, van der Velden TJ, Russel FG, et al. Novel conditionally immortalized human proximal tubule cell line expressing functional influx and efflux transporters. Cell Tissue Res. 2010;339(2):449-57.
308. Duval K, Grover H, Han L-H, Mou Y, Pegoraro AF, Fredberg J, Chen Z. Modeling Physiological Events in 2D vs. 3D Cell Culture. Physiology. 2017;32(4):266-77.
309. Yeste J, Illa X, Alvarez M, Villa R. Engineering and monitoring cellular barrier models. J Biol Eng. 2018;12(1):18.
310. Chung HH, Mireles M, Kwarta BJ, Gaborski TR. Use of porous membranes in tissue barrier and co-culture models. Lab Chip. 2018;18(12):1671-89.
311. Cereijido M, Robbins ES, Dolan WJ, Rotunno CA, Sabatini DD. Polarized monolayers formed by epithelial cells on a permeable and translucent support. J Cell Biol. 1978;77(3):853-80.
312. Blackburn JG, Hazen-Martin DJ, Detrisac CJ, Sens DA. Electrophysiology and ultrastructure of cultured human proximal tubule cells. Kidney Int. 1988;33(2):508-16.
313. Rabito CA, Karish MV. Polarized amino acid transport by an epithelial cell line of renal origin (LLC-PK1). The basolateral systems. J Biol Chem. 1982;257(12):6802-8.
314. Hidalgo IJ, Raub TJ, Borchardt RT. Characterization of the human colon carcinoma cell line (Caco-2) as a model system for intestinal epithelial permeability. Gastroenterology. 1989;96(3):736-49.
315. Elwi AN, Damaraju VL, Kuzma ML, Mowles DA, Baldwin SA, Young JD, et al. Transepithelial fluxes of adenosine and 2′-deoxyadenosine across human renal proximal tubule cells: roles of nucleoside transporters hENT1, hENT2, and hCNT3. Am J Physiol Renal Physiol. 2009;296(6):F1439-F51.
316. Shamir ER, Ewald AJ. Three-dimensional organotypic culture: experimental models of mammalian biology and disease. Nat Rev Mol Cell Biol. 2014;15(10):647-64.
317. Cho MJ, Thompson DP, Cramer CT, Vidmar TJ, Scieszka JF. The Madin Darby canine kidney (MDCK) epithelial cell monolayer as a model cellular transport barrier. Pharm Res. 1989;6(1):71-7.
318. Dukes JD, Whitley P, Chalmers AD. The MDCK variety pack: choosing the right strain. BMC Cell Biol. 2011;12:43.

319. Pentecost M, Otto G, Theriot JA, Amieva MR. Listeria monocytogenes invades the epithelial junctions at sites of cell extrusion. PLOS Pathog. 2006;2(1):e3.
320. Yu Q, Wang L-C, Di Benigno S, Stein DC, Song W. Gonococcal invasion into epithelial cells depends on both cell polarity and ezrin. PLOS Pathog. 2021;17(12):e1009592.
321. Golovkine G, Faudry E, Bouillot S, Elsen S, Attrée I, Huber P. Pseudomonas aeruginosa Transmigrates at Epithelial Cell-Cell Junctions, Exploiting Sites of Cell Division and Senescent Cell Extrusion. PLOS Pathog. 2016;12(1):e1005377.
322. Clayson ET, Compans RW. Entry of simian virus 40 is restricted to apical surfaces of polarized epithelial cells. Mol Cell Biol. 1988;8(8):3391-6.
323. Tseng C-TK, Tseng J, Perrone L, Worthy M, Popov V, Peters CJ. Apical entry and release of severe acute respiratory syndrome-associated coronavirus in polarized Calu-3 lung epithelial cells. J Virol. 2005;79(15):9470-9.
324. Katoh H, Nakatsu Y, Kubota T, Sakata M, Takeda M, Kidokoro M. Mumps Virus Is Released from the Apical Surface of Polarized Epithelial Cells, and the Release Is Facilitated by a Rab11-Mediated Transport System. J Virol. 2015;89(23):12026-34.
325. Capelli N, Marion O, Dubois M, Allart S, Bertrand-Michel J, Lhomme S, et al. Vectorial Release of Hepatitis E Virus in Polarized Human Hepatocytes. J Virol. 2019;93(4).
326. Lin W-HW, Tsay AJ, Lalime EN, Pekosz A, Griffin DE. Primary differentiated respiratory epithelial cells respond to apical measles virus infection by shedding multinucleated giant cells. Proc Natl Acad Sci U S A. 2021;118(11):e2013264118.
327. Simian M, Bissell MJ. Organoids: A historical perspective of thinking in three dimensions. J Cell Biol. 2017;216(1):31-40.
328. Barrila J, Crabbé A, Yang J, Franco K, Nydam SD, Forsyth RJ, et al. Modeling Host-Pathogen Interactions in the Context of the Microenvironment: Three-Dimensional Cell Culture Comes of Age. Infect Immun. 2018;86(11).
329. Barrila J, Radtke AL, Crabbé A, Sarker SF, Herbst-Kralovetz MM, Ott CM, Nickerson CA. Organotypic 3D cell culture models: using the rotating wall vessel to study host–pathogen interactions. Nat Rev Microbiol. 2010;8(11):791-801.
330. Drummond CG, Nickerson CA, Coyne CB. A Three-Dimensional Cell Culture Model To Study Enterovirus Infection of Polarized Intestinal Epithelial Cells. mSphere. 2016;1(1):e00030-15.
331. Bramley JC, Drummond CG, Lennemann NJ, Good CA, Kim KS, Coyne CB. A Three-Dimensional Cell Culture System To Model RNA Virus Infections at the Blood-Brain Barrier. mSphere. 2017;2(3).
332. Corry J, Arora N, Good CA, Sadovsky Y, Coyne CB. Organotypic models of type III interferon-mediated protection from Zika virus infections at the maternal–fetal interface. Proc Natl Acad Sci U S A. 2017;114(35):9433-8.
333. Carterson AJ, Bentrup KHz, Ott CM, Clarke MS, Pierson DL, Vanderburg CR, et al. A549 Lung Epithelial Cells Grown as Three-Dimensional Aggregates: Alternative Tissue Culture Model for Pseudomonas aeruginosa Pathogenesis. Infect Immun. 2005;73(2):1129-40.
334. Łaniewski P, Gomez A, Hire G, So M, Herbst-Kralovetz MM. Human Three-Dimensional Endometrial Epithelial Cell Model To Study Host Interactions with Vaginal Bacteria and Neisseria gonorrhoeae. Infect Immun. 2017;85(3):10.1128/iai.01049-16.
335. Liu D, Chen S, Win Naing M. A review of manufacturing capabilities of cell spheroid generation technologies and future development. Biotechnol Bioeng. 2021;118(2):542-54.
336. Velasco V, Shariati SA, Esfandyarpour R. Microtechnology-based methods for organoid models. Microsys Nanoeng. 2020;6(1):76.

337. Costa EC, Moreira AF, de Melo-Diogo D, Gaspar VM, Carvalho MP, Correia IJ. 3D tumor spheroids: an overview on the tools and techniques used for their analysis. Biotechnol Adv. 2016;34(8):1427-41.
338. Pampaloni F, Reynaud EG, Stelzer EHK. The third dimension bridges the gap between cell culture and live tissue. Nat Rev Mol Cell Biol. 2007;8(10):839-45.
339. Celis T, Bullens DMA, Hoet PHM, Ghosh M. Development and validation of a human bronchial epithelial spheroid model to study respiratory toxicity in vitro. Arch Toxicol. 2024;98(2):493-505.
340. Kosheleva NV, Efremov YM, Shavkuta BS, Zurina IM, Zhang D, Zhang Y, et al. Cell spheroid fusion: beyond liquid drops model. Sci Rep. 2020;10(1):12614.
341. Yonemura S. Differential Sensitivity of Epithelial Cells to Extracellular Matrix in Polarity Establishment. PLOS One. 2014;9(11):e112922.
342. Wohlwend A, Montesano R, Vassalli JD, Orci L. LLC-PK1 cysts: a model for the study of epithelial polarity. J Cell Physiol. 1985;125(3):533-9.
343. Hall HG, Farson DA, Bissell MJ. Lumen formation by epithelial cell lines in response to collagen overlay: a morphogenetic model in culture. Proc Natl Acad Sci U S A. 1982;79(15):4672-6.
344. Schutgens F, Clevers H. Human Organoids: Tools for Understanding Biology and Treating Diseases. Annual Review of Pathology: Mechanisms of Disease. 2020;15(1):211-34.
345. Zhao Z, Chen X, Dowbaj AM, Sljukic A, Bratlie K, Lin L, et al. Organoids. Nat Rev Methods Primers. 2022;2(1):94.
346. Kim J, Koo B-K, Knoblich JA. Human organoids: model systems for human biology and medicine. Nat Rev Mol Cell Biol. 2020;21(10):571-84.
347. Gijzen L, Yousef Yengej FA, Schutgens F, Vormann MK, Ammerlaan CME, Nicolas A, et al. Culture and analysis of kidney tubuloids and perfused tubuloid cells-on-a-chip. Nat Protoc. 2021;16(4):2023-50.
348. Sato T, Stange DE, Ferrante M, Vries RGJ, van Es JH, van den Brink S, et al. Long-term Expansion of Epithelial Organoids From Human Colon, Adenoma, Adenocarcinoma, and Barrett's Epithelium. Gastroenterology. 2011;141(5):1762-72.
349. Schutgens F, Rookmaaker MB, Margaritis T, Rios A, Ammerlaan C, Jansen J, et al. Tubuloids derived from human adult kidney and urine for personalized disease modeling. Nat Biotechnol. 2019;37(3):303-13.
350. Takasato M, Er PX, Becroft M, Vanslambrouck JM, Stanley EG, Elefanty AG, Little MH. Directing human embryonic stem cell differentiation towards a renal lineage generates a self-organizing kidney. Nat Cell Biol. 2014;16(1):118-26.
351. Takasato M, Er PX, Chiu HS, Little MH. Generation of kidney organoids from human pluripotent stem cells. Nat Protoc. 2016;11(9):1681-92.
352. Hofer M, Lutolf MP. Engineering organoids. Nat Rev Mater. 2021;6(5):402-20.
353. Miller AJ, Dye BR, Ferrer-Torres D, Hill DR, Overeem AW, Shea LD, Spence JR. Generation of lung organoids from human pluripotent stem cells in vitro. Nat Protoc. 2019;14(2):518-40.
354. Sachs N, Papaspyropoulos A, Zomer-van Ommen DD, Heo I, Böttinger L, Klay D, et al. Long-term expanding human airway organoids for disease modeling. EMBO J. 2019;38(4):e100300.
355. Lancaster MA, Renner M, Martin C-A, Wenzel D, Bicknell LS, Hurles ME, et al. Cerebral organoids model human brain development and microcephaly. Nature. 2013;501(7467):373-9.
356. Co JY, Margalef-Català M, Li X, Mah AT, Kuo CJ, Monack DM, Amieva MR. Controlling Epithelial Polarity: A Human Enteroid Model for Host-Pathogen Interactions. Cell Rep. 2019;26(9):2509-20.e4.

357. Huh D, Hamilton GA, Ingber DE. From 3D cell culture to organs-on-chips. Trends Cell Biol. 2011;21(12):745-54.
358. van Duinen V, Trietsch SJ, Joore J, Vulto P, Hankemeier T. Microfluidic 3D cell culture: from tools to tissue models. Curr Opin Biotechnol. 2015;35:118-26.
359. Aguilar C, Alves da Silva M, Saraiva M, Neyazi M, Olsson IAS, Bartfeld S. Organoids as host models for infection biology – a review of methods. Exp Mol Med. 2021;53(10):1471-82.
360. Bhatia SN, Ingber DE. Microfluidic organs-on-chips. Nat Biotechnol. 2014;32(8):760-72.
361. Villenave R, Wales SQ, Hamkins-Indik T, Papafragkou E, Weaver JC, Ferrante TC, et al. Human Gut-On-A-Chip Supports Polarized Infection of Coxsackie B1 Virus In Vitro. PLOS One. 2017;12(2):e0169412.
362. Nieskens TTG, Persson M, Kelly EJ, Sjögren A-K. A Multicompartment Human Kidney Proximal Tubule-on-a-Chip Replicates Cell Polarization–Dependent Cisplatin Toxicity. Drug Metab Dispos. 2020;48(12):1303-11.
363. Klasse PJ. Neutralization of Virus Infectivity by Antibodies: Old Problems in New Perspectives. Advances in Biology. 2014;2014:157895.
364. Deschamps T, Kalamvoki M. Impaired STING Pathway in Human Osteosarcoma U2OS Cells Contributes to the Growth of ICP0-Null Mutant Herpes Simplex Virus. J Virol. 2017;91(9).
365. Reus JB, Trivino-Soto GS, Wu LI, Kokott K, Lim ES. SV40 Large T Antigen Is Not Responsible for the Loss of STING in 293T Cells but Can Inhibit cGAS-STING Interferon Induction. Viruses. 2020;12(2).
366. Sui H, Zhou M, Imamichi H, Jiao X, Sherman BT, Lane HC, Imamichi T. STING is an essential mediator of the Ku70-mediated production of IFN-λ1 in response to exogenous DNA. Sci Signal. 2017;10(488).
367. Forero A, Giacobbi NS, McCormick KD, Gjoerup OV, Bakkenist CJ, Pipas JM, Sarkar SN. Simian Virus 40 Large T Antigen Induces IFN-Stimulated Genes through ATR Kinase. J Immunol. 2014;192(12):5933-42.
368. Wang F, Barrett JW, Ma Y, Dekaban GA, McFadden G. Induction of Alpha/Beta Interferon by Myxoma Virus Is Selectively Abrogated When Primary Mouse Embryo Fibroblasts Become Immortalized. J Virol. 2009;83(11):5928-32.
369. Shinohara T, Matsuda M, Cheng SH, Marshall J, Fujita M, Nagashima K. BK virus infection of the human urinary tract. J Med Virol. 1993;41(4):301-5.
370. Acott PD, O'Regan PA, Lee SH, Crocker JF. Utilization of vero cells for primary and chronic BK virus infection. Transplant Proc. 2006;38(10):3502-5.
371. Maraldi NM, Barbanti Brodano G, Portolani M, La Placa M. Ultrastructural aspects of BK virus uptake and replication in human fibroblasts. J Gen Virol. 1975;27(1):71-80.
372. Leuenberger D, Andresen PA, Gosert R, Binggeli S, Strom EH, Bodaghi S, et al. Human polyomavirus type 1 (BK virus) agnoprotein is abundantly expressed but immunologically ignored. Clin Vaccine Immunol. 2007;14(8):959-68.
373. Bernhoff E, Gutteberg TJ, Sandvik K, Hirsch HH, Rinaldo CH. Cidofovir inhibits polyomavirus BK replication in human renal tubular cells downstream of viral early gene expression. Am J Transplant. 2008;8(7):1413-22.
374. Detrisac CJ, Sens MA, Garvin AJ, Spicer SS, Sens DA. Tissue culture of human kidney epithelial cells of proximal tubule origin. Kidney Int. 1984;25(2):383-90.
375. Humes HD, Fissell WH, Weitzel WF, Buffington DA, Westover AJ, MacKay SM, Gutierrez JM. Metabolic replacement of kidney function in uremic animals with a bioartificial kidney containing human cells. Am J Kidney Dis. 2002;39(5):1078-87.

376. Luo Y, Motamedi N, Magaldi Thomas G, Gee Gretchen V, Atwood Walter J, DiMaio D. Interaction between Simian Virus 40 Major Capsid Protein VP1 and Cell Surface Ganglioside GM1 Triggers Vacuole Formation. mBio. 2016;7(2):10.1128/mbio.00297-16.
377. Tremolada S, Akan S, Otte J, Khalili K, Ferrante P, Chaudhury PR, et al. Rare subtypes of BK virus are viable and frequently detected in renal transplant recipients with BK virus-associated nephropathy. Virology. 2010;404(2):312-8.
378. Takemoto KK, Mullarkey MF. Human papovavirus, BK strain: biological studies including antigenic relationship to simian virus 40. J Virol. 1973;12(3):625-31.
379. Pietrobon S, Bononi I, Mazzoni E, Lotito F, Manfrini M, Puozzo A, et al. Specific IgG Antibodies React to Mimotopes of BK Polyomavirus, a Small DNA Tumor Virus, in Healthy Adult Sera. Front Immunol. 2017;8:236.
380. An P, Sáenz Robles MT, Cantalupo PG, Naik AS, Sealfon R, Imperiale MJ, Pipas JM. Cultured Renal Proximal Tubular Epithelial Cells Resemble a Stressed/Damaged Kidney While Supporting BK Virus Infection. J Virol. 2023;97(5):e0034323.
381. Procario MC, Sexton JZ, Halligan BS, Imperiale MJ. Single-Cell, High-Content Microscopy Analysis of BK Polyomavirus Infection. Microbiol Spectr. 2023;11(3):e00873-23.
382. Rinaldo CH, Gosert R, Bernhoff E, Finstad S, Hirsch HH. 1-O-hexadecyloxypropyl cidofovir (CMX001) effectively inhibits polyomavirus BK replication in primary human renal tubular epithelial cells. Antimicrob Agents Chemother. 2010;54(11):4714-22.
383. Hirsch HH, Yakhontova K, Lu M, Manzetti J. BK Polyomavirus Replication in Renal Tubular Epithelial Cells Is Inhibited by Sirolimus, but Activated by Tacrolimus Through a Pathway Involving FKBP-12. Am J Transplant. 2016;16(3):821-32.
384. Ferrell N, Cheng J, Miao S, Roy S, Fissell WH. Orbital Shear Stress Regulates Differentiation and Barrier Function of Primary Renal Tubular Epithelial Cells. ASAIO J. 2018;64(6):766-72.
385. Duan Y, Gotoh N, Yan Q, Du Z, Weinstein AM, Wang T, Weinbaum S. Shear-induced reorganization of renal proximal tubule cell actin cytoskeleton and apical junctional complexes. Proc Natl Acad Sci U S A. 2008;105(32):11418-23.
386. Shaughnessey EM, Kann SH, Azizgolshani H, Black LD, Charest JL, Vedula EM. Evaluation of rapid transepithelial electrical resistance (TEER) measurement as a metric of kidney toxicity in a high-throughput microfluidic culture system. Sci Rep. 2022;12(1):13182.
387. Omer D, Pleniceanu O, Gnatek Y, Namestnikov M, Cohen-Zontag O, Goldberg S, et al. Human Kidney Spheroids and Monolayers Provide Insights into SARS-CoV-2 Renal Interactions. J Am Soc Nephrol. 2021;32(9):2242-54.
388. Krautkrämer E, Lehmann MJ, Bollinger V, Zeier M. Polar release of pathogenic Old World hantaviruses from renal tubular epithelial cells. Virol J. 2012;9(1):299.
389. Van der Hauwaert C, Savary G, Gnemmi V, Glowacki F, Pottier N, Bouillez A, et al. Isolation and characterization of a primary proximal tubular epithelial cell model from human kidney by CD10/CD13 double labeling. PLOS One. 2013;8(6):e66750-e.
390. Bartfeld S, Clevers H. Organoids as Model for Infectious Diseases: Culture of Human and Murine Stomach Organoids and Microinjection of Helicobacter Pylori. Journal of visualized experiments : JoVE. 2015(105).
391. Qi W, Johnson DW, Vesey DA, Pollock CA, Chen X. Isolation, propagation and characterization of primary tubule cell culture from human kidney. Nephrology. 2007;12(2):155-9.
392. Lorentzen EM, Henriksen S, Rinaldo CH. Modelling BK Polyomavirus dissemination and cytopathology using polarized human renal tubule epithelial cells. PLOS Pathog. 2023;19(8):e1011622.
393. Wang WH, Chang LK, Liu ST. Molecular interactions of Epstein-Barr virus capsid proteins. J Virol. 2011;85(4):1615-24.

394. Tugizov SM, Berline JW, Palefsky JM. Epstein-Barr virus infection of polarized tongue and nasopharyngeal epithelial cells. Nat Med. 2003;9(3):307-14.
395. Parvate A, Williams EP, Taylor MK, Chu YK, Lanman J, Saphire EO, Jonsson CB. Diverse Morphology and Structural Features of Old and New World Hantaviruses. Viruses. 2019;11(9).
396. Krautkrämer E, Zeier M. Hantavirus causing hemorrhagic fever with renal syndrome enters from the apical surface and requires decay-accelerating factor (DAF/CD55). J Virol. 2008;82(9):4257-64.
397. Matthijnssens J, Attoui H, Bányai K, Brussaard CPD, Danthi P, del Vas M, et al. ICTV Virus Taxonomy Profile: Sedoreoviridae 2022. J Gen Virol. 2022;103(10).
398. Realpe M, Espinosa R, López S, Arias CF. Rotaviruses require basolateral molecules for efficient infection of polarized MDCKII cells. Virus Res. 2010;147(2):231-41.
399. Butcher SJ, Aitken J, Mitchell J, Gowen B, Dargan DJ. Structure of the Human Cytomegalovirus B Capsid by Electron Cryomicroscopy and Image Reconstruction. J Struct Biol. 1998;124(1):70-6.
400. Hemmings DG, Guilbert LJ. Polarized Release of Human Cytomegalovirus from Placental Trophoblasts. J Virol. 2002;76(13):6710-7.
401. Stuart DI, Ren J, Wang X, Rao Z, Fry EE. Hepatitis A Virus Capsid Structure. Cold Spring Harb Perspect Med. 2019;9(5).
402. Blank CA, Anderson DA, Beard M, Lemon SM. Infection of Polarized Cultures of Human Intestinal Epithelial Cells with Hepatitis A Virus: Vectorial Release of Progeny Virions through Apical Cellular Membranes. J Virol. 2000;74(14):6476-84.
403. Snooks MJ, Bhat P, Mackenzie J, Counihan NA, Vaughan N, Anderson DA. Vectorial Entry and Release of Hepatitis A Virus in Polarized Human Hepatocytes. J Virol. 2008;82(17):8733-42.
404. Gatherer D, Depledge DP, Hartley CA, Szpara ML, Vaz PK, Benkő M, et al. ICTV Virus Taxonomy Profile: Herpesviridae 2021. J Gen Virol. 2021;102(10).
405. Topp KS, Rothman AL, Lavail JH. Herpes Virus Infection of RPE and MDCK Cells: Polarity of Infection. Exp Eye Res. 1997;64(3):343-54.
406. Rima B, Balkema-Buschmann A, Dundon WG, Duprex P, Easton A, Fouchier R, et al. ICTV Virus Taxonomy Profile: Paramyxoviridae. J Gen Virol. 2019;100(12):1593-4.
407. Ciarlet M, Crawford SE, Estes MK. Differential infection of polarized epithelial cell lines by sialic acid-dependent and sialic acid-independent rotavirus strains. J Virol. 2001;75(23):11834-50.
408. Tucker S, Melsen L, Compans R. Migration of polarized epithelial cells through permeable membrane substrates of defined pore size. Eur J Cell Biol. 1992;58:280-90.
409. Gong T, Liu L, Jiang W, Zhou R. DAMP-sensing receptors in sterile inflammation and inflammatory diseases. Nat Rev Immunol. 2020;20(2):95-112.
410. DeWolf SE, Kasimsetty SG, Hawkes AA, Stocks LM, Kurian SM, McKay DB. DAMPs Released From Injured Renal Tubular Epithelial Cells Activate Innate Immune Signals in Healthy Renal Tubular Epithelial Cells. Transplantation. 2022;106(8):1589-99.
411. Huerfano S, Ryabchenko B, Forstová J. Nucleofection of expression vectors induces a robust interferon response and inhibition of cell proliferation. DNA Cell Biol. 2013;32(8):467-79.
412. Motamedi N, Sewald X, Luo Y, Mothes W, DiMaio D. SV40 Polyomavirus Activates the Ras-MAPK Signaling Pathway for Vacuolization, Cell Death, and Virus Release. Viruses. 2020;12(10).
413. Miyamura T, Kitahara T. Early cytoplasmic vacuolization of African green monkey kidney cells by SV40. Arch Virol. 1975;48(2):147-56.

414. Giepmans BNG, Adams SR, Ellisman MH, Tsien RY. The Fluorescent Toolbox for Assessing Protein Location and Function. Science. 2006;312(5771):217-24.
415. Crivat G, Taraska JW. Imaging proteins inside cells with fluorescent tags. Trends Biotechnol. 2012;30(1):8-16.
416. Chong ZX, Yeap SK, Ho WY. Transfection types, methods and strategies: a technical review. PeerJ. 2021;9:e11165.
417. Stepanenko AA, Heng HH. Transient and stable vector transfection: Pitfalls, off-target effects, artifacts. Mutat Res Rev Mutat Res. 2017;773:91-103.
418. Bykov YS, Cortese M, Briggs JA, Bartenschlager R. Correlative light and electron microscopy methods for the study of virus-cell interactions. FEBS Lett. 2016.
419. Bozzola JJ. Conventional Specimen Preparation Techniques for Transmission Electron Microscopy of Cultured Cells. In: Kuo J, editor. Electron Microscopy: Methods and Protocols. Totowa, NJ: Humana Press; 2014. p. 1-19.
420. Ellis EA. Staining Sectioned Biological Specimens for Transmission Electron Microscopy: Conventional and En Bloc Stains. In: Kuo J, editor. Electron Microscopy: Methods and Protocols. Totowa, NJ: Humana Press; 2014. p. 57-72.
421. Webster P. Microwave-Assisted Processing and Embedding for Transmission Electron Microscopy. In: Kuo J, editor. Electron Microscopy: Methods and Protocols. Totowa, NJ: Humana Press; 2014. p. 21-37.
422. Murk JLAN, Posthuma G, Koster AJ, Geuze HJ, Verkleij AJ, Kleijmeer MJ, Humbel BM. Influence of aldehyde fixation on the morphology of endosomes and lysosomes: quantitative analysis and electron tomography. J Microsc. 2003;212(1):81-90.
423. Wegener CS, Malerød L, Pedersen NM, Prodiga C, Bakke O, Stenmark H, Brech A. Ultrastructural characterization of giant endosomes induced by GTPase-deficient Rab5. Histochem Cell Biol. 2010;133(1):41-55.
424. Funk GA, Gosert R, Comoli P, Ginevri F, Hirsch HH. Polyomavirus BK replication dynamics in vivo and in silico to predict cytopathology and viral clearance in kidney transplants. Am J Transplant. 2008;8(11):2368-77.
425. Funk GA, Hirsch HH. From plasma BK viral load to allograft damage: rule of thumb for estimating the intrarenal cytopathic wear. Clin Infect Dis. 2009;49(6):989-90.
426. Seifert ME, Mannon RB, Nellore A, Young J, Wiseman AC, Cohen DJ, et al. A multicenter prospective study to define the natural history of BK viral infections in kidney transplantation. Transpl Infect Dis. 2024:e14237.
427. David-Neto E, Agena F, Silva Ribeiro David D, Paula FJ, Camera Pierrotti LC, Domingues Fink MC, Fonseca de Azevedo LS. Effect of polyoma viremia on 3-year allograft kidney function. Transpl Infect Dis. 2019;21(2):e13056.
428. Elfadawy N, Flechner SM, Schold JD, Srinivas TR, Poggio E, Fatica R, et al. Transient versus Persistent BK Viremia and Long-Term Outcomes after Kidney and Kidney–Pancreas Transplantation. Clin J Am Soc Nephrol. 2014;9(3):553-61.
429. Huang G, Wang C-x, Zhang L, Fei J-g, Deng S-x, Qiu J, et al. Monitoring of polyomavirus BK replication and impact of preemptive immunosuppression reduction in renal-transplant recipients in China: a 5-year single-center analysis. Diagn Microbiol Infect Dis. 2015;81(1):21-6.
430. Hardinger KL, Koch MJ, Bohl DJ, Storch GA, Brennan DC. BK-Virus and the Impact of Pre-Emptive Immunosuppression Reduction: 5-Year Results. Am J Transplant. 2010;10(2):407-15.
431. Ginevri F, Azzi A, Hirsch HH, Basso S, Fontana I, Cioni M, et al. Prospective monitoring of polyomavirus BK replication and impact of pre-emptive intervention in pediatric kidney recipients. Am J Transplant. 2007;7(12):2727-35.

432. Weiss AS, Gralla J, Chan L, Klem P, Wiseman AC. Aggressive Immunosuppression Minimization Reduces Graft Loss Following Diagnosis of BK Virus-Associated Nephropathy: A Comparison of Two Reduction Strategies. Clin J Am Soc Nephrol. 2008.
433. Broeders EN, Hamade A, El Mountahi F, Racapé J, Hougardy J-M, Le Moine A, Vereerstraeten P. Preemptive reduction of immunosuppression upon high urinary polyomavirus loads improves patient survival without affecting kidney graft function. Transpl Infect Dis. 2016;18(6):872-80.
434. Simard-Meilleur MC, Bodson-Clermont P, St-Louis G, Pâquet MR, Girardin C, Fortin MC, et al. Stabilization of renal function after the first year of follow-up in kidney transplant recipients treated for significant BK polyomavirus infection or BK polyomavirus-associated nephropathy. Transpl Infect Dis. 2017;19(3).
435. Schaub S, Hirsch HH, Dickenmann M, Steiger J, Mihatsch MJ, Hopfer H, Mayr M. Reducing immunosuppression preserves allograft function in presumptive and definitive polyomavirus-associated nephropathy. Am J Transplant. 2010;10(12):2615-23.
436. Celik B, Shapiro R, Vats A, Randhawa PS. Polyomavirus allograft nephropathy: sequential assessment of histologic viral load, tubulitis, and graft function following changes in immunosuppression. Am J Transplant. 2003;3(11):1378-82.
437. Brennan DC, Agha I, Bohl DL, Schnitzler MA, Hardinger KL, Lockwood M, et al. Incidence of BK with tacrolimus versus cyclosporine and impact of preemptive immunosuppression reduction. Am J Transplant. 2005;5(3):582-94.
438. Seifert ME, Gunasekaran M, Horwedel TA, Daloul R, Storch GA, Mohanakumar T, Brennan DC. Polyomavirus Reactivation and Immune Responses to Kidney-Specific Self-Antigens in Transplantation. J Am Soc Nephrol. 2017;28(4):1314-25.
439. Dakroub F, Touzé A, Sater FA, Fiore T, Morel V, Tinez C, et al. Impact of pre-graft serology on risk of BKPyV infection post-renal transplantation. Nephrol Dial Transplant. 2021;37(4):781-8.
440. Schmitt C, Raggub L, Linnenweber-Held S, Adams O, Schwarz A, Heim A. Donor origin of BKV replication after kidney transplantation. J Clin Virol. 2014;59(2):120-5.
441. Bird SW, Kirkegaard K. Escape of non-enveloped virus from intact cells. Virology. 2015;479-480:444-9.
442. Owusu IA, Quaye O, Passalacqua KD, Wobus CE. Egress of non-enveloped enteric RNA viruses. J Gen Virol. 2021;102(3).
443. Gudipaty SA, Rosenblatt J. Epithelial cell extrusion: Pathways and pathologies. Semin Cell Dev Biol. 2017;67:132-40.
444. Moshiri J, Craven AR, Mixon SB, Amieva MR, Kirkegaard K. Mechanosensitive extrusion of Enterovirus A71-infected cells from colonic organoids. Nat Microbiol. 2023;8:629-39.
445. Knodler LA, Vallance BA, Celli J, Winfree S, Hansen B, Montero M, Steele-Mortimer O. Dissemination of invasive Salmonella via bacterial-induced extrusion of mucosal epithelia. Proc Natl Acad Sci U S A. 2010;107(41):17733-8.
446. Liesman RM, Buchholz UJ, Luongo CL, Yang L, Proia AD, DeVincenzo JP, et al. RSV-encoded NS2 promotes epithelial cell shedding and distal airway obstruction. J Clin Invest. 2014;124(5):2219-33.
447. Shkarina K, Hasel de Carvalho E, Santos JC, Ramos S, Leptin M, Broz P. Optogenetic activators of apoptosis, necroptosis, and pyroptosis. J Cell Biol. 2022;221(6):e202109038.
448. Santacreu BJ, Romero DJ, Pescio LG, Tarallo E, Sterin-Speziale NB, Favale NO. Apoptotic cell extrusion depends on single-cell synthesis of sphingosine-1-phosphate by sphingosine kinase 2. Biochim Biophys Acta Mol Cell Biol Lipids. 2021;1866(4):158888.

449. Drachenberg CB, Hirsch HH, Ramos E, Papadimitriou JC. Polyomavirus disease in renal transplantation: review of pathological findings and diagnostic methods. Hum Pathol. 2005;36(12):1245-55.
450. Drachenberg RC, Drachenberg CB, Papadimitriou JC, Ramos E, Fink JC, Wali R, et al. Morphological spectrum of polyoma virus disease in renal allografts: diagnostic accuracy of urine cytology. Am J Transplant. 2001;1(4):373-81.
451. Hirsch HH, Knowles W, Dickenmann M, Passweg J, Klimkait T, Mihatsch MJ, Steiger J. Prospective study of polyomavirus type BK replication and nephropathy in renal-transplant recipients. N Engl J Med. 2002;347(7):488-96.
452. Zhong P, Agosto LM, Munro JB, Mothes W. Cell-to-cell transmission of viruses. Curr Opin Virol. 2013;3(1):44-50.
453. Monel B, Compton AA, Bruel T, Amraoui S, Burlaud-Gaillard J, Roy N, et al. Zika virus induces massive cytoplasmic vacuolization and paraptosis-like death in infected cells. EMBO J. 2017;36(12):1653-68-68.
454. Liu Y, Sun Y, Xu Y, Dong T, Qian L, Zheng H, et al. Targeting VPS41 induces methuosis and inhibits autophagy in cancer cells. Cell Chem Biol. 2023;30(2):130-43.e5.
455. Maltese WA, Overmeyer JH. Methuosis: Nonapoptotic Cell Death Associated with Vacuolization of Macropinosome and Endosome Compartments. Am J Pathol. 2014;184(6):1630-42.
456. Compton LM, Ikonomov OC, Sbrissa D, Garg P, Shisheva A. Active vacuolar H+ ATPase and functional cycle of Rab5 are required for the vacuolation defect triggered by PtdIns(3,5)P2 loss under PIKfyve or Vps34 deficiency. Am J Physiol Cell Physiol. 2016;311(3):C366-77.
457. Sharma G, Guardia CM, Roy A, Vassilev A, Saric A, Griner LN, et al. A family of PIKFYVE inhibitors with therapeutic potential against autophagy-dependent cancer cells disrupt multiple events in lysosome homeostasis. Autophagy. 2019;15(10):1694-718.
458. Capurro MI, Greenfield LK, Prashar A, Xia S, Abdullah M, Wong H, et al. VacA generates a protective intracellular reservoir for Helicobacter pylori that is eliminated by activation of the lysosomal calcium channel TRPML1. Nat Microbiol. 2019;4(8):1411-23.
459. Cover TL, Blaser MJ. Purification and characterization of the vacuolating toxin from Helicobacter pylori. J Biol Chem. 1992;267(15):10570-5.
460. Bright NA, Davis LJ, Luzio JP. Endolysosomes Are the Principal Intracellular Sites of Acid Hydrolase Activity. Curr Biol. 2016;26(17):2233-45.
461. Kartenbeck J, Stukenbrok H, Helenius A. Endocytosis of simian virus 40 into the endoplasmic reticulum. J Cell Biol. 1989;109(6):2721-9.
462. McIlroy D, Hönemann M, Nguyen N-K, Barbier P, Peltier C, Rodallec A, et al. Persistent BK polyomavirus viruria is associated with accumulation of VP1 mutations and neutralization escape. Viruses. 2020;12(8):824.
463. Lauver MD, Goetschius DJ, Netherby-Winslow CS, Ayers KN, Jin G, Haas DG, et al. Antibody escape by polyomavirus capsid mutation facilitates neurovirulence. eLife. 2020;9:e61056.

Appendix: Paper 1

Lorentzen et al. Virology Journal (2020) 17:5
https://doi.org/10.1186/s12985-019-1275-9

Virology Journal

CASE REPORT Open Access

Early fulminant BK polyomavirus-associated nephropathy in two kidney transplant patients with low neutralizing antibody titers receiving allografts from the same donor

Elias Myrvoll Lorentzen[1,2], Stian Henriksen[1,2], Amandeep Kaur[3], Grete Birkeland Kro[4,5], Clara Hammarström[6], Hans H. Hirsch[3,7], Karsten Midtvedt[8] and Christine Hanssen Rinaldo[1,2*]

Abstract

Background: BK Polyomavirus (BKPyV) causes premature graft failure in 1 to 15% of kidney transplant (KT) recipients. High-level BKPyV-viruria and BKPyV-DNAemia precede polyomavirus-associated nephropathy (PyVAN), and guide clinical management decisions. In most cases, BKPyV appears to come from the donor kidney, but data from biopsy-proven PyVAN cases are lacking. Here, we report the early fulminant course of biopsy-proven PyVAN in two male KT recipients in their sixties, receiving kidneys from the same deceased male donor.

Case presentations: Both recipients received intravenous basiliximab induction, and maintenance therapy consisting of tacrolimus (trough levels 3–7 ng/mL from time of engraftment), mycophenolate mofetil 750 mg bid, and prednisolone. At 4 weeks post-transplant, renal function was satisfactory with serum creatinine concentrations of 106 and 72 μmol/L in recipient #1 and recipient #2, respectively. Plasma BKPyV-DNAemia was first investigated at 5 and 8 weeks post-transplant being 8.58×10^4 and 1.12×10^6 copies/mL in recipient #1 and recipient #2, respectively. Renal function declined and biopsy-proven PyVAN was diagnosed in both recipients at 12 weeks post-transplant. Mycophenolate mofetil levels were reduced from 750 mg to 250 mg bid while tacrolimus levels were kept below 5 ng/mL. Recipient #2 cleared BKPyV-DNAemia at 5.5 months post-transplant, while recipient #1 had persistent BKPyV-DNAemia of 1.07×10^5 copies/mL at the last follow-up 52 weeks post-transplant. DNA sequencing of viral DNA from early plasma samples revealed apparently identical viruses in both recipients, belonging to genotype Ib-2 with archetype non-coding control region. Retrospective serological work-up, demonstrated that the donor had high BKPyV-IgG-virus-like particle ELISA activity and a high BKPyV-genotype I neutralizing antibody titer, whereas both KT recipients only had low neutralizing antibody titers pre-transplantation. By 20 weeks post-transplant, the neutralizing antibody titer had increased by > 1000-fold in both recipients, but only recipient #2 cleared BKPyV-DNAemia.

Conclusions: Low titers of genotype-specific neutralizing antibodies in recipients pre-transplant, may identify patients at high risk for early fulminant donor-derived BKPyV-DNAemia and PyVAN, but development of high neutralizing antibody titers may not be sufficient for clearance.

Keywords: Kidney transplantation, BK polyomavirus, BKPyV-DNAemia, PyVAN, Neutralizing antibodies

* Correspondence: christine.rinaldo@unn.no
[1]Department of Microbiology and Infection Control, University Hospital of North Norway, Tromsø, Norway
[2]Metabolic and Renal Research Group, UiT The Arctic University of Norway, Tromsø, Norway
Full list of author information is available at the end of the article

Background

BK Polyomavirus (BKPyV) infects about 90% of the world's population [3, 14]. After primary infection, which usually goes unnoticed, the virus persists quietly in the epithelial cells of the reno-urinary tract. Asymptomatic low-level virus shedding in the urine has been detected in healthy immunocompetent blood donors indicating immune escape of BKPyV [6, 17]. In kidney transplant (KT) recipients, where the immune system is suppressed by immunosuppressive drugs in order to avoid rejection, the prevalence of viruria increases to more than 60%, and about half of these viruric patients develop high-level BKPyV viruria defined as >7 $\log_{10}$ copies (c) per mL and shed decoy cells. About 2 to 6 weeks later, approximately half of these patients progress to BKPyV-DNAemia and biopsy-proven polyomavirus-associated nephropathy (PyVAN). The disease is characterized by persisting high-level BKPyV replication in the tubular epithelial cells of the kidney allograft, causing cytopathic loss. The disruption of the epithelial cell monolayer leads to leakage of virus and viral DNA into the tissue and blood stream i.e. BKPyV DNAemia, and is followed by a local inflammation [4, 12, 22]. In addition, high-level BKPyV replication in the multilayered epithelium of the renal pelvis and the bladder, contribute to the viruria. As antiviral drugs for treatment of PyVAN are lacking, the mainstay therapy is a stepwise reduction of immunosuppression [13]. Without this intervention, more than 90% of affected KT recipients will show a declining kidney allograft function and experience premature graft loss.

BKPyV has a circular double-stranded DNA genome of about 5 kb. The genetic heterogeneity in the *VP1* gene encoding the major capsid protein Vp1, can be used to divide BKPyV into four sero–/genotypes (I, II, III, IV) [15], two of which can be further divided into subtypes (Ia, Ib-1, Ib-2, Ic, IVa-I, IVa-2, IVb-1, IVb-2, IVc-I and IVc-2) [38]. Another genome sequence used to characterize the virus is the non-coding control region (*NCCR*) which comprises the origin of viral genome replication and promoter/enhancer functions. In urine from immunocompetent individuals, BKPyV typically has an archetype NCCR architecture that has been arbitrarily divided into five sequence blocks denoted O_{142} - P_{68} - Q_{39} - R_{63} - S_{63}, where the subscript number indicates the number of base pairs. Early in the course of PyVAN, BKPyV strains with an archetype NCCR are found in urine and plasma. Presumably due to the lack of a functional T-cell immunity, these strains are gradually replaced by faster replicating strains with a rearranged NCCRs showing an up-regulated expression of the early regulatory protein large T-antigen (LTag) [9, 23, 24].

Since PyVAN preferentially affects KT recipients, PyVAN has been suggested to arise mainly due to donor-derived infection [2]. This concept is supported by the detection of identical BKPyV-genotypes and/or strains in the donor urine pre-transplant and in the recipients urine and/or plasma post-transplant [2, 29, 30, 35, 37]. Moreover, a study of 21,575 recipient pairs receiving kidneys from the same donor supported this concept, as BKPyV replication was reported in twice as many recipient pairs ($n = 174$) than expected by chance [32]. However, data from recipient pairs with biopsy-proven nephropathy are lacking.

Here, we describe the course of two KT patients developing early fulminant biopsy-proven PyVAN after receiving their allografts from the same deceased donor. Retrospective sequencing of the BKPyV genome indicated that PyVAN developed as a result of transmission of donor-derived BKPyV. Detailed serological studies identified low neutralizing antibody titers in both recipients pre-transplant as a potential marker of low antiviral immune control and increased risk for BKPyV-DNAemia and PyVAN. Although both recipients developed a more than 1000-fold increase in neutralizing antibody (NAb) titers, only one recipient cleared BKPyV-DNAemia. The potential role of viral and immune markers for screening, monitoring and follow-up is discussed.

Case presentation

Deceased donor

The donor was a 62-year old male who died from a subarachnoid hemorrhage. He was IgG-seropositive for cytomegalovirus (CMV) and had blood group A. Retrospective investigation of his plasma using three different serological methods (reviewed in [17]) demonstrated high-levels of BKPyV neutralizing antibodies. In more detail, using a neutralization assay, a more than 50% inhibition of genotype I-pseudovirus infectivity was obtained when a 640-fold plasma dilution was used, which corresponds to a NAb titer of 640 half maximal inhibitory concentration (IC_{50}). The method used was modified from a protocol by Pastrana and colleagues [25] by using a pseudovirus containing pEGFP-N1 instead of phGluc. As a consequence, infectivity was measured as fluorescent intensity instead of luciferase activity. The hemagglutination inhibition assay (HIA) [21], measured a HIA-titer of 320. Finally, the BKPyV-IgG specific enzyme-linked immunosorbent assay (ELISA) using Vp1-derived virus-like particles [16], gave a normalized optical density (nOD) of 2.329 for a plasma dilution of 400, but no IgM was detectable. Moreover, using a validated quantitative real-time PCR assay [5], no BKPyV-DNA was detectable in the donor plasma. Besides, immunohistochemistry of the baseline kidney biopsy using a commercial antibody directed against SV40 LTag (Pab416, Merck) but known to cross-react with BKPyV LTag, was negative.

Case 1

Recipient #1 was a 68 year old male with end-stage kidney disease due to granulomatosis with polyangiitis requiring hemodialysis for the last two years. At the time of transplantation, he had a serum creatinine (s-Cr) of 457 μmol/L (Fig. 1a). Human leukocyte antigen (HLA) typing showed one HLA-A, one HLA-B and one HLA-DR mismatches. His blood group was the same as for the donor and he was seropositive for CMV-IgG, thus yielding an intermediate risk for CMV (D+/R+). No known panel reactive antibody (PRA) or donor specific antibodies (DSA) were detected i.e. the recipient had a standard immunologic risk. He received standard immunosuppressive therapy; intravenous (i.v.) basiliximab induction, prednisolone, tacrolimus (trough levels 3–7 ng/mL from time of engraftment), and mycophenolate mofetil (MMF) 750 mg bid. Four days post-transplant, his s-Cr level was 302 μmol/L, decreasing to 106 μmol/L by 4 weeks post-transplant (Fig. 1a). One week later (5 weeks post-transplant), his plasma was, for the first time, analyzed for BKPyV-DNAemia and 8.58×10^4 c/mL were detected (Fig. 1b), giving him the diagnosis presumptive PyVAN.

At 12 weeks post-transplant, his BKPyV plasma load had increased by 3 orders of magnitude to 1.66×10^7 c/mL (Fig. 1b), and the s-Cr level had increased to 139 μmol/L (Fig. 1a). Therefore, an allograft biopsy was taken. The biopsy showed no interstitial inflammation, no intimal arteritis, and no rejection, but mild tubulitis (Banff score of i0t1v0, C4d negative) (Fig. 2a). In addition, positive immunostaining for LTag was observed in some tubular epithelial cells (Fig. 2b), establishing the diagnosis of proven-PyVAN (Stage-B1) [13]. Therefore, MMF was reduced from 750 mg to 250 mg bid while tacrolimus treatment with already low trough levels was left unchanged.

Seven weeks later (19 weeks post-transplant), the plasma BKPyV load had decreased to 6.35×10^5 c/mL (Fig. 1b). Subsequently, the patient was seen in his local hospital, where the s-Cr was reported as stable and plasma BKPyV-DNAemia was not examined. At the planned one-year post-transplant surveillance control, the s-Cr was stable at 135 μmol/L, the plasma BKPyV-load was still 1.07×10^5 c/mL (Fig. 1b), and the urine BKPyV-load was high with 6.71×10^9 c/mL (Fig. 1b). The protocol biopsy showed no signs of inflammation or rejection

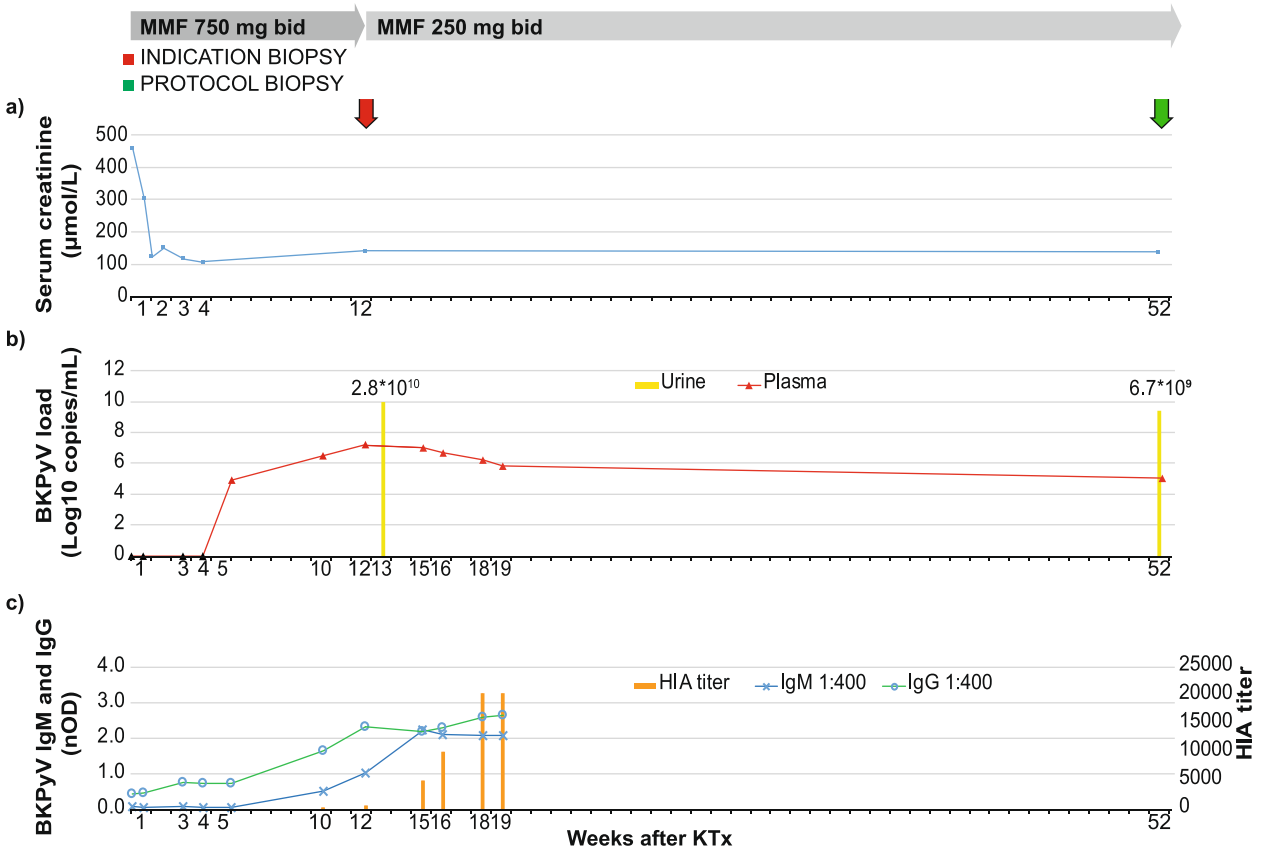

Fig. 1 Treatment and Clinical Course of Recipient #1. The X-axis is labeled with the week after transplantation when the sample was taken. Arrows indicate biopsies. Y-axis: **a** Serum creatinine concentration in μmol/L. **b** BKPyV-DNA genome levels in plasma (red triangles) and in urine (yellow bar) in $\log_{10}$ c/mL. Retrospectively tested plasma samples (black triangles). **c** BKPyV-antibody IgG (green line) and IgM (blue line) shown as nOD at the left Y-axis; HIA-titer (orange bar) at the right Y-axis

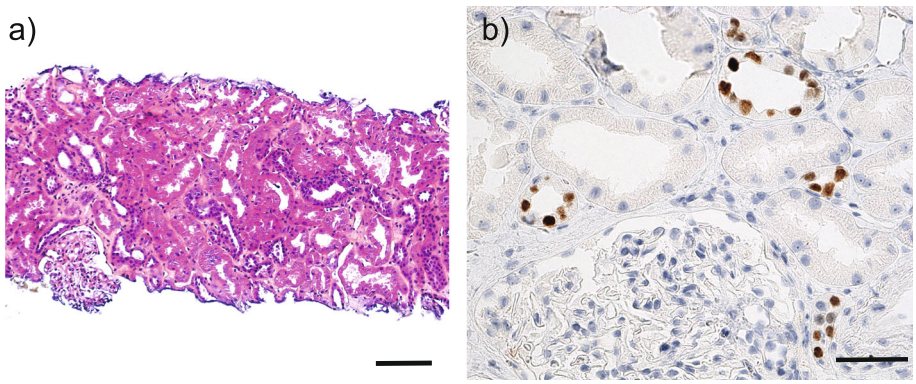

Fig. 2 Histological analysis of a renal allograft biopsy from recipient #1 at 12 weeks post-transplant. **a** HES (hematoxylin, eosin and saffron) stained section. Original magnification 200x, scale bar =100 μm. **b** Immunohistochemistry staining of the same biopsy as in a), viral LTag expression (brown colour) in tubular epithelial cells using the cross-reacting monoclonal anti-SV40 LTag antibody Pab416 (Merck). Original magnification 400x, scale bar =50 μm

(Banff score of i0t0v0, C4d negative) and no detectable LTag staining (results not shown) (Fig. 1a).

Retrospective testing of plasma samples taken the first four weeks post-transplant did not detect BKPyV-DNAemia (Fig. 1b, black triangles). Nevertheless, BKPyV-ELISA revealed that recipient #1 was IgG seropositive (0.442 nOD) and IgM seronegative pre-transplantation. Of note, the pre-transplant HIA-titer was 80 (Fig. 1c), and the BKPyV-genotype I NAb-titer was only 10 IC_{50}.

During the first 5 weeks post-transplant, a slow but continuous increase of the ELISA-IgG activity was found. Then a more rapid increase was seen with a peak value of nOD 2.646 at 19 weeks post-transplant (the last measured time point). During this last phase, the BKPyV-IgM became detectable and peaked at 15 weeks post-transplant (Fig. 1c), indicating a significant immune response to BKPyV-antigens.

At 19 weeks post-transplant, the ELISA IgG and the HIA-titer had increased by six-fold and 256-fold, whereas the NAb-titer had increased by > 1000-fold to > 10,240 IC_{90} i.e. the plasma inhibited more than 90% of the infectious activity at 1:10240 dilution.

Case 2

Recipient #2 was a 62 year old male with autosomal polycystic kidney disease. He had a s-Cr of 401 μmol/L pre-transplantation (Fig. 3a). HLA typing showed one HLA-A, two HLA-B, and one HLA-DR mismatches. The recipient's blood group was the same as the donor's and he had an intermediate risk for CMV (D+/R+). No known PRA or DSA were detected and he received the same immunosuppressive therapy as recipient #1. His baseline renal function was good with serum s-Cr levels decreasing from 112 μmol/L at 4 days post-transplant to 72 μmol/L at 5 weeks post-transplant (Fig. 3a).

However, at 6 weeks post-transplant, the s-Cr suddenly increased to 124 μmol/L (Fig. 3a). At 8 weeks post-transplant, the plasma was for the first time analyzed for BKPyV-DNAemia and 1.12×10^6 c/mL was detected (Fig. 3b), giving the diagnosis of presumptive PyVAN. An allograft biopsy was taken, but HES staining showed no signs of inflammation or rejection (Banff score i0t0v0, C4d negative) and immunohistochemical staining was negative for LTag (data not shown). The plasma BKPyV-DNAemia persisted at levels > 6 $\log_{10}$ c/mL (Fig. 3b), and at 12 weeks post-transplant a second allograft biopsy was taken. This time the biopsy showed focal interstitial inflammation and severe tubulitis (Banff score i2t3v0, C4d negative) (Fig. 4a). In addition, immunostaining revealed LTag-positive epithelial cells (Fig. 4b) giving the diagnosis of biopsy-proven PyVAN (stage B1). MMF was reduced from 750 mg to 250 mg bid, while tacrolimus treatment was left unchanged (trough levels ng/mL). At 20 weeks post-transplant, the plasma BKPyV-DNA load had declined to 3.56×10^4 c/mL and at 29 weeks post-transplant, BKPyV-DNAemia was no longer detectable (Fig. 3b). Concurrently the s-Cr was 155 μmol/L (Fig. 3a). One year post-transplantation, the s-Cr had declined to 130 μmol/L (Fig. 3a), plasma was still negative for BKPyV-DNAemia (Fig. 3b) while urine was positive with a low BKPyV load of 1.6×10^5 c/mL (Fig. 3b). The protocol biopsy showed limited inflammation and mild tubulitis (Banff score of i1t1v0, corresponding to Banff borderline for rejection, C4d negative) and negative LTag staining (results not shown).

Retrospective testing of plasma BKPyV-DNAemia revealed 2.59×10^3 c/mL in plasma already at 4 weeks post-transplant (Fig. 3b, black triangles). Besides, BKPyV-ELISA demonstrated that recipient #2 was IgG seropositive (nOD of 0.191) and IgM seronegative pre-transplantation. As for recipient #1, the pre-transplant HIA-titer was 80 (Fig. 3c), and the BKPyV-genotype I NAb-titer was only 10 IC_{50}. During the first 7 weeks post-transplant, a slow but continuous increase of the

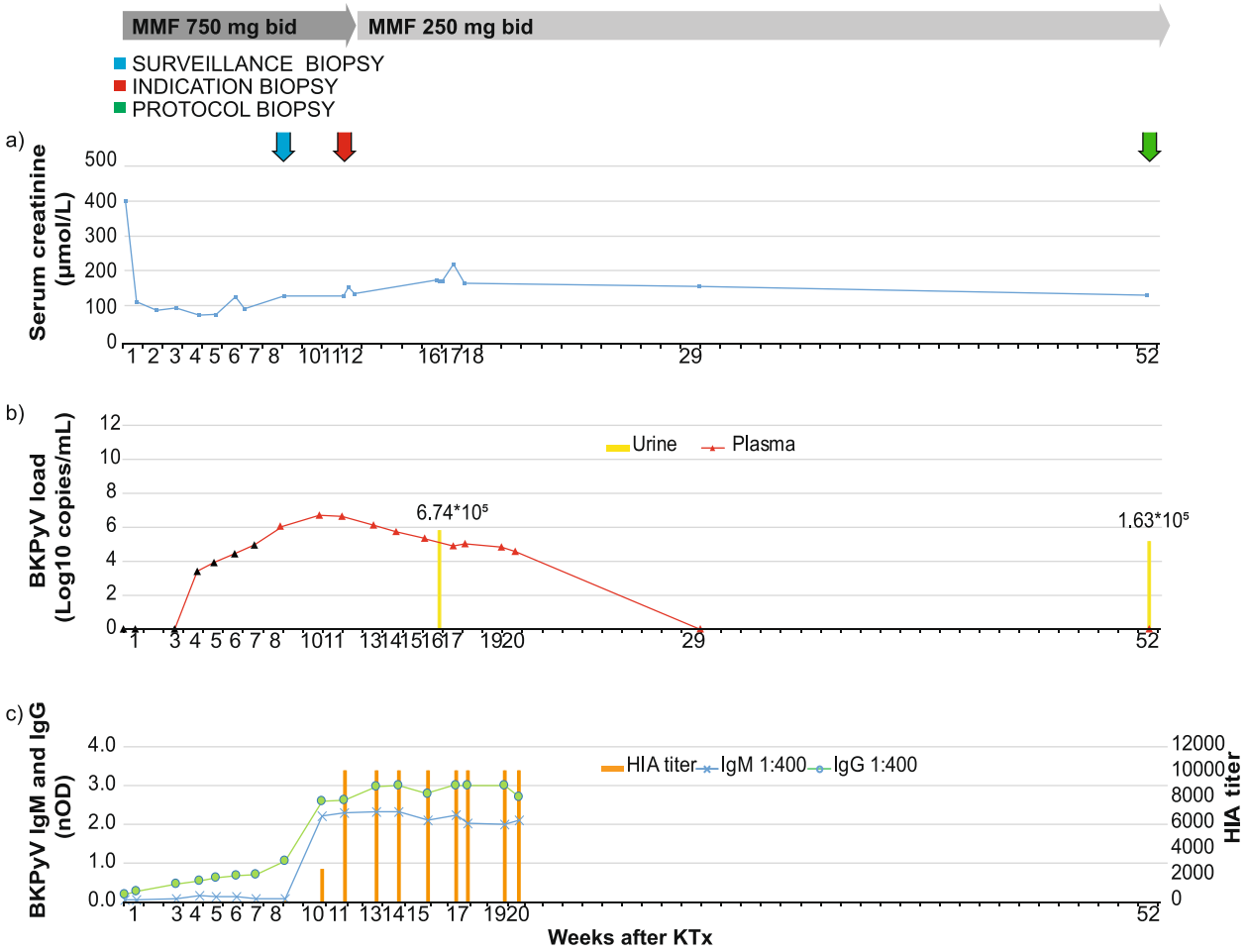

Fig. 3 Treatment and Clinical Course of Recipient #2. The X-axis is labeled with the week after transplantation when the sample was taken. Arrows indicate biopsies. Y-axis: **a** Serum creatinine concentration in µmol/L. **b** BKPyV-DNA genome levels in plasma (red triangles) and in urine (yellow bar) in $\log_{10}$ c/mL. Retrospectively tested plasma samples (black triangles). **c** BKPyV-antibody IgG (green line) and IgM (blue line) shown as nOD at the left Y-axis; HIA-titer (orange bar) at the right Y-axis.

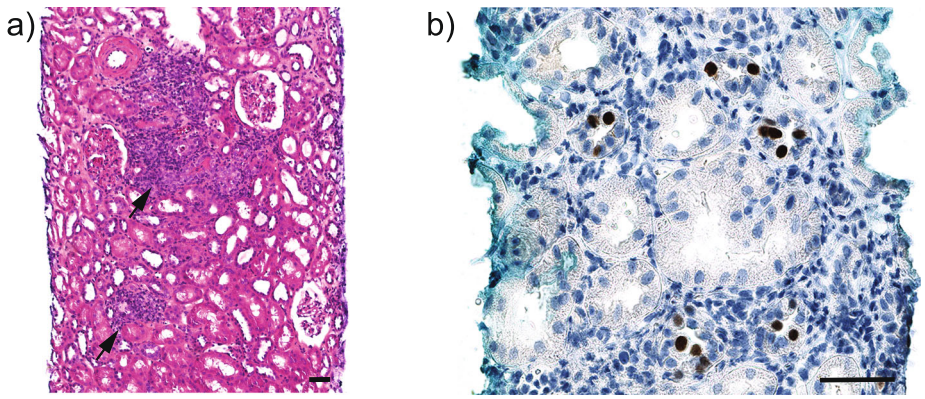

Fig. 4 Histological analysis of a renal allograft biopsy from recipient #2 at 12 weeks post-transplant. **a** HES (hematoxylin, eosin and saffron) stained section showing inflammation (arrows). Original magnification 200x, scale bar = 100 µm. **b** Immunohistochemistry staining of the same biopsy as in a), showing LTag expression (brown colour) in tubular epithelial cells when the monoclonal anti–SV40 LTag antibody Pab416 (Merck) is used. Original magnification 400x, scale bar = 50 µm

BKPyV-IgG titer was found. Then a more rapid increase was seen until the IgG titer plateaued from 13 weeks post-transplant with a maximum nOD of 3.017 at 17 weeks post-transplantation. From 4 weeks post-transplant the BKPyV-IgM became positive and from 11 weeks post-transplant the HIA-titer peaked with 10,240 (Fig. 3c). At 20 weeks post-transplant, the ELISA IgG and the HIA-titer had increased by 16-fold and 128-fold, whereas the NAb-titer had increased by > 1000-fold to > 10,240 IC_{90}.

Genetic analysis of BKPyV DNA in plasma and urine samples from both patients

In order to investigate the genotype and strain of BKPyV in plasma and urine samples, two nested PCRs were used to amplify a 330 base pair fragment of the VP1 gene and the complete NCCR [19]. The sequence results from both early plasma samples and urine samples from both recipients revealed virus of genotype Ib-2 having identical archetype NCCR. These results suggest that both recipients were infected with an identical BKPyV strain. However, one year post-transplant plasma sample of recipient #1, also contained strains with NCCR rearrangements, including one strain denoted RH-20 (GenBank Accession number MN627732), having a 60 bp deletion in the Q- and R-block removing the Sp1–4 transcription factor binding site [1].

Discussion and conclusions

In this study we report the parallel onset of early fulminant biopsy-proven PyVAN in two KT patients having received one kidney each from the same deceased donor. DNA sequencing of BKPyV DNA amplified from early plasma and urine samples, revealed an apparently identical virus of genotype Ib-2 with archetype NCCRs, in both recipients. This together with the clinical course, supports the notion of donor kidney transmission of BKPyV. Both recipients shared several previously reported risk factors for PyVAN [13] such as being males in their sixties and receiving treatment with tacrolimus-mycophenolic acid, whereas other risk factors such as lymphocyte-depleting induction or acute rejection episodes treated with steroid pulses were not present.

Our retrospective analyses revealed that the donor and both recipients were BKPyV-IgG seropositive before transplantation, but significantly differed in their NAb-titers for the replicating BKPyV genotype, which was almost 100-fold higher in the donor than in the recipients. These observations in the recipients are in line with a recent study by Solis and colleagues [31]. They reported that low NAb-titers against the donor BKPyV genotype, here defined as less than 4 $\log_{10}$ IC_{50}, was associated with an increased risk of BKPyV-DNAemia and PyVAN. Despite this striking similarity, the titers may not be directly comparable, since they used a slightly different protocol.

Remarkably, the BKPyV-genotype I NAb-titers increased in both of our patients by more than 1000-fold to 10,240 IC_{90}, thereby, reaching titers associated with clearance of BKPyV DNAemia [31]. Indeed, following MMF reduction, BKPyV-DNAemia declined in recipient #2, and cleared with 3 months. In contrast, recipient #1 had persistent BKPyV-DNAemia levels above 10^5 c/mL and high-level viruria detectable at one year post-transplant. Moreover, as previously reported [9, 23], the archetype NCCR of the BKPyV genome was now replaced by a rearranged NCCR in line with on-going intra-patient evolution and insufficient antiviral immunity. In particular, CD8 T cells directed against immunodominant 9mer epitopes derived from the viral early protein LTag has been implicated in clearance of BKPyV-DNAemia [17, 20]. Such immunodominant epitopes are presented by HLA-B51 which alone or in combination with HLA-B7 and -B8 has been associated with a lower risk of BKPyV DNAemia [34, 36]. Both recipients lacked these HLA types, except recipient #2 having HLA-B7. Possibly, lack of these HLA-types contributed to the rapid onset and protracted course of PyVAN.

Although we cannot exclude a synergizing role of neutralizing antibodies in the control of BKPyV replication in the affected tubulus of a given nephron, it remains unclear how sufficient antibodies can prevent the well documented cell to cell spread in the nephron.

We noted that the donor was in an age group that is characterized by low titers of BKPyV-specific IgG [10, 18, 28]. In our comprehensive serological assessment using three different assays, however, the donor had high BKPyV-IgG ELISA activity (2.329 nOD), a high HIA-titer (320) as well as a high NAb-titer (> 640 IC_{50}). These results suggest that the immune system of the donor had been exposed to BKPyV recently. Considering the donor's age and the undetectable BKPyV-IgM, this exposure was probably not due to a primary infection, but rather a recent reactivation leading to increased viral loads in his kidneys. Although no pre-transplant viruria samples from the donor were available, the high neutralizing activity against BKPyV of genotype I and the fact that BKPyV genotypes are serologically distinct [26], argues for transmission of genotype I, which also was found in the recipients.

Our parallel kidney transplant case studies from a single donor are also notable for further specific details. Unlike in the donor, the BKPyV-specific antibodies measured by ELISA and by the neutralization assay were discordant in both recipients with respect to the level at the time of transplantation, being higher in the former assay, but nearly undetectable in the latter. This suggest that the ELISA is more sensitive, but less specific for a given BKPyV genotype than the neutralization assay. This may also explain the lack of association of recipient ELISA antibody levels with BKPyV-DNAemia seen in a

recent study of living donor-recipient pairs [11]. Moreover, from three weeks post-transplant, the ELISA titers started to increase suggesting a CD4-T cell help independent memory B-cell response to viral antigen exposure, for example resulting from donor virus replication in both kidney allografts directly after transplantation. This interpretation is supported by the fact that the antibody levels increased in parallel with increasing BKPyV-DNAemia before immunosuppression was reduced.

Another aspect is the observation that the first biopsy of recipient #2 was negative for BKPyV-LTag expression although BKPyV-DNAemia was higher than $> 10^6$ c/ml. Only a second biopsy taken 4 weeks later confirmed proven PyVAN. This suggests that the biopsy must have missed the typically focally arranged LTag positive epithelial cells, which has been previously documented in a study involving 41 KT recipients with persisting high-level BKPyV-DNAemia [4]. In this study multiple biopsy cores were taken at the same time, and discordant LTag-positive and LTag-negative biopsy cores were found in more than 30% of the cases. The focal nature of PyVAN may also explain why the baseline biopsy at transplantation and the protocol biopsy taken one year post-transplant of recipient #1 were negative. Cases of allograft nephrectomy have clearly demonstrated that BKPyV-DNAemia is derived directly from the renal allograft [7, 8] and BKPyV-DNAemia is now considered a direct biological marker of PyVAN [13]. Importantly this has been implemented in the recently updated guidelines on BKPyV in solid organ transplantation [13]. A renal allograft biopsy is only needed to decide on immunosuppression reduction in patients with an increased risk of acute rejection (i.e. the presence of DSA or known PRA positivity) or impaired baseline renal function of unknown origin. For all other patients, a preemptive treatment algorithm is recommended. To better reflect the continuum of BKPyV replication, immunosuppression reduction is recommended for KT patients with plasma BKPyV-DNAemia of 1000 c/ml sustained for more than three weeks (probable PyVAN), or more than 10,000 c/ml (presumptive PyVAN).

Finally, while supporting the potential of neutralizing antibodies as markers of increased risk, our case studies raise questions about the potential of neutralizing antibodies for prophylaxis or therapy. As commercial human i.v. immunoglobulin (Ig) has been shown to contain BKPyV neutralizing antibodies [27], recently monthly i.v. Ig injections during the first three critical months post-transplant was suggested as an initiative to prevent PyVAN development [33]. Others have suggested pre-vaccination of KT recipients with a multivalent VLP-based vaccine against all BKPyV sero−/genotypes [25]. However, the question has been raised whether or not the apparently beneficial neutralizing antibody activity observed in patients represents surrogates of their corresponding CD4 and/or CD8 activity (reviewed in [17, 20]). It is conceivable that the efficacy of administrating intravenous immunoglobulins may differ when given prophylactically before significant BKPyV spread in the renal allograft has occurred, or when administered in patients with significant BKPyV-DNAemia and PyVAN. Randomized controlled clinical trials are needed to address both situations. However, our study and that of others suggests that the antibody status pre-transplantation should be assessed in order to obtain meaningful results.

In this paired kidney case report, donor-derived transmission with rapid progression to presumptive and proven PyVAN probably occurred due to the combination of a recent BKPyV exposure in the donor and initial low levels of BKPyV-genotype I neutralizing antibodies in both recipients. More evidence is needed to evaluate whether measurement of neutralizing antibodies pre-transplant can be useful in organ allocation or more intense post-transplant screening. Until then, monthly screening for BKPyV-DNAemia followed by a rapid reduction of immunosuppression remains the standard measure to prevent allograft damage and loss due to PyVAN.

Abbreviations

Bid: Twice a day; BKPyV: BK polyomavirus; c: Copies; CMV: Cytomegalovirus; DSA: Donor specific antibodies; ELISA: Enzyme-linked immunosorbent assay; HIA: Hemagglutination inhibition assay; HLA: Human leukocyte antigen; i.v: Intravenous; IC: Inhibitory concentration; KT: Kidney transplant; LTag: Large tumor antigen; MMF: Mycophenolate mofetil; NAb: Neutralizing antibody; NCCR: Non-coding control region; nOD: Normalized optical density; PRA: Panel reactive antibody; PyVAN: Polyomavirus-associated nephropathy; s-Cr: Serum creatinine

Acknowledgements

The authors are grateful to the recipients for their willingness to participate in the study and also wish to thank Dr. Dorian McIlroy at the University of Nantes, France, for providing the plasmids for BKPyV-genotype I pseudovirus production and Dr. Garth D. Tylden at Uit The Arctic University of Norway, for critical reading of the manuscript. The publication charges for this article have been funded by a grant from the publication fund of UiT The Arctic University of Norway.

Authors' contributions

EML performed the HIA, the neutralization assay, part of the VP1 and NCCR PCR and DNA sequencing and wrote the first draft of the manuscript. SH determined the BKPyV load by quantitative real-time PCR, and performed part of the VP1 and NCCR PCR and DNA sequencing and provided the summary of results in Fig. 1 and Fig. 3. AK performed the normalized BKPyV-VLP ELISA for IgG and IgM activity. GBK provided the samples from the clinical biobank and validated the CMV-status data. CH evaluated the kidney biopsies and the immunohistochemical staining, and provided the corresponding Figs. 2 and 4. HHH supervised the VLP-ELISA, interpreted the data, and contributed to the study design, and to writing the manuscript. KM was in charge of the clinical management in the initial post-transplant period and during the one-year post-transplant surveillance control, provided the HLA-typing, the s-Cr data, and initiated the investigation of the potential donor-derived infection in both recipients. CHR designed the study, initiated and coordinated the entire retrospective laboratory work, interpreted the laboratory and clinical data, and wrote the finale manuscript. All authors read and approved the final manuscript.

Funding

We had no external funding for this project.

Availability of data and materials
Data sharing is not applicable to this article as no datasets were generated or analyzed during the current study.

Ethics approval and consent to participate
Ethics approval was obtained from the Norwegian Data Protection Authority (266–2005-142234). Written informed consents were obtained from the KT recipients.

Consent for publication
Written informed consents were obtained from the KT recipients. Copies of the written consents are available for review of the Editor-in-Chief of this journal.

Competing interests
The authors declare that they have no competing interests.

Author details
[1]Department of Microbiology and Infection Control, University Hospital of North Norway, Tromsø, Norway. [2]Metabolic and Renal Research Group, UiT The Arctic University of Norway, Tromsø, Norway. [3]Department Biomedicine Transplantation & Clinical Virology, University of Basel, Basel, Switzerland. [4]Department of Microbiology, Oslo University Hospital, Rikshospitalet, Oslo, Norway. [5]Institute of Clinical Medicine, University of Oslo, Oslo, Norway. [6]Department of Pathology, Oslo University Hospital, Rikshospitalet, Oslo, Norway. [7]Infectious Diseases & Hospital Epidemiology, University Hospital Basel, Basel, Switzerland. [8]Department of Transplantation, Medicine, Section of Nephrology, Oslo University Hospital, Rikshospitalet, Oslo, Norway.

Received: 11 November 2019 Accepted: 20 December 2019
Published online: 10 January 2020

References

1. Bethge T, Hachemi HA, Manzetti J, Gosert R, Schaffner W, Hirsch HH. Sp1 sites in the noncoding control region of BK polyomavirus are key regulators of bidirectional viral early and late gene expression. J Virol. 2015;89:3396–411.
2. Bohl DL, Storch GA, Ryschkewitsch C, Gaudreault-Keener M, Schnitzler MA, Major EO, Brennan DC. Donor origin of BK virus in renal transplantation and role of HLA C7 in susceptibility to sustained BK viremia. Am J Transplant. 2005;5:2213–21.
3. DeCaprio JA, Garcea RL. A cornucopia of human polyomaviruses. Nat Rev Microbiol. 2013;11:264–76.
4. Drachenberg CB, Papadimitriou JC, Hirsch HH, Wali R, Crowder C, Nogueira J, Cangro CB, Mendley S, Mian A, Ramos E. Histological patterns of polyomavirus nephropathy: correlation with graft outcome and viral load. Am J Transplant. 2004;4:2082–92.
5. Dumoulin A, Hirsch HH. Reevaluating and optimizing polyomavirus BK and JC real-time PCR assays to detect rare sequence polymorphisms. J Clin Microbiol. 2011;49:1382–8.
6. Egli A, Infanti L, Dumoulin A, Buser A, Samaridis J, Stebler C, Gosert R, Hirsch HH. Prevalence of polyomavirus BK and JC infection and replication in 400 healthy blood donors. J Infect Dis. 2009;199:837–46.
7. Funk GA, Gosert R, Comoli P, Ginevri F, Hirsch HH. Polyomavirus BK replication dynamics in vivo and in silico to predict cytopathology and viral clearance in kidney transplants. Am J Transplant. 2008;8:2368–77.
8. Funk GA, Steiger J, Hirsch HH. Rapid dynamics of polyomavirus type BK in renal transplant recipients. J Infect Dis. 2006;193:80–7.
9. Gosert R, Rinaldo CH, Funk GA, Egli A, Ramos E, Drachenberg CB, Hirsch HH. Polyomavirus BK with rearranged noncoding control region emerge in vivo in renal transplant patients and increase viral replication and cytopathology. J Exp Med. 2008;205:841–52.
10. Gossai A, Waterboer T, Nelson HH, Doherty JA, Michel A, Willhauck-Fleckenstein M, Farzan SF, Christensen BC, Hoen AG, Perry AE, Pawlita M, Karagas MR. Prospective study of human polyomaviruses and risk of cutaneous squamous cell carcinoma in the United States. Cancer Epidemiol Biomark Prev. 2016;25:736–44.
11. Grellier J, Hirsch HH, Mengelle C, Esposito L, Hebral AL, Belliere J, Weissbach F, Izopet J, Del Bello A, Kamar N. Impact of donor BK polyomavirus replication on recipient infections in living donor transplantation. Transpl Infect Dis. 2018;20:e12917.
12. Hirsch HH. BK virus: opportunity makes a pathogen. Clin Infect Dis. 2005;41:354–60.
13. Hirsch HH, Randhawa PS, AST Infectious Diseases Community of Practice. BK polyomavirus in solid organ transplantation-Guidelines from the American Society of Transplantation Infectious Diseases Community of Practice. Clin Transpl. 2019;33:e13528.
14. Hirsch HH, Steiger J. Polyomavirus BK. Lancet Infect Dis. 2003;3:611–23.
15. Jin L. Molecular methods for identification and genotyping of BK virus. In: Raptis L, editor. SV40 Protocols. Totowa: Humana Press; 2001. p. 33–48.
16. Kardas P, Leboeuf C, Hirsch HH. Optimizing JC and BK polyomavirus IgG testing for seroepidemiology and patient counseling. J Clin Virol. 2015;71:28–33.
17. Kaur A, Wilhelm M, Wilk S, Hirsch HH. BK polyomavirus-specific antibody and T-cell responses in kidney transplantation: update. Curr Opin Infect Dis. 2019;32:575–83.
18. Kean JM, Rao S, Wang M, Garcea RL. Seroepidemiology of human polyomaviruses. PLoS Pathog. 2009;5:e1000363.
19. Koskenvuo M, Dumoulin A, Lautenschlager I, Auvinen E, Mannonen L, Anttila VJ, Jahnukainen K, Saarinen-Pihkala UM, Hirsch HH. BK polyomavirus-associated hemorrhagic cystitis among pediatric allogeneic bone marrow transplant recipients: treatment response and evidence for nosocomial transmission. J Clin Virol. 2013;56:77–81.
20. Leboeuf C, Wilk S, Achermann R, Binet I, Golshayan D, Hadaya K, Hirzel C, Hoffmann M, Huynh-Do U, Koller MT, Manuel O, Mueller NJ, Mueller TF, Schaub S, van Delden C, Weissbach FH, Hirsch HH, Swiss Transplant Cohort S. BK polyomavirus-specific 9mer CD8 T cell responses correlate with clearance of BK viremia in kidney Transplant recipients: first report from the Swiss Transplant Cohort study. Am J Transplant. 2017;17:2591–600.
21. Neel JV, Major EO, Awa AA, Glover T, Burgess A, Traub R, Curfman B, Satoh C. Hypothesis: "rogue cell"-type chromosomal damage in lymphocytes is associated with infection with the JC human polyoma virus and has implications for oncopenesis. Proc Natl Acad Sci U S A. 1996;93:2690–5.
22. Nickeleit V, Hirsch HH, Binet IF, Gudat F, Prince O, Dalquen P, Thiel G, Mihatsch MJ. Polyomavirus infection of renal allograft recipients: from latent infection to manifest disease. J Am Soc Nephrol. 1999;10:1080–9.
23. Olsen GH, Andresen PA, Hilmarsen HT, Bjorang O, Scott H, Midtvedt K, Rinaldo CH. Genetic variability in BK virus regulatory regions in urine and kidney biopsies from renal-transplant patients. J Med Virol. 2006;78:384–93.
24. Olsen GH, Hirsch HH, Rinaldo CH. Functional analysis of polyomavirus BK non-coding control region quasispecies from kidney transplant recipients. J Med Virol. 2009;81:1959–67.
25. Pastrana DV, Brennan DC, Cuburu N, Storch GA, Viscidi RP, Randhawa PS, Buck CB. Neutralization serotyping of BK polyomavirus infection in kidney transplant recipients. PLoS Pathog. 2012;8:e1002650.
26. Pastrana DV, Ray U, Magaldi TG, Schowalter RM, Cuburu N, Buck CB. BK polyomavirus genotypes represent distinct serotypes with distinct entry tropism. J Virol. 2013;87:10105–13.
27. Randhawa P, Pastrana DV, Zeng G, Huang Y, Shapiro R, Sood P, Puttarajappa C, Berger M, Hariharan S, Buck CB. Commercially available immunoglobulins contain virus neutralizing antibodies against all major genotypes of polyomavirus BK. Am J Transplant. 2015;15:1014–20.
28. Schmidt T, Adam C, Hirsch HH, Janssen MW, Wolf M, Dirks J, Kardas P, Ahlenstiel-Grunow T, Pape L, Rohrer T, Fliser D, Sester M, Sester U. BK polyomavirus-specific cellular immune responses are age-dependent and strongly correlate with phases of virus replication. Am J Transplant. 2014;14:1334–45.
29. Schmitt C, Raggub L, Linnenweber-Held S, Adams O, Schwarz A, Heim A. Donor origin of BKV replication after kidney transplantation. J Clin Virol. 2014;59:120–5.
30. Schwarz A, Linnenweber-Held S, Heim A, Framke T, Haller H, Schmitt C. Viral origin, clinical course, and renal outcomes in patients with BK virus infection after living-donor renal transplantation. Transplantation. 2016;100:844–53.
31. Solis M, Velay A, Porcher R, Domingo-Calap P, Soulier E, Joly M, Meddeb M, Kack-Kack W, Moulin B, Bahram S, Stoll-Keller F, Barth H, Caillard S, Fafi-Kremer S. Neutralizing antibody-mediated response and risk of BK virus-associated nephropathy. J Am Soc Nephrol. 2018;29:326–34.
32. Thangaraju S, Gill J, Wright A, Dong J, Rose C, Gill J. Risk factors for BK Polyoma virus treatment and Association of Treatment with Kidney Transplant Failure: insights from a paired kidney analysis. Transplantation. 2016;100:854–61.
33. Velay A, Solis M, Benotmane I, Gantner P, Soulier E, Moulin B, Caillard S, Fafi-Kremer S. Intravenous immunoglobulin administration significantly increases BKPyV genotype-specific neutralizing antibody titers in kidney Transplant recipients. Antimicrob Agents Chemother. 2019;63:e00393–19.

34. Willhelm M, Wilk S, Kaur A, Hirsch HH, Swiss Transplant Cohort S. Can HLA-B51 protect against BKPyV-DNAemia? Transplantation. 2019;103:e384–5.
35. Wunderink HF, De Brouwer CS, Gard L, De Fijter JW, Kroes ACM, Rotmans JI, Feltkamp MCW. Source and relevance of the BK polyomavirus genotype for infection after kidney transplantation. Open Forum Infect Dis. 2019a;6:ofz078.
36. Wunderink HF, Haasnoot GW, de Brouwer CS, van Zwet EW, Kroes ACM, de Fijter JW, Rotmans JI, Claas FHJ, Feltkamp MCW. Reduced risk of BK polyomavirus infection in HLA-B51-positive kidney Transplant recipients. Transplantation. 2019b;103:604–12.
37. Wunderink HF, van der Meijden E, van der Blij-de Brouwer CS, Mallat MJ, Haasnoot GW, van Zwet EW, Claas EC, de Fijter JW, Kroes AC, Arnold F, Touze A, Claas FH, Rotmans JI, Feltkamp MC. Pretransplantation donor-recipient pair Seroreactivity against BK polyomavirus predicts viremia and nephropathy after kidney transplantation. Am J Transplant. 2017;17:161–72.
38. Zhong S, Randhawa PS, Ikegaya H, Chen Q, Zheng HY, Suzuki M, Takeuchi T, Shibuya A, Kitamura T, Yogo Y. Distribution patterns of BK polyomavirus (BKV) subtypes and subgroups in American, European and Asian populations suggest co-migration of BKV and the human race. J Gen Virol. 2009;90:144–52.

Publisher's Note

Appendix: Paper 2

PLOS PATHOGENS

RESEARCH ARTICLE

Modelling BK Polyomavirus dissemination and cytopathology using polarized human renal tubule epithelial cells

Elias Myrvoll Lorentzen[1,2], **Stian Henriksen**[1,2], **Christine Hanssen Rinaldo**[1,2]*

1 Department of Microbiology and Infection Control, University Hospital of North Norway, Tromsø, Norway, **2** Metabolic and Renal Research Group, Department of Clinical Medicine, UiT The Arctic University of Norway, Tromsø, Norway

* christine.rinaldo@unn.no

Citation: Lorentzen EM, Henriksen S, Rinaldo CH (2023) Modelling BK Polyomavirus dissemination and cytopathology using polarized human renal tubule epithelial cells. PLoS Pathog 19(8): e1011622. https://doi.org/10.1371/journal.ppat.1011622

Editor: Walter J. Atwood, Brown University, UNITED STATES

Received: July 21, 2023

Accepted: August 17, 2023

Published: August 28, 2023

Peer Review History: PLOS recognizes the benefits of transparency in the peer review process; therefore, we enable the publication of all of the content of peer review and author responses alongside final, published articles. The editorial history of this article is available here: https://doi.org/10.1371/journal.ppat.1011622

Data Availability Statement: All relevant data are within the manuscript and its supporting Information files.

Abstract

Most humans have a lifelong imperceptible BK Polyomavirus (BKPyV) infection in epithelial cells lining the reno-urinary tract. In kidney transplant recipients, unrestricted high-level replication of donor-derived BKPyV in the allograft underlies polyomavirus-associated nephropathy, a condition with massive epithelial cell loss and inflammation causing premature allograft failure. There is limited understanding on how BKPyV disseminates throughout the reno-urinary tract and sometimes causes kidney damage. Tubule epithelial cells are tightly connected and have unique apical and basolateral membrane domains with highly specialized functions but all *in vitro* BKPyV studies have been performed in non-polarized cells. We therefore generated a polarized cell model of primary renal proximal tubule epithelial cells (RPTECs) and characterized BKPyV entry and release. After 8 days on permeable inserts, RPTECs demonstrated apico-basal polarity. BKPyV entry was most efficient via the apical membrane, that *in vivo* faces the tubular lumen, and depended on sialic acids. Progeny release started between 48 and 58 hours post-infection (hpi), and was exclusively detected in the apical compartment. From 72 hpi, cell lysis and detachment gradually increased but cells were mainly shed by extrusion and the barrier function was therefore maintained. The decoy-like cells were BKPyV infected and could transmit BKPyV to uninfected cells. By 120 hpi, the epithelial barrier was disrupted by severe cytopathic effects, and BKPyV entered the basolateral compartment mimicking the interstitial space. Addition of BKPyV-specific neutralizing antibodies to this compartment inhibited new infections. Taken together, we propose that during *in vivo* low-level BKPyV replication, BKPyV disseminates inside the tubular system, thereby causing minimal damage and delaying immune detection. However, in kidney transplant recipients lacking a well-functioning immune system, replication in the allograft will progress and eventually cause denudation of the basement membrane, leading to an increased number of decoy cells, high-level BKPyV-DNAuria and DNAemia, the latter a marker of allograft damage.

Funding: This work was supported by a grant from the Northern Norway Regional Health Authority – project number HNF1571-21 to CHR. The funders had no role in study design, data collection and analysis, decision to publish, or preparation of the manuscript.

Competing interests: The authors have declared that no competing interests exist.

Author summary

BKPyV causes polyomavirus-associated nephropathy, a severe condition affecting kidney transplant recipients. Besides, BKPyV is commonly detected in urine of healthy individuals. The renal tubules are lined by polarized epithelial cells that form a physical barrier with specialized functions. This is the first *in vitro* study of BKPyV replication in polarized tubule epithelial cells, a model reflecting the renal tubule anatomy. Cytopathic effects described in patients with polyomavirus-associated nephropathy, such as cell lysis and cell shedding, were recreated. Moreover, we demonstrate that BKPyV enters epithelial cells from the apical side and that viral progeny and infected cells are released into the apical compartment, which is mimicking the tubular lumen, without disrupting the epithelial barrier. Eventually the barrier was disrupted and BKPyV leaked into the basolateral compartment, mimicking the interstitial space. Our results suggest that in healthy individuals, viral progeny disseminates in the tubular fluid, thus delaying immune detection. In kidney transplant recipients with a suppressed immune system, BKPyV replication in the allograft may progress and cause massive cell loss and leakage of BKPyV-DNA into blood. Summarized, we have established a useful model to study renal BKPyV infection and used it to deepen our understanding of BKPyV dissemination and cytopathic effects.

Introduction

BK Polyomavirus (BKPyV), one of the 13 known human polyomaviruses [1,2], infects more than 90% of the population worldwide [3]. BKPyV persists in epithelial cells of the reno-urinary tract and is intermittently shed in the urine of healthy individuals without causing symptoms [4]. In immunosuppressed individuals, mainly kidney transplant and allogeneic stem cell transplant recipients, unrestricted BKPyV replication causes polyomavirus-associated nephropathy (PyVAN) [5] and polyomavirus-associated hemorrhagic cystitis [6], respectively. Moreover, some PyVAN patients develop bladder cancer years later [7–9]. PyVAN affects 1–15% of kidney transplant patients. The early phase is characterized by uncontrolled BKPyV replication in tubule epithelial cells in isolated nephrons of the allograft, resulting in BKPyV viruria with little impact on renal function. Somehow BKPyV disseminates to multiple nephrons, which is causing high-level viruria, urinary decoy cells and high-level BKPyV DNAemia [10–14]. Finally, interstitial and tubular inflammatory infiltrates become prominent, contributing to the declining allograft function. As no effective anti-viral therapies are available and reduced immunosuppression is the only treatment option, PyVAN is an important cause of reduced allograft function and premature allograft loss [5].

The replication cycle of BKPyV has been studied in various non-polarized cell cultures such as African green monkey kidney cell lines [15] and more recently in primary human renal proximal tubule epithelial cells (RPTECs) [16]. However, these cell cultures differ greatly from epithelial cells *in vivo*, where apico-basal polarity yields two unique membrane domains which are essential for the cell shape and function [17]. Apico-basal polarity can have important influence on the viral replication cycle [18]. For instance, polarized distribution of viral receptors can restrict viral entry to one membrane domain while directional protein sorting can lead to directional progeny release [18]. The influence of apico-basal polarity on BKPyV entry and release is not characterized and we therefore have limited understanding of how BKPyV disseminate from tubule epithelial cells and spread throughout the reno-urinary tract and sometimes causes kidney damage. In an effort to answer these questions, we established an *in*

vitro model of polarized human RPTECs and used this model to characterize major steps of the BKPyV replication cycle.

Results

Renal proximal tubule epithelial cells develop a polarized morphology and functionality

To examine if virus entry and release is polarized, we needed access to both membrane domains. We therefore chose to utilize permeable cell culture inserts (Fig 1A), previously used for polarization of renal epithelial cells [19–22]. To examine if RPTECs developed a polarized morphology, they were cultured on Falcon-inserts with pore size 1.0 μm. At 8 days post-seeding (dps), immunofluorescence staining and confocal microscopy demonstrated hallmarks of polarized epithelial cells such as basolateral distribution of sodium-potassium ATPase (Na/K-ATPase) (Fig 1B), apical primary cilia shown by acetylated α-tubulin (Fig 1B) and intercellular tight junctions represented by zonula occludens-1 (ZO-1) (Fig 1C).

In the nephron, the epithelium in the proximal tubule is known to be leakier than the epithelium in the distal parts of the nephron [23,24]. To investigate the integrity of the tight junctions in polarized RPTECs, we measured the transepithelial electrical resistance (TEER). It gradually increased during culture and plateaued at 20–30 $\Omega * cm^2$ from 8 dps (Fig 1D). The barrier function was further examined by measuring the diffusion of FITC-dextran across the cell layer. Compared to non-polarized RPTECs (at 2–3 dps), diffusion across polarized RPTECs (at 8–10 dps) was reduced by 65% (Fig 1E).

Epithelial cells of the proximal tubule have several drug transporters, including the P-glycoprotein (P-gp) efflux pump [25]. To evaluate the functionality of P-gp, the cell-permeant calcein AM and the P-gp inhibitor Psc-833 can be used [26]. If P-gp is inhibited, calcein AM accumulates intracellularly and is hydrolyzed into fluorescent calcein. Polarized RPTECs were exposed to calcein AM in the presence or absence of Psc-833 before fluorescence was measured. Inhibition of P-gp increased the intracellular fluorescence by approximately 70% (Fig 1F), confirming that polarized RPTECs have an active P-gp efflux pump. Transwell-inserts with pore size 0.4 μm yielded results similar to pore size 1.0 μm for polarity markers, FITC-diffusion and P-gp activity (S1A–S1E Fig). Falcon-inserts with pore size 3.0 μm were unsuitable, as RPTECs migrated through the pores (S1F Fig).

In summary, our morphological and functional assessment confirmed that RPTECs cultured on inserts develop a polarized morphology and exhibit functions similar to epithelial cells in the proximal tubule. The subsequent virus experiments were performed from 8 dps, when TEER values plateaued.

Polarized RPTECs support BKPyV replication

We next investigated if the polarized RPTECs were permissive for BKPyV. Two hours after apical infection, confocal microscopy demonstrated punctate Vp1-staining (Fig 2A), indicating binding and internalization of BKPyV. Transmission electron microscopy (TEM) confirmed binding of BKPyV to the apical membrane (Fig 2B) and a polarized morphology with microvilli, tight junctions and basal labyrinths (Fig 2B). At 72 hours post-infection (hpi), immunofluorescence staining (Fig 2C) and immunoblot (Fig 2D) showed expression of BKPyV proteins, while confocal microscopy demonstrated enlarged nuclei with inclusions (Fig 2E).

In summary, we found that polarized RPTECs supported BKPyV replication and may therefore be a suitable model for studying entry and release of BKPyV.

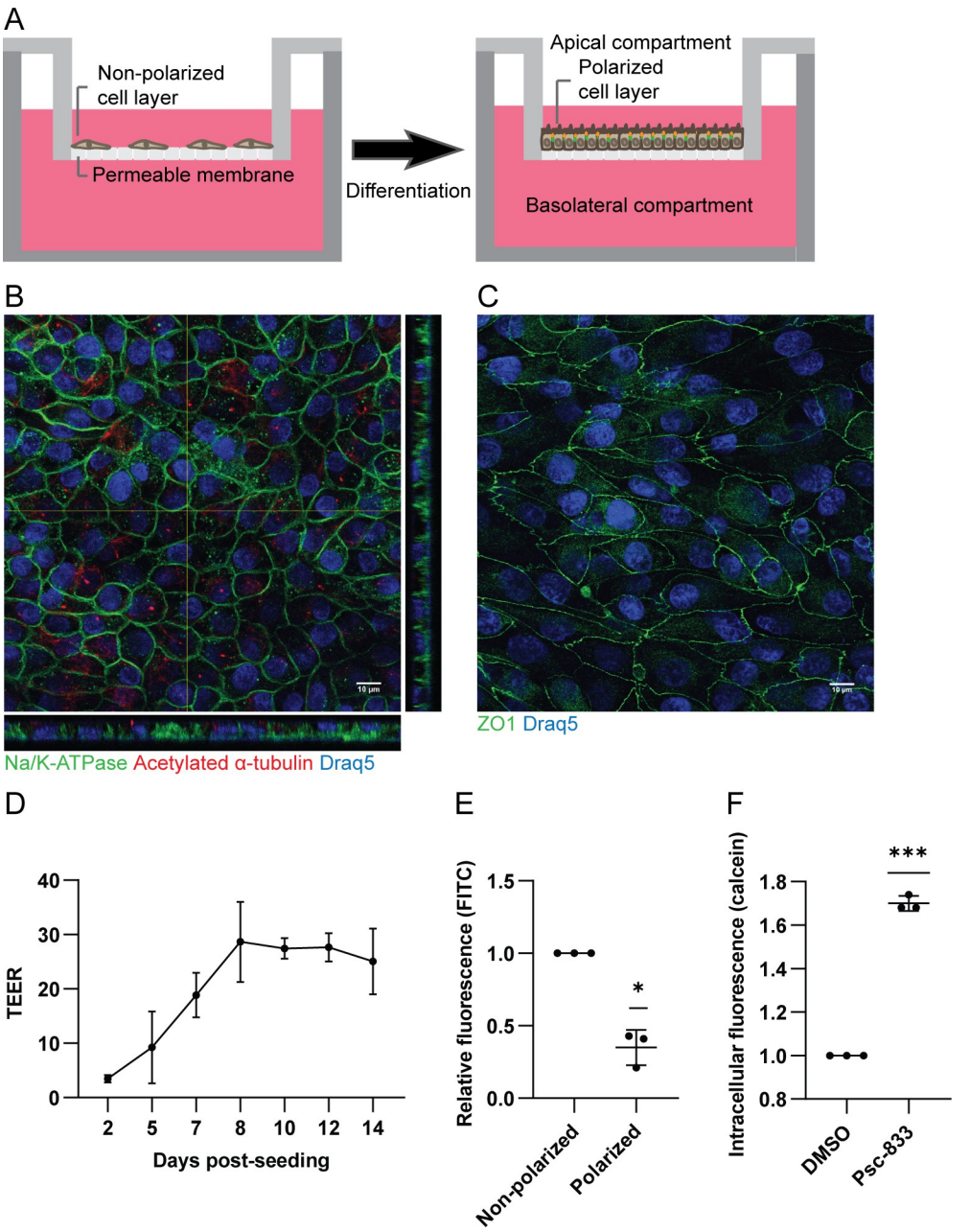

Fig 1. RPTECs develop a polarized morphology and functionality on cell culture inserts. (A) Scheme of cells cultured on a permeable cell culture insert. (B and C) At 8 days post-seeding (dps), RPTECs on Falcon-inserts were fixed and stained for: (B) Na/K-ATPase (green) and acetylated α-tubulin (red), and (C) ZO-1 (green). Nuclei were stained with Draq5 (blue). Images are representative images from at least three independent experiments. Scale bar 10 μm. (D) Transepithelial electrical resistance (TEER) values of RPTECs at 2 to 14 dps. Data is derived from two to four biological replicates per timepoint. Data are shown as means and error bars represent ± standard deviation (SD). (E) Diffusion of FITC-dextran from the apical to the basolateral compartment across polarized and non-polarized RPTECs. Data is normalized to the non-polarized control, n = 3 and error bars represent ± SD. * = $P < 0.05$, one sample *t* test. (F) Accumulation of intracellular calcein AM in the presence or absence of the P-gp inhibitor Psc-833, quantified by fluorescence measurement using a plate reader. Data is normalized to the untreated control, n = 3 and error bars represent ± SD. *** = $P < 0.001$, one sample *t* test.

https://doi.org/10.1371/journal.ppat.1011622.g001

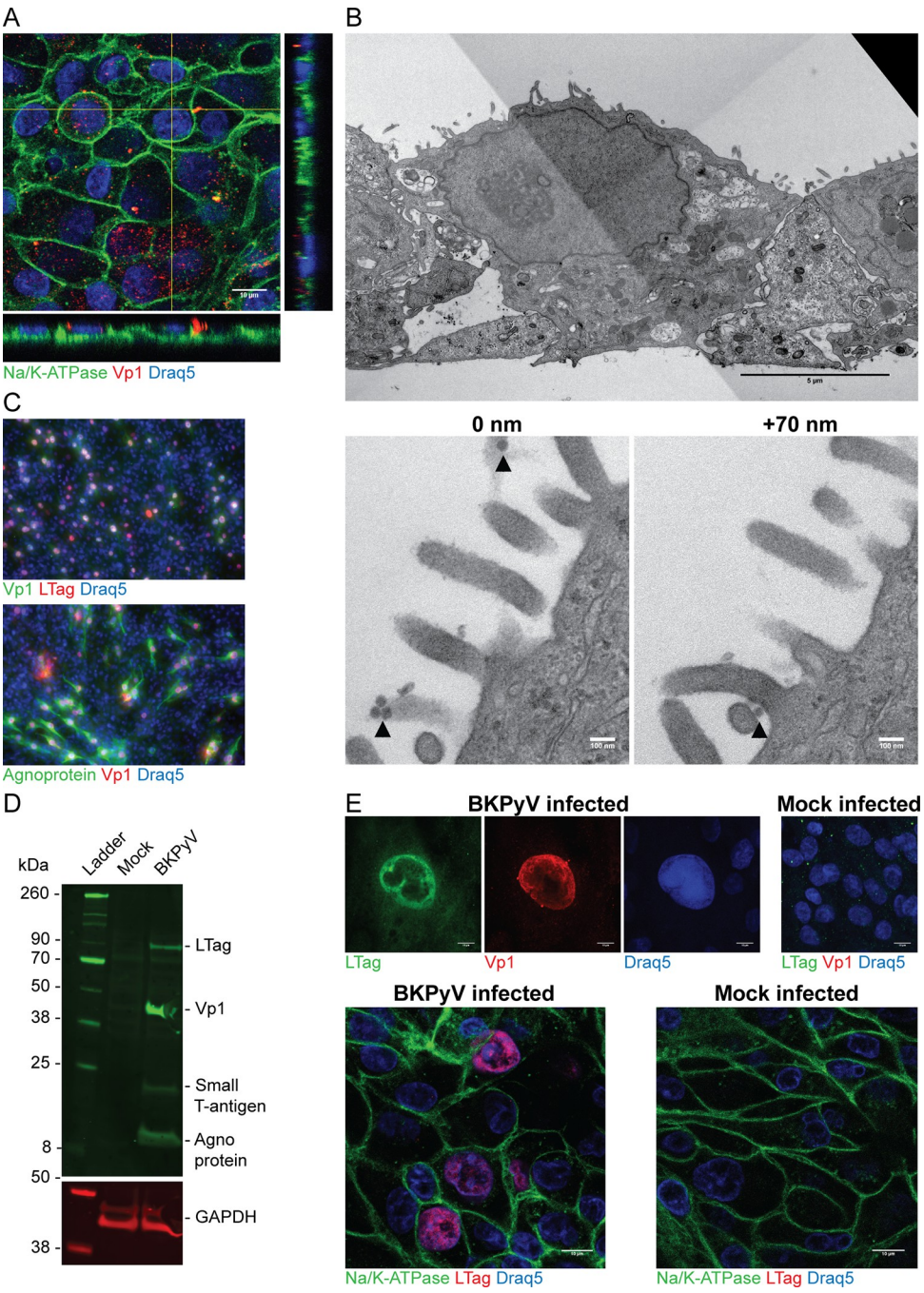

Fig 2. Polarized RPTECs support BKPyV infection. (A) Binding and internalization of BKPyV (MOI 0.1) in polarized RPTECs at 2 hours post infection (hpi) demonstrated by immunofluorescence staining against Vp1 (4942) (red) and Na/K-ATPase (green). Scale bar is 10 μm. (B) Transmission electron micrographs of polarized RPTECs that have been inoculated with BKPyV for 2 hours. Top image is an overview image with scale bar 5 μm. Bottom images are representative images from 70 nm serial sections of virions on the cell surface (black arrowhead). Scale bar 100 nm. Productive BKPyV infection in polarized RPTECs at 3 days post infection (dpi) with BKPyV (MOI 1) is demonstrated by: (C) Immunofluorescence staining against Vp1 (rabbit serum) (green) and LTag (Pab416) (red) (top image) or agnoprotein (green) and Vp1 (4942) (red) (bottom image). (D) Western blot using rabbit serums against N-terminal LTag, Vp1 and agnoprotein. Lysates of mock infected cells were used as negative control and a GAPDH antibody was used as a loading control. (E) Confocal microscopy images of BKPyV infected cells. Top images are stained with rabbit serum against N-terminal LTag (green) and an antibody against Vp1 (4942) (red). Bottom images are stained for Na/K-ATPase (green) and LTag (Pab416) (red). Mock infected cells are included as a negative control. Scale bar 10 μm. In (A), (C) and (E), nuclei are stained with Draq5 (blue) and representative images from three independent experiments are shown.

https://doi.org/10.1371/journal.ppat.1011622.g002

BKPyV preferentially enters polarized RPTECs through the apical membrane

It is not known which compartment BKPyV must access to infect renal tubule epithelial cells *in vivo*. To shed light on this, we examined the entry of BKPyV in our polarized model. To ensure that BKPyV could traverse the insert, we first determined the diffusion of BKPyV through empty inserts. Approximately 19% of applied virus diffused across Falcon-inserts (1.0 μm) while only 5% diffused across the Transwell-inserts (0.4 μm). Based on this, the Falcon-inserts and a 5.3x higher BKPyV concentration for basolateral infections were used for subsequent experiments.

We infected polarized RPTECs via the apical membrane or the basolateral membrane and determined infectivity by immunofluorescence staining. Basolateral infection yielded 71% fewer infected cells than apical infection (Figs 3A and S2A). We hypothesized that this was caused by poorer binding of BKPyV to the basolateral membrane. To examine this, we repeated the previous experiment except that we performed immunofluorescence staining at 2 hpi and compared the intensity of the Vp1-signal. Apical infection yielded a significantly stronger Vp1-signal (Fig 3B and 3C), indicating that more Vp1 bound to the apical membrane than the basolateral membrane. As a control, we infected RPTECs at 2 dps i.e. prior to polarization, and found no difference in infectivity between apical and basolateral infection (Figs 3D and S2B). This confirms that apico-basal polarity is necessary for preferential apical entry.

It has previously been shown that BKPyV can utilize sialic acids and gangliosides on non-polarized Vero cells as receptors [27–31]. To assess if sialic acids are necessary for BKPyV infection in polarized RPTECs, we performed a neuraminidase pre-treatment. This reduced infectivity by 90% (Figs 3E and S2C), confirming that sialic acids are indispensable for BKPyV infection in polarized RPTECs.

In lack of suitable antibodies against gangliosides, Texas-Red conjugated wheat-germ-agglutinin (WGA) was used to examine the distribution of sialic acids. WGA-staining was almost exclusively seen on the apical membrane (Fig 3F). In non-polarized RPTECs, both apical and basolateral application of WGA yielded visible staining (S2D Fig).

We conclude that BKPyV mainly enters RPTECs through the apical membrane, possibly because of more sialic acids at the apical membrane. All subsequent infections were done via the apical compartment.

BKPyV is mainly released into the apical compartment

In vivo, the direction of virus release has important consequences as it influences if viruses disseminate systemically or cause local infection [18]. For viruses infecting tubule epithelial cells, apical release will result in viruria while basolateral release will result in virus in the interstitial space and potentially viremia. To investigate if BKPyV undergo directional release, we infected polarized RPTECs (MOI 0.3), sampled the supernatants before removal of the inoculum at 2 hpi and at several later timepoints up to 120 hpi and analyzed BKPyV-DNA loads. At 2 hpi only 0.4% of the extracellular BKPyV-DNA load was detected in the basolateral compartment (S3A Fig), confirming that the epithelial cells formed a tight barrier. At 48 and 58 hpi, the extracellular BKPyV-DNA load in the apical compartment had increased by 0.7 log and 1 log from input, i.e. the inoculum left after washing (Fig 4A), suggesting that progeny release had started. The apical BKPyV-DNA load increased up to the last timepoint, 120 hpi, at which a 3.1 log increase was found (Fig 4A). Up to 58 hpi, the BKPyV-DNA load in the basolateral compartment was 2.4 to 2.8 log lower than in the apical compartment. The difference decreased to 1.3 log at 120 hpi. BKPyV infection with MOI 3 and 30 yielded similar results,

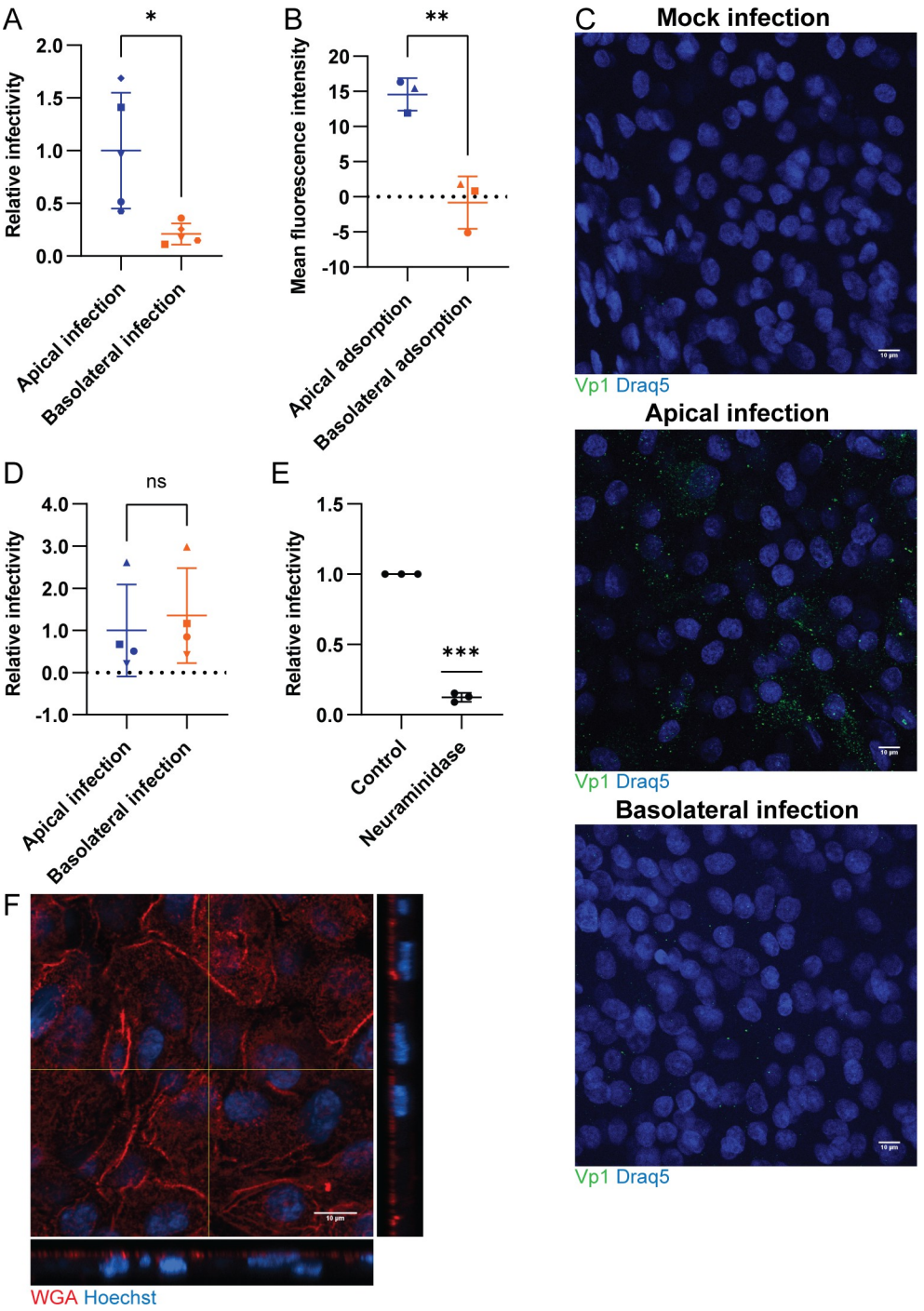

Fig 3. BKPyV preferentially enters polarized RPTECs via the apical membrane. (A) BKPyV infectivity following apical and basolateral infection. Apical infection was performed with MOI 0.1 while basolateral infection was done with 5.3x more virus. Data represents the number of infected cells based on immunofluorescence staining for Vp1 (4942) and agnoprotein at 3 dpi and is presented as relative infectivity normalized to the mean number of infected cells for apical infection. n = 5 and error bars represent ± SD. * = $P < 0.05$, two-tailed *t* test (B) Detection of BKPyV at 2 hours after apical and basolateral infection, respectively. Immunofluorescence staining for Vp1 (4942) was performed and followed by confocal microscopy and acquisition of z-stacks. Vp1-staining intensity was measured in sum z-projections and is represented as mean fluorescence intensity. Z-stacks of mock infected cells were used as a negative control and subtracted as background. Error bars represent ± SD and n = 3. ** = $P < 0.01$, two-tailed *t* test. (C) Representative z-slices from (B) stained for Vp1 (4942) (green) and Draq5 (blue). Scale bar 10 μm. (D) BKPyV infectivity in non-polarized RPTECs following apical or basolateral infection at 2 dps. Apical infection was performed

with approximately MOI 0.1 while basolateral infection was done with 5.3x more virus. Data represents the number of infected cells based on immunofluorescence staining for Vp1 (4942) and agnoprotein at 3 dpi and is presented as relative infectivity normalized to the mean number of infected cells for apical infection. n = 4 and error bars represent ± SD. ns = P > 0.05, two-tailed *t* test (E) BKPyV infectivity after neuraminidase-pretreatment. Data represents the number of infected cells based on immunofluorescence staining for Vp1 (4942) and agnoprotein at 3 dpi and is presented as relative infectivity normalized to the untreated control. n = 3 and error bars represent ± SD. *** = P < 0.001, one sample *t* test. (F) Representative apical z-slice from a z-stack of polarized RPTECs stained with Texas Red conjugated wheat germ agglutinin (red) and Hoechst (blue). Scale bar 10 μm.

https://doi.org/10.1371/journal.ppat.1011622.g003

except that the basolateral BKPyV-DNA load increased slightly earlier (S3B and S3C Fig). Of note, at 120 hpi, we observed considerable cytopathic effects (CPE).

Next, we examined if the extracellular BKPyV-DNA corresponded to infectious BKPyV by inoculating supernatants onto non-polarized RPTECs. Up to 72 hpi, virus was exclusively found in supernatants from the apical compartment (Fig 4B). In supernatants from the basolateral compartment, virus was detected at 120 hpi (Fig 4B), coincident with the observed CPE. Notably, the infectious BKPyV load was still about 2 log lower than in the apical supernatants.

We conclude that BKPyV is preferentially released into the apical compartment and that basolateral BKPyV represents leakage from the apical compartment. Detection of apical progeny release between 48 and 58 hpi, suggests that the BKPyV replication cycle is of similar length as in non-polarized RPTECs [32].

BKPyV replication causes late cell death in polarized RPTECs

Due to the detection of CPE, we decided to examine the morphology of cells throughout BKPyV infection (MOI 3.0). Cytoplasmic vacuolization, cell rounding and loss of the cobblestone-pattern emerged at 72 hpi, increased over time and was most evident at 120 hpi (Fig 5A). We also noted that a reduced infectious dose (MOI 1 or 0.3) gave less CPE (results not shown).

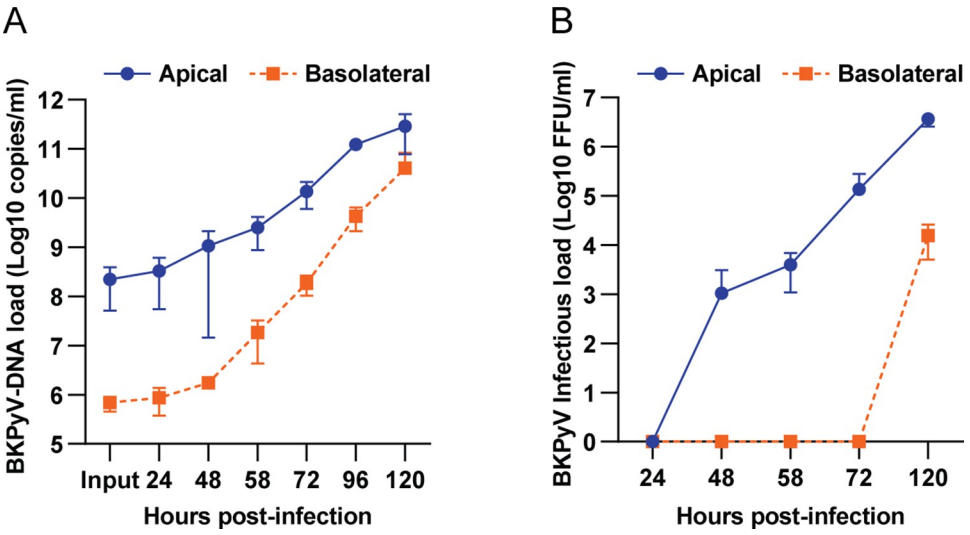

Fig 4. BKPyV is mainly released into the apical compartment. (A) Polarized RPTECs were apically infected (MOI 0.3) and supernatants were collected at the indicated timepoints for BKPyV-DNA load (log 10 copies/ml) determination by qPCR. Data was generated from at least three independent experiments, except the 96 hpi timepoint which was derived from two independent experiments. (B) Polarized RPTECs were apically infected (MOI 1) and supernatants were collected at the indicated timepoints for determination of BKPyV infectious load (log 10 FFU/ml) by infectivity assay. Infectious load at 24 hpi was defined as input and subtracted as background. Data was generated from six independent experiments. Error bars represent ± SD for (A) and (B).

https://doi.org/10.1371/journal.ppat.1011622.g004

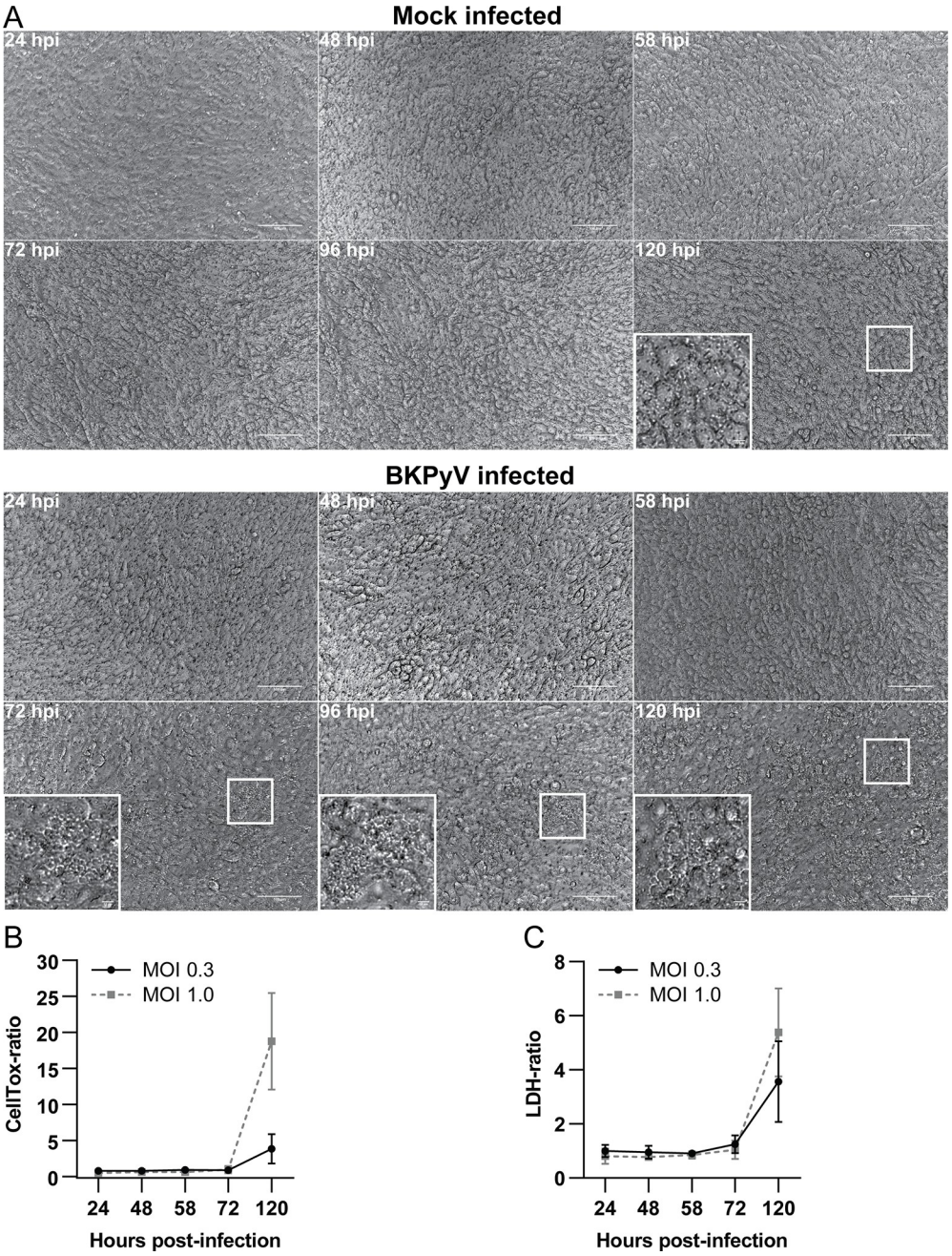

Fig 5. BKPyV induced cytopathic effects and cell death in polarized RPTECs. (A) Phase-contrast images of mock infected and BKPyV infected RPTECs (MOI 3) from 24 to 120 hpi. Representative images from two independent experiments are shown. Scale bar 100 μm. (B) Widefield microscopy of mock infected and BKPyV infected RPTECs incubated with CellTox dye. Data is presented as CellTox-ratio (mean total fluorescence from infected inserts/mean total fluorescence from mock infected inserts). Error bars represent ± SD and data is derived from at least three independent experiments. (C) Release of LDH into apical supernatants as measured by Promega LDH-Glo Cytotoxicity assay. Data is presented as LDH-ratio (infected-RLU/mock-RLU). Error bars represent ± SD and data is derived from at least three independent experiments.

https://doi.org/10.1371/journal.ppat.1011622.g005

Studies have suggested that BKPyV is released after host cell necrosis [10,11,33]. A common feature of cell death with necrotic morphology is permanent plasma membrane permeabilization [34]. We therefore examined the plasma membrane integrity of mock infected and

BKPyV infected RPTECs from 24 to 120 hpi by measuring CellTox-fluorescence and LDH release. Up to 72 hpi, BKPyV caused no increase in CellTox-fluorescence, but at 120 hpi, a 5- and 20-fold increase was found with BKPyV MOI 0.3 and MOI 1, respectively (Fig 5B) indicating host cell lysis. Similarly, no increase in extracellular LDH was observed up to 72 hpi, while at 120 hpi a 4- and 6-fold increase was detected for MOI 0.3 and MOI 1, respectively (Fig 5C). BKPyV infections with higher MOI (3 and 30) caused earlier and more prominent increase in CellTox-fluorescence and LDH release (S3D and S3E Fig).

Next, we investigated the plasma membrane integrity of individual cells by utilizing CellTox dye and live-cell imaging (Fig 6A and S1–S2 Video). An increase in CellTox-positive cells was exclusively observed in the infected inserts. The first increase was detected at 72 hpi with a mean of 32 new CellTox-positive cells per image, representing a 2.8-fold increase. The increase continued up to 120 hpi with 336 new CellTox-positive cells, representing a 30-fold increase (Fig 6A and 6B and S1 Video). Additionally, we observed cell ballooning and lysis in real-time (S1 Video). In contrast, the number of CellTox-positive cells consistently decreased throughout imaging for mock infected inserts (Fig 6A and 6B and S2 Video).

As BKPyV infection leads to widespread cell death, we investigated if this affected the barrier function. Up to 3 days post-infection (dpi), we detected a slight increase in TEER for BKPyV infected RPTECs. However, at 5 dpi we detected a negative trend in TEER with a 14% and 34% reduction for MOI 1 and MOI 10, progressing to a 20% and 50% reduction at 7 dpi, respectively (Fig 6C), indicating a disrupted barrier function.

We conclude that BKPyV induces CPE and lytic cell death in polarized RPTECs, but that this mainly occurs from 3 dpi. Despite CPE and increasing cell death, we first detected a downward trend in TEER at 5 dpi, allowing leakage of BKPyV from the apical to the basolateral compartment.

BKPyV replication leads to extensive cell detachment

Many viruses are known to cause detachment of infected cells [35–37], including BKPyV as urinary shedding of infected epithelial cells, i.e decoy cells [38,39], is commonly observed in PyVAN patients [11,14]. Although a well-known phenomenon, this feature of BKPyV infection has not been studied *in vitro*.

First, we harvested supernatants from mock infected and BKPyV infected RPTECs (MOI 1) at 5 dpi and imaged them for detached cells. All supernatants contained detached cells, but the infected inserts yielded markedly more cells. Addition of CellTox dye revealed that most of the cells were permeabilized and appeared non-viable (Fig 7A). Papanicolaou staining, commonly used to detect decoy cells, followed by widefield microscopy demonstrated that detached cells had enlarged nuclei, intranuclear inclusion bodies and small and irregular cytoplasms (Figs 7B and S5), reminiscent of decoy cells type 1 [38,39]. Additionally, most decoy-like cells had intact nuclei and some cells displayed membrane ballooning (S5 Fig). Immunofluorescence staining revealed that the majority of decoy-like cells expressed agnoprotein and Vp1 (Fig 7C), and immunoblot confirmed the expression of viral proteins (Fig 7D). Next, we examined if decoy-like cells could transmit BKPyV. Cells were washed and pelleted before inoculation onto RPTECs. As a control, we included the last wash-supernatant. Immunofluorescence staining demonstrated that infection with decoy-like cells yielded strikingly more infected cells compared to the control supernatant (Fig 7E), demonstrating that the decoy-like cells harbor infectious virus.

We next investigated the detachment of BKPyV infected RPTECs by live-cell imaging in the presence of CellTox dye and the membrane stain CellMask. Due to focus-distance limitations, we used confluent RPTEC-monolayers in chamberslides. Z-stacks of RPTEC-

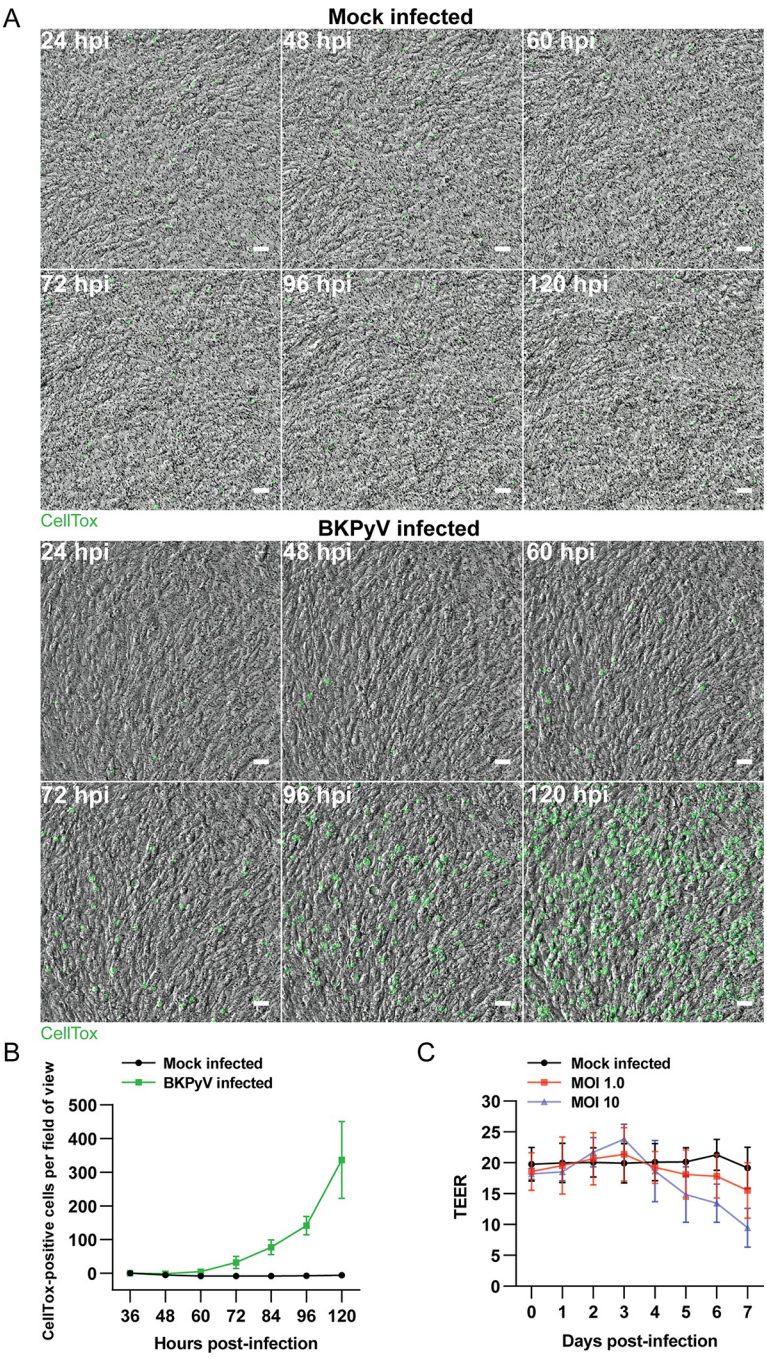

Fig 6. Time-lapse imaging and TEER-monitoring throughout BKPyV replication. (A) Time-lapse imaging of mock infected and BKPyV infected (MOI 1) polarized RPTECs. Nuclei of permeabilized cells are stained with CellTox dye. Representative images from two independent experiments at 24, 48, 60, 72, 96 and 120 hpi are shown. Scale bar 50 μm. (B) Quantitation of cell permeabilization in (A). Presented is the number of new CellTox-positive cells from 36 hpi. Error bars represent ± SD, n = 2. (C) TEER-values of mock infected and BKPyV infected (MOI 0.1 and 10) polarized RPTECs from 0 to 7 dpi. Data is derived from three to six biological replicates and error bars represent ± SD.

https://doi.org/10.1371/journal.ppat.1011622.g006

monolayers at 4 dpi revealed that CellTox-fluorescent cells were localized 10 to 20 μm above the non-permeabilized monolayer, indicating that permeabilized cells detached from the monolayer (S4 Fig).

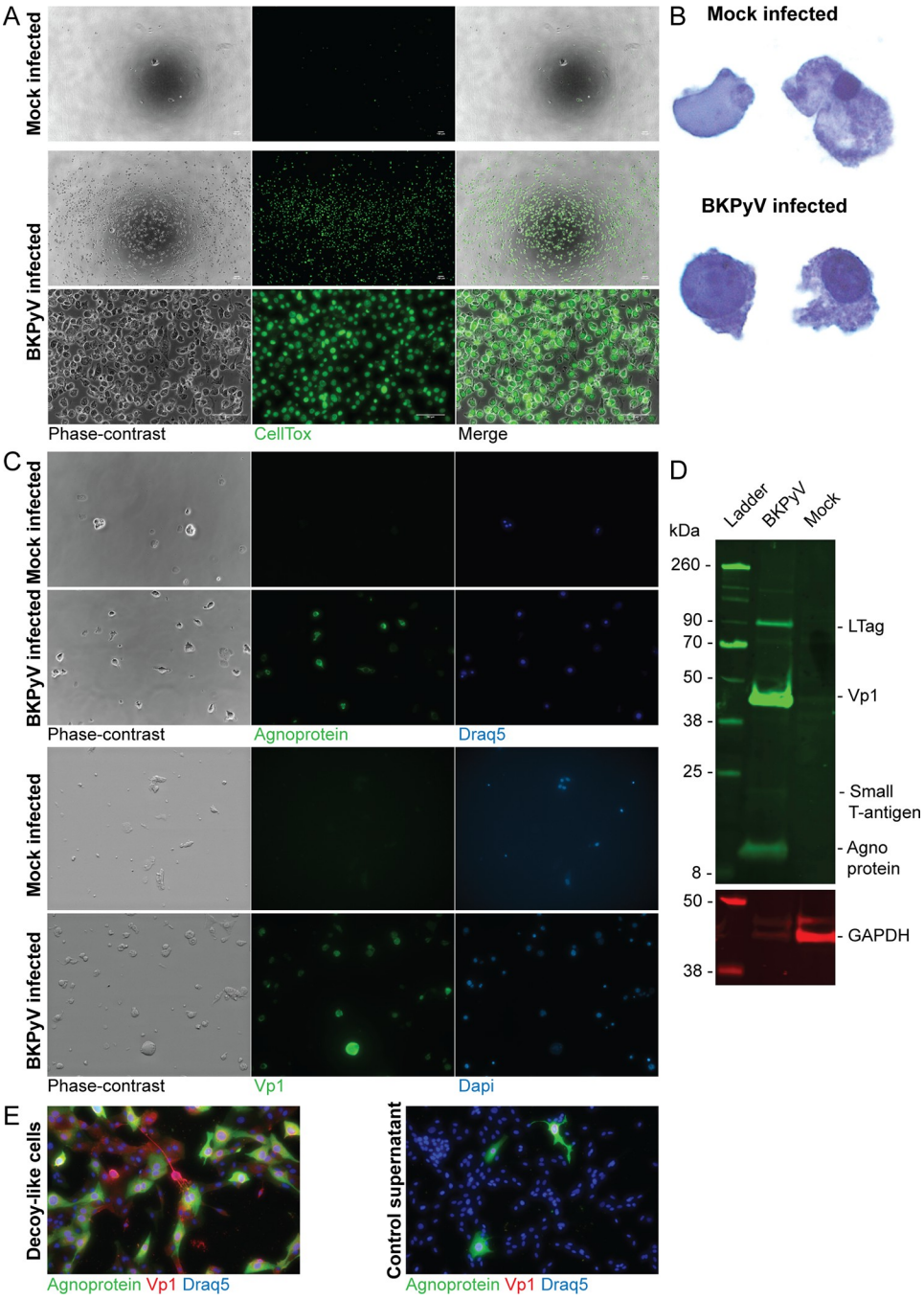

Fig 7. BKPyV replication leads to shedding of infectious decoy cells. Widefield microscopy of detached cells harvested from supernatants of mock infected and BKPyV infected (MOI 1) polarized RPTECs at 5 dpi. Harvested cells were imaged with phase-contrast and fluorescence microscopy. All images are representative images from two independent experiments, except (B) which is derived from one experiment. (A) Detached cells incubated with CellTox dye (green) and imaged with a combination of phase-contrast and fluorescence microscopy. Scale bar 100 μm. (B) Detached cells after Papanicolaou staining. (C) Immunofluorescence staining of detached cells from mock infected and BKPyV infected (MOI 1) polarized RPTECs using rabbit serums against Vp1 and agnoprotein. (D) Western blot of lysates of detached RPTECs harvested at 5 dpi from BKPyV infected (MOI 1) RPTECs. Mock infected RPTEC-lysate was used as the negative control. The membrane was probed with rabbit serums against N-terminal LTag, Vp1 and agnoprotein and an antibody against GAPDH. A representative blot from two experiments is shown. (E) Immunofluorescence staining of non-polarized RPTECs after infection with decoy cells harvested from BKPyV infected polarized RPTECs. A rabbit serum against agnoprotein (green) and an antibody against Vp1 (4942) (red) were used. Prior to infection, the decoy cells were washed and centrifuged five times. The supernatant from the last centrifugation was used as a control. Images are representative images from two independents experiments.

https://doi.org/10.1371/journal.ppat.1011622.g007

Epithelial tissues have a special mechanism, denoted extrusion, for removal of dead or unwanted cells whilst maintaining the integrity of the epithelial barrier [40]. Besides, some viruses have been reported to trigger extrusion in intestinal and airway epithelium [36,37]. To investigate if BKPyV infected RPTECs undergo extrusion, we performed time-lapse imaging with CellTox and CellMask dye [41], to visualize detachment at the single-cell level. We observed that most detaching cells were permeabilized and appeared to undergo extrusion as demonstrated by compression and subsequent upward migration of the permeabilized cell while the confluent monolayer was maintained (Fig 8A and S3 Video). However, some cells sloughed off the surface, leaving a hole in the monolayer (Fig 8B and S4 Video). Quantification of cell fate revealed that over 80% of the CellTox-fluorescent cells were detached (Fig 8C) and 70% of detached cells appeared to undergo extrusion while 30% sloughed off (Fig 8D).

We conclude that BKPyV infection induces cell death and subsequent detachment into the apical compartment. The detached cells resembled decoy cells and could transmit BKPyV. Extrusion of dead cells seems to preserve the epithelial barrier integrity.

Neutralizing antibodies inhibit BKPyV spread in polarized cell layers

Antibodies have been shown to undergo transepithelial transport across polarized cells and inhibit viral infection [42–44]. To investigate if BKPyV-specific antibodies could undergo transepithelial transport and inhibit *de novo* BKPyV infection, we infected polarized RPTECs (MOI 0.1) and added a neutralizing BKPyV-specific Vp1-antibody in the basolateral compartment at 24 hpi. Immunofluorescence staining at 120 hpi revealed about 35% fewer infected cells compared to control inserts where a non-neutralizing antibody was added (Fig 8E).

We conclude that neutralizing antibodies traverse the tight RPTEC-layer, possibly by transcytosis, and inhibit spread of BKPyV infection.

Discussion

Current *in vitro* studies on BKPyV replication have been performed in non-polarized cell cultures. In this study we established a polarized human renal epithelial cell model by culturing primary RPTECs on permeable inserts. Using this model, we demonstrate that BKPyV preferentially enters RPTECs via the apical membrane and that BKPyV replication results in lytic release and shedding of decoy-like cells. As cell shedding mainly occurs by extrusion, the epithelial barrier is maintained for some time, retaining viral progeny in the apical compartment. However, high-level BKPyV replication is gradually damaging the barrier, allowing virus and viral DNA to leak into the basolateral compartment. Basolateral addition of BKPyV-specific neutralizing antibodies inhibited *de novo* infections. BKPyV replication in our model closely emulates BKPyV replication in tubule epithelial cells *in vivo* and gives new insight into BKPyV reno-urinary dissemination and cytopathology.

BKPyV preferentially entered the cells via the apical membrane. Directional virus entry in epithelial cells depends on receptor distribution [18]. For instance, entry of the closely related polyomavirus SV40 and of rotavirus is suggested to be apical due to apical distribution of entry receptors [45–47]. In non-polarized cells, BKPyV has been shown to use gangliosides [27,28] and a N-linked glycoprotein containing α(2,3)-linked sialic acid [29] as receptors. In polarized cells, gangliosides and sialic acids are known to be asymmetrically distributed to the apical membrane [47–50]. In agreement with this, WGA-staining showed more sialic acids on the apical than the basolateral membrane. Moreover, neuraminidase pre-treatment reduced BKPyV infectivity, demonstrating that BKPyV infection of polarized RPTECs rely on sialic acids on the apical membrane.

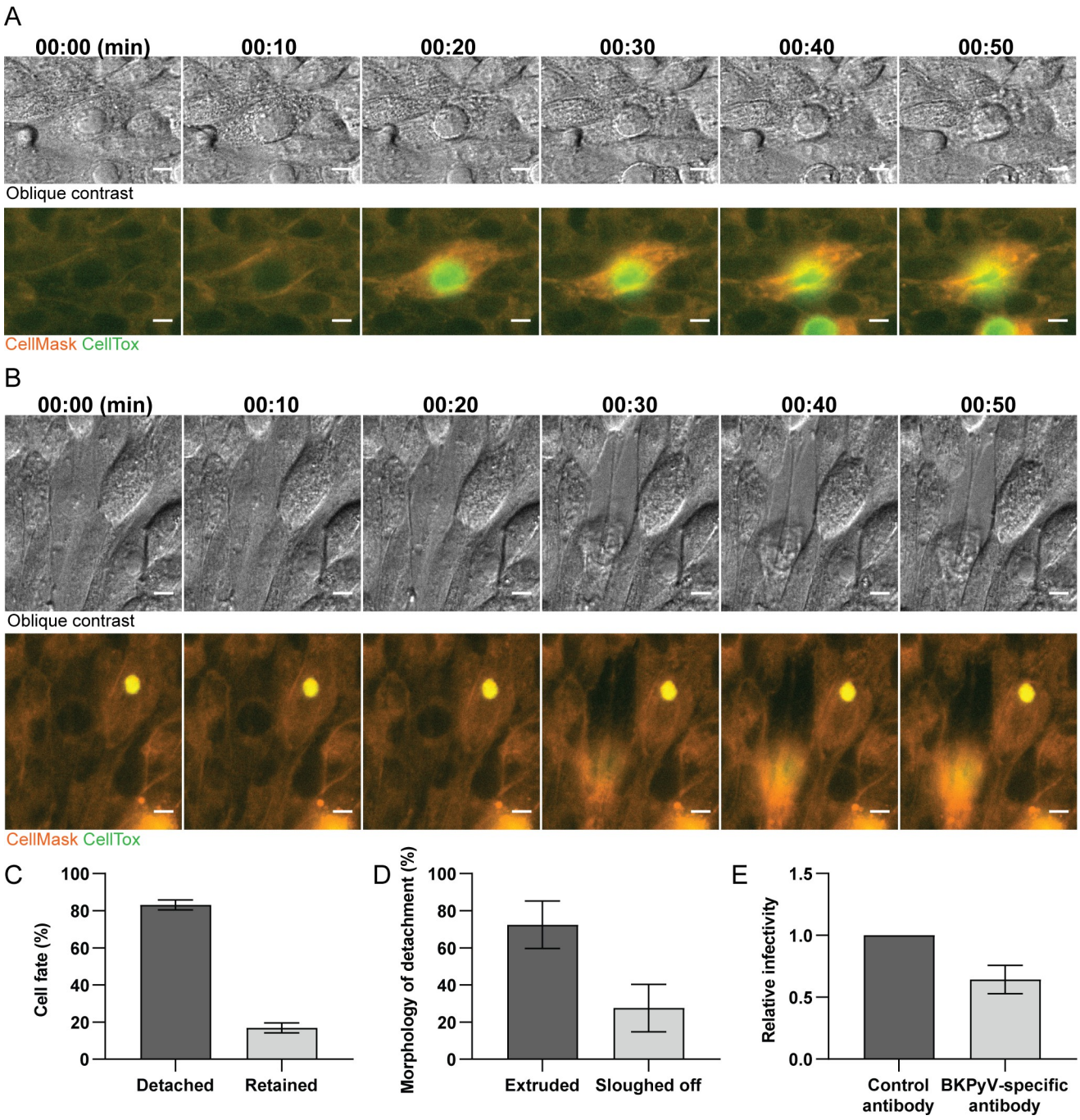

Fig 8. Cell shedding mainly occurs via extrusion. (A and B) Representative time-lapses with oblique contrast and fluorescence microscopy of a cell undergoing extrusion (A) or sloughing off (B). Membranes are stained with CellMask (orange) and the nuclei of permeabilized cells are stained with CellTox dye (green). Scale bar 10 μm. Images are representative time-lapses from two independent experiments. (C) Quantification of cell fate of CellTox-positive cells at 4 dpi. Data is derived from two independent experiments where 653 cells have been examined. Error bars represent ± SD. (D) Classification of the morphology of detachment for CellTox-positive cells at 4 dpi (extrusion vs. slough off). Data is derived from two independent experiments and 71 examined cells. Error bars represent ± SD. (E) Neutralizing antibodies undergo transepithelial transport and inhibit spread of BKPyV infection. Polarized RPTECs were infected with a low MOI (0.1) and at 24 hpi, a BKPyV-specific neutralizing antibody or control antibody was added to the basolateral compartment. At 5 dpi, cells were stained for LTag with a mouse antibody (Pab416) and a C-terminal LTag rabbit serum and the number of infected cells were counted. Data is derived from two independent experiments and error bars represent ± SD.

https://doi.org/10.1371/journal.ppat.1011622.g008

The primary mode of progeny release for non-enveloped DNA viruses is considered to be host cell lysis [51]. For BKPyV, this is supported by studies of renal allograft biopsies from PyVAN patients [10,11,33]. On the other hand, non-lytic release has been suggested for BKPyV [30,52] as well as for SV40 [53]. When we measured cell lysis by CellTox-fluorescence and LDH release, no increase in lysis was detected up to 72 hpi, a timepoint when considerable progeny release into the apical compartment had taken place. However, live-cell imaging of single cells at 72 hpi did reveal a small increase in dead cells, suggesting that progeny was indeed released by host cell lysis. Although host cell lysis seems to be the most important mechanism for BKPyV release from polarized RPTECs, we cannot exclude a parallel non-lytic release mechanism.

Even though lytic virus release normally is considered non-directional [47], several factors may explain why BKPyV was exclusively detected in the apical compartment up to 120 hpi. Firstly, since the cells were cultured in the apical compartment, lysis released BKPyV into the apical compartment. Secondly, due to shedding of infected cells by extrusion, the cell layer was intact until 5 dpi, preventing released BKPyV from leaking into the basolateral compartment. Of note, this is the first time that shedding of BKPyV infected epithelial cells by extrusion is suggested. Third, released virions presumably bound to the apical membranes, further hindering virus from traversing the insert. The two latter points are supported by the virus release assay (Figs 4A and S3A), which demonstrates that with an intact cell layer, only miniscule amounts of the inoculating virus can cross from the apical to the basolateral compartment. Lastly, apically shed cells harbored virus and contributed to the high apical BKPyV load.

How do our results fit with *in vivo* findings and increase our understanding of BKPyV dissemination and cytopathology in the reno-urinary tract? BKPyV infected polarized RPTECs showcased cytopathic changes described in renal allografts from PyVAN patients. These were enlarged nuclei with inclusions, cell rounding, cytoplasmic vacuolization, cell lysis and detachment [10,11,14,54]. Furthermore, our finding of preferential BKPyV release into the apical compartment agrees with observations in PyVAN patients, as they always have higher urinary- than plasma BKPyV load and develop viruria prior to DNAemia [12,55,56]. Apical entry also fits well with the suggested importance of ureteric reflux for multi-site spread of BKPyV in the allograft [12].

Despite BKPyV replication causing more than a 100-fold increase in viral progeny in the apical compartment and abundant cell shedding, the epithelial barrier seemed intact until 5 dpi, presumably due to extrusion of lysed BKPyV infected cells. Based on these findings, we propose that during low-level BKPyV replication in the kidneys of immunocompetent individuals or renal allografts of kidney transplant recipients, progeny virus is mainly released into the tubular lumen and disseminate intra-luminally along the tubular system. Importantly, extrusion of BKPyV infected cells keeps the epithelial lining of the tubular lumen intact. In immunocompetent individuals, we expect that infected tubule epithelial cells will eventually interact with the immune system [57] and viral replication will be inhibited.

After five days of high-level BKPyV replication in polarized RPTECs, the number of decoy-like cells increased, the epithelial barrier was disrupted and BKPyV leaked into the basolateral compartment. This suggests that during unrestricted high-level replication of donor-derived BKPyV in the kidney allograft [58], widespread cell lysis will eventually disrupt the epithelial barrier. BKPyV and intracellular BKPyV-DNA from lysed cells will leak into the interstitial fluid and blood and an increased number of decoy cell will be found in urine, together giving the diagnosis presumptive PyVAN [5]. The decoy cells can potentially act as vessels to promote further spread of BKPyV in the reno-urinary tract.

We observed that neutralizing antibodies could cross the epithelial cell layer and reduce *de novo* BKPyV infection, suggesting that treatment with intravenous BKPyV-specific

neutralizing antibodies could be beneficial as treatment of PyVAN. However, to clear BKPyV infected cells, BKPyV-specific cytotoxic T cells are needed [59]. Currently, there are several ongoing clinical trials with BKPyV-specific neutralizing antibodies and donor-derived cytotoxic T lymphocytes [60].

To establish a persistent BKPyV infection in epithelial cells of the reno-urinary tract, BKPyV must be able to evade immune sensing. BKPyV miRNA has been reported to target the stress-induced protein ULBP3 to reduce killing by natural killer cells [61]. Furthermore, Manzetti *et al* demonstrated that BKPyV evades innate immunity by disrupting the mitochondrial network and promoting mitophagy [62]. Here we for the first time demonstrate that extrusion of BKPyV infected epithelial cells leads to containment of viral progeny in the apical compartment, which is expected to delay the contact with the immune system [63]. Together, this highlights that BKPyV utilizes multiple strategies for immune evasion.

In order to fully understand the pathogenesis of BKPyV infection, including primary infection and entry, multiplication, spread within the body, the immune response and the potential kidney damage, an animal model would be very useful. Unfortunately, this is lacking. Polarized cell culture models, such as ours, is a valuable alternative tool to study BKPyV under conditions that more closely reflects the renal epithelium and tubular system than traditional cell cultures.

Taken together, we utilized a novel cell model of polarized renal tubule epithelial cells to characterize local BKPyV dissemination and cytopathological changes associated with BKPyV infection. Using this model, we establish a preferential apical entry of BKPyV, a predominant release of viral progeny into the apical compartment via host cell lysis and decoy cell shedding and finally that extrusion contain BKPyV in the apical compartment, suggesting that BKPyV *in vivo* spreads intra-luminally along the nephron to the pelvis and bladder and thereby delay immune detection.

Materials and methods

Cells and virus

Primary human RPTECs (Lonza) were cultured in renal epithelial growth medium (REGM; Lonza) containing 0.5% fetal bovine serum in a humidified 5% CO_2 incubator at 37˚C. Cesium-chloride gradient purified BKPyV Dunlop was used for all infections.

Culture and infection of polarized RPTECs

For polarization, RPTECs were seeded on collagen-coated (recombinant human collagen type I; Sigma-Aldrich) permeable polyester-membrane cell culture inserts and cultured for 8 to 15 days. The following inserts were used: Falcon inserts with pore size 1.0 μm or 3.0 μm and Corning Transwell-inserts with pore size 0.4 μm, all with 0.3 cm^2 growth area.

Polarized RPTECs were infected with an inoculum of 100 μl. Apical infection was done by adding inoculum inside the insert. Basolateral infection was performed by temporarily inverting inserts and adding inoculum on top. Infections were performed for 2 hours at 37˚C.

For neuraminidase-experiments, cells were pretreated with 100 mU/ml neuraminidase type V from clostridium perfringens (Merck) for 1 hour prior to apical infection.

For neutralization experiments, polarized RPTECs were apically infected (MOI 0.1). At 24 hpi, a mouse monoclonal BKPyV-specific antibody (Virostat 4942) or control antibody (Virostat 4944) was added to the basolateral compartment at a concentration of 7 μg/ml. At 5 dpi, the number of infected cells was determined with immunofluorescence staining.

Immunofluorescence staining, microscopy and image analysis

Cells were fixed in ice-cold methanol or 4% paraformaldehyde for 10–15 minutes. PFA-fixed cells were permeabilized with permeabilization buffer (DPBS with 1% BSA and 0.1% Triton-X100) for 10 minutes. Immunofluorescence staining was performed as previously described [64] except that primary and secondary antibody staining was performed for 1 hour at room temperature. The following antibodies and serums were used to stain for viral proteins:, mouse anti-BKPyV Vp1 (4942; 2.8 ug/ml; Virostat), mouse anti-LTag (Pab416; 1:100; Merck Millipore), rabbit serums against BKPyV agnoprotein (1:1000) [65], BKPyV N-terminal LTag (1:1000) [66,67], BKPyV C-terminal LTag (1:1000) [67] and BKPyV Vp1 (1:1000) [68]. The following antibodies were used to stain for cellular proteins: rabbit monoclonal anti-Na/K-ATPase (ab76020; 1:500; Abcam), rabbit polyclonal anti-ZO-1 (61–7300; 1:100; Invitrogen) and mouse monoclonal anti-acetylated α-tubulin (sc-23950; 1:100; SCBT). Secondary antibodies used were goat anti-rabbit Alexa Fluor 488 and anti-mouse Alexa Fluor 568 (Invitrogen). Staining with Texas Red-conjugated WGA (10 μg/ml; Thermo Fisher) was performed for 30 minutes on living cells. Insert-membranes was cut out and mounted on a cover glass with mowiol or ProLong Diamond mounting medium.

Widefield microscopy was performed using a Nikon TE2000-microscope with a 4x (NA 0.13) and 20x objective (NA 0.45) and NIS Elements Basic Research software. Confocal microscopy was performed using a Zeiss LSM800 confocal microscope with a 40x water-objective (NA 1.2) and Zeiss ZEN blue software. All images were processed with FIJI/ImageJ.

To measure Vp1-staining, z-stacks of equal size were acquired. Identical acquisition settings were used for each replicate. Using ImageJ, sum z-projections were generated and mean fluorescence was measured. The mean fluorescence in z-projections from mock infected inserts were subtracted as background.

Transepithelial resistance

TEER was measured using a Millicell ERS-2 voltohmmeter with an adjustable electrode (STX02) in a 12-well plate. TEER (Ohm * cm^2) was calculated by subtracting the background of an empty insert from the average TEER and multiplying the value by the surface area (0.3 cm^2). All measurements were done in duplicate or triplicate.

FITC-Dextran diffusion assay

The assay was adapted from two publications [69,70]. Polarized RPTECs were incubated with 100 μl of 0.1 mg/ml FITC-Dextran MW 20k (Merck) in the apical compartment for 1 hour at 37˚C. Supernatant was harvested from the basolateral compartment and fluorescence was measured using a Tecan Infinite 200 Pro plate reader with an excitation wavelength of 488 nm and emission wavelength of 518 nm. All measurements were performed in duplicate or triplicate.

P-glycoprotein assay

The assay was adapted from the following studies [26,69,71]. Polarized RPTECs were pre-treated with 5 μM of the P-gp inhibitor PSC-833 (Merck) or solvent (0.125% DMSO), followed by addition of REGM with 1 μM Calcein-AM (Invitrogen) and 5 μM PSC-833 or solvent. After incubation at 37˚C for 1 hour, cells were washed twice with DPBS and lysed with 1% Triton X-100. Fluorescence in each sample was measured using a plate reader as described for the FITC-dextran diffusion assay.

Transmission electron microscopy

The protocol was adapted from two reports [72,73]. Samples were fixed in 0.5% glutaraldehyde and 4% formaldehyde in PHEM-buffer (60 mM PIPES, 25 mM HEPES, 10 mM EGTA, 4 mM $MgSO_4 \cdot 7H_2O$) for 30 minutes before fixing again with 4% formaldehyde, 0.5% glutaraldehyde, and 0.05% malachite green in PHEM-buffer (2 min vacuum on-off-on-off-on-off-on, 100 W) using a Ted Pella microwave processor. Samples were post-fixed with 1% osmium tetroxide, 1% $K_3Fe(CN)_6$ in 0.1 M cacodylic acid buffer, post-stained with 1% tannic acid and 1% uranyl acetate and dehydrated in increasing ethanol series before embedding in an Epon-equivalent. 70 nm sections were imaged using a Hitachi HT7800 transmission electron microscope with a Xarosa-camera.

Immunoblots

Immunoblot was performed as previously described [74] except Halt protease- and phosphatase-inhibitor was used in the lysis buffer, lysates were pretreated with Pierce nuclease and membranes were blocked with LI-COR Intercept TBS blocking buffer. The following primary antibody and serums were used: rabbit serums against BKPyV Vp1 (1:10 000) [68], BKPyV N-terminal LTag (1:2000) [67], BKPyV agnoprotein (1:10 000) [65] and mouse anti-GAPDH (ab8245; 1:2000; Abcam). The secondary antibodies used were goat anti-rabbit 800CW and goat anti-mouse 680RD from LI-COR Biosciences. Detection was done with the Odyssey CLx imaging system and Image studio.

Virus diffusion assay

Cell-free collagen-coated Transwell-inserts (pore size 0.4 μm) and Falcon-inserts (pore size 1.0 μm) were incubated with 100 μl of CsCl-purified BKPyV in REGM (250 000–500 000 fluorescent focus units (FFU)) inside the insert for two hours at 37˚C. The basal medium was then harvested and inoculated on non-polarized RPTECs. Infectivity was determined by immunofluorescent staining for agnoprotein and Vp1 (4942) at 3 dpi. To calculate the percentage of virus that diffused across the insert, the infectivity of the basal medium and the initial virus suspension was compared.

Virus release assay

Polarized RPTECs on Falcon-inserts were apically infected before supernatants were harvested at the indicated timepoints and analyzed for BKPyV-DNA or infectious BKPyV. BKPyV-DNA was quantitated by a BKPyV-specific qPCR targeting the BKPyV LTag gene [75]. Infectivity was measured by inoculating diluted supernatants onto non-polarized RPTECs. At 3 dpi, immunofluorescence staining against agnoprotein and Vp1 (4942) was performed and infected cells were counted using the object count feature of the NIS Elements basic research software. All replicates were performed in duplicate.

Cell viability

Cell viability and CPE were examined by phase-contrast microscopy, by LDH release (Promega LDH-Glo Cytotoxicity assay according to the manufacturer's instructions) and by the use of the plasma membrane impermeable CellTox dye (x1) from the Promega CellTox Green cytotoxicity assay. For the CellTox-experiments, CellTox dye was added to the medium before images were acquired. ImageJ was used to measure the total fluorescence per image. Each measurement was performed in duplicate.

Live-cell imaging

Live-cell imaging of inserts were done with Falcon-inserts in a 24-well plate with confocal glass bottom (CellVis P24-1.5H-N) in REGM with CellTox dye (1x) and Hoechst (0,1 μg/ml). Images were acquired using an automated Zeiss CellDiscoverer 7 microscope with a 5x objective (NA 0.35) and 2x tube lens at 37˚C with humidity and 5% CO_2.

To visualize detachment, RPTECs were cultured in fibronectin-coated Lab-Tek 8-well chamberslides (#1 coverglass). RPTECs were infected (MOI 1) when fully confluent monolayers had formed. At 4 dpi, CellMask (0.5x) and CellTox dye (1x) were added, and live-cell imaging was performed as above, but with a 20x objective (NA 0.95) and 2x tube lens. Images were acquired every 10 minutes.

CellTox-fluorescent cells were classified as detached if the nucleus was out of focus or the cell was floating on top of the monolayer, while cells that were adherent and had the nucleus in the same focus plane as the monolayer were classified as retained. Cells that detached without leaving a gap in the monolayer were classified as extruded while cells that left a gap were classified as sloughed off.

Harvest and examination of detached cells

Detached cells were harvested by gently aspirating the apical supernatant, washing once and then pooling supernatants and wash-medium. For immunofluorescence or standard Papanicolaou staining, cells were fixed with ThinPrep PreservCyt-solution and processed with the ThinPrep 5000 Processor before staining. For immunoblot, cells were processed identically as RPTEC lysates. For widefield microscopy, supernatants were transferred to wells to sediment followed by imaging with a Nikon TE2000-microscope (20x objective) or a Zeiss CellDiscoverer 7 microscope (20x objective, 2x tubelens). To examine the infectivity of detached cells, detached cells were washed and centrifuged five times to remove extracellular virus before the cells were inoculated onto non-polarized RPTECs. Wash supernatant was used as a control.

Supporting information

S1 Data. Excel spreadsheet containing the numerical values used for graphs and statistical analysis for figure panels 1D, 1E, 1F, 3A, 3B, 3D, 3E, 4A, 4B, 5B, 5C, 6B, 6C, 8C, 8D, 8E, S1E, S3A, S3B, S3C, S3D and S3E.
(XLSX)

S1 Fig. RPTECs grown on cell culture inserts with 0.4 μm and 3.0 μm pore size. Immunofluorescence staining of RPTECs at 10 dps on Transwell-inserts, pore size 0.4 μm, against markers of apico-basal polarity: (A) Na/K-ATPase (green), (B) acetylated α-tubulin (red) and (C) ZO-1 (green). Nuclei were stained with Draq5 (blue). Images are representative images from at least three independent experiments. (D) Diffusion of FITC-dextran across polarized and non-polarized RPTECs. Data is normalized to the non-polarized control, n = 7 and error bars represent ± SD. *** = $P < 0.001$, one sample *t* test. (E) Accumulation of intracellular calcein AM with or without Psc-833, quantified by measuring intracellular fluorescence with a plate reader. Data is normalized to the untreated control. Error bars represent ± SD and n = 3. * = $P < 0.05$, one sample *t* test. (F) Confocal microscopy of RPTECs grown on Falcon-inserts with 3.0 μm pore size at 9 dps. Cell membranes were stained with CellMask (orange) while nuclei were stained with Draq5 (blue). Representative images from a z-stack from two independent experiments.
(TIF)

S2 Fig. Supplemental images to Fig 3. Immunofluorescence staining against agnoprotein (green) and Vp1 (4942) (red) in polarized RPTECs (A) or non-polarized RPTECs (B), infected via the apical or basolateral compartment. (C) Immunofluorescence staining for Vp1 (4942) (red) in polarized RPTECs treated with or without neuraminidase prior to infection. Nuclei were stained with Draq5 in all images. All images are representative images from at least three independent experiments. (D) Confocal microscopy of non-polarized RPTECs stained with Texas Red conjugated wheat germ agglutinin (red) via the apical or basolateral membrane. Scale bar 10 μm.
(TIF)

S3 Fig. Virus release and cell viability with increased MOI. (A) Purified BKPyV was added to the apical compartment. After 2 hours, apical and basolateral supernatants were collected, BKPyV-DNA load (log10 copies/ml) was determined by qPCR and apical and basolateral distribution was calculated. Data was generated from three independent experiments and error bars represent ± SD. (B and C) BKPyV-DNA load (log10 copies/ml) in apical and basolateral supernatants collected from infected polarized RPTECs at indicated timepoints. (B) MOI 3 and (C) MOI 30. Data is generated from three independent experiments and error bars represent ± SD. (D) Widefield microscopy of uninfected and infected (MOI 3 and 30) RPTECs incubated with CellTox dye. Data is presented as CellTox-ratio (mean total fluorescence from infected inserts/mean total fluorescence from mock infected inserts). Error bars represent ± SD and n = 2. (E) Release of LDH into apical supernatants as measured by Promega LDH-Glo Cytotoxicity assay. Data is presented as LDH-ratio (infected-RLU/mock-RLU). Error bars represent ± SD and n = 2.
(TIF)

S4 Fig. Permeabilized cells lie in a different z-plane than the viable monolayer. Fully confluent RPTECs were BKPyV infected (MOI 1) and at 4 dpi cells were stained with CellTox dye (green) and CellMask (orange) followed by live-cell imaging and acquisition of z-stacks. Shown is oblique contrast (top row), CellTox (green, second row), CellMask (orange, third row), merge of oblique contrast and CellTox (fourth row) and merge of CellMask and CellTox (bottom row). Each column displays the same z-slice. Images are from a representative z-stack derived from two independent experiments. Scale bar 20 μm.
(TIF)

S5 Fig. Widefield microscopy of detached cells. Harvested cells incubated with CellTox dye (green) and Hoechst (blue) and imaged with a combination of oblique contrast and fluorescence microscopy using a Zeiss Celldiscoverer 7 with a 20x objective and 2x tube lens. Images are derived from two independent experiments. Scale bar 10 μm.
(TIF)

S1 Video. Time-lapse microscopy of polarized RPTECs infected with BKPyV (MOI 1) from 5 to 120 hpi with image acquisition every 30 minutes. The nuclei of permeabilized cells are stained with CellTox dye (green). Scale bar 50 μm.
(AVI)

S2 Video. Time-lapse microscopy of mock infected polarized RPTECs from 5 to 120 hpi with image acquisition every 30 minutes. The nuclei of permeabilized cells are stained with CellTox dye (green). Scale bar 50 μm.
(AVI)

S3 Video. Time-lapse microscopy of cell undergoing extrusion as showcased by compression of the permeabilized cell and subsequent upwards migration of the cell. Membranes

are stained with CellMask (orange) and the nuclei of permeabilized cells are stained with CellTox dye (green). Left panel shows oblique contrast, right panel shows CellMask and CellTox. Images were acquired every 10 minutes. Scale bar 10 μm.
(AVI)

S4 Video. Time-lapse microscopy of cell sloughing off from surface. Membranes are stained with CellMask (orange) and the nuclei of permeabilized cells are stained with CellTox dye (green). Left panel shows oblique contrast, right panel shows CellMask and CellTox. Images were acquired every 10 minutes. Scale bar 10 μm.
(AVI)

Acknowledgments

We thank Garth D. Tylden (University Hospital of North Norway, UNN) for helpful discussions and critical reading of the manuscript, Kristian Prydz (University of Oslo) for helpful discussions, the Advanced Microscopy Core Facility at UiT–The Arctic University of Norway for the use of instruments, Randi Olsen (UiT), Kenneth Bowitz Larsen (UiT) and Mona Antonsen (UNN) for technical assistance and reagents.

Author Contributions

Conceptualization: Elias Myrvoll Lorentzen, Christine Hanssen Rinaldo.

Data curation: Elias Myrvoll Lorentzen.

Formal analysis: Elias Myrvoll Lorentzen, Stian Henriksen.

Funding acquisition: Elias Myrvoll Lorentzen, Christine Hanssen Rinaldo.

Investigation: Elias Myrvoll Lorentzen, Stian Henriksen.

Methodology: Elias Myrvoll Lorentzen, Stian Henriksen.

Project administration: Christine Hanssen Rinaldo.

Supervision: Christine Hanssen Rinaldo.

Visualization: Elias Myrvoll Lorentzen.

Writing – original draft: Elias Myrvoll Lorentzen.

Writing – review & editing: Elias Myrvoll Lorentzen, Stian Henriksen, Christine Hanssen Rinaldo.

References

1. Moens U, Calvignac-Spencer S, Lauber C, Ramqvist T, Feltkamp MCW, Daugherty MD, et al. ICTV Virus Taxonomy Profile: Polyomaviridae. J Gen Virol. 2017; 98(6):1159–60. https://doi.org/10.1099/jgv.0.000839 PMID: 28640744
2. DeCaprio JA, Imperiale MJ, Hirsch HH. Fields Virology: DNA viruses. In: Howley PM, Knipe DM, Cohen JL, Damania BA, editors. Fields Virology. 7th ed: Wolters Kluwer; 2021.
3. Kamminga S, van der Meijden E, Feltkamp MCW, Zaaijer HL. Seroprevalence of fourteen human polyomaviruses determined in blood donors. PLoS One. 2018; 13(10):e0206273. https://doi.org/10.1371/journal.pone.0206273 PMID: 30352098
4. Imperiale MJ, Jiang M. Polyomavirus persistence. Annual Review of Virology. 2016; 3(1):517–32. https://doi.org/10.1146/annurev-virology-110615-042226 PMID: 27501263
5. Hirsch HH, Randhawa PS, AST Infectious Diseases Community of Practice. BK polyomavirus in solid organ transplantation—Guidelines from the American Society of Transplantation Infectious Diseases Community of Practice. Clin Transplant. 2019; 33(9):e13528.

6. Cesaro S, Dalianis T, Rinaldo CH, Koskenvuo M, Pegoraro A, Einsele H, et al. ECIL guidelines for the prevention, diagnosis and treatment of BK polyomavirus-associated haemorrhagic cystitis in haematopoietic stem cell transplant recipients. J Antimicrob Chemother. 2017; 73(1):12–21.
7. Starrett GJ, Yu K, Golubeva Y, Lenz P, Piaskowski ML, Petersen D, et al. Evidence for virus-mediated oncogenesis in bladder cancers arising in solid organ transplant recipients. eLife. 2023; 12:e82690. https://doi.org/10.7554/eLife.82690 PMID: 36961501
8. Jin Y, Zhou Y, Deng W, Wang Y, Lee RJ, Liu Y, et al. Genome-wide profiling of BK polyomavirus integration in bladder cancer of kidney transplant recipients reveals mechanisms of the integration at the nucleotide level. Oncogene. 2021; 40(1):46–54. https://doi.org/10.1038/s41388-020-01502-w PMID: 33051598
9. Papadimitriou JC, Randhawa P, Rinaldo CH, Drachenberg CB, Alexiev B, Hirsch HH. BK Polyomavirus infection and renourinary tumorigenesis. Am J Transplant. 2016; 16(2):398–406. https://doi.org/10.1111/ajt.13550 PMID: 26731714
10. Drachenberg CB, Papadimitriou JC, Wali R, Cubitt CL, Ramos E. BK polyoma virus allograft nephropathy: ultrastructural features from viral cell entry to lysis. Am J Transplant. 2003; 3(11):1383–92. https://doi.org/10.1046/j.1600-6135.2003.00237.x PMID: 14525599
11. Nickeleit V, Hirsch HH, Binet IF, Gudat F, Prince O, Dalquen P, et al. Polyomavirus infection of renal allograft recipients: from latent infection to manifest disease. J Am Soc Nephrol. 1999; 10(5):1080–9. https://doi.org/10.1681/ASN.V1051080 PMID: 10232695
12. Funk GA, Gosert R, Comoli P, Ginevri F, Hirsch HH. Polyomavirus BK replication dynamics in vivo and in silico to predict cytopathology and viral clearance in kidney transplants. Am J Transplant. 2008; 8(11):2368–77. https://doi.org/10.1111/j.1600-6143.2008.02402.x PMID: 18925904
13. Ramos E, Drachenberg CB, Papadimitriou JC, Hamze O, Fink JC, Klassen DK, et al. Clinical Course of Polyoma Virus Nephropathy in 67 Renal Transplant Patients. J Am Soc Nephrol. 2002; 13(8):2145–51. https://doi.org/10.1097/01.asn.0000023435.07320.81 PMID: 12138148
14. Binet I, Nickeleit V, Hirsch HH, Prince O, Dalquen P, Gudat F, et al. Polyomavirus disease under new immunosuppressive drugs: a cause of renal graft dysfunction and graft loss. Transplantation. 1999; 67(6):918–22. https://doi.org/10.1097/00007890-199903270-00022 PMID: 10199744
15. Gardner SD, Field AM, Coleman DV, Hulme B. New human papovavirus (B.K.) isolated from urine after renal transplantation. Lancet. 1971; 1(712):1253–7. https://doi.org/10.1016/s0140-6736(71)91776-4 PMID: 4104714
16. Low J, Humes HD, Szczypka M, Imperiale M. BKV and SV40 infection of human kidney tubular epithelial cells in vitro. Virology. 2004; 323(2):182–8. https://doi.org/10.1016/j.virol.2004.03.027 PMID: 15193914
17. Pieczynski J, Margolis B. Protein complexes that control renal epithelial polarity. Am J Physiol Renal Physiol. 2011; 300(3):F589–F601. https://doi.org/10.1152/ajprenal.00615.2010 PMID: 21228104
18. Blau DM, Compans RW. Polarization of viral entry and release in epithelial cells. Semin Virol. 1996; 7(4):245–53.
19. Cereijido M, Robbins ES, Dolan WJ, Rotunno CA, Sabatini DD. Polarized monolayers formed by epithelial cells on a permeable and translucent support. J Cell Biol. 1978; 77(3):853–80. https://doi.org/10.1083/jcb.77.3.853 PMID: 567227
20. Elwi AN, Damaraju VL, Kuzma ML, Mowles DA, Baldwin SA, Young JD, et al. Transepithelial fluxes of adenosine and 2′-deoxyadenosine across human renal proximal tubule cells: roles of nucleoside transporters hENT1, hENT2, and hCNT3. Am J Physiol Renal Physiol. 2009; 296(6):F1439–F51. https://doi.org/10.1152/ajprenal.90411.2008 PMID: 19297449
21. Ronco P, Antoine M, Baudouin B, Geniteau-legendre M, Lelongt B, Chatelet F, et al. Polarized membrane expression of brush-border hydrolases in primary cultures of kidney proximal tubular cells depends on cell differentiation and is induced by dexamethasone. J Cell Physiol. 1990; 145(2):222–37. https://doi.org/10.1002/jcp.1041450206 PMID: 1978836
22. Di Mise A, Tamma G, Ranieri M, Svelto M, Heuvel Bvd, Levtchenko EN, et al. Conditionally immortalized human proximal tubular epithelial cells isolated from the urine of a healthy subject express functional calcium-sensing receptor. Am J Physiol Renal Physiol. 2015; 308(11):F1200–F6. https://doi.org/10.1152/ajprenal.00352.2014 PMID: 25656364
23. Shaughnessey EM, Kann SH, Azizgolshani H, Black LD, Charest JL, Vedula EM. Evaluation of rapid transepithelial electrical resistance (TEER) measurement as a metric of kidney toxicity in a high-throughput microfluidic culture system. Sci Rep. 2022; 12(1):13182. https://doi.org/10.1038/s41598-022-16590-9 PMID: 35915212
24. Gonzalez-Mariscal L, Namorado MC, Martin D, Luna J, Alarcon L, Islas S, et al. Tight junction proteins ZO-1, ZO-2, and occludin along isolated renal tubules. Kidney Int. 2000; 57(6):2386–402. https://doi.org/10.1046/j.1523-1755.2000.00098.x PMID: 10844608

25. Yin J, Wang J. Renal drug transporters and their significance in drug–drug interactions. Acta Pharmaceutica Sinica B. 2016; 6(5):363–73. https://doi.org/10.1016/j.apsb.2016.07.013 PMID: 27709005

26. Liminga G, Nygren P, Larsson R. Microfluorometric Evaluation of Calcein Acetoxymethyl Ester as a Probe for P-Glycoprotein-Mediated Resistance: Effects of Cyclosporin A and Its Nonimmunosuppressive Analogue SDZ PSC 833. Exp Cell Res. 1994; 212(2):291–6. https://doi.org/10.1006/excr.1994.1146 PMID: 7910563

27. Neu U, Allen S-aA, Blaum BS, Liu Y, Frank M, Palma AS, et al. A structure-guided mutation in the major capsid protein retargets BK Polyomavirus. PLoS Pathog. 2013; 9(10):e1003688. https://doi.org/10.1371/journal.ppat.1003688 PMID: 24130487

28. Low JA, Magnuson B, Tsai B, Imperiale MJ. Identification of gangliosides GD1b and GT1b as receptors for BK virus. J Virol. 2006; 80(3):1361–6. https://doi.org/10.1128/JVI.80.3.1361-1366.2006 PMID: 16415013

29. Dugan AS, Eash S, Atwood WJ. An N-linked glycoprotein with alpha(2,3)-linked sialic acid is a receptor for BK virus. J Virol. 2005; 79(22):14442–5. https://doi.org/10.1128/JVI.79.22.14442-14445.2005 PMID: 16254379

30. Handala L, Blanchard E, Raynal P-I, Roingeard P, Morel V, Descamps V, et al. BK Polyomavirus Hijacks Extracellular Vesicles for En Bloc Transmission. J Virol. 2020; 94(6):e01834–19. https://doi.org/10.1128/JVI.01834-19 PMID: 31896595

31. Sorin MN, Di Maio A, Silva LM, Ebert D, Delannoy CP, Nguyen N-K, et al. Structural and functional analysis of natural capsid variants suggests sialic acid-independent entry of BK polyomavirus. Cell Rep. 2023; 42(2):112114. https://doi.org/10.1016/j.celrep.2023.112114 PMID: 36790933

32. Bernhoff E, Gutteberg TJ, Sandvik K, Hirsch HH, Rinaldo CH. Cidofovir inhibits polyomavirus BK replication in human renal tubular cells downstream of viral early gene expression. Am J Transplant. 2008; 8(7):1413–22. https://doi.org/10.1111/j.1600-6143.2008.02269.x PMID: 18510636

33. Seemayer CA, Seemayer NH, Durmuller U, Gudat F, Schaub S, Hirsch HH, et al. BK virus large T and VP-1 expression in infected human renal allografts. Nephrol Dial Transplant. 2008; 23(12):3752–61. https://doi.org/10.1093/ndt/gfn470 PMID: 18784088

34. Galluzzi L, Vitale I, Aaronson SA, Abrams JM, Adam D, Agostinis P, et al. Molecular mechanisms of cell death: recommendations of the Nomenclature Committee on Cell Death 2018. Cell Death Differ. 2018; 25(3):486–541. https://doi.org/10.1038/s41418-017-0012-4 PMID: 29362479

35. Lin W-HW, Tsay AJ, Lalime EN, Pekosz A, Griffin DE. Primary differentiated respiratory epithelial cells respond to apical measles virus infection by shedding multinucleated giant cells. Proc Natl Acad Sci U S A. 2021; 118(11):e2013264118. https://doi.org/10.1073/pnas.2013264118 PMID: 33836570

36. Moshiri J, Craven AR, Mixon SB, Amieva MR, Kirkegaard K. Mechanosensitive extrusion of Enterovirus A71-infected cells from colonic organoids. Nat Microbiol. 2023; 8:629–39. https://doi.org/10.1038/s41564-023-01339-5 PMID: 36914754

37. Liesman RM, Buchholz UJ, Luongo CL, Yang L, Proia AD, DeVincenzo JP, et al. RSV-encoded NS2 promotes epithelial cell shedding and distal airway obstruction. J Clin Invest. 2014; 124(5):2219–33. https://doi.org/10.1172/JCI72948 PMID: 24713657

38. Singh HK, Bubendorf L, Mihatsch MJ, Drachenberg CB, Nickeleit V. Urine cytology findings of polyomavirus infections. Adv Exp Med Biol. 2006; 577:201–12. https://doi.org/10.1007/0-387-32957-9_15 PMID: 16626038

39. Fogazzi GB, Cantu M, Saglimbeni L. 'Decoy cells' in the urine due to polyomavirus BK infection: easily seen by phase-contrast microscopy. Nephrol Dial Transplant. 2001; 16(7):1496–8. https://doi.org/10.1093/ndt/16.7.1496 PMID: 11427650

40. Gudipaty SA, Rosenblatt J. Epithelial cell extrusion: Pathways and pathologies. Semin Cell Dev Biol. 2017; 67:132–40. https://doi.org/10.1016/j.semcdb.2016.05.010 PMID: 27212253

41. Shkarina K, Hasel de Carvalho E, Santos JC, Ramos S, Leptin M, Broz P. Optogenetic activators of apoptosis, necroptosis, and pyroptosis. J Cell Biol. 2022; 221(6):e202109038. https://doi.org/10.1083/jcb.202109038 PMID: 35420640

42. Kobayashi N, Suzuki Y, Tsuge T, Okumura K, Ra C, Tomino Y. FcRn-mediated transcytosis of immunoglobulin G in human renal proximal tubular epithelial cells. Am J Physiol Renal Physiol. 2002; 282(2):F358–F65. https://doi.org/10.1152/ajprenal.0164.2001 PMID: 11788451

43. Rojas R, Apodaca G. Immunoglobulin transport across polarized epithelial cells. Nat Rev Mol Cell Biol. 2002; 3(12):944–56. https://doi.org/10.1038/nrm972 PMID: 12461560

44. Bai Y, Ye L, Tesar DB, Song H, Zhao D, Björkman PJ, et al. Intracellular neutralization of viral infection in polarized epithelial cells by neonatal Fc receptor (FcRn)-mediated IgG transport. Proc Natl Acad Sci U S A. 2011; 108(45):18406–11. https://doi.org/10.1073/pnas.1115348108 PMID: 22042859

45. Clayson ET, Compans RW. Entry of simian virus 40 is restricted to apical surfaces of polarized epithelial cells. Mol Cell Biol. 1988; 8(8):3391–6. https://doi.org/10.1128/mcb.8.8.3391-3396.1988 PMID: 2850491

46. Basak S, Turner H, Compans RW. Expression of SV40 receptors on apical surfaces of polarized epithelial cells. Virology. 1992; 190(1):393–402. https://doi.org/10.1016/0042-6822(92)91225-j PMID: 1326810

47. Ciarlet M, Crawford SE, Estes MK. Differential infection of polarized epithelial cell lines by sialic acid-dependent and sialic acid-independent rotavirus strains. J Virol. 2001; 75(23):11834–50. https://doi.org/10.1128/JVI.75.23.11834-11850.2001 PMID: 11689665

48. Crespo PM, von Muhlinen N, Iglesias-Bartolomé R, Daniotti JL. Complex gangliosides are apically sorted in polarized MDCK cells and internalized by clathrin-independent endocytosis. FEBS J. 2008; 275(23):6043–56. https://doi.org/10.1111/j.1742-4658.2008.06732.x PMID: 19021775

49. Ulloa F, Real FX. Differential distribution of dialic acid in α2,3 and α2,6 linkages in the apical membrane of cultured epithelial cells and tissues. J Histochem Cytochem. 2001; 49(4):501–9.

50. Murata F, Tsuyama S, Suzuki S, Hamada H, Ozawa M, Muramatsu T. Distribution of glycoconjugates in the kidney studied by use of labeled lectins. J Histochem Cytochem. 1983; 31(1A_suppl):139–44.

51. Bird SW, Kirkegaard K. Escape of non-enveloped virus from intact cells. Virology. 2015; 479–480:444–9. https://doi.org/10.1016/j.virol.2015.03.044 PMID: 25890822

52. Evans GL, Caller LG, Foster V, Crump CM. Anion homeostasis is important for non-lytic release of BK polyomavirus from infected cells. Open Biol. 2015; 5(8):150041. https://doi.org/10.1098/rsob.150041 PMID: 26246492

53. Clayson ET, Brando LV, Compans RW. Release of simian virus 40 virions from epithelial cells is polarized and occurs without cell lysis. J Virol. 1989; 63(5):2278–88. https://doi.org/10.1128/JVI.63.5.2278-2288.1989 PMID: 2539518

54. Zhao G-D, Gao R, Hou X-T, Zhang H, Chen X-T, Luo J-Q, et al. Endoplasmic Reticulum Stress Mediates Renal Tubular Vacuolation in BK Polyomavirus-Associated Nephropathy. Front Endocrinol. 2022; 13:834187. https://doi.org/10.3389/fendo.2022.834187 PMID: 35464062

55. Hirsch HH, Knowles W, Dickenmann M, Passweg J, Klimkait T, Mihatsch MJ, et al. Prospective study of polyomavirus type BK replication and nephropathy in renal-transplant recipients. N Engl J Med. 2002; 347(7):488–96. https://doi.org/10.1056/NEJMoa020439 PMID: 12181403

56. Brennan DC, Agha I, Bohl DL, Schnitzler MA, Hardinger KL, Lockwood M, et al. Incidence of BK with tacrolimus versus cyclosporine and impact of preemptive immunosuppression reduction. Am J Transplant. 2005; 5(3):582–94. https://doi.org/10.1111/j.1600-6143.2005.00742.x PMID: 15707414

57. Cantaluppi V, Quercia AD, Dellepiane S, Ferrario S, Camussi G, Biancone L. Interaction between systemic inflammation and renal tubular epithelial cells. Nephrol Dial Transplant. 2014; 29(11):2004–11. https://doi.org/10.1093/ndt/gfu046 PMID: 24589723

58. Lorentzen EM, Henriksen S, Kaur A, Kro GB, Hammarström C, Hirsch HH, et al. Early fulminant BK polyomavirus-associated nephropathy in two kidney transplant patients with low neutralizing antibody titers receiving allografts from the same donor. Virol J. 2020; 17(1):5. https://doi.org/10.1186/s12985-019-1275-9 PMID: 31924245

59. Kaur A, Wilhelm M, Wilk S, Hirsch HH. BK polyomavirus-specific antibody and T-cell responses in kidney transplantation: update. Curr Opin Infect Dis. 2019; 32(6):575–83. https://doi.org/10.1097/QCO.0000000000000602 PMID: 31567736

60. ClinicalTrials.Gov [19.07.2023]. Available from: https://www.clinicaltrials.gov/search?cond=BK%20Polyomavirus&viewType=Table&limit=100&page=1.

61. Bauman Y, Nachmani D, Vitenshtein A, Tsukerman P, Drayman N, Stern-Ginossar N, et al. An identical miRNA of the human JC and BK polyoma viruses targets the stress-induced ligand ULBP3 to escape immune elimination. Cell Host Microbe. 2011; 9(2):93–102. https://doi.org/10.1016/j.chom.2011.01.008 PMID: 21320692

62. Manzetti J, Weissbach FH, Graf FE, Unterstab G, Wernli M, Hopfer H, et al. BK Polyomavirus Evades Innate Immune Sensing by Disrupting the Mitochondrial Network and Promotes Mitophagy. iScience. 2020; 23(7):101257. https://doi.org/10.1016/j.isci.2020.101257 PMID: 32599557

63. Hirsch HH, Steiger J. Polyomavirus BK. Lancet Infect Dis. 2003; 3(10):611–23. https://doi.org/10.1016/s1473-3099(03)00770-9 PMID: 14522260

64. Rinaldo CH, Gosert R, Bernhoff E, Finstad S, Hirsch HH. 1-O-hexadecyloxypropyl cidofovir (CMX001) effectively inhibits polyomavirus BK replication in primary human renal tubular epithelial cells. Antimicrob Agents Chemother. 2010; 54(11):4714–22. https://doi.org/10.1128/AAC.00974-10 PMID: 20713664

65. Rinaldo CH, Traavik T, Hey A. The agnogene of the human polyomavirus BK is expressed. J Virol. 1998; 72(7):6233–6. https://doi.org/10.1128/JVI.72.7.6233-6236.1998 PMID: 9621096

66. Sharma BN, Li R, Bernhoff E, Gutteberg TJ, Rinaldo CH. Fluoroquinolones inhibit human polyomavirus BK (BKV) replication in primary human kidney cells. Antiviral Res. 2011; 92(1):115–23. https://doi.org/10.1016/j.antiviral.2011.07.012 PMID: 21798289

67. Hey AW, Johnsen JI, Johansen B, Traavik T. A two fusion partner system for raising antibodies against small immunogens expressed in bacteria. J Immunol Methods. 1994; 173(2):149–56. https://doi.org/10.1016/0022-1759(94)90294-1 PMID: 8046249

68. Rinaldo CH, Myhre MR, Alstad H, Nilssen O, Traavik T. Human polyomavirus BK (BKV) transiently transforms and persistently infects cultured osteosarcoma cells. Virus Res. 2003; 93(2):181–7. https://doi.org/10.1016/s0168-1702(03)00096-0 PMID: 12782366

69. Schutgens F, Rookmaaker MB, Margaritis T, Rios A, Ammerlaan C, Jansen J, et al. Tubuloids derived from human adult kidney and urine for personalized disease modeling. Nat Biotechnol. 2019; 37(3):303–13. https://doi.org/10.1038/s41587-019-0048-8 PMID: 30833775

70. Petit L, Gibert M, Gourch A, Bens M, Vandewalle A, Popoff MR. Clostridium perfringens epsilon toxin rapidly decreases membrane barrier permeability of polarized MDCK cells. Cell Microbiol. 2003; 5(3):155–64. https://doi.org/10.1046/j.1462-5822.2003.00262.x PMID: 12614459

71. Jansen J, Schophuizen CM, Wilmer MJ, Lahham SH, Mutsaers HA, Wetzels JF, et al. A morphological and functional comparison of proximal tubule cell lines established from human urine and kidney tissue. Exp Cell Res. 2014; 323(1):87–99. https://doi.org/10.1016/j.yexcr.2014.02.011 PMID: 24560744

72. Pokrovskaya ID, Szwedo JW, Goodwin A, Lupashina TV, Nagarajan UM, Lupashin VV. Chlamydia trachomatis hijacks intra-Golgi COG complex-dependent vesicle trafficking pathway. Cell Microbiol. 2012; 14(5):656–68. https://doi.org/10.1111/j.1462-5822.2012.01747.x PMID: 22233276

73. Cocchiaro JL, Kumar Y, Fischer ER, Hackstadt T, Valdivia RH. Cytoplasmic lipid droplets are translocated into the lumen of the Chlamydia trachomatis parasitophorous vacuole. Proc Natl Acad Sci U S A. 2008; 105(27):9379–84. https://doi.org/10.1073/pnas.0712241105 PMID: 18591669

74. Henriksen S, Hansen T, Bruun JA, Rinaldo CH. The presumed polyomavirus viroporin VP4 of simian virus 40 or human BK Polyomavirus is not required for viral progeny release. J Virol. 2016; 90(22):10398–413. https://doi.org/10.1128/JVI.01326-16 PMID: 27630227

75. Dumoulin A, Hirsch HH. Reevaluating and optimizing polyomavirus BK and JC real-time PCR assays to detect rare sequence polymorphisms. J Clin Microbiol. 2011; 49(4):1382–8. https://doi.org/10.1128/JCM.02008-10 PMID: 21325560

Appendix: Paper 3